REPORT NO. FRA/ORD-80/21

OPERATIONAL PARAMETERS IN ACOUSTIC SIGNATURE INSPECTION OF RAILROAD WHEELS

D. Dousis
R.D. Finch

UNIVERSITY OF HOUSTON
Department of Mechanical Engineering
Houston TX   77004

APRIL 1980
FINAL REPORT

Prepared for

1. Report No. FRA/ORD-80/21	2. Government Accession No.	3. Recipient's Catalog No. PB81 116766
4. Title and Subtitle OPERATIONAL PARAMETERS IN ACOUSTIC SIGNATURE INSPECTION OF RAILROAD WHEELS		5. Report Date April 1980
		6. Performing Organization Code
7. Author's) D. Dousis, R. D. Finch		8. Performing Organization Report No. DOT-TSC-FRA-80-9
9. Performing Organization Name and Address University of Houston* Department of Mechanical Engineering Houston TX 77004		10. Work Unit No. (TRAIS) RR031/R0312
		11. Contract or Grant No. DOT-TSC-1187
12. Sponsoring Agency Name and Address U.S. Department of Transportation Federal Railroad Administration Office of Research and Development Washington DC 20590		13. Type of Report and Period Covered Final Report March 1976-Oct. 1978
		14. Sponsoring Agency Code

15. Supplementary Notes *under contract to:	U.S. Department of Transportation Research and Special Programs Administration Transportation Systems Center Cambridge MA 02142

16. Abstract

A brief summary is given of some prior studies which established the feasibility of using acoustic signatures for inspection of railroad wheels. The purpose of the present work was to elucidate operational parameters which would be of importance for the development of a prototype system. Experimental and theoretical investigations were conducted to obtain more information on the effects on wheel vibrations of geometrical variations, wear, internal stress etc. Hardware improvements and interfacing were carried out for a wayside installation, in addition to software development for real time data acquisition and processing. Field tests were made to evaluate system performance, to permit follow-up on certain wheels and to obtain tape recordings from a sample of axle sets in service. These tape recordings were used to optimize the data processing software and to attempt to correlate identifiable wheel conditions with characteristics of the acoustic signature. The greatest signature differences were obtained when one of a pair of wheels was cracked. Differential wear was found to be a major cause of differences in the signatures of good wheel pairs. It is claimed that the knowledge gained from this study is sufficient to warrant the installation of a prototype system with a reasonable likelihood of success. Another important finding is that the frequencies of certain resonant modes shift slightly with changes in residual stress.

17. Key Words Railroad Wheels Acoustic Signature Inspection Systems Residual Stress	18. Distribution Statement DOCUMENT IS AVAILABLE TO THE PUBLIC THROUGH THE NATIONAL TECHNICAL INFORMATION SERVICE, SPRINGFIELD, VIRGINIA 22161

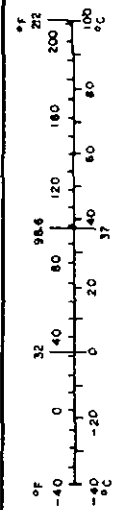| 19. Security Classif. (of this report) Unclassified	20. Security Classif. (of this page) Unclassified	21. No. of Pages	22. Price

METRIC CONVERSION FACTORS

Approximate Conversions to Metric Measures

Symbol	When You Know	Multiply by	To Find	Symbol
LENGTH				
in	inches	2.5	centimeters	cm
ft	feet	30	centimeters	cm
yd	yards	0.9	meters	m
mi	miles	1.6	kilometers	km
AREA				
in²	square inches	6.5	square centimeters	cm²
ft²	square feet	0.09	square meters	m²
yd²	square yards	0.8	square meters	m²
mi²	square miles	2.6	square kilometers	km²
	acres	0.4	hectares	ha
MASS (weight)				
oz	ounces	28	grams	g
lb	pounds	0.45	kilograms	kg
	short tons (2000 lb)	0.9	tonnes	t
VOLUME				
tsp	teaspoons	5	milliliters	ml
Tbsp	tablespoons	15	milliliters	ml
fl oz	fluid ounces	30	milliliters	ml
c	cups	0.24	liters	l
pt	pints	0.47	liters	l
qt	quarts	0.95	liters	l
gal	gallons	3.8	liters	l
ft³	cubic feet	0.03	cubic meters	m³
yd³	cubic yards	0.76	cubic meters	m³
TEMPERATURE (exact)				
°F	Fahrenheit temperature	5/9 (after subtracting 32)	Celsius temperature	°C
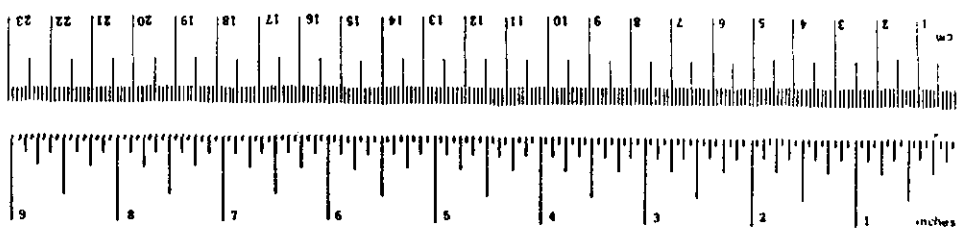
Approximate Conversions from Metric Measures

Symbol	When You Know	Multiply by	To Find	Symbol
LENGTH				
mm	millimeters	0.04	inches	in
cm	centimeters	0.4	inches	in
m	meters	3.3	feet	ft
m	meters	1.1	yards	yd
km	kilometers	0.6	miles	mi
AREA				
cm²	square centimeters	0.16	square inches	in²
m²	square meters	1.2	square yards	yd²
km²	square kilometers	0.4	square miles	mi²
ha	hectares (10,000 m²)	2.5	acres	
MASS (weight)				
g	grams	0.035	ounces	oz
kg	kilograms	2.2	pounds	lb
t	tonnes (1000 kg)	1.1	short tons	
VOLUME				
ml	milliliters	0.03	fluid ounces	fl oz
l	liters	2.1	pints	pt
l	liters	1.06	quarts	qt
l	liters	0.26	gallons	gal
m³	cubic meters	35	cubic feet	ft³
m³	cubic meters	1.3	cubic yards	yd³
TEMPERATURE (exact)				
°C	Celsius temperature	9/5 (then add 32)	Fahrenheit temperature	°F

°F
    -40   0   32   98.6   160   200   212
-40   -20   0   20   37   40   60   80   100
°C

TABLE OF CONTENTS

CONTENTS (Cont'd)

CONTENTS (Cont'd)

LIST OF ILLUSTRATIONS

ILLUSTRATIONS (Cont'd)

ILLUSTRATIONS (Cont'd)

LIST OF TABLES

1. INTRODUCTION

1.1 Background

The impetus to the work covered in this report came
from a feasibility study on the use of acoustic signatures
for inspection of railroad wheels [1]. The basic idea was
to see if it would be possible to automate the art of the
carman, who by banging wheels with a hammer, can tell a
defective one by its sound. There is a need for a fully
automatic testing system to inspect freight car wheels.
At present the standard way of finding cracked or over-
heated wheels depends on the visual acuity of inspectors
stationed in pits at switching yards. These men have to
watch for a variety of possible mechanical defects as the
cars move past the pit. Although the inspectors are
remarkably adept at finding problems there are still a
number of mechanical defects which are not readily
apparent and subsequently can result in derailments.
Table 1.1.1 shows the AAR list of wheel failures for
1976 indicating the relative importance of different
defects.

Having indicated the motivation for the research it is
appropriate to proceed to summarize the findings of the earlier
feasibility study [1]. The present work had the general
objective of improving the laboratory demonstration system
to the point that actual operating parameters could be

TABLE 1.1.1 LIST OF WHEEL FAILURES FOR 1976

From: Association of American Railroads
Mechanical Division Circular D.V. 1895

REPORT OF AAR WHEEL FAILURES FOR YEAR 1976	Total Failures	CAUSE – INTERCHANGE RULE 41 – SEC. F 6								
		Cracked or Broken Flange	Cracked or Broken Rim	Shattered Rim	Spread Rim	Thermal Cracks	Tread Shelled	Burst Hub	Cracked or Broken Plate	Subsurface Defect
		66	68	71	72	74	75	82	83	88
28 "										
1W – CS	21		18			1	2			
1W – WS	36		1	16		6			13	
2W & MW – CS										
2W & MW – WS	1		1							
TOTAL	58		20	16		7	2		13	
33 "										
1W – CS	273	3	30	17		176	25	1	20	1
1W – WS	255	5	63	75	1	25	22	1	63	
2W & MW – CS	16	1	3			9	2		1	
2W & MW – WS	87	2	12	30		26	7	1	9	
TOTAL	631	11	108	122	1	236	56	3	93	1
36 "										
1W – CS	69	8		2		17	37	1	4	
1W – WS	367	4	47	211		18	71		16	
2W & MW – CS	25		1	4		12	7		1	
2W & MW – WS	94	2	12	27	1	15	22		15	
TOTAL	555	14	60	244	1	62	137	1	36	
38 "										
1W – CS										
1W – WS	7			2		2	2		1	
2W & MW – CS										
2W & MW – WS	3		1			2				
TOTAL	10		1	2		4	2		1	
GRAND TOTAL	1254	25	189	384	2	309	197	4	143	1

1W = Single Wear

MW = Multiple Wear

CS = Cast Steel

WS = Wrought Steel

established and a secondary objective was to find if residual stresses could change the acoustic signature and in what manner. The specific objectives of the present program will be defined after the summary of the feasibility study.

1.2 Types of Defects

It is appropriate to summarize the principal in-service defects of wheels*, and their causes. A good summary of this subject has been given by Carter and Caton [30]. At present one of the most frequently occurring classes of defect is the thermal crack, due to extended periods of brake shoe application and rapid cooling. The cracks may be found on only one or both wheels of an axle set. The cracks appear as hair lines on the tread or flange and there are frequently numerous cracks around the circumference of the wheel. Despite the barely visible exterior manifestation of this type of crack, below the surface it may occupy a sizeable fraction of the rim cross section. When a wheel with thermal cracks is withdrawn from service and subjected to metallurgical examination the cracks are typically found to extend over about a square inch in area perpendicular to the surface (see Fig. 1.2.1). This area is usually blackened, suggesting that the cracks may persist for long periods before progressing through the plate to cause a catastrophic failure. This final stage of the failure is surmised to be a result of changes in the internal state

---

*The Association of American Railroads standard nomenclature for the parts of a wheel is illustrated in Fig. 1.2.1.
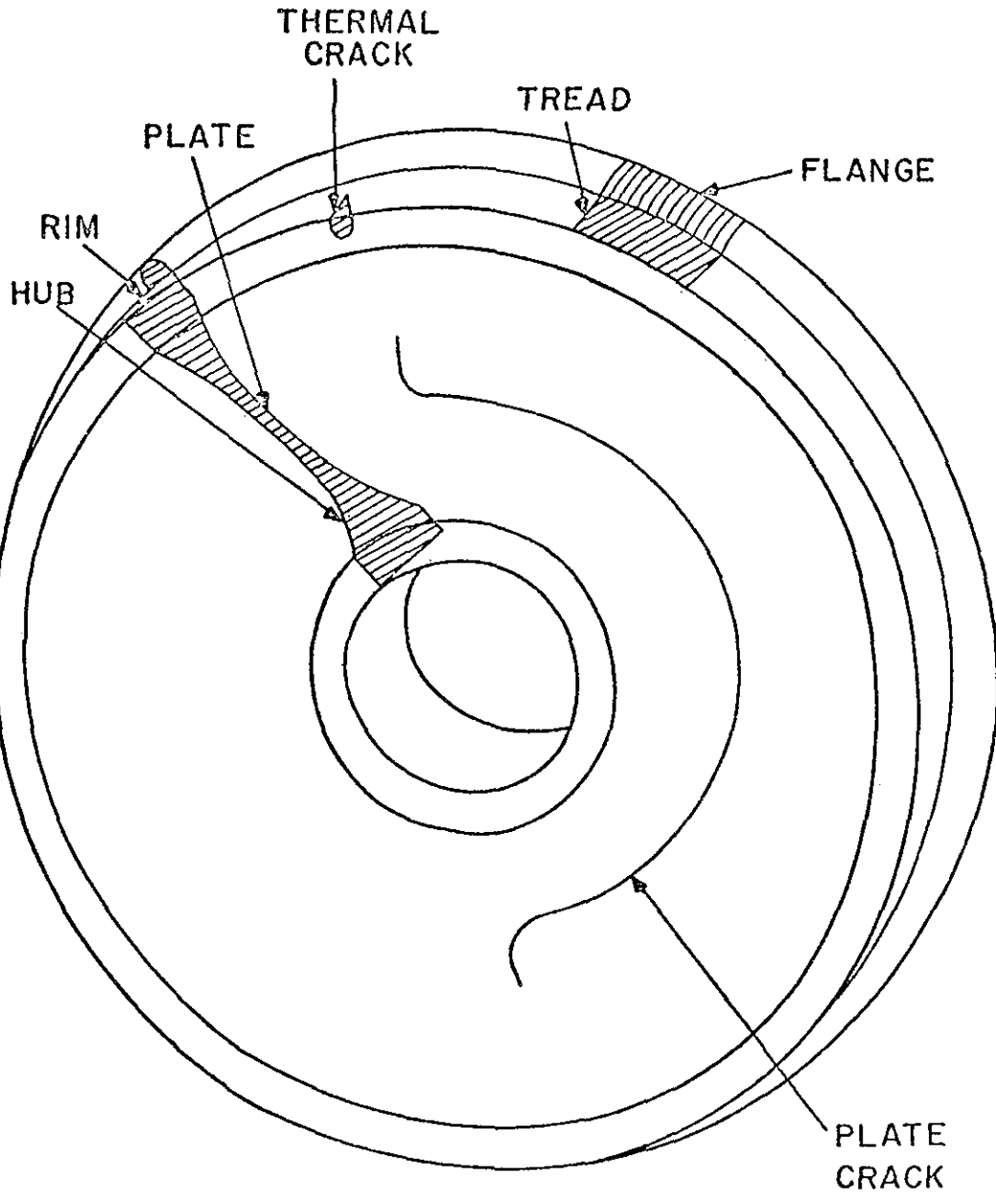
FIG. 1.2.1 WHEEL SHOWING TYPICAL CRACKS

of stress of the wheel. A method for detecting thermal
cracks using ultrasonic surface waves has been described in
an earlier publication by Bray et al. [3], but acoustic
signature inspection is an alternative method.

Changes in internal stress are not readily measured, even
under laboratory conditions, and so most railroads make it
a practice to remove wheels showing a burnt or cindered road
dirt and oil mixture or a typical discoloration associated
with overheating. A means of determining internal stress on
an automatic basis therefore would be a highly desirable
feature of any wheel inspection system. Some evidence is
presented in this report that changes in internal stress
can be detected from acoustic signature inspection.

Plate cracks are usually found as extensive bow shape
fractures running round the hub and extending into the plate.
Cracks in the plate can develop due to lateral stresses in
service or tension due to rim heating during drag braking.
Some plate cracks have been ascribed to manufacturing defects.
This type of defect is not found as frequently as thermal
cracking or overheating but some of the most catastrophic wheel
failures have been ascribed to plate cracks. The detection of
plate cracks by acoustic signature inspection was investigated
extensively as reported later.

Shattered rims, due to the growth of subsurface defects,
are encountered quite often. Another common problem is the
occurrence of flat spots on the tread, due to sliding along
the rail when the brake locks the wheels. Large flat spots

cause repeated impacting which results in further damage to both the rail and the wheels. These tread surface defects can be detected using very simple acoustic signature inspection.

1.3 Elements of Acoustic Signature Analysis

The elements of an acoustic signature inspection system are illustrated schematically in Fig. 1.3.1. The excitation, in principle, could occur in normal railroad operations: impact at joints, friction of brakes and retarders; or simply the forces due to rolling. Flat spots provide their own source of excitation by periodic impact on the rail. Alternatively, it may be necessary to introduce an excitation, such as a hammer blow, which does not occur in normal operations. One of the objectives of the feasibility study was to decide which of these forms of excitation would be most suitable for a flaw detection system.

The vibratory mechanical energy of the excited wheel is partially degraded by sound radiated into the air and vibration of the track. It is these sounds and vibrations which are termed the acoustic signature. Sound can be picked up by a microphone, and vibration, by a rail mounted accelerometer. A second objective of the feasibility study was to decide whether sound or vibration is the better form of acoustic signature to monitor in the detection of various types of flaw.

The sound or vibration signal after transduction may be represented in various formats. The simplest of these is an overall, RMS sound level. Various weighting networks as
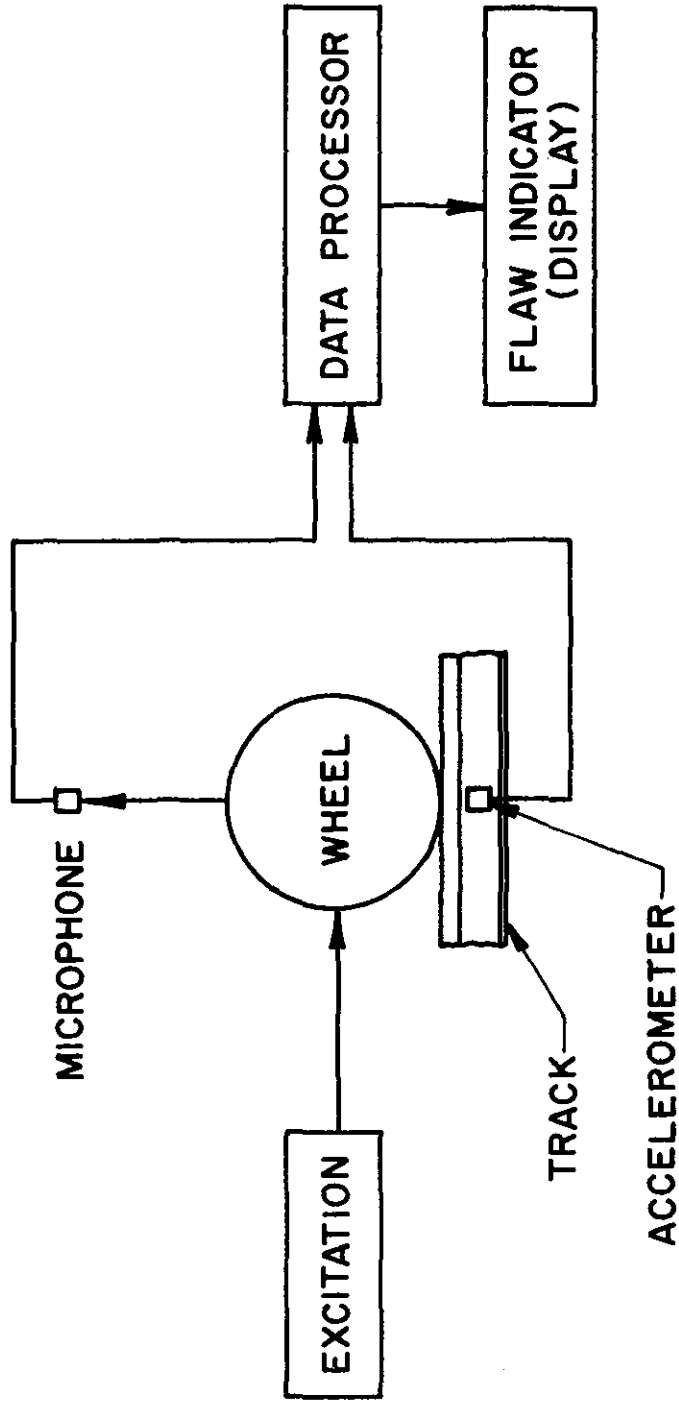
FIG. I.3.I SCHEMATIC OF ACOUSTIC SIGNATURE
INSPECTION SYSTEM COMPONENTS

well as band-pass filtering may be used to attenuate or
exclude noise components in the signal. The frequency
spectrum of the signal is a function of the filtering method
employed. Both one-third octave band and constant bandwidth
(250 channels per 10 kHz) analyzers were used in the
feasibility study. Railroad wheel sound spectra were found
to be dominated by high frequency components in the range of
1 to 5 kHz. One-third octave bands in this frequency range
are wide, so that all the information from a wheel's acoustic
signature is compressed into a few bands. Changes in the
acoustic signature result in relatively small level changes
in these 1/3 octave bands. However, when narrow constant
bandwidth analyzers are used, the wheel signature is represented
by more bands, thus perception of signature changes is
considerably improved. The disadvantage is increased
analysis time due to the increased amount of data.

The spectrum of a given signal can be processed with
a minicomputer by comparison to reference spectra. Various
possible comparison schemes were considered and are discussed
later. Finally if the comparisons show that a wheel is
defective, some form of flaw indicator is actuated. In the
present research system this indication is made with a
teletype.

1.4 Theory

A completely theoretical design procedure could be
envisaged. The railroad wheel could be modelled using finite

element analysis so that various forcing functions, various wheel geometries and various defects could then be simulated. The wheel vibrations could then be related to sound radiated to obtain predictions of acoustic signatures. This information could then be used in selecting excitation, detection and data processing methods. Some progress on such a theoretical approach was made during the feasibility study. The free vibration frequencies of a wheel without damping were found. Figure 1.4.1 shows these theoretical results for the first 15 resonance frequencies and mode shapes of the wheel. Comparison with experimental results for 33" good wheels showed good agreement at the lower frequencies. The higher frequency resonances obtained using finite element analysis differed from experimental values (see Fig. 1.4.2), because at higher frequencies the wavelength becomes comparable to the size of the element.

Resonance changes were obtained with the finite element program for a 33" wheel having a simulated plate crack. The reason for studying the plate crack was that it appeared to present a particular challenge to other NDE methods such as inspection with ultrasonic surface waves on the tread. Figure 1.4.3 shows the first six resonances and mode shapes for the cracked wheel. In Fig. 1.4.4 comparison is made between the resonances of a good and a bad wheel from the finite element model. The outstanding feature of this comparison is the apparent increase in the model density of the flawed wheel.
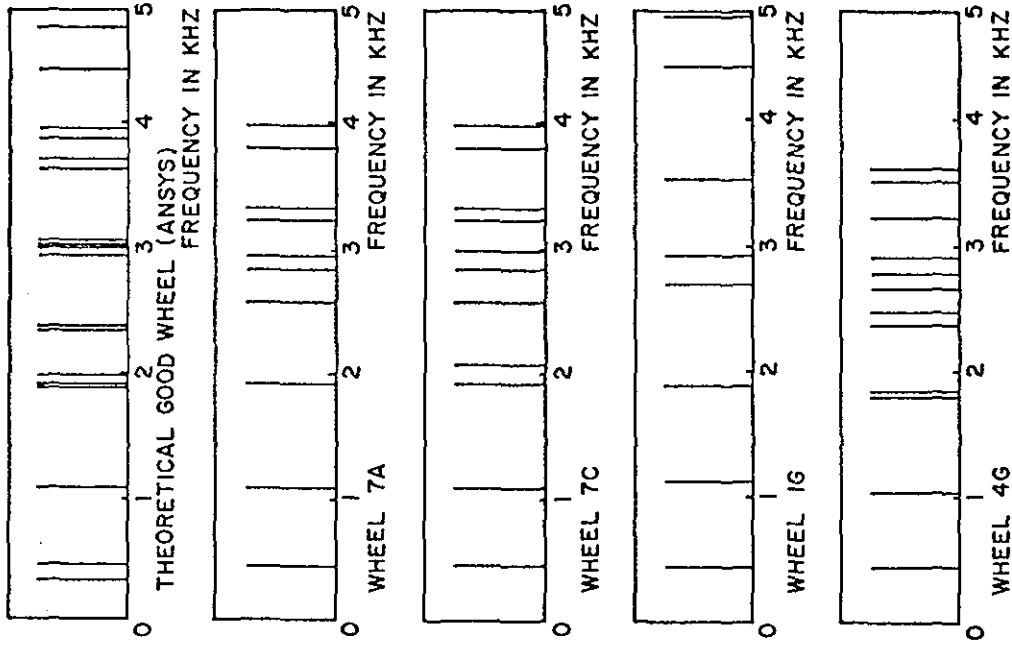
FIG. 1.4.2 LINE SPECTRA OF RESONANCES OBTAINED FROM THE ANSYS PROGRAM, COMPARED WITH EXPERIMENTAL SPECTRA FOR 33" GOOD WHEELS, OBTAINED BY USING A RAIL-MOUNTED ACCELERO-METER

THEORETICAL GOOD WHEEL (ANSYS)
FREQUENCY IN KHZ

WHEEL 7A
FREQUENCY IN KHZ

WHEEL 7C
FREQUENCY IN KHZ

WHEEL 1G
FREQUENCY IN KHZ

WHEEL 4G
FREQUENCY IN KHZ

317 HZ
(DOUBLE RESONANCE)

443 HZ
(DOUBLE RESONANCE)

455 HZ

1087 HZ
(DOUBLE RESONANCE)

1897 HZ
(DOUBLE RESONANCE)

1912 HZ

1999 HZ
(DOUBLE RESONANCE)

2360 HZ
(DOUBLE RESONANCE)

NODAL CIRCLE ON RIM

2386 HZ
(DOUBLE RESONANCE)
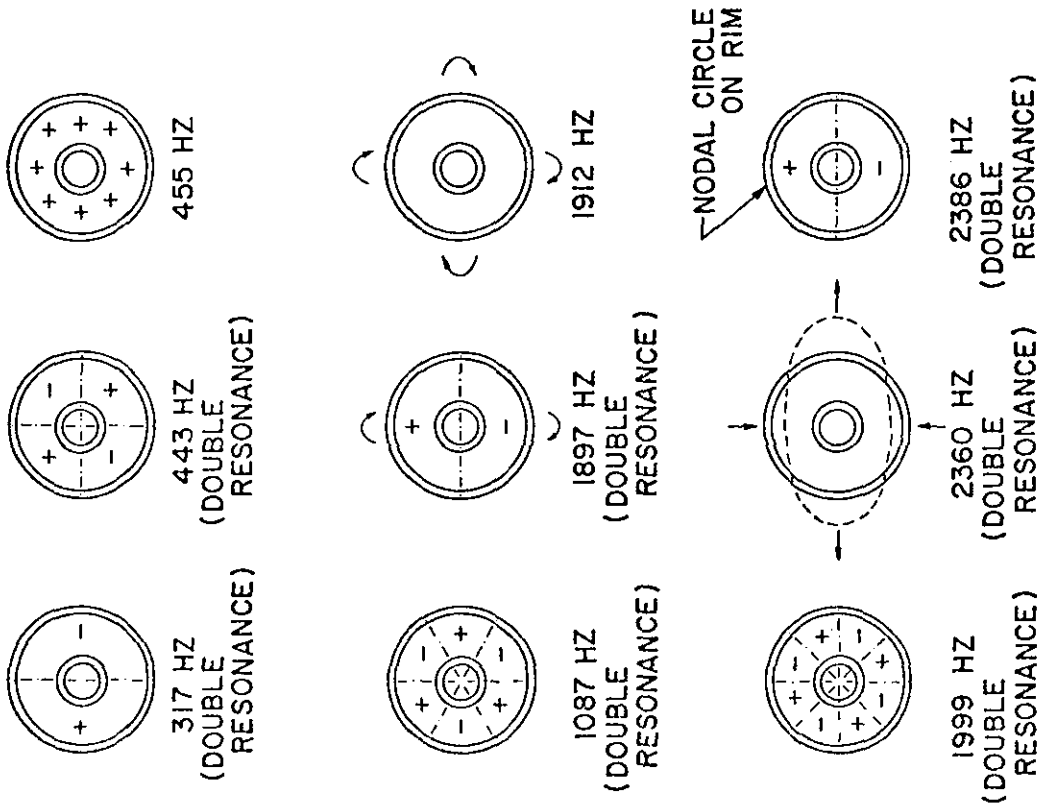
FIG. 1.4.1 MODE SHAPES OBTAINED WITH FINITE ELEMENT PROGRAM FOR 33" GOOD WHEEL. NOTE: THE HUB IS FIXED FOR ALL MODE SHAPES.

FREQUENCY IN KHZ

THEORETICAL RESONANCES OF A GOOD WHEEL

FREQUENCY IN KHZ

THEORETICAL RESONANCES OF A WHEEL WITH A PLATE FLAW

FIG.14.4 LINE SPECTRA OF RESONANCES OBTAINED FROM THE ANSYS PROGRAM FOR 33" GOOD AND FLAWED WHEELS

148.5 HZ

255.13 HZ

347.3 HZ

421.7 HZ

429.7 HZ

764.5 HZ
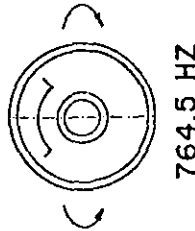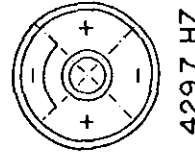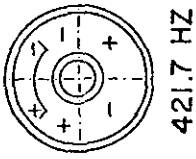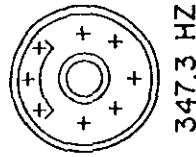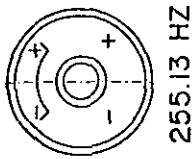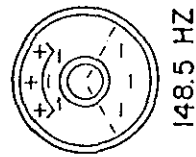
FIG. 14.3 MODE SHAPES OBTAINED WITH ANSYS PROGRAM FOR 33" WHEEL WITH PLATE CRACK

1.5 Experiments on Excitation and Detection Methods

In order to determine which of the various excitation methods would be most suitable a series of experiments were performed, during the feasibility study, both in the laboratory and in the field. Rolling noise was found to be predominantly low frequency sound from many sources and to mask the response of the wheel. Impact at a rail joint masks the wheel signature and even though some of the higher wheel resonances seem to be excited the response varies from wheel to wheel and with train speed. When passing through a retarder a wheel sometimes emits an intense screeching sound. It was found in this situation that only a few resonances of the wheel were excited, and different resonances were excited during successive passages of the wheel through the retarder. This lack of repeatability and the excitation of only one or two resonances ruled out the retarder as a choice of excitation.

When using active excitation methods, energy is imparted to the wheel from a device which is not part of normal railroad operations. In the feasibility study an electrodynamic shaker was used with random noise and sine wave inputs. This method of excitation does not appear to be feasible for field use. Tapping with a steel pendulum or a hammer excites a rich spectrum of wheel resonances (see Figs. 1.6.2 - 1.6.5). To obtain repeatability with this mode of excitation, it was found that there must be a good control of the momentum of the impacting hammer.

Various microphone and accelerometer configurations were experimented with. Except in the detection of flat spots [4], rail mounted accelerometers are not regarded as the best choice, the reason being that there are natural modes of vibration of the rail in the same frequency range as the wheel modes. These rail modes can be superimposed on the wheel signature thus compounding the difficulties of data processing. When a microphone is used only the sound from the wheel is detected because of the relatively small radiating area of the rail and its weak coupling to the wheel. Regulations permit installation of devices at ground level so that the microphone to receive airborne sound is best located close to the rails.

1.6 Variables in the Acoustic Signature

As part of the feasibility study wheel and axle sets were rolled over an automatic impacter (see Fig. 1.6.1) on the laboratory track. Unfortunately at the time this data was taken there was no provision in the system for a triggering pulse so that the timing of the scan made by the instrument could not be controlled relative to the duration of the impact sound. Even with this difficulty several interesting features were discovered.

Figure 1.6.2 shows the superposition of impact spectra from two good and equally worn Griffin 9 riser 33" wheels on either end of the same axle. The signal amplitudes differ somewhat but the values of the resonance frequencies are very closely reproduced. In contrast Fig. 1.6.3 shows the spectrum of one of these same wheels in comparison with the spectrum of a good Armco Wrought 33" wheel. There are some pronounced differences in the resonance frequencies. Even more differences in the resonance frequencies are
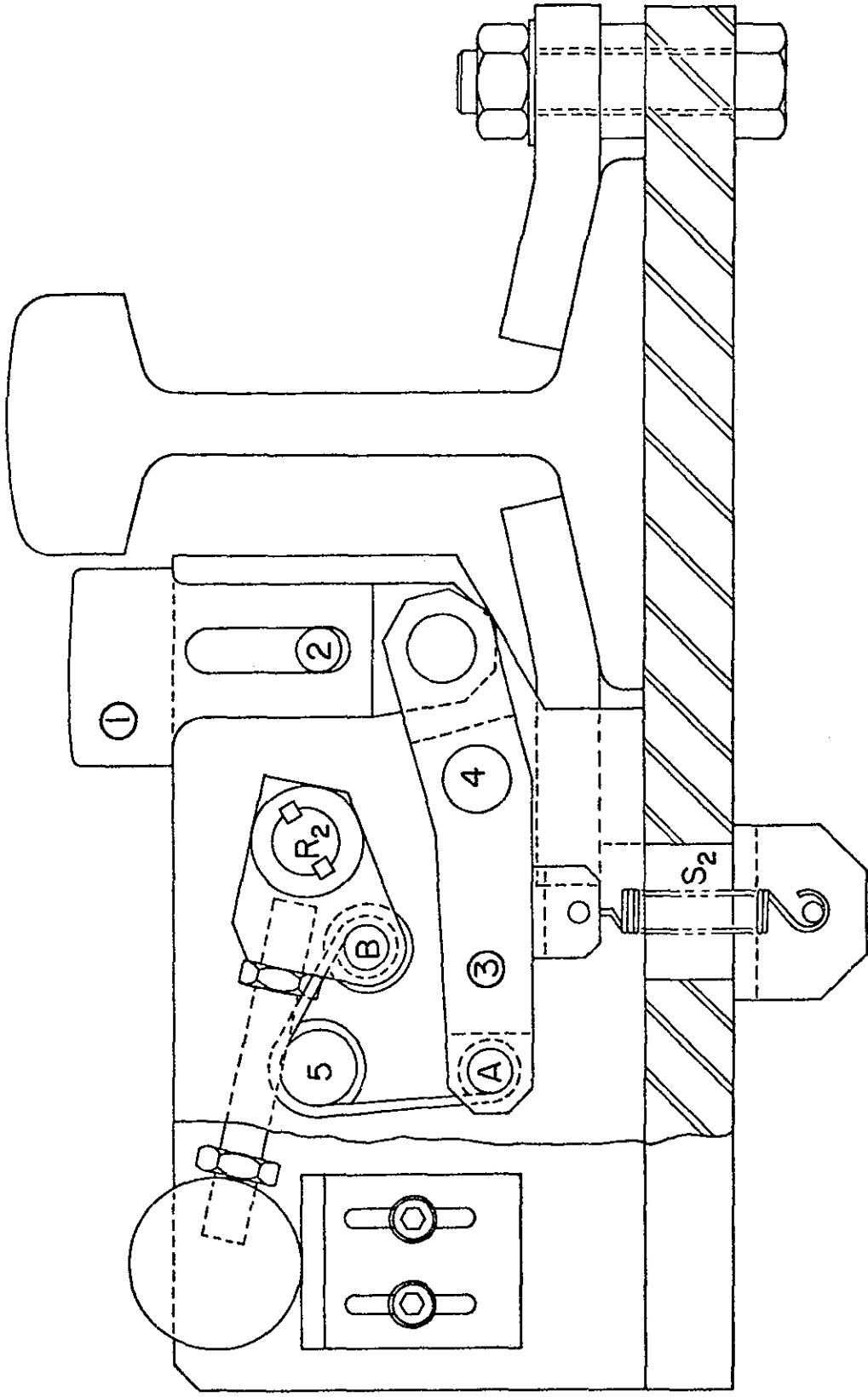
FIG. 1.6.1 DRAWING OF IMPACTER USED IN FIRST TEST
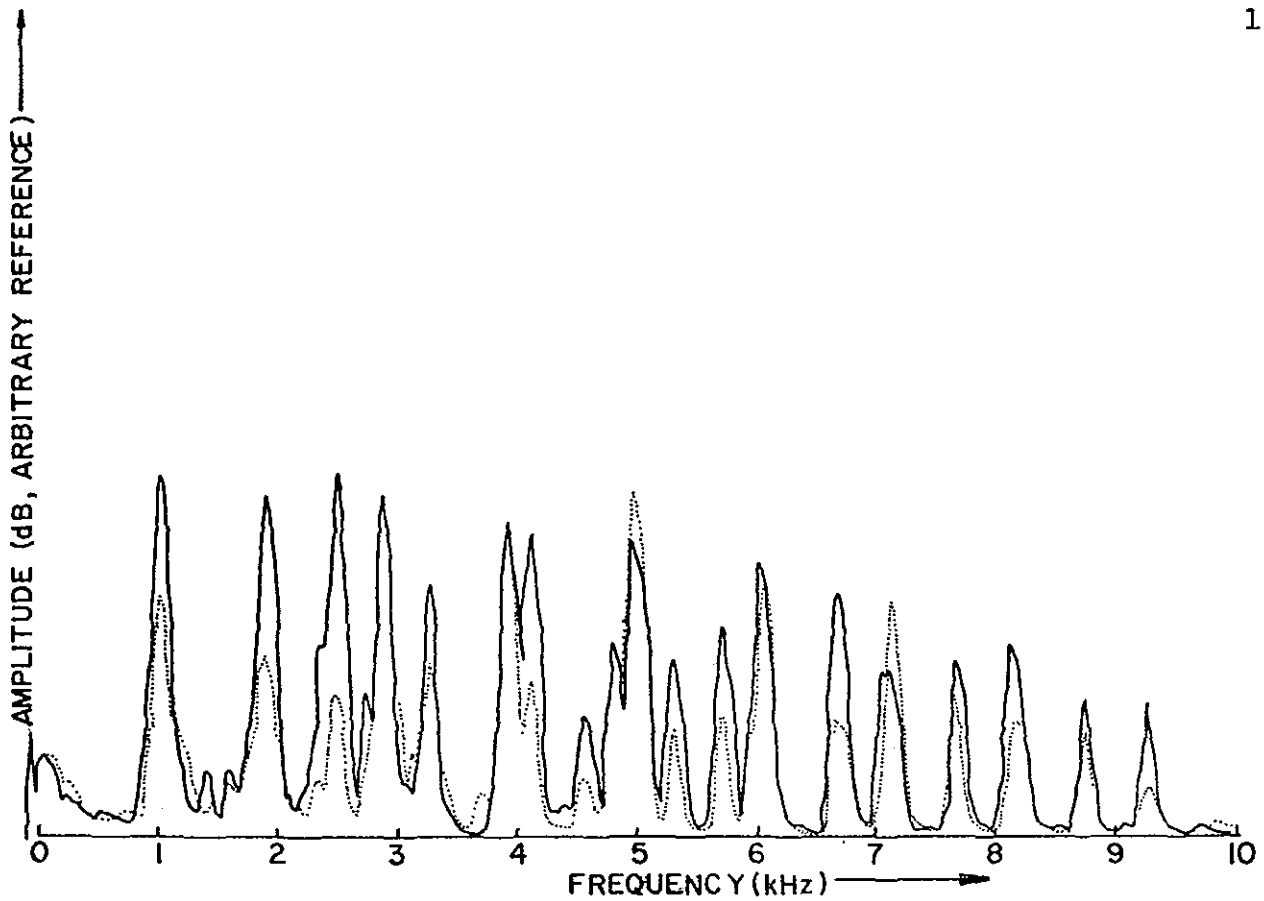
FIGURE 1.6.2   FIXED BAND SPECTRA OF IMPACT ON GOOD 33"
WHEELS ON EITHER END OF THE SAME AXLE

————GRIFFIN 9 RISER
·········ARMCO WROUGHT
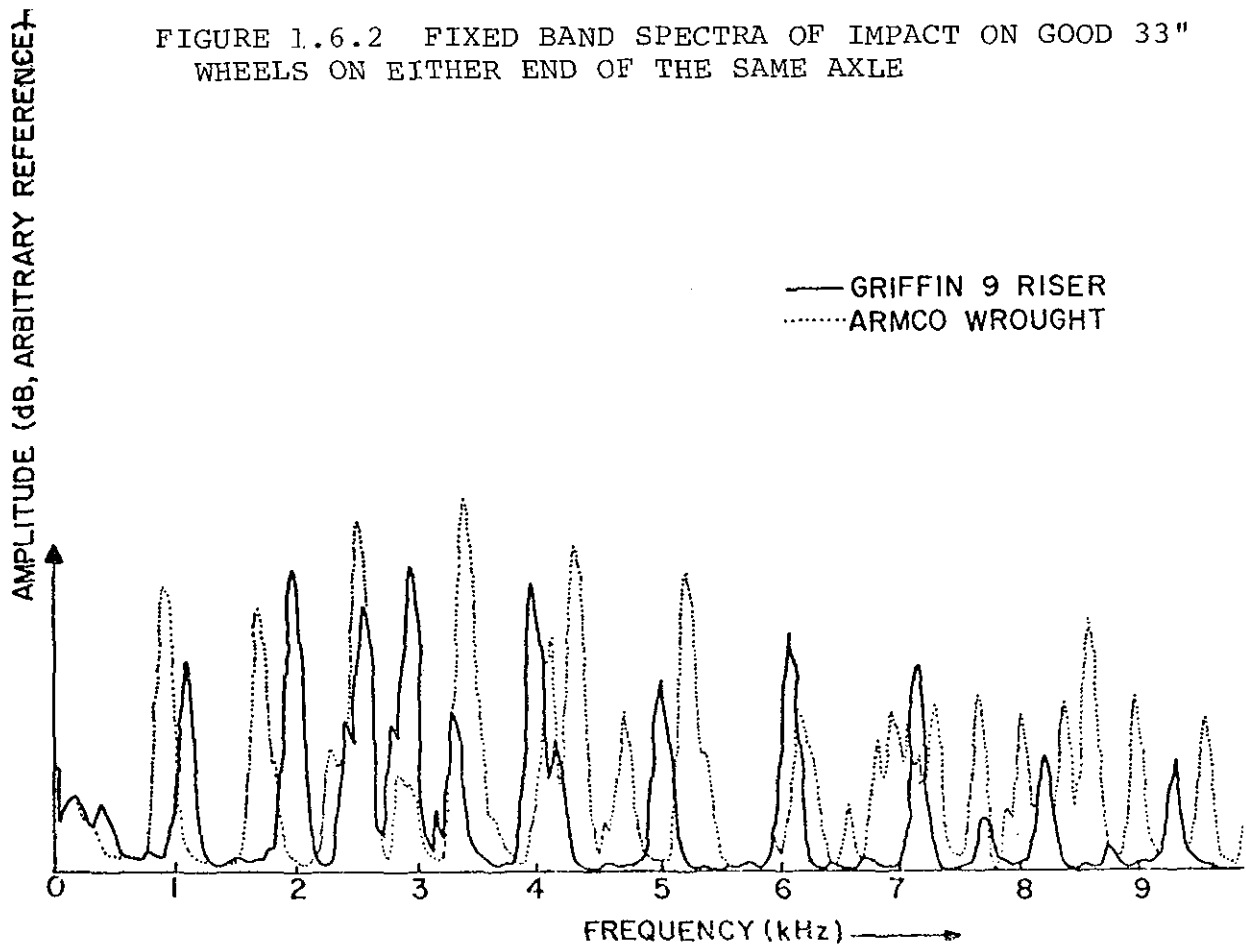
FIGURE 1.6.3   FIXED BAND SPECTRA OF IMPACT ON TWO GOOD 33"
WHEELS ONE A GRIFFIN 9 RISER, ONE AN ARMCO WROUGHT

found between the spectra displayed in Fig. 1.6.4. These
were obtained from two Southern 33" wheels on the same
axle. One of them, however, has a thermal crack which has
propagated clear through to the hub. Finally, Fig. 1.6.5
shows the comparison of the spectra of two identical good wheels
(33" Southern), one of which has a heavy layer of grease.
The most interesting aspect of the spectrum of the greasy
wheel is the complete absence of sound above about 4 kHz.
This was presumably due to damping of the plate vibrations.
This feature, i.e., the damping of high frequency resonances,
could be used as a means of identifying the spectra of greasy
wheels, which might otherwise be mistaken for cracked
wheels and give rise to a false alarm.

Also as a part of the feasibility study some labora-
tory experiments were performed with wheel pairs in a
stationary load frame using a hydraulic jacking system to
simulate loads up to 20 tons. Figure 1.6.6 shows a series
of spectral analyses, each with increasing load. The
traces are superimposed on one another but slightly offset
to give a three dimensional perspective. Some resonances
are enchanced by the load; some are diminished. Most shift
slightly in frequency and some split into two separate
resonance peaks. On the other hand, if one does not use
too fine discrimination, it is clear that the changes do
not produce complete disorder in the three-dimensional plot.

1.7 Laboratory Demonstration System for Finding Cracks

As the last part of the feasibility study a laboratory
demonstration system was assembled to simulate field opera-
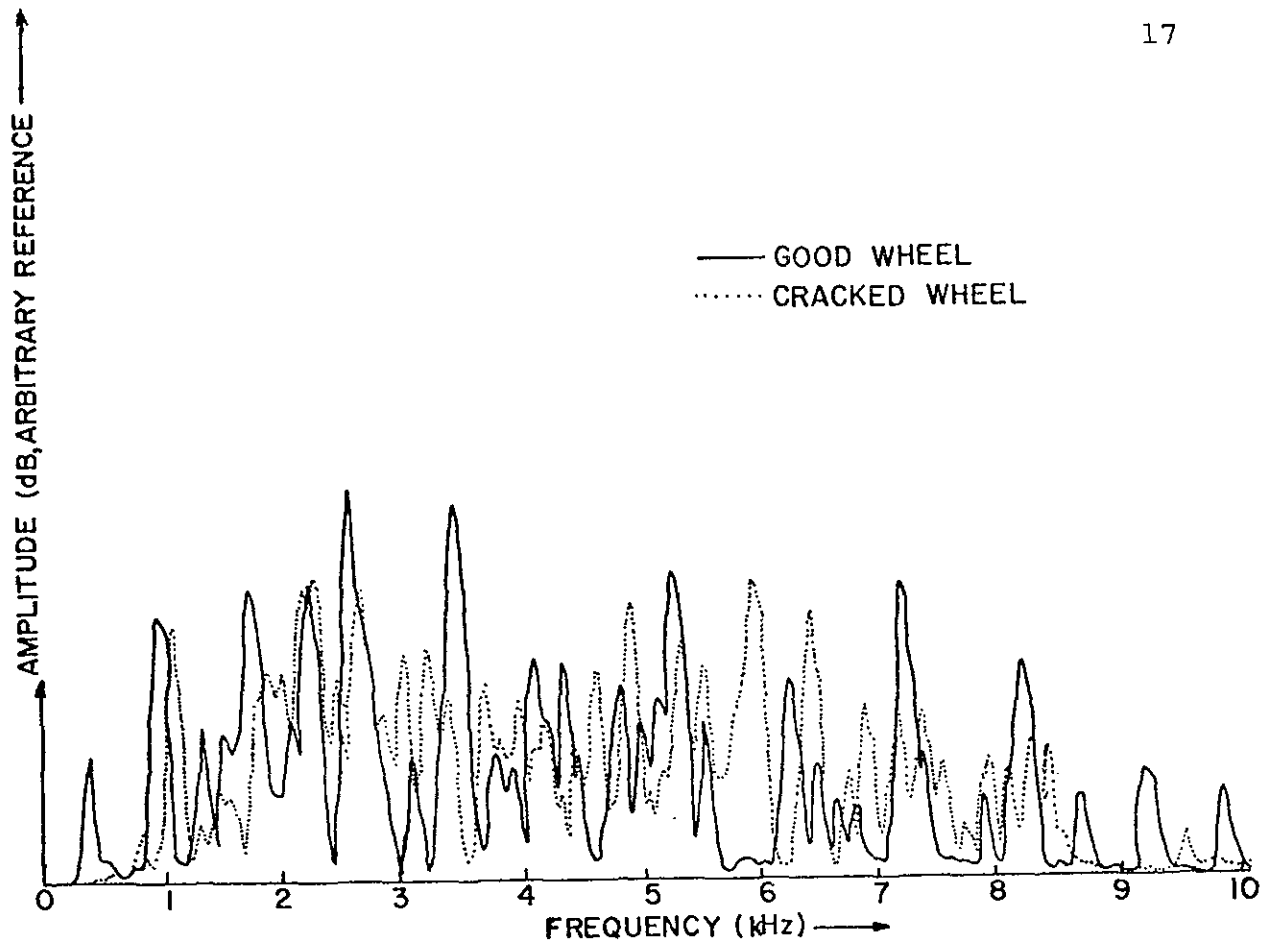
FIGURE 1.6.4   FIXED BAND SPECTRA OF IMPACT ON 33" SOUTHERN
WHEELS, ONE WITH A LARGE THERMAL CRACK
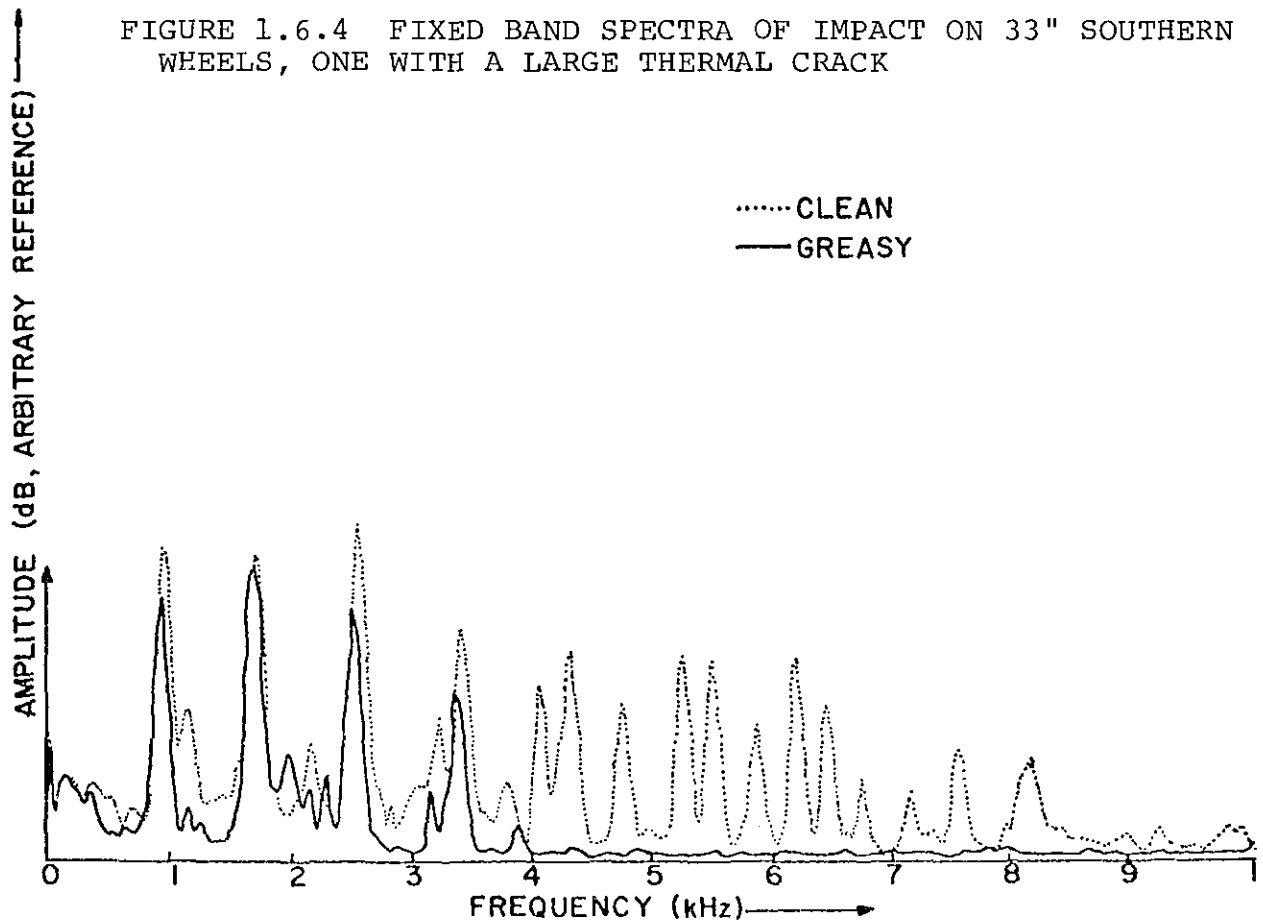
FIGURE 1.6.5   FIXED BAND SPECTRA OF IMPACT ON TWO 33" SOUTHE[
WHEELS, ONE WITH A THICK LAYER OF GREESE
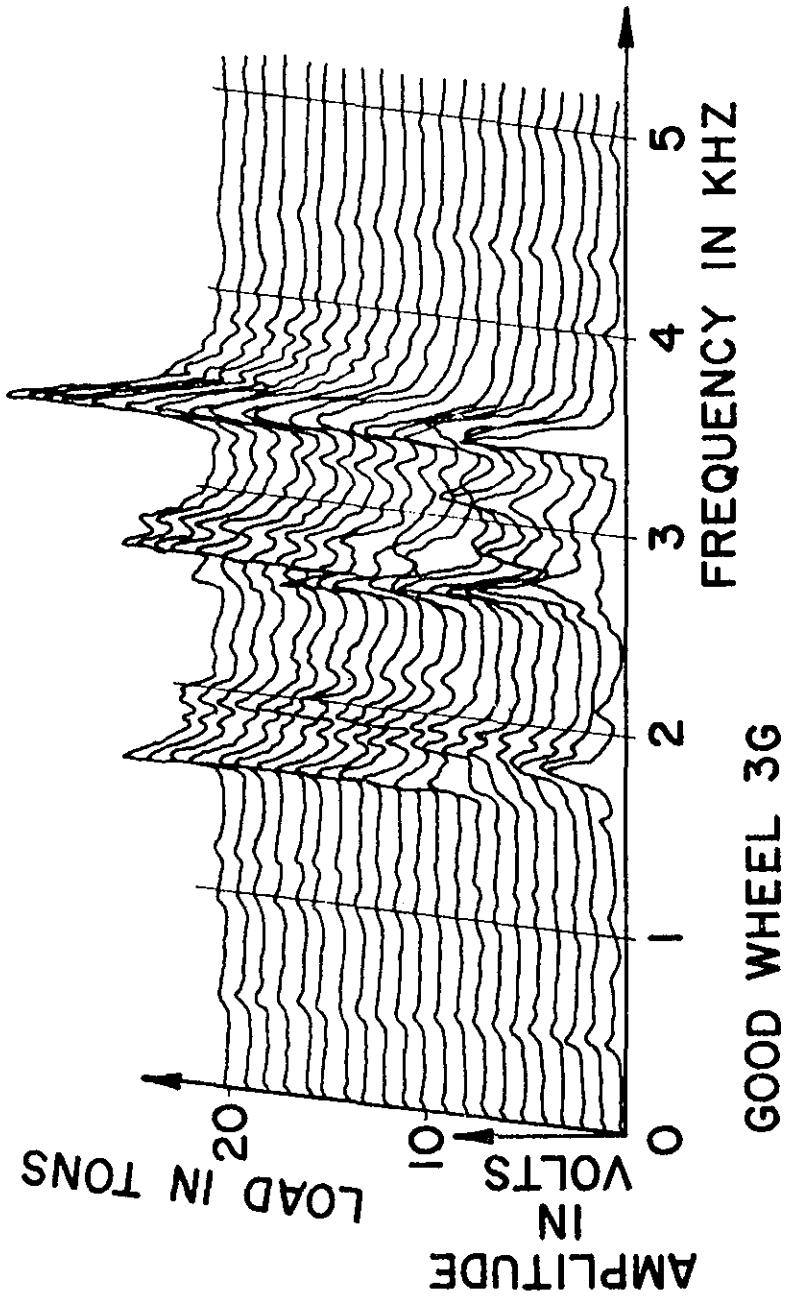
FIG. I.6.6 VARIATION OF WHEEL SIGNATURE WITH
LOAD FOR WHEEL 3G. (ACCELEROMETER PICKUP)

tions as far as possible. For this phase of the work only the third octave band analyzer was available. This was interfaced with the NOVA minicomputer. The minicomputer was programmed to read a given spectrum, generated by impact of a hammer or pendulum, and to compare this spectrum with either: 1) a standard spectrum, i.e., the average spectrum of good wheels, continuously averaged on a weighted basis, or 2) the spectrum of the mating wheel on the same axle. The output of the program was a number which is the sum of the squares of the differences in dB between the two spectra in the various third octave bands.

In Table 1.7.1 are tabulated values that were calculated in this way for a set of wheel signatures obtained from impact tests. Of all the wheels that were tested there was one wheel where the performance of the classifier was questionable. Wheel 8G did not have any apparent cracks, but it was worn beyond serviceable limits.

1.8 Preliminary Field Tests

Subsequent to the feasibility study, two preliminary field tests of the impacting system for crack detection were carried out. The first test was performed at the Omaha East Yard of the Union Pacific. Only one impacter was available so that across axle comparison was not possible. No timing pulse was provided for and the hammer arm broke at a train speed of about 17 mph. The second test, performed at the Southern Pacific's Englewood Yard in Houston, was more successful and will be briefly described. Because of the variations in signature due to wheel geometry,

TABLE 1.7.1   SUMS OF DIFFERENCES OF WHEEL SPECTRA FROM AVERAGE
GOOD WHEEL SPECTRUM (IMPACT EXCITATION)

NOTE: a) Good wheel average based on all good wheels,

b) Summing of differences in dB for 1/3 octave bands
with center frequencies of 1.6 KHz to 8 KHz,

c) All spectra for this table were obtained by tapping
on the rim of the wheels with a steel bar.

WHEELS	ACTUAL CONDITION	CONDITION INDICATED BY CLASSIFIER WITH DISCRIMINATION LEVEL=70	DIFFERENCE FROM AVERAGE SIGNATURE	DIFFERENCE BETWEEN SIGNATURES OF WHEELS ON SAME AXLE
1G	Good	Good	27	157
1B	Flawed	Flawed	184	
3G	Good	Good	35	49
3B	Flawed	Flawed	84	
4G	Good	Good	41	82
4B	Flawed	Flawed	123	
8G *Mispick	Good Badly Worn	Flawed	128	7
8B	Flawed	Flawed	121	
7A	Good	Good	42	4
7C	Good	Good	38	
9A	Good	Good	51	100
9C	Flawed	Flawed	151	
10A	Good	Good	63	4
10C	Good	Good	67	
11A	Good	Good	28	26
11C	Good	Good	54	

load, grease etc., the basis of this test was a comparison of spectra from wheels at either end of axle. Figure 1.8.1 shows the train consist in the test. Identical impacters were installed on the two rails, one train length apart. There were two defective wheels. Wheel N15 had a larger thermal crack and wheel S12, a shattered rim. The train was run forward and backward in successive runs and the sound tape recorded for laboratory processing.

Figure 1.8.2 shows typical printout using cross axle comparison with third octave band analysis. Car 5 is the engine. The numbers in the column labelled "Across Axle Comparison" are the sums of the algebraic differences in third octave band spectra of the two wheels. The decision that a wheel is bad is based upon this number exceeding 10.

1.9 Objectives of the Present Study

It was concluded from the feasibility study that it should be possible to use acoustic signature inspection for detection of thermal and plate cracks in railroad wheels. It appeared that the best form of excitation for detecting cracks is by impact and that the best sensor is a microphone. The cracks cause shifts in resonance frequencies and these shifts can be observed best in narrow band analysis but are also manifest in third octave band analysis. Grease layers cause damping of resonance lines above about 5 kHz. Recognition of defective wheels can be carried out by comparing sound spectra with a standard or by comparing the sound spectra of wheels on either end of an axle.

CAR	AXLE	AVERAGE SPECTRUM COMPARISON		ACROSS AXLE COMP.	DECISION
		FIRST SIDE	SECOND SIDE		
1	1	34	24	8	GOOD
1	2	11	20	11	BAD
1	3	6	8	4	GOOD
1	4	9	6	3	GOOD
2	1	6	4	12	BAD
2	2	10	2	7	GOOD
2	3	8	1	4	GOOD
2	4	8	1	2	GOOD
3	1	1	0	1	GOOD
3	2	0	3	3	GOOD
3	3	1	1	1	GOOD
3	4	2	2	0	GOOD
4	1	3	1	7	GOOD
4	2	3	0	6	GOOD
4	3	1	0	2	GOOD
4	4	2	0	4	GOOD
5	1	2	0	1	GOOD
5	2	2	15	10	GOOD
5	3	1	3	1	GOOD
5	4	13	5	3	GOOD

FIG. 1.8.2   COMPUTER OUTPUT FOR AN EASTBOUND RUN AT 6 MPH. RELIABILITY WAS 100%. ENGINE IS CAR 5. DECISION LIMIT IS 11.

FIG. 1.8.1   TRAIN CONSIST FOR SECOND TEST

It was with this background that the present project was formulated. The overall objective was to obtain information on the parameters that might affect or limit the performance of an acoustic signature inspection in actual operation, as opposed to laboratory operation or operation in controlled field tests. To achieve this end the program was divided into three parts: first, to improve and expand scientific knowledge of the wheel's acoustic signatures; second, to improve the design of various system components; third, to test the improved system for an extended period under actual operating conditions.

Regarding the first part of the program, improvement of scientific knowledge, both experimental and theoretical studies were planned. The intention was to obtain a better grasp of the effect on signatures of wheel geometry, wheel wear, the wheel's internal state of stress, and various environmental conditions. Some of these studies were carried out at the DOT's Transportation Test Center at Pueblo, Colorado, some at the Griffin Wheel Company's plant at Bessemer, Alabama, and some at the Westinghouse plant at Wilmerding, Pennsylvania. It was decided to extend the theory of wheel vibrations to gain additional insight into the effects of a) variations in wheel geometry, b) variations in crack sizes and locations, c) various forcing functions and d) variation in internal stress.

Under the second part of the program, improvements in system component design, there were several major

developments. Firstly, the design of the excitation
mechanism was subjected to some scrutiny, with a view to
improving its reliability and operating speed range. The
second major change was the acquisition of a narrow band
RTA, its interfacing with the existing NOVA computer and
the addition and interfacing of a diskette memory unit.
Finally, reliable commercially made microphones and wheel
sensors were acquired.

The final system test, the third part of the program,
was carried out at the Southern Pacific's Englewood Yard
in Houston. The objectives of this test were to elucidate
remaining problems with the system and to ascertain, if
possible, information on false alarm rates.

The study was concluded with a sensitivity analysis
of the data recorded during the field tests. System problems
were elucidated, an optimum form of the difference index
(DI) equation was ascertained and the major cause of high
DI values in uncracked wheels was determined.

2. THEORY OF RAILROAD WHEEL VIBRATIONS

2.1 Introduction

A brief summary of previous work on wheel vibrations was presented in Section 1. In these earlier studies a number of elementary models were considered and commercially available computer programs were used to simulate the vibrations of good and defective wheels. The cross section of a typical railroad wheel is shown in Figure 2.1.1. Ring or circular plate models are the simplest approximations that can be used. In the feasibility study of flaw detection in wheels using acoustic signatures, Nagy modeled the one-fourth scale model wheels and later full size wheels as flat annular plates. He also reviewed the literature on these subjects and concluded that the ring model gave a better fit to wheel data. The most accurate theoretical approach is to analyze the actual wheel geometry using finite element analysis. Nagy used the ANSYS program to study the vibrations of a good 33-inch wheel and compared those with the response of a defective wheel having a plate crack. His work was extended later by Chaudhari who studied the vibrations of wheels with different types and sizes of cracks, applying single or repetitive impulse excitation. Chaudhari's work improved on Nagy's by using more elements and more realistic boundary conditions. (The wheels were fixed at the hub and

WHERE: a= 16.5"
       b= 4.12"
       r= 15.92"
       w= 5.75"
       h= 1.2"
       H= 1.2"
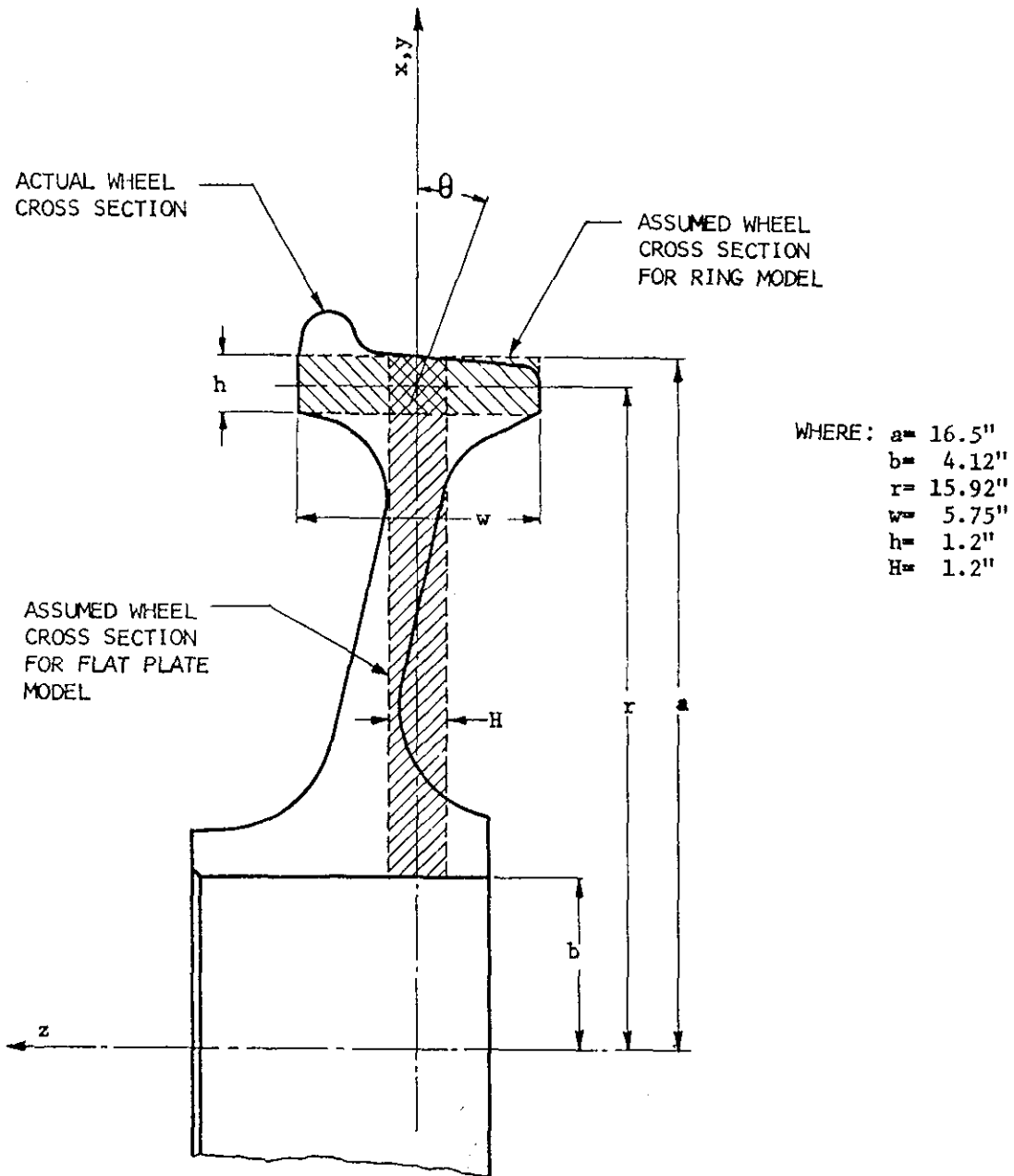
Fig. 2.1.1 Assumed and Actual Wheel Cross Sections

in addition at one node on the tread to simulate the con-
tact of the wheel with the rail.) An abbreviated version
of Chaudhari's work is presented in Appendix F.

Although the finite element approach is ultimately
the most accurate it is expensive and time consuming.
The more elementary models, especially Stappenbeck's [17]
ring theory, can be used to gain an insight into certain
effects, as explained in later sections, with comparative
ease.

2.2 Stappenbeck's Ring Model of Wheel Vibrations

Stappenbeck [17] showed that the well known theory
of the vibrations of rings could give a good explanation
of the sounds emitted by a vibrating railroad wheel. To
see why this is so it is appropriate to review his reason-
ing. The vibration of rings was first treated in 1890
by Mitchell [52], as an extension of the theory of bars,
by regarding the ring as a curved bar whose two ends are
joined together. Flexural modes of vibration, with
displacements either in the plane of the ring or out of
the plane, are the most readily excited.

For out-of-plane flexure the resonant frequencies
are given by:

$$f_n = \frac{1}{2\pi} \left[\frac{EI_x}{\rho Ar^4} \frac{n^2(n^2-1)^2}{(n^2+1+\nu)} \right]^{1/2} \quad \text{for } n = 1,2,3, \ldots \quad (2.2.1)$$

where

E = Young's modulus

A = the cross sectional area,

I_x = the moment of inertia of cross section with

    respect to an axis in the plane of the ring,

r = the radius of the ring,

ν = Poisson's ratio,

n = the ratio of the number of wavelengths to the

    circumference,

and ρ = the density of the ring.

It should be noted that the case for n = 1 yields a zero
resonant frequency. This is not a vibrational mode and the
motion consists of a free rotation about a diameter. The
lowest vibrational mode occurs when n = 2, in which case
there are four nodal points on the ring.

Now consider the addition of a thin circular plate
within the ring. Again, in the case of a plate, the most
readily excited modes are flexural. Thus when the coupling
of ring and plate modes is considered, it may be seen that
the out-of-plane flexure of the ring will readily couple
with plate modes having an integral number of nodal dia-
meters. Because the wheel rim is massive in comparison
to the plate this was the model Stappenback proposed for
the vibrations of the wheel and he demonstrated that the
sound radiated from 765 mm diameter streetcar wheels con-
tained a series of prominent resonances whose frequency
ratios corresponded closely to values obtained from
eqn (2.2.1). (Assuming the fundamental mode occurs
when n = 2, the ratios of the frequencies of the higher
order modes to the fundamental are 2.87, 5.53, 8.98,

13.2, ... for n = 3, 4, 5, 6, ... respectively). With

this viewpoint in mind the massive rim forces the plate

into vibration, and the plate is then the primary sound

source because of its larger radiating surface. An alter-

native model, in which the plate forces the rim into vibration,

was investigated by Nagy [1]. The ratios of the prominent

resonance frequencies did not fit the experimental results.

The conclusion is then that the prominent resonances

in the acoustic spectrum are due to wheel modes with two,

three, four or more nodal diameters. This does not imply

that other modes of vibration cannot be excited. Indeed

the author has been able to excite the wheel in a vibratory

mode with a single nodal diameter. (The hub of the wheel

provides a stiffness for this mode which would not exist

for an unconstrained plate.) Such a mode is also revealed

by the finite element analysis. Numerical results for such

experiments are shown in Table 2.2.1. The two columns

showing the experimental results are for two different

types of 33-inch wheel. The left-hand column corresponds

to a wheel having the same cross-section as in Fig. 2.1.1,

and the right-hand column corresponds to a 33-inch Griffin

wheel having cross section as in Fig. 4.2.1. Three

variations of calculations using the ring model are

given. In column A the results are those given by Nagy.

An attempt to improve these results was made by modeling

the wheel as a ring with cross section identical to the

TABLE 2.2.1   LIST OF RESONANCES CALCULATED WITH

THE RING MODEL COMPARED WITH ANSYS

RESULTS AND EXPERIMENTAL DATA

Modes with Ring Model (Flexural Modes Perpendicular to Plane of Ring)					Experimental Resonances for 33" Wheel		ANSYS
n	approx. shape	frequency in Hz			freq. in Hz		freq. in Hz
		A	B	C			
1	┤	0	· 0	0	—	324	317
2	+	549	476	417	420	435	443
3	✳	1579	1365	1196	1093	1147	1087
4	✳	3049	2632	2308	1890	2018	1999
5	✳	4948	4271	3743	—	2990	—
6	✳	7272	6275	5501	—	4012	—

Note: Columns undermarked with an asterisk show results obtained by Nagy.
A, B, C are three assumed ring cross-sections, as shown in Fig. 2.2.1
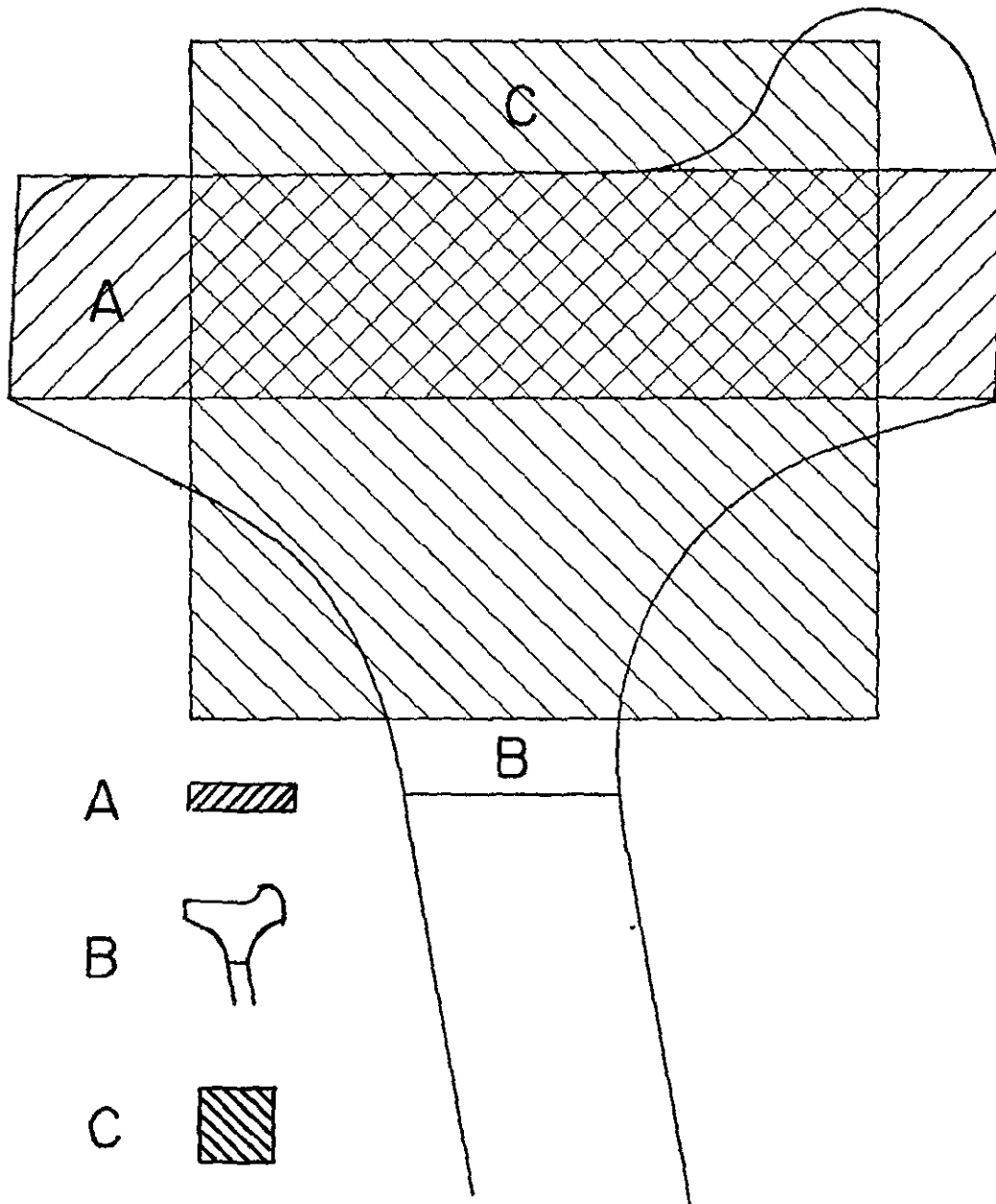
FIG. 2.2.1 CROSS SECTIONS FOR RING MODEL

rim. The radius of the ring was estimated after evaluating the centroid of the cross section by numerical-graphic integration. The area moment of inertia about the neutral axis was evaluated in a similar way. The results, shown in column B, are a much closer fit to experimental measurements than obtained from the rectangular cross section (see Fig. 2.2.1) model used by Nagy. Even better results are obtained using an "equivalent" square cross section. The optimum selection was a 4" x 4" cross section with corresponding radius of 15.1". The mode evaluation based on this model shows almost identical frequencies for the two nodal diameter mode and reasonable correspondence with experiment for the other nodal diameter modes. Comparison with the results from the ANSYS program also shows good agreement. The major point to be made is that Stappenbeck's ring model is a surprisingly good predictor of the prominent resonances of the acoustic spectrum of actual wheels.

2.3 The Effect of Uneven Wear on Wheels Across the Axle

A theoretical explanation of the effect of uneven wear can be given in terms of Stappenbeck's simple theory of wheel vibrations. The series of resonant frequencies is given by the expression (2.2.1). It is clear that uneven wear on a wheel pair will result in differences for I_x, A and r for the two wheels. Rewriting eqn. (2.2.1) to break out these factors, which are related to the wheel geometry, we have:

$$f_n = \frac{1}{2\pi} \left[\frac{E}{\rho}\right]^{1/2} \left[\frac{I_x}{Ar^4}\right]^{1/2} \left[\frac{n^2(n^2-1)^2}{n^2+1+\nu}\right]^{1/2}$$

or

$$f_n = B \left[\frac{I_x}{Ar^4}\right]^{1/2} \left[\frac{n^2(n^2-1)^2}{n^2+1+\nu}\right]^{1/2}$$

where B is a constant dependent on the material properties

of the wheel. We shall assume that these properties are

unaffected by wear. Assuming that the rim can be modelled

as a ring of rectangular cross section (see Fig. 2.2.1),

with width w and thickness h,

$$A = hw$$

and

$$I_x = \frac{hw^3}{12}$$

Hence,

$$f_n = \frac{B}{\sqrt{12}} \frac{w}{r^2} \left[\frac{n^2(n^2-1)^2}{n^2+1+\nu}\right]^{1/2} \qquad (2.3.1)$$

The effect of wear will be to reduce the effective radius

r, but not the rim width w. Hence the change in frequency

of the nth mode will be:

$$|\Delta f_n| = \frac{2B}{\sqrt{12}} \left[\frac{n^2(n^2-1)^2}{n^2+1+\nu}\right]^{1/2} \frac{w\Delta r}{r^3}$$

$$= (2\frac{\Delta r}{r}) f_n$$

Finally, since a change in the effective radius is

approximately one half of a change in rim thickness, Δh,

for small changes,

$$|\Delta f_n| = \left|\frac{\Delta h}{r}\right| f_n \qquad (2.3.2)$$

Thus, for a given wheelset, a difference in wear on the two wheels, in the amount Δh, should result in frequency shifts proportional to the resonant frequencies. Experimental results which are in agreement with this finding, to a first approximation, are given in Section 7.

2.4 The Effect of Residual Stress*

The current interest in residual stress and its influence on the creation and propagation of cracks in wheels can be seen from the number of recent papers on this topic. Bray [18] cited 15 papers related to the subject at the 5th International Wheelset Conference in 1976. Wetenkamp and Kipp [19] and Yavelak and Scott [53] have also given papers on this subject recently.

The most general treatment of the dynamics of elastic media under intial stress was given by Biot [20, 21] who concluded that the presence of an initial stress tends to modify the effective rigidity of the medium. In general, tension tends to increase the rigidity, whereas compression tends to decrease it. The result is a corresponding increase or decrease in the frequency of the natural modes of a finite body. There are a number of well known examples of such effects, the vibrations of strings under tension and rods under load being among the best known.

---

*The definition of residual stress in this context refers to the system of stresses which can exist in a body when it is free from external forces, temperature gradients and rotational motion. In the case of a wheel these stresses are located in manufacture and may be modified in service.

There have also been a number of recent papers on the effect of in-plane forces on the vibration of plates [22-27]. For present purposes it is of considerable interest to realize that the well known effect of axial load on the natural modes of a bar can be applied to the problem of measuring wheel stresses. Following Stappenbeck's model, a compressive or tensile stress in the wheel rim should have an effect similar to that found in a loaded bar.

For a simply supported vibrating beam under compression the natural frequencies of flexural vibrations are given [50] by:

$$\omega_n^2 = \frac{EI\, n^4\pi^4 - F\ell^2 n^2\pi^2}{\rho A\ell^4} \quad , \tag{2.4.1}$$

where

ℓ = the length of the beam,

F = the compressive axial force,

A = the cross sectional area,

ρ = the density,

EI = the flexural rigidity,

but the frequency of the nth mode of the beam without external

stress is
$$\omega_{n_0}^2 = \frac{EI\, n^4\pi^4}{\rho A\ell^4} \quad . \tag{2.4.2}$$

Then
$$\omega_{n_0}^2 - \omega_n^2 = \frac{F n^2\pi^2}{\rho A\ell^2} \quad ,$$

For small frequency changes

$$\omega_{n_o} + \omega_n \simeq 2 \omega_{n_o} \, .$$

Thus

$$(\omega_{n_o} - \omega_n) \, 2\omega_{n_o} = \frac{F n^2 \pi^2}{\rho A \ell^2} \, ,$$

or

$$\Delta\omega_n = \frac{F}{2\{EI\rho A\}^{1/2}} \, . \qquad (2.4.3)$$

This result implies that the frequency shifts are the

same for all modes and are proportional to the applied

force. Since the ring model simply assumes that the rim

is a circular bar, flexural vibrations of wheels with uniform

compressive or tensile residual stresses in the rim should

show similar effects; i.e., if a uniform stress is induced in the

rim, all modes should show the same numerical change in

resonant frequency. Some experimental results which appear

to be consistent with this concept are presented in

Section 4.

3.   EXPERIMENTS ON WHEEL GEOMETRY

AND MINIMUM DETECTABLE CRACK SIZE

3.1   Introduction

There were certain questions which could not be readily answered from the theoretical study and it was decided to tackle these by obtaining experimental data.   There were two main tasks in this work: firstly, the compilation of a data bank of signatures of wheels with different geometries and from various manufacturers, and secondly, a study of the minimum detectable crack size.

3.2   Data Bank of Wheel Types

In brief, the idea behind this study was that the acoustic signatures of all types of good wheels and the signatures of all types of defective wheels might belong in two different clusters and there might be no over-lapping in their characteristics.   If this were the case a decision scheme for flaw detection could be based on the comparison of the signature of the wheel under test with a set of good wheel signatures.   If the signature matched any of the good wheel signatures it would be declared a good wheel of a certain type, and if not, defective.   A computer or other type of file that has the signatures of all geometrical variations of good wheels would house the data bank.

In order to develop the data bank, the Southern
Pacific Transportation Company provided a number of new
and used wheels for testing in their Houston repair shop
facilities. A total of 34 wheels were tested and 136
wheel signatures were obtained. The sample included
wheels of cast and wrought construction, having flat
and dished plate configurations. Single wear and multiple
wear rims were also encountered. The information acquired
was kept in a data bank book, in the form of a series of
description sheets as shown in Fig. 3.2.1a, accompanied
by the signature plots, one of which is shown in Fig.
3.2.1b. For these tests an inclined guideway was
constructed (see Fig. 3.2.2) and was used as a path
guide for a 1.5 inch steel ball. Near the bottom end
of the incline a photosensor unit was installed to detect
the presence of the ball immediately before the impact.
The photosensor's signal was recorded on the triggering
pulse channel of a dual channel GR* recorder for later
acoustic signature analysis in the laboratory. The
design assured reproducible and constant force impact on
the lower inner rim of the wheel. Acoustic signature
tests were conducted on the wheels listed in Table 3.2.1.

3.3 Results from Data Bank Tests

About ten different types of wheels were tested
in the SP shops. Another 14 axles having good/good and

---

*General Radio

Peak, Other
No. of Averages _____
Input ATT, dB __20__
Tape No. __101__

Exciter: M, PV, B, R; _____
Frequency Range; _10KHz_
Y = LIN/LOG
Y Range, dB/dB

Wheel Ref.: _1-1_
Wheel Condition
  G, Gr, R N V
Train ID: _____

FREQUENCY
dB
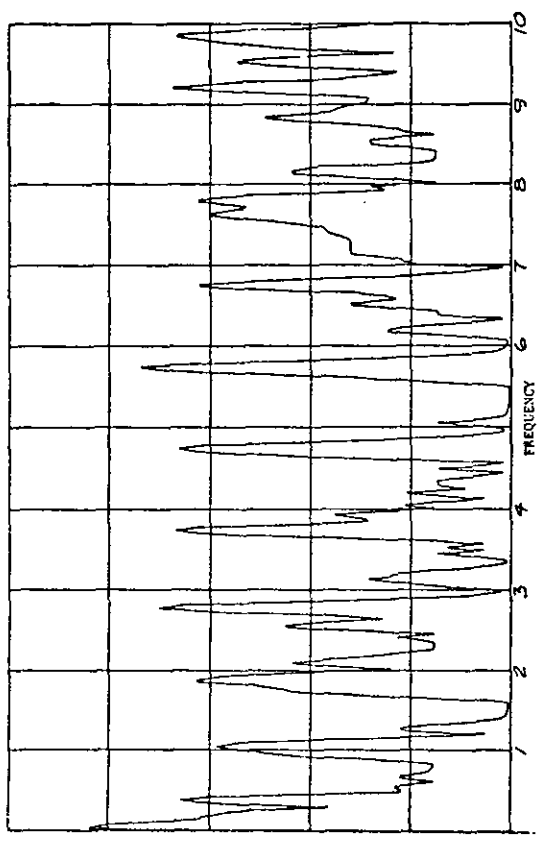
UH ME DEPT.
DATE: 6/20/76 BY: D.P.

FIG. 3.2.1b   ACOUSTIC SIGNATURE PLOT FORM

WHEEL DESCRIPTION

WHEEL ID: _J-10-76   CJ5724 @ CJ73_

MANUFACTURER: _SOUTHERN_

DIAMETER: 28   30   33   36   40

CAST √ WROUGHT __ PLATE: DISHED __ FLAT √ WEAR: 1W √ MW __

CONDITION: GOOD __ BAD __ GREASY __ RUSTY __ NEW √ USED __

DEFECTS: SLID FLAT __ THERMAL CRACK __ CRACKED PLATE __
         OVERHEATED __ OTHER __

TEST INFORMATION

LOCATION: UH   SPR   OTHER

TRAIN ID: _____

RECORDER TYPE: GR   N   9   TAPE SPEED: 7 1/2   3 3/4

BACKGROUND LEVEL: _62_ PEAK SPL: _96_ ATTENUATION: 70   80   90   100

IMPACTOR TYPE: MECHANICAL __ PNEUMATIC __ ROTARY __
         ROLLING BALL BEARING √ 1/2 √ FULL √ ANGLE _20_

LOCATION ON THE TRACK: N   B   D   W   L   R

ROLLING WHEEL DIRECTION: N   S   E   W   STATIONARY √

AXLE SPEED: _____

NOTES & COMMENTS

UH NUMBER: _____
UH CODE: _____
TAPE NUMBER: _102_
EVENTS RECORDED: _1,2,3,4_
DATE TESTED: _15 June 76_

UH ME DEPT.
DATE: _18 June 76_
BY: W. Peters

FIG. 3.2.1a   WHEEL INFORMATION AND
              TEST DESCRIPTION FORM

FIG. 3.2.2 ROLLING BALL APPARATUS

Table 3.2.1

INVENTORY OF WHEELS TESTED AT SOUTHERN PACIFIC ENGLEWOOD YARD

18 June 1976

AXLE NO.	EAST WHEEL IDENTIFICATION	WEST WHEEL IDENTIFICATION	DESIGN	TAPE NO. AND EVENTS RECORDED
1.	3/10/76 C532340 SOUTHERN	3/10/76 C532311 SOUTHERN	33" NEW, CAST FLAT, IW	102: 1, 2, 3, 4 (E) / 5, 6, 7, 8 (W)
2.	3/76 GL 87022 CJ33 GRIFFIN	3/76 GL 87183 CJ33 GRIFFIN	33" NEW, CAST DISHED, IW	102: 9, 10, 11, 12 (W) / 13, 14, 15, 16 (E)
3.	3/76 GL 67249 CJ33 GRIFFIN	3/76 GL 87204 CJ33 GRIFFIN	33" NEW, CAST DISHED, IW	102: 17, 18, 19, 20 (E) / 21, 22, 23, 24 (W)
4.	5/66 GL 91686 CS-2 GRIFFIN	5/66 GL 91690 CS-2 GRIFFIN	33" USED, CAST, DISHED, MW	102: 25, 26, 27, 28 (W) / 29, 30, 31, 32 (E)
5.	10/70 GL 17646 CM33 GRIFFIN	10/70 GL 17522 CM-33 GRIFFIN	33" USED, CAST, DISHED, MW	102: 33, 34, 35, 36 (W) / 37, 38, 39, 40 (E)
6.	3/15/76 C995514 CH-36B, SOUTHERN	3/15/76, C995524 CH-36B, SOUTHERN	36" NEW, CAST, FLAT, IW	102: 41, 42, 43, 44 (E) / 45, 46, 47, 48 (W)
7.	3/15/76, C995745 CH-36B, SOUTHERN	3/15/76, C995518 CH-36B, SOUTHERN	36" NEW, CAST FLAT, IW	102: 49, 50, 51, 52 (W) / 53, 54, 55, 56 (E)
8.	10/68, GB02936 CCH-36, GRIFFIN	10/68, GB02939 CCH-36, GRIFFIN	36" USED, CAST DISHED, IW	102: 57, 58, 59, 60 (E) / 61, 62, 63, 64 (W)
9.	10/74 ±S ±15217 H36 STANDARD	9/74 ±S ±7750 H36 STANDARD	36" USED, WROUGHT FLAT, IW	102: 65, 66, 67, 68 (W) / 69, 70, 71, 72 (E)
10.	3/73 ±S ±8952 H-36 STANDARD	3/73 ±S ±9482 H-36 STANDARD	36" USED, WROUGHT FLAT, IW	102: 73, 74, 75, 76 (E) / 103: 1, 2, 3, 4 (W)

General Radio Recorder set at 7½ tape speed.
Attenuation on all recordings, 90 dB.
Impactor: Rolling Ball device set at 30°, first two events at full height; second two events at ½ height.

TABLE 3.2.1 (Cont'd)

AXLE NO.	EAST WHEEL IDENTIFICATION	WEST WHEEL IDENTIFICATION	DESIGN	TAPE NO. AND EVENTS RECORDED
11.	4/74 C24094 J-36, USS	4/74 C24224 J-36, USS	36" USED, WROUGHT, FLAT, MW	103: 5, 6, 7, 8 (W) 9,10,11,12 (E)
12.	4/61 B8749647C027 BETHLEHEM	8/61 B10468650D003 BETHLEHEM	33" USED, WROUGHT FLAT, MW	103: 13, 14, 15, 16 (W) 17, 18, 19, 20 (E)
13.	NONE –	NONE –	36" USED, WROUGHT FLAT, MW, VERY HEAVY RIM	103: 21, 22, 23, 24 (W) 25, 26, 27, 28 (E)
14.	10/66 G75969 73M705, USS	10/66 G75758 G1M498, USS	36" USED, WROUGHT FLAT, IW	103: 29, 30, 31, 32 (E) 33, 34, 35, 36 (W)
15.	8/29/73 C607153 CH-36 SOUTHERN	8/27/73 C606076 CH-36 SOUTHERN	36" CAST, USED FLAT, IW	103: 37, 38, 39, 40 (W) 41, 42, 43, 44 (E)
16.	2/73 GY 45037 B CB28	2/73 GY 43344 B CB28	28" USED, CAST DISHED, IW	103: 45, 46, 47, 48 (E) 49, 50, 51, 52 (W)
17.	3/73 GY 44187 B CB28	2/73 GY 43019 B CB28	28" USED, CAST DISHED, IW	103: 53, 54, 55, 56 (E) 57, 58, 59, 60 (W)

good/defective wheels were tested in the University
laboratory (hammer impact testing). The conclusions
from these tests were as follows:

a. The relative amplitude of the wheel resonances
    depends on the magnitude of the impact.

b. The relative amplitude of the wheel resonances
    depends on the direction of the impact.

c. Each type of wheel has a characteristic signature.

d. Signature changes with wear. An axle with wheels
    whose flanges show different amounts of wear has
    spectral differences mostly above 4 kHz (see
    Fig. 3.3.1). The importance of this finding was
    not completely appreciated at the time of the earlier
    laboratory tests. After the field test it was
    realized that differential wear is a major cause of
    signature differences and further work on the
    subject was performed (see Section 7).

e. The signature of a used worn wheel compared to
    the signatures of standard new wheels may show
    spectral differences of the same order as a cracked
    wheel.

It was already known that load on wheels has some
effect on wheel signature, (see Fig. 1.6.6). Variations
with wear and load are enough to exclude the use of the
data bank as a classifier for the decision process in
field tests. Another important reason is the extremely
lengthy processing that would be necessary due to the
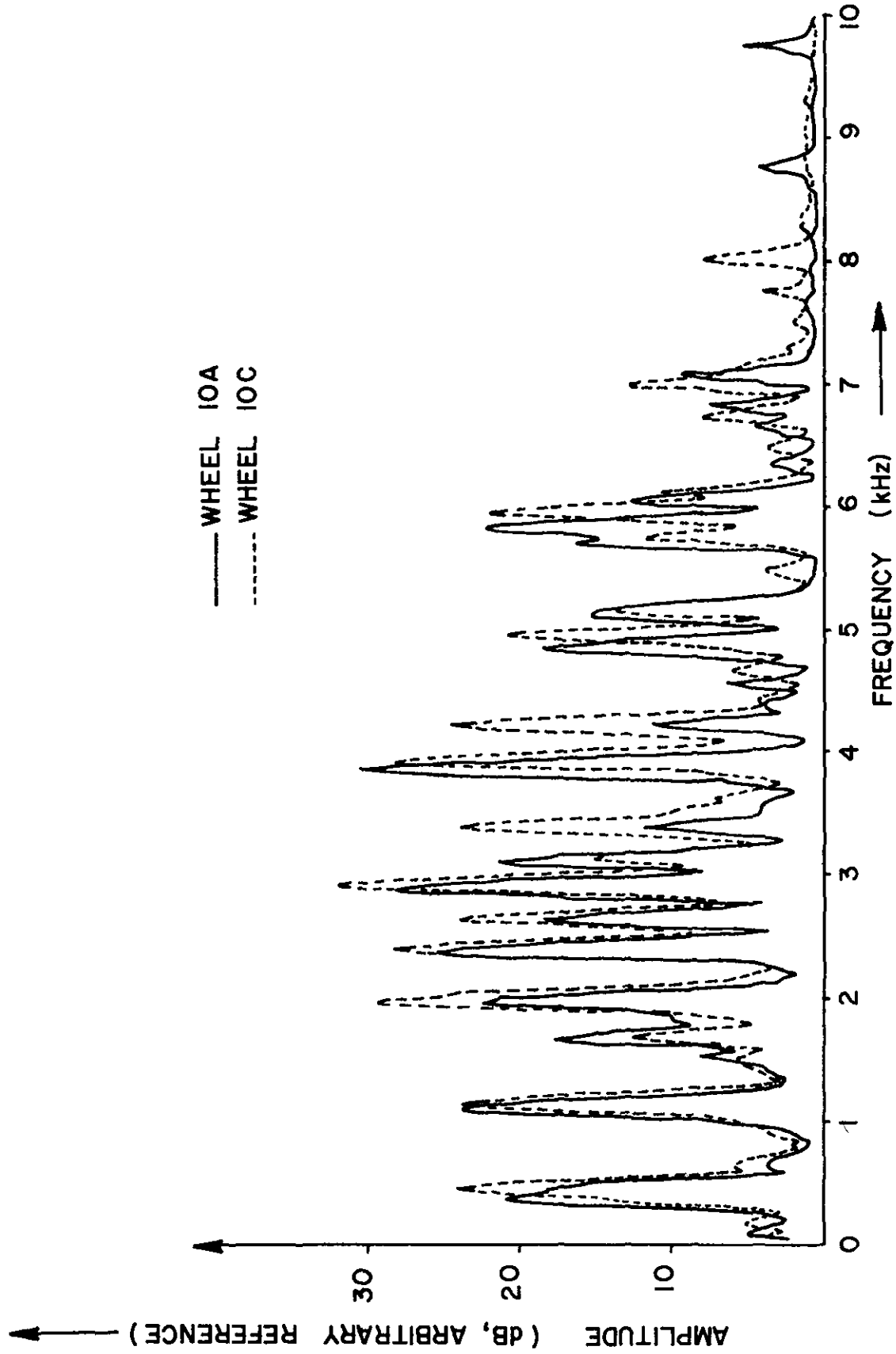
FIGURE 3.3.1 SIGNATURES OF IMPACT ON TWO WHEELS ON THE
SAME AXLE WITH UNEVENLY WORN FLANGES

large number of comparisons between the signature of an
unknown wheel type and the standard signatures. One
single comparison takes about 30 seconds, and there are
over 40 different types of wheel in use. It was concluded
that across the axle comparison is therefore the only
practical scheme.

3.4 Investigation of Minimum Detectable Crack Size

As mentioned earlier, one of the questions which
arose from the feasibility study was the issue of the
smallest crack that could be detected by signature analysis.
In Appendix F it is shown on a theoretical basis that a
single crack, not much larger than a dormant thermal
crack, will change the signature slightly. The doubt
remained however as to whether an experimental system
would be capable of finding such a slight change.
Consequently it was decided to perform some experiments
to address this issue. As discussed in section 4
the critical crack length is at least one tenth of an inch. The
key question is therefore whether or not the system can
detect the presence of cracks of critical size. This
leads to the difficulty that there is little agreement on
what this size is. In practice cracked wheels are
removed from service when they are found by visual
inspection and thus it was decided to investigate wheel
sets with the smallest cracks discovered in this way.

Firstly, it was decided to investigate the
chances of finding thermal cracks. Some experiments
were performed on a 36" wheel and axle set. One of these
wheels had eight thermal cracks visible on the front
face of the rim and extending onto the tread, i.e., at
about the same location as that of the crack illustrated
in Fig. 1.2.1. No cracks were visible on the other wheel.
The experiments were performed using a 1.5" hard steel
ball bearing on the end of a 3 ft. pendulum string.
Analysis was performed in real time, using the third octave
band RTA*. At a given site on the wheel, five impacts
were made, the starting point of the pendulum's fall
being accurate to about 1 mm and the maximum overall
sound level of the impact being reproducible to about
1 dB. The RTA was set to read the maximum level in
each spectral band and these values were transferred to
the computer and stored after each impact. Two impact
sites on the good wheel were chosen, one on the front
face of the rim and one on the plate. The precisely
equivalent locations on the bad wheel were then impacted.
For each set of 5 impacts on the good wheel an average
spectrum was computed. Each of the individual spectra
for a given location on either wheel was then compared
with the appropriate good wheel average. The algebraic
sum of the deviations in dB in each spectral band was
then calculated. The results are shown in Table 3.4.1.

---

*RTA (Real Time Analyzer)

TABLE 3.4.1

RANGE OF DEVIATIONS FROM GOOD WHEEL SPECTRAL
AVERAGES IN EXPERIMENTS WITH THERMAL CRACKS

Run Number	Good Wheel		Bad Wheel	
	Flange Impact	Plate Impact	Flange Impact	Plate Impact
1	200-500	300-800	1300-2800	700-1000
2	200-650	250-650	1100-2600	700-1400

The conclusion was reached that there was a definite difference between the good and bad wheel spectra. Some measurements were also made of decay times of impact sound levels, but no significant differences were found in that case.

These results indicate that the wheel with the thermal cracks should be readily distinguished from its mating wheel. The point should be made that the wheel under test had a large number of cracks, although each one is presumably not much greater than a square inch in area. However, the occurrence of dormant thermal cracks in such numbers on a wheel is probably the normal way for such cracks to appear, so it was concluded that there is a good chance of detecting them in the field.

It was also of some interest to know the smallest plate crack which could be detected. Railroad representatives were asked for help to find a small plate crack. The closest approximation that has come to our attention so far is a wheelset where one wheel (UH inventory number 15A) has a typical large plate crack as shown in Fig. 3.4.1 and wheel 15C, its mate, has a crack on the front plate near the hub (see Fig. 3.4.2a) which is not visible on the back side of the plate (see Fig. 3.4.2b). To be sure about the extent of the crack, a liquid penetrant test was performed on the
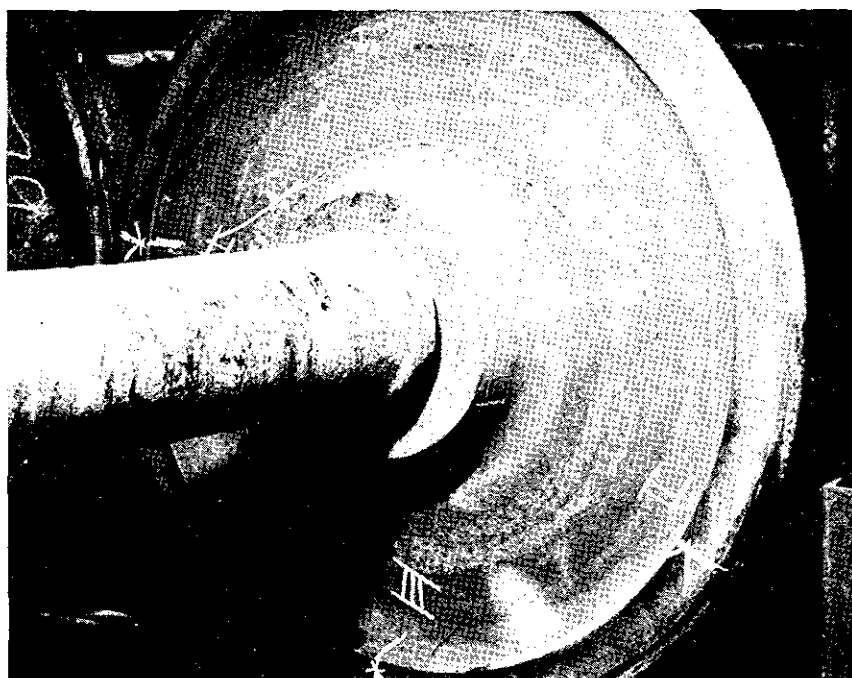
FIG. 3.4.1 VIEW OF WHEEL 15A
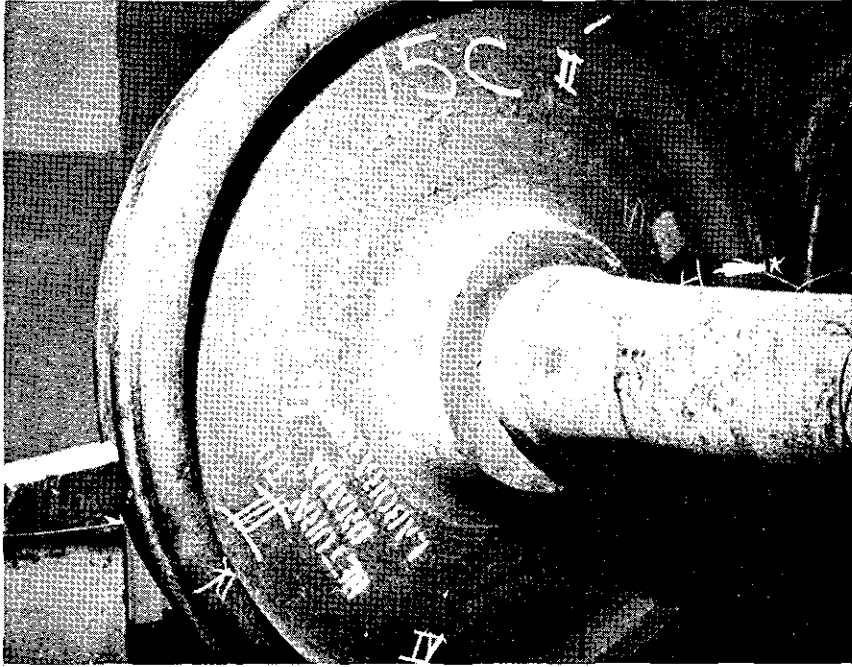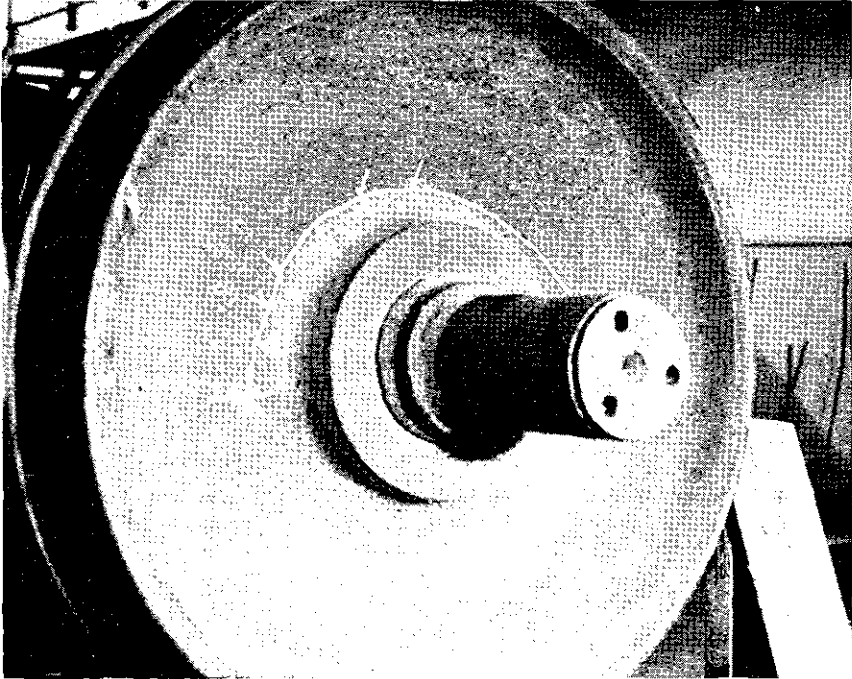
FIG. 3.4.2a VIEW OF WHEEL 15C (front side)
      b VIEW OF WHEEL 15C (back side)

wheel. The suspected area was properly cleaned of dust and rust and then a liquid penetrant was applied as an aerosol spray. The penetrant was of the fluorescent type so inspection under ultraviolet light showed clearly the presence of a 20" crack around the hub on the front plate of wheel 15C, but nothing on the back plate. Acoustic signature comparison between the wheels showed only a 20% matching with line spectra comparison vs. 50-80% for most good wheels. The signatures of the two wheels are shown in Fig. 3.4.3.

A comparison was made of the signature of wheel 15C, the partially cracked wheel, with the signatures of wheels 4G and 1G which are good wheels of the same type. The results are shown in Fig. 3.4.4. The results showed 28% line spectra matching for wheel 4G compared to 15C, as also for wheel 1G compared to 15C. Comparison between 4G and 1G showed a better matching, 37%. These numbers indicate that it is possible to find small plate defects on wheels.
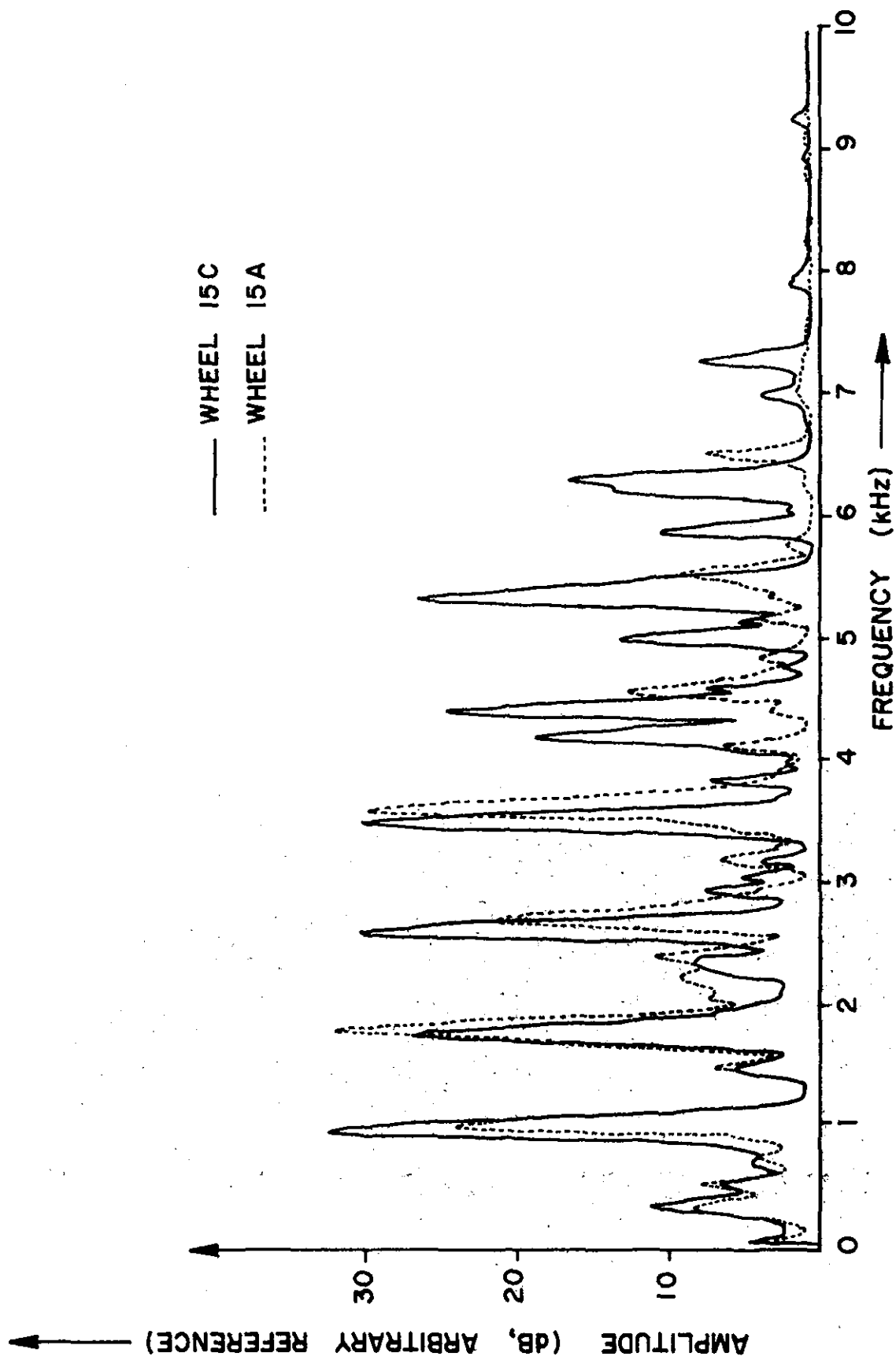
FIGURE 3.4.3 SIGNATURES OF WHEELS, 15C WITH A PARTIAL PLATE
CRACK AND 15A WITH A FULL PLATE CRACK

Percentage of Matching Lines

20%

28%

28%

37%
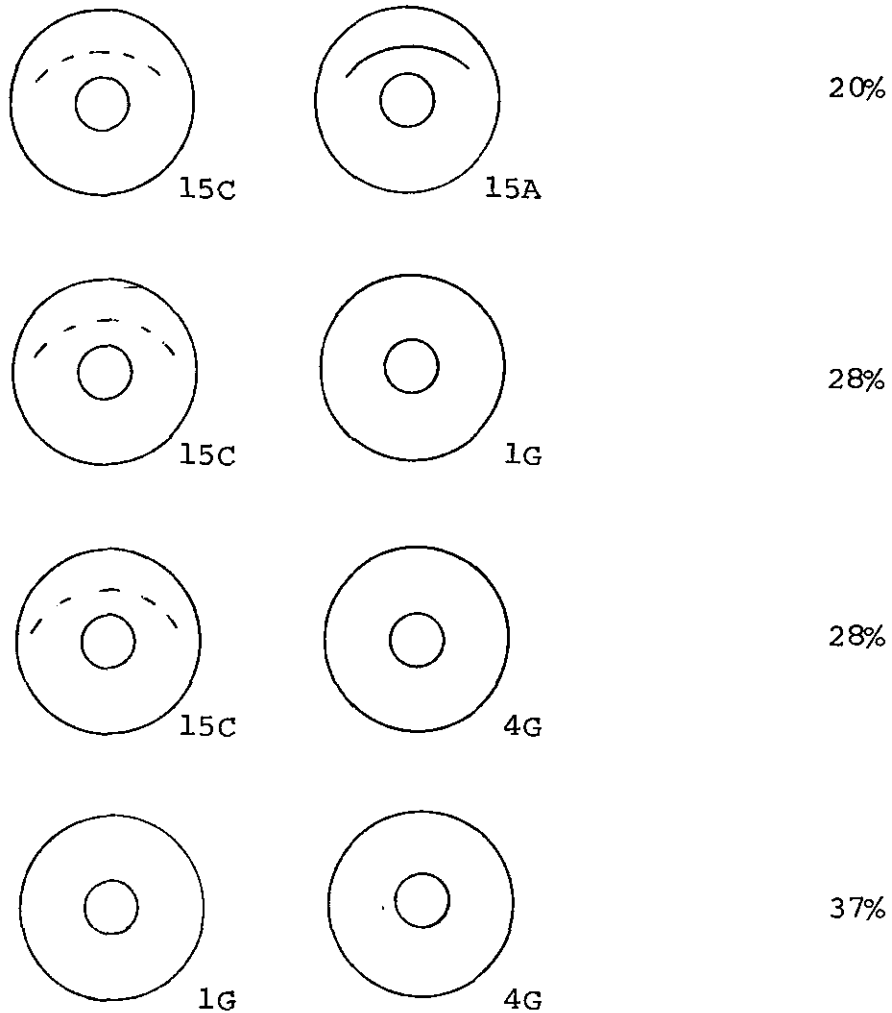
FIG. 3.4.4 SPECTRAL LINE COMPARISON TESTS BETWEEN A WHEEL
WITH A PARTIAL PLATE CRACK (15C), A WHEEL WITH
A FULL PLATE CRACK (15A) AND TWO GOOD WHEELS OF
THE SAME TYPE (1G AND 4G)

4. RESIDUAL STRESS EVALUATION IN RAILROAD WHEELS USING ACOUSTIC SIGNATURE ANALYSIS

4.1 Introduction

The residual stress in a wheel may be as important in influencing wheel failure as the presence of an incipient crack. The reason for this, in terms of fracture mechanics, is apparent from the relationship

$$K_{IC} = A \sigma c^{1/2}$$

where K_{IC} is the fracture toughness parameter, a property of the material. Carter and Caton [30] give values of K_{IC} ranging from 25 to 40 Ksi in$^{1/2}$, depending on the wheel class. A is a constant which Carter and Caton found to vary from 0.9 to 1.98 for different crack locations. σ is the applied tension needed to cause the crack to grow and c is the surface length of the crack. Carter and Caton quote 55 Ksi tensile stress as being representative of the peak of the stress generated during drag braking and hence conclude that critical crack lengths are a minimum of 0.1 inch for corner cracks in class U wheels to 0.65 inch for surface cracks in class A wheels.

However it does not follow that such cracks will cause a wheel to break. New wheels are manufactured with a residual compressive stress in the rim, which is usually in the range 20-25 Ksi according to Wandrisco and Dewez [31] . The plate of a new wheel is in tension. Extended periods of brake application can overheat the wheel and

eventually change the signs of the internal residual stresses. Clearly then the residual stress plays a major role in determining the growth of small cracks. Even if a crack grows through the rim it may be arrested in the plate for a long period before finally causing the wheel to disintegrate.

Some estimates of the number of wheels containing small rim cracks are quite high. However, on an annual basis there are less than 1000 derailments due to broken wheels. It might be concluded that many small cracks are not a problem. Hirooka et al. [33] have confirmed this impression as a result of drag brake tests and stated that such cracks are only dangerous if the rim has a high tensile stress. One concludes that a sensible inspection program would aim to find large cracks and wheels in which the compressive stresses in the rim have changed to a high tensile value. Large cracks are found quite effectively using ASI* but the measurement of residual stress is problematic.

None of the methods of residual stress measurement is readily applicable in this situation. The velocity of sound can be measured at ultrasonic frequencies and changes of the order of 1 part in 10^4 can be found per Ksi change in residual stress [43]. Obviously great accuracy and careful calibration is required, implying careful surface preparation. This method does have the advantage that the stress in the bulk of the material is measured.

*ASI (Acoustic Signature Inspection)

X-rays can be used in evaluation of lattice dimensions in homogeneous materials. Residual stresses can be deduced by evaluating strain from lattice dimensions. The method is restricted to surface stress-evaluation over a small area and careful surface preparation is necessary [32]. Barkhausen noise can also be used in residual stress evaluation [34]. Again in this case the most obvious limitation is surface preparation of the test material and only surface stress evaluation can be made. In the case of a wheel in service surface residual stresses on the tread, front and back rim are different from the "bulk" rim stresses due to braking action from retarders and the high local loading on the tread of a rolling wheel.

The objective of the work reported here was to investigate the possibility of using acoustic signature inspection to evaluate residual stress. The basic idea is that applied stress changes the natural frequencies of flexural vibrations in an object. The simplest example is the change of the natural modes of a string under different tension. For rigid bodies such as a beam, or column, there is a well known theoretical treatment and experimental evidence that the response changes with load, which has to be allowed for in the design of chimney stacks and the like. A similar effect occurs in the case of high speed turbine blades where the frequencies of the natural modes changes with speed. This question has been discussed in Section 2.

Nagy [1] showed that changes in resonant frequencies of wheels occurred under load. This gave rise to the idea that change in residual stress might be detectable from changes in resonant frequencies.

4.2 Test on Wheels with Different Heat Treatment in the Griffin Wheel Manufacturing Plant at Bessemer, Alabama

A first attempt to study this problem was made in the Griffin Wheel Manufacturing Plant at Bessemer, Alabama. A variety of manufacturing treatments had been applied to the wheels to generate a wide range of residual stresses. Acoustic signatures were recorded from 33 and 36-inch wheels that had normal treatment, and also from wheels that had high internal tension stresses. The standard procedure for measuring residual stresses is destructive testing by saw cut described in the manual of standards and recommended practices of the Association of American Railroads (AAR) [36]. In Fig. 4.2.1 are shown the results of strain test on a 33 inch one wear Griffin wheel. This figure was obtained from the Car and Locomotive Cyclopedia [37].

All wheels tested were sitting on their hubs on a concrete floor, so the plates and rims were free of contact. The following measurements were taken:

1. Hammer impacts on each wheel.

   a. Ten impacts were made on three different points on the circumference of the front rim of the wheel. The relative location of the impact points were approximately 120° apart.
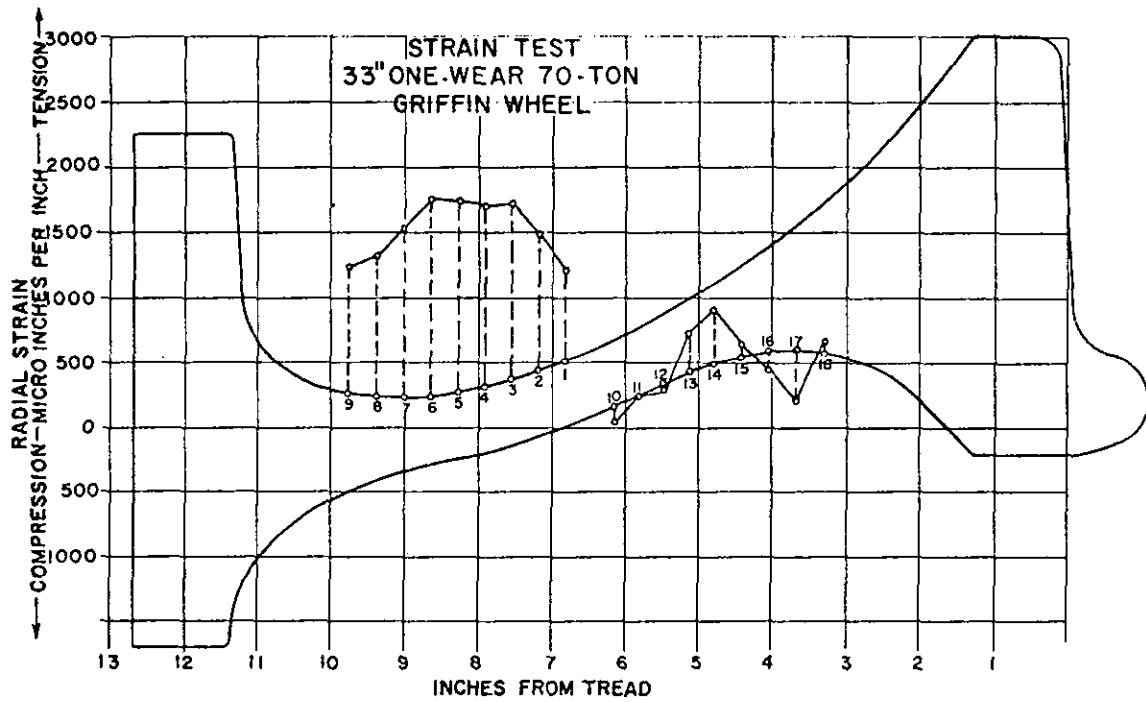
FIG. 4.2.1 STRAIN TEST ON A 33-INCH ONE WEAR 70 TON GRIFFIN
          WHEEL

b. Five impacts on the plate, midway from the center
to the rim of the wheel.

c. Five impacts on the flange, along a radius.

For steps 1a, b, and c sound was detected by a
microphone. The hammer is shown in Fig. 4.2.2. This
design provides a triggering pulse simultaneously with
the impact. Signals were recorded on a dual channel
recorder.

2. Shaker excitation. In this series of tests a shaker
was used as an exciter and the vibrations were picked
up by a GR type 1560-P52 accelerometer. Input
signals were:

a. random noise,

and b. slowly sweeping sine signal from a Wavetek
Model 134 signal generator, in the range from
400 to 2000 Hz.

Most of the analyses were made from impact recordings.
The wheel manufacturing steps are as follows:

1. Pressure Pouring Pit: Steel wheels are formed as
air pressure forces molten steel up from a sealed
chamber into graphite molds. A mold is filled in
20 seconds.

2. Wheel Transfer: Depending upon the metal temperature
at pouring, the wheel casting will solidify in five
to seven minutes. The cope (top) of the mold is
removed, and the wheel is lifted by the hub and
conveyed to the final finishing and inspection stations.
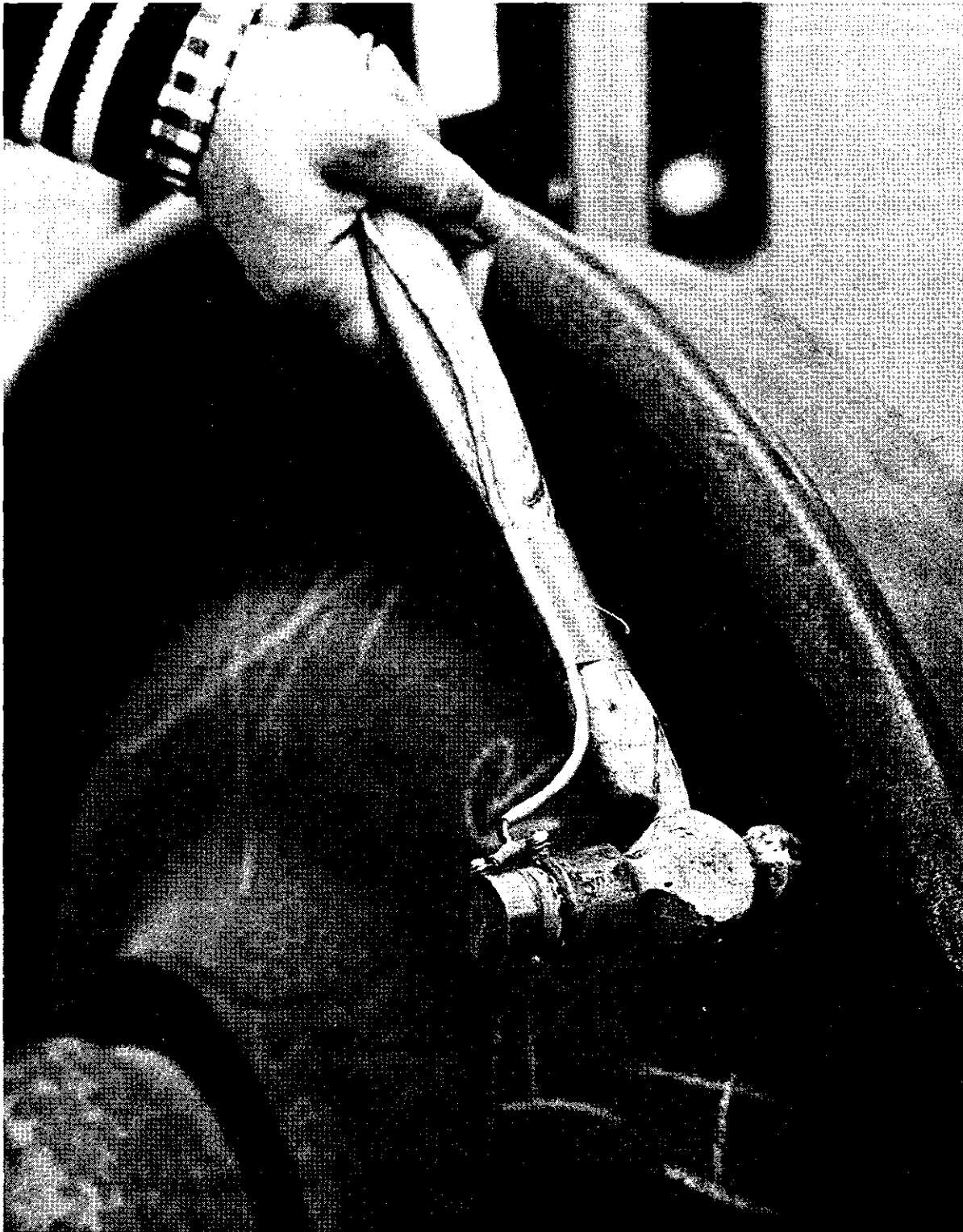
FIG. 4.2.2   VIEW OF THE HAMMER WITH A PZT DISK BETWEEN HAMMER
AND CYLINDER TO PROVIDE THE TRIGGERING PULSE ON
IMPACT WITH THE TEST OBJECT

3. Cooling Kiln: Wheels are cooled from 2,000°F to 1,000°F to reduce stress formation.

4. Stopper Pipe Cut off and Shot Blast: Each wheel's stopper pipe is automatically cut off and the graphite stopper removed from the hub.

5. Torch Cutting: (a) Riser stubs are taken off with an electric arc torch. (b) An oxyacetylene torch automatically cuts out the wheel's hub bore.

6. Heat Treating: Wheels are moved by conveyor to a rotary hearth normalizing furnace, where they are heat treated.

7. Rim Quench: Following heat treatment, rims are quenched to harden the treads for more severe service.

8. Draw Furnace: The wheels are tempered again.

9. Hub Cooling: Final heat treatment for proper residual stress formation.

10. Shot Blasting: Each wheel is shot blasted to remove scale and permit surface inspection.

11. Magnaglo Test: Magnaglo testing detects surface and subsurface defects.

12. Ultrasonic Test: An additional test is made, using pulse echoes. This is to further insure that there are no subsurface flaws.

The manufacturing steps are shown in a schematic diagram in Fig. 4.2.3. If the wheel has been taken off line before the normalizing furnace, steps 3 to 6, it has a high stress. After step 6 it has normal stress.
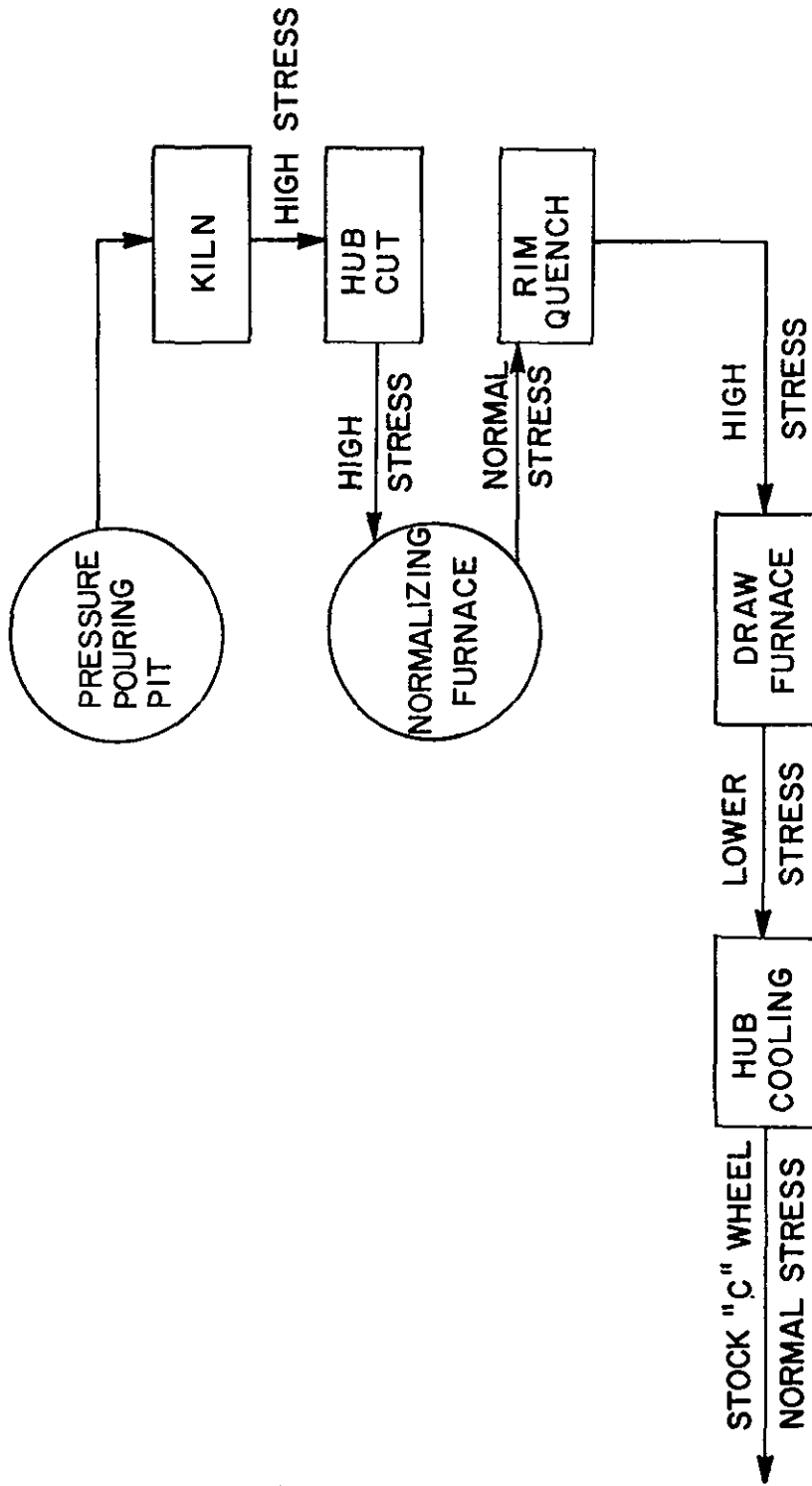
FIG. 4.2.3   SCHEMATIC   DIAGRAM   OF   CAST   WHEEL   MANUFACTURING

Between steps 7 and 8 it has high stress. After step 8
it has lower stress and after step 9 it has the normal
stress configuration. A list of wheels tested at the
Griffin Wheel Plant in Bessemer, Alabama is presented in
Table 4.2.1. The first column has the wheel identification,
type and number. The second column has the tape numbers
of tests as recorded. The third column has the
description of the manufacturing treatment and the last
column the estimated stress according to the treatment.

Preliminary results from comparisons between the
acoustic signatures of the wheels are listed in Table 4.2.2.
The difference index is based on a decision scheme which
is a combination of line spectra and sum of the differences
comparison between two spectra. There were only two
conflicting results out of 25 tests. In run No. 5, the
Difference Index for high/normal stressed wheels is small.
In run No. 9, although wheels CJ36 26 425 and CJ 36 26 171
had the same heat treatment, history, and structure, they have
a Difference Index of 10. One possible explanation is
the existence of small geometric differences indicated
by the rough surface appearance (the wheels were removed
from the line before step 4).

A detailed study of the acoustic signatures was made
using a spectrum translator to measure small shifts in
resonance frequencies. This instrument was used in con-
junction with the SD330 RTA. The spectrum translator can
separate frequency bands from a spectrum and expand them,

TABLE 4.2.1

LIST OF WHEELS TESTED AT THE GRIFFIN WHEEL
MANUFACTURING PLANT IN BESSEMER, ALABAMA
FOR RESIDUAL STRESS EVALUATION

WHEEL NO. AND TYPE	TAPE NO.	DESCRIPTION	STRESS
CJ36-26425 "C"	141, 141A, 142, 155A	Hub Left In	High Stress
CJ36-26171 "C"	143A, 144	Hub Left In	High Stress
CH36-17180 "C"	147A, 149	Hubcut, Not Normalized	High Stress
CJ36-27910 "C"	145, 146A	Hubcut, Quenched Skipped Draw Furnace	High Stress
CJ36-27636 "C"		Hubcut, Quenched and Tempered but Not Hub Cooled	Lower Stress
CJ36-32784 "C"	145, 146A	Stock	Normal Stress
CJ36-23089 "U"	147A, 148	Stock	Normal Stress
CJ36-32769	153A, 154	Stock	Normal Stress
CJ33-30695	151A, 152	Hub Left In	High Stress
CJ33-31029	149, 150A	Hubcut, Quenched Skipped Draw Furnace	High Stress
CJ33-30695	149, 151A	Hubcut, Quenched Skipped Draw Furnace	High Stress
CJ33-97803 "C"	149, 150A	Stock	Normal Stress
CJ33-11092 "U"	151A, 152	Stock	Normal Stress
CJ33-21226 "U"	152, 153A	Stock	Normal Stress

TABLE 4.2.2

PRELIMINARY RESULTS - RESIDUAL STRESS TESTS, BESSEMER, ALABAMA
(-H INDICATES HIGHLY STRESSED WHEEL, -N INDICATES NORMAL WHEEL)

RUN	TEST #	WHEEL #1	WHEEL #2	DIFFERENCE INDEX*	COMMENT
1	1	CJ36 26425-H	SAME	1	SAME WHEEL COMPARISON
2	18	CJ33 97803-N	SAME	3	SAME WHEEL COMPARISON
3	12	CJ36 32784-N	CJ36 23089-N	5	
4	27	CJ36 32769-N	CJ36 32784-N	5	
5	22	CJ33 30695-H	CJ33 11092-N	6	THIS IS ONLY CONFLICTING RESULT FROM 25 TEST
6	21	CJ33 97803-N	CJ33 11092-N	7	
7	19	CJ33 97803-N	CJ33 31029-H	9	
8	13	CJ36 27910-H	CJ36 23089-N	9	
9	5	CJ36 26425-H	CJ36 26171-H	10	**
10	10	CJ36 26171-H	CJ36 32784-N	10	
11	14	CJ36 23089-N	CH36 17180-H	27	DIFFERENT TREAD
12	25	CJ33 97803-N	CJ36 32769-N	29	33" COMPARED TO 36"
13	17	CH36 17180-H	CJ33 97803-N	33	33" COMPARED TO 36" DIFFERENT TREAD

* THE DIFFERENCE INDEX IS OBTAINED BY SUMMING THE DIFFERENCE BETWEEN SPECTRA TAKEN CHANNEL BY CHANNEL. BEFORE SUMMING, EACH SPECTRA IS NORMALIZED BY DIVIDING ALL ITS CHANNEL VALUES (IN dB) BY THE MAXIMUM VALUE. FURTHERMORE, WHEN RESONANCE LINES CO-INCIDE BETWEEN THE TWO SPECTRA, THEN THE CENTER CHANNEL AND ADJACENT CHANNELS FOR SUCH RESONANCES ARE DISREGARDED IN THE SUM.

** THIS MIGHT BE DUE TO SMALL GEOMETRIC DIFFERENCES (NO SURFACE TREATMENT)

thus improving the frequency resolution. In the range
of 10 kHz the analyzer has a 40 Hz resolution. With the
spectrum translator, translated bands had a 100 Hz range
and 0.4 Hz resolution. In the range of 10 kHz the sampling
period is 50 ms, for the 100 Hz range it is 2500 ms, hence
only slowly decaying signals (resonances) can be analyzed.
With the use of a spectrum translator significant dif-
ferences in the resonant frequencies were revealed.
Spectral plots were obtained for most of the strong wheel
resonances. An example is shown in Fig. 4.2.4. The
resonances of the normally stressed wheels were separated
from those of the highly stressed wheels by more than
8 Hz. The estimated frequency shift for those resonances
due to geometrical tolerance in manufacturing is 1 Hz.

A list of the measurements taken is presented in
Table D.1 in Appendix D.1. The results are also shown in
Fig. 4.2.5 for CJ36 type wheels and in Fig. 4.2.6 for CJ33
type wheels. These are rather unusual presentations and
some explanation is needed. The points on the plot repre-
sent resonant frequencies. All the points lie on lines
parallel to the Y axis. For example, the line AA' in
Fig. 4.2.5 has the resonances of the CJ36 type wheels near
390 Hz. Dots represent resonances of normally stressed
wheels and asterisks represent highly stressed wheels. At each
wheel resonance, the value for the normally stressed wheel
was set on the X-axis. The intersection of AA' and the
X-axis represents the resonance of the wheel CJ 36 32784
at 390.8 Hz. The rest of the indications on AA' show the

67
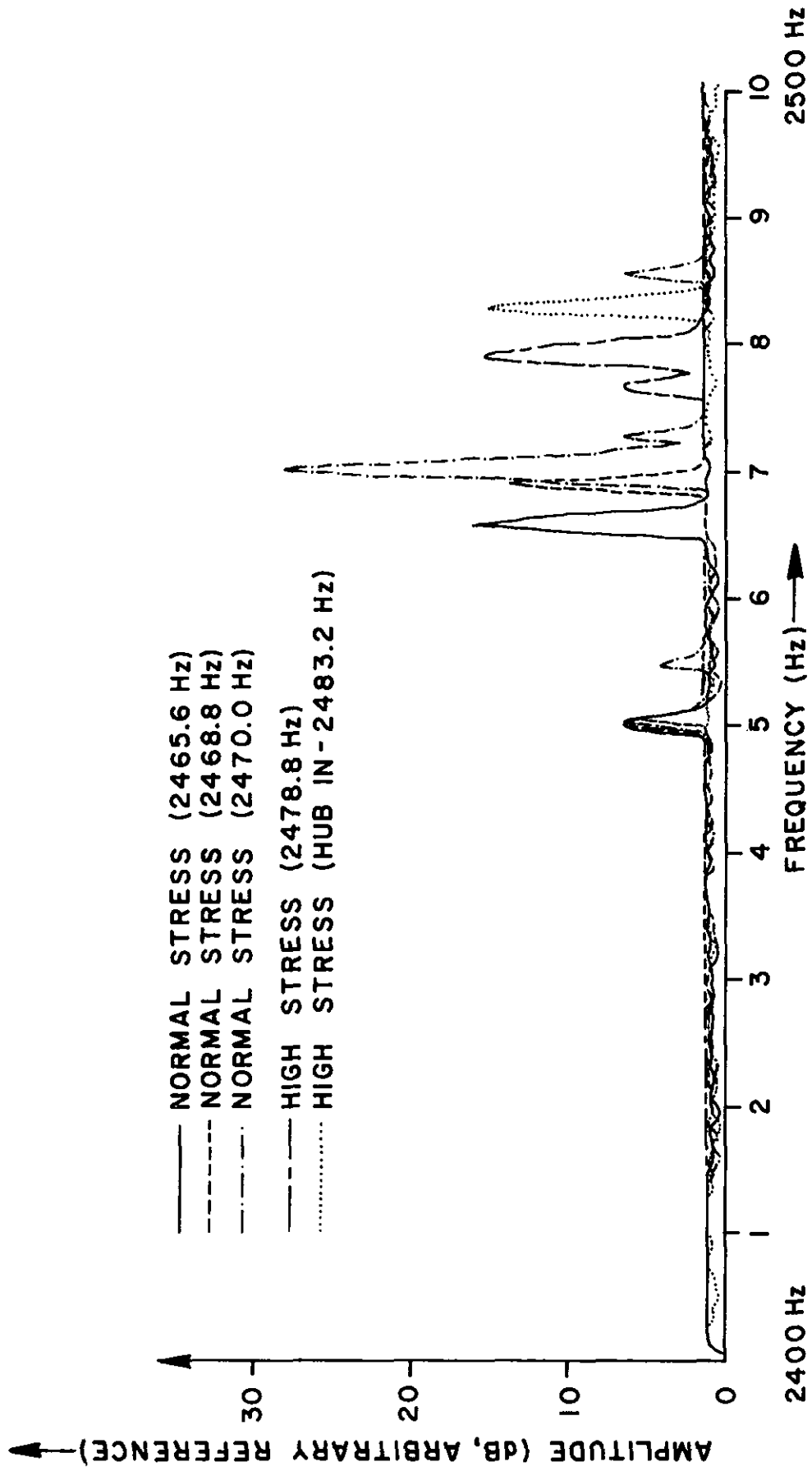
FIGURE 4.2.4   SPECTRA PLOTS FOR CJ36 WHEELS WITH DIFFERENT INTERNAL
STRESS DISTRIBUTION, BETWEEN 2400 and 2500 Hz
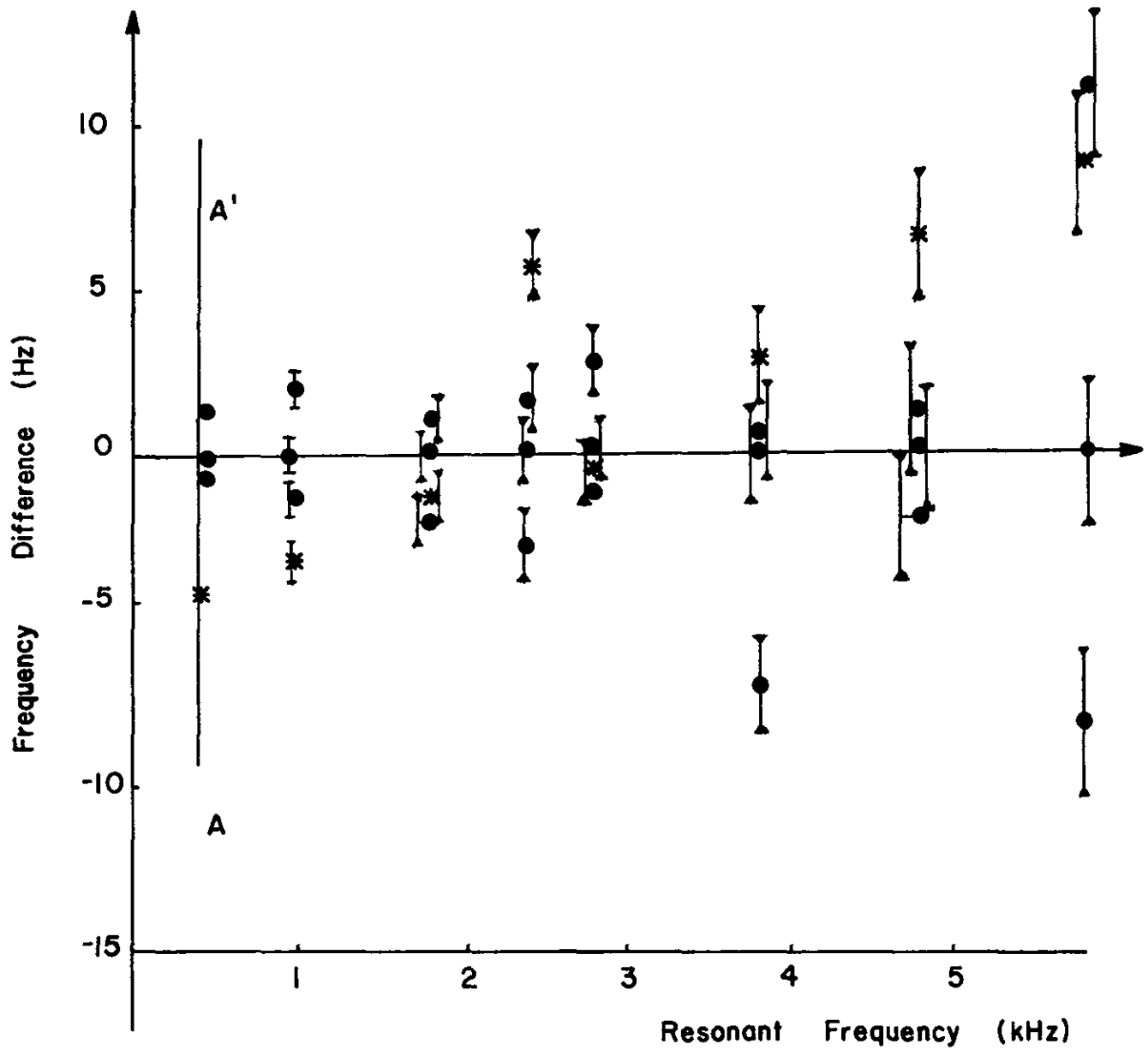
FIG. 4.2.5 DIFFERENCES IN RESONANT FREQUENCY FOR CJ36
WHEELS
● NORMALLY STRESSED WHEELS;
✳ HIGHLY STRESSED WHEELS
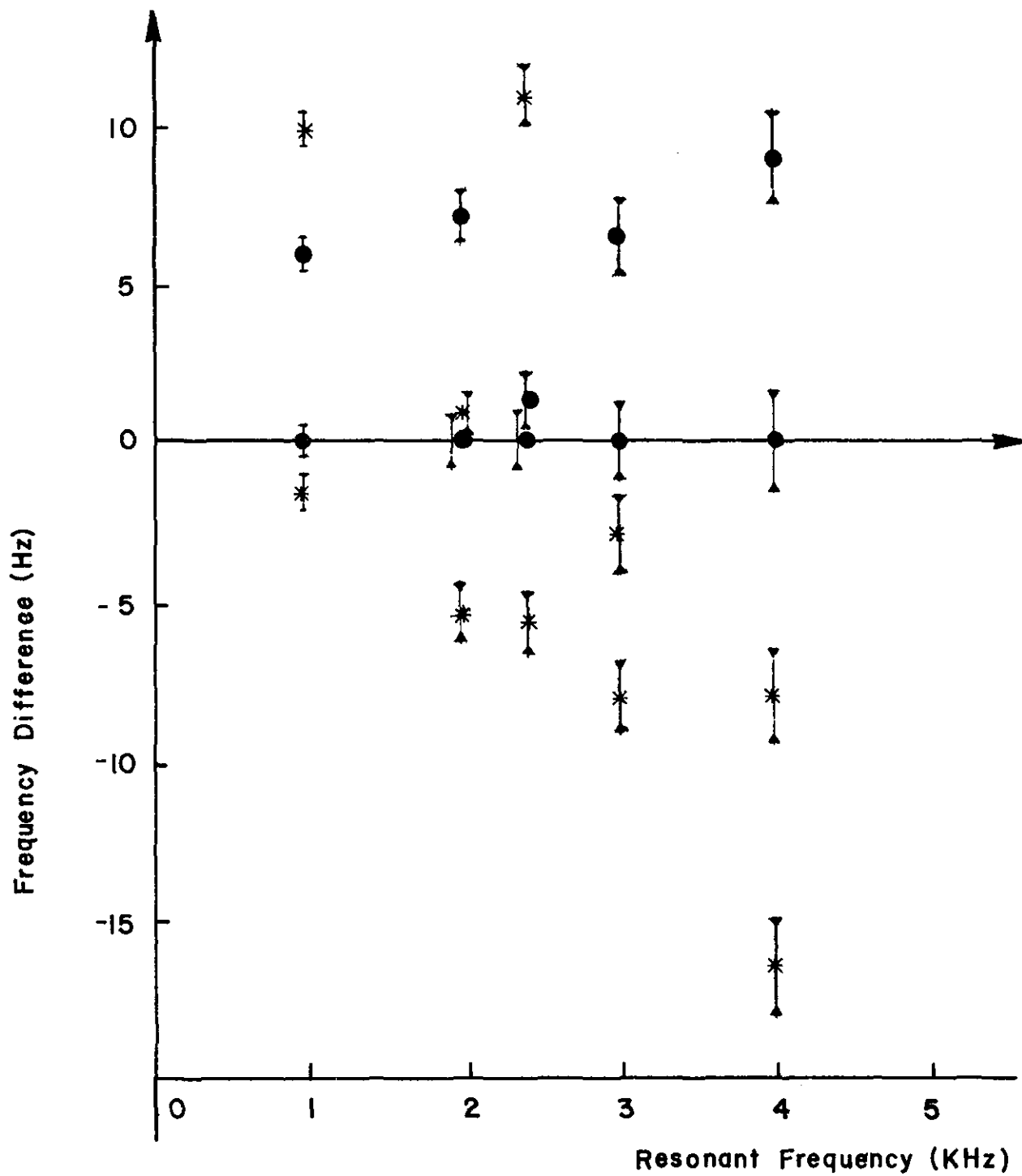
FIG. 4.2.6   DIFFERENCES IN RESONANT FREQUENCY FOR CJ33 WHEELS.
● NORMALLY STRESSED WHEELS;   ✳ HIGHLY STRESSED WHEELS

frequency deviation from that value of the corresponding
resonance for other wheels in Hz. Positive deviations
correspond to resonances above 390.8 Hz and negative
deviations to lower values. In some cases the resonance
of a highly stressed wheel lies among the resonances of
the normally stressed wheels, but in other cases it is
above or below. Thus, although the shift may be to higher
or lower frequencies, in general there is a separation
between the resonances of normally and highly stressed
wheels. Hence a known type of wheel with unknown stress
could be checked for stress distribution by comparing a
few small portions of its signature with the same signature
portions of normally stressed wheels. These frequency
shifts could conceivably be due to variations in the
geometry of the wheels because of dimensional tolerances.
For this reason it was decided to estimate frequency
shifts due to extreme variations in the dimensional
tolerances.

The manufacturing error for a 36" wheel is about 5 lb
or about 0.5% in weight; hence the volume error, ε_v, is
also 0.5%

$$\text{i.e. } \varepsilon_v = 0.5\%. \tag{4.2.1}$$

Approximating the wheel to a disk, the volume of the
wheels is

$$v = \pi r^2 h. \tag{4.2.2}$$

Differentiating (4.2.2)

$$dv = 2\pi rhdr + \pi r^2 dh,$$

or,

$$\varepsilon_v = \frac{dv}{v} = \frac{2\pi rh}{\pi r^2 h} dr + \frac{\pi r^2}{\pi r^2 h} dh \qquad (4.2.3)$$

$$= \frac{2dr}{r} + \frac{dh}{h} = \varepsilon_r + \varepsilon_h$$

where ε_r is the error due to the change in the radial direction and ε_h is the error due to the change in the thickness. Assuming $\varepsilon_r = \varepsilon_h$, for the sake of argument, $\varepsilon_r = 2.5 \times 10^{-4}$ and $\Delta r = \frac{r}{2} \times 2.5 \times 10^{-4}$,

or

$$\frac{\Delta r}{r} = 1.25 \times 10^{-4}, \qquad (4.2.4)$$

The resonance frequencies are given by

$$f_n = \frac{n(n-1)}{(n^2+\nu)^{\frac{1}{2}}} \frac{1}{2\pi} (EI_x/\rho Ar^4)^{1/2},$$

or

$$f_n = \frac{C}{r^2} \quad (4.2.5) \quad , \quad C = \text{constant.} \qquad (4.2.5)$$

Thus

$$\Delta f_n = \frac{3C}{r^3} \Delta r, \qquad (4.2.6)$$

and finally from (4.2.4), (4.2.5) and (4.2.6) the frequency error is

$$\varepsilon_f = \frac{\Delta f_n}{f_n} \simeq 4 \times 10^{-4}. \qquad (4.2.7)$$

In Table 4.2.3 the estimated frequency error is given in Hz for the main resonances of the CJ33 and CJ36 type wheels. The estimated frequency shifts due to geometrical variations are much less than those measured.

TABLE 4.2.3

ERROR EVALUATION FOR STRONG
RESONANCES ON CJ33 AND CJ36 WHEELS

WHEEL TYPE	RESONANT FREQUENCY	FREQUENCY ERROR Δf_1 Hz	MAX. FREQUENCY ERROR Δf_2 Hz
CJ33	440	0.2	0.4
	1130	0.5	1.0
	3010	1.2	2.4
	4040	1.6	3.2
CJ36	390	0.2	0.4
	1040	0.4	0.8
	1860	0.8	1.6
	2470	1.0	2.0
	2790	1.1	2.2
	3780	1.5	3.0
	4810	1.9	3.8
	5860	2.3	4.6

4.3 Dynamometer Tests at Wilmerding, Pennsylvania

An opportunity to correlate numerical stress indications with changes in the acoustic signature was offered by the Union Pacific Railroad Company (UPRR) who invited the University to participate in a series of dynamometer tests in the Westinghouse Plant at Wilmerding, Pennsylvania.

4.3.1 Description of Tests

The objective of the Union Pacific's test team was to study the thermal damage and premature wear to the tread and flange portion of the wheel. Preliminary internal study of the problem by the UPRR focused attention on three potential causes of the phenomena:

1. misalignment of the brake shoe with respect to the wheel center line,

2. misapplied brake shoe,

and 3. high energy drag braking applications. Subsequent discussion and correspondence between representatives of the Union Pacific Railroad and Westinghouse Air Brake Division (WABD) resulted in a proposal to conduct a dynamometer research test program to investigate the possible effect of these factors on usable wheel life. This program was conducted by WABD under contract to UPRR.

The dynamometer test program consisted of both stop tests and drag tests. The stop tests were emergency stops from 80 mph. Five stops were made on each wheel used. The drag test was run at a speed of 60 mph with a

shoe force simulating a 15 psi brake pipe reduction. Five

drag tests were made on each wheel. Two different positions

of the shoe on the wheel were tested: in the center of

the tread, with the shoe overriding the outer edge of the

tread, and with the shoe riding on the flange. Several

types of brake shoes were used.

The acoustic signature of the wheel after each stop

was obtained using the setup shown in Fig. 4.3.1. For

excitation of the wheel a 16 oz, standard hammer was used

and the wheel was impacted five times. In a few tests a

32 oz. hammer in addition to the 16 oz. one was used. The

stress readings were obtained from three SR-4 foil strain

gauges (BLH Electronics) welded on the wheel as shown in

Fig. 4.3.2. The strain readings were obtained using two

types of strain indicators. The first device was a

multichannel indicator with an internal calibration to zero

the initial reading, so that any subsequent reading indi-

cated the change in strain directly. The second device

gave indications whereby any strain change could be

evaluated by subtracting the indication from the initial

reading. In the following description the three gauges

will be referred to as A, B, and C (see Fig. 4.3.2). The

SR-4 gauge specifications indicate that the maximum

advisable operational temperature without special coating

is 705°F.

Acoustic signatures from a total of six wheels were

obtained. All wheels tested were Griffin CJ33 and were

Wheel Microphone

NAGRA
TAPE
500 HP   RECORDER
DC MOTOR   SLM

2'
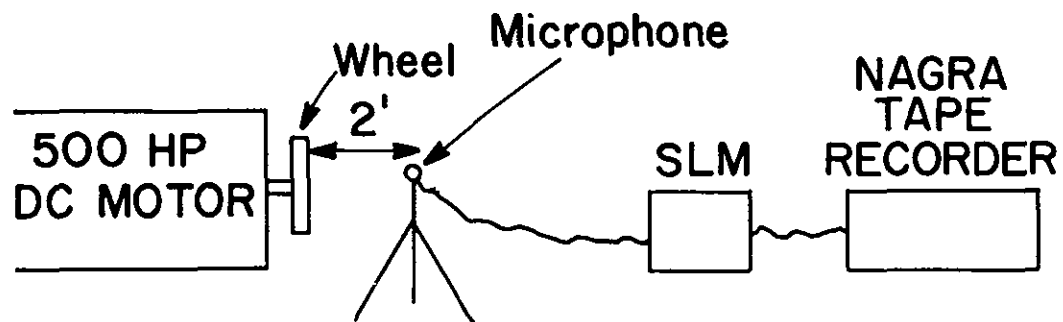
BACKGROUND NOISE : 88 dBA
IMPACT LEVEL   : II3 dBA on fast at 2 feet
SLM   : GR
TAPE RECORDER   : NAGRA IV

FIG. 4.3.I SETUP FOR ACOUSTIC SIGNATURE RECORDING
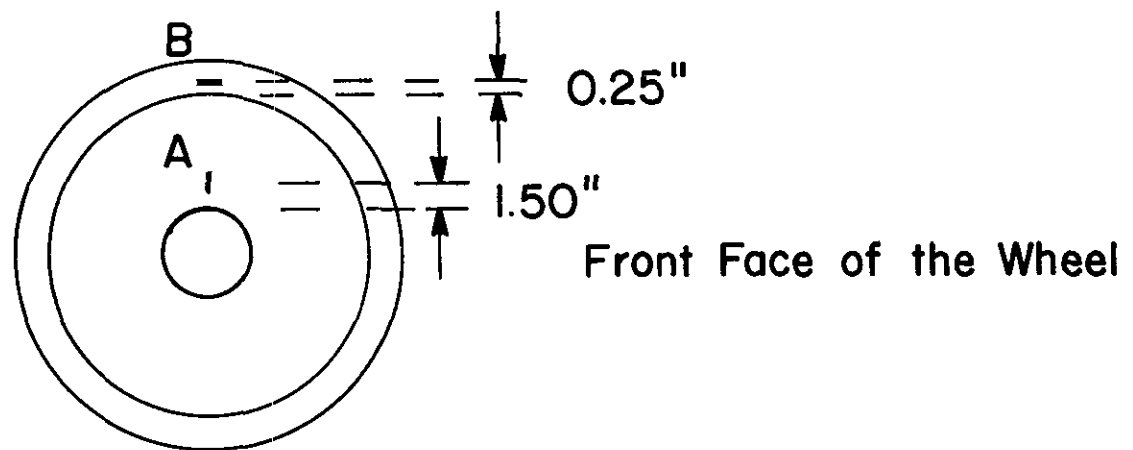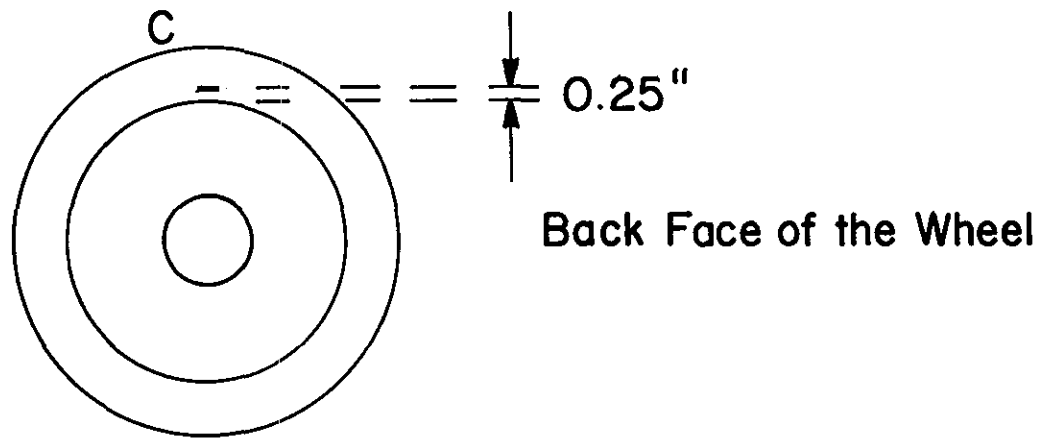
FIG. 4.3.2   STRAIN GAUGE ARRANGEMENT

identified as UP 12, 19, 20, 17, 27, and 28. In wheels
UP 12, 19, 20 and 17 emergency braking tests were per-
formed with different brake shoes and shoe positions. On
wheels UP 27 and 28 drag braking tests were performed
applying COBRA composition brake shoes. As was expected
the highest stress changes occurred in the drag braking
tests because of the high final wheel tread temperature of
600°F to 1100°F, as compared to emergency stops in which
final temperatures are generally in the range of $150°F$ to
550°F.

4.3.2 Data Processing

The tape recordings were returned to the University
for processing. An attempt to see changes in the signature
using the SD 330 A RTA failed because of the low frequency
resolution of 20-40 Hz while the range of interest is
0-10 Hz. By courtesy of the Shell Oil Co., a Hewlett
Packard (HP 5445) real-time spectrum analyzer was made
available. This instrument has a variety of features and
options for optimum signal processing. Identification of
the important resonances was achieved in a preliminary run
shown in Fig. 4.3.3. Because of limited access time with
the analyzer only signatures from wheels UP 27 and 28
(drag braking) could be obtained.

4.3.3 Results

The results are summarized in Table 4.3.1 and 4.3.2.
These tables contain: in column 1, the test number; in

TABLE 4.3.1   STRAIN GAUGE INDICATION VERSUS ACOUSTIC SIGNATURE

CHANGES FROM DRAG BRAKING TESTS ON WHEEL UP 28

TEST No.	TAPE No.	STRAIN GAUGE INDICATIONS			ΔA	ΔB	ΔC	RESONANCE in Hz			
		A	B	C				420.70	3001.2	4034.3	5091.4
32	203	0 (-1248)	0 (+2227)	0 (+510)							
33	"	-392 (-1648)	(-980) (+1239)	+140 (+646)	-392 (-400)	-980 (-988)	140 (136)	.62	-1.2	-1.8	-2.7
34	"	-826 (-2104)	-1125 (+1074)	+279 (+788)	-826 (-856)	-1125 (-1153)	279 (278)	—	0.4	0.1	-1.5
35	"	-1342 (-2613)	GAUGE BURNED OFF	+809 (+1329)	-1342 (-1365)	NR	810 (819)	3.52	5.1	5.2	4.3
36	204	-1674 (-2960)	NR	(+825) (+1327)	-1674 (-1712)	NR	825 (817)	—	5.4	4.7	5.1
37	"	-1703 (-2985)	NR	+884 (1409)	-1703 (-1737)	NR	884 (899)	—	6.0	6.7	6.6

Note: The Strain Gauge Readings are in microinches per inch. An Indication of 1000 Corresponds to about 30 Ksi.

TABLE 4.3.2 STRAIN GAUGE INDICATION VERSUS ACOUSTIC SIGNATURE

CHANGES FROM DRAG BRAKING TESTS ON WHEEL UP 27

TEST No.	TAPE No.	STRAIN GAUGE INDICATION			ΔA	ΔB	ΔC	RESONANCES in Hz				
		A	B	C				2012.1	2990.6	4019.5	5069.5	6129.4
25	203	0 (-340)	0 (+312)	0 (+1260)								
26	"	-330 (-674)	-800 (-500)	+120 (+1374)	-330 (-334)	-800 (-812)	+120 (+114)	0	0	-1.1	-1.2	-1.4
27	"	-764 (-1106)	-879 (537)	+286 (+1548)	-764 (-766)	-879 (-849)	+286 (+288)	2.2	2.6	2.4	2.1	3.0
28	"	-1412 (-1775)	NR	+51 (+1305)	-1412 (-1435)	NR	+51 (+45)	4.3	4.3	3.5	3.1	4.0
29	"	-1378 (-1732)	NR	+129 (+1403)	-1378 (-1392)	NR	+129 (+143)	—	3.7	1.1	0	-0.4
30	"	-1356 (-1725)	NR	+404 (+1675)	-1356 (-1385)	NR	+404 (+415)	—	4.7	3.9	3.0	3.0

column 2, the magnetic tape number; in columns 3, 4, 5,

the strain gauge indications from A, B and C gauges; in

columns 6, 7, 8, the changes in strain are evaluated from

columns 3, 4 and 5, and the last five columns show the initial

resonant frequency and the frequency shift that occurred

in the subsequent braking stops. Table 4.3.3 is an example

of the machine setup data for narrow band analysis which

includes information about the type of measurement, the

number of averages, the type of signal, the type of trigger,

the center frequency, the bandwidth, and the sampling time

length, from which the frequency error ΔF is given,

about 0.4 Hz. The frequency shift shown in the last

columns of Tables 4.3.1 and 4.3.2 was obtained from 54

graphs, such as those shown in Figs. 4.3.4 through 4.3.9.

These figures correspond to the signature of wheel UP 28

at about 3000 Hz, taken before the drag braking test

started (Fig. 4.3.4) and after each successive drag test

(Fig. 4.3.5 through 4.3.9).

The limited results shown in Tables 4.3.1 and 4.3.2

show the interesting feature of a frequency shift almost

independent of the resonant mode. This behavior is con-

sistent with the theory discussed in Section 2. It is

interesting to compare this frequency shift with the

theoretical result given by eqn 2.4.3. Rearranging this

equation one obtains

$$\frac{F}{A} = \sigma = 2\pi\Delta f_n \left[\frac{EI\rho}{A}\right]^{1/2}$$

TABLE 4.3.3

SETUP STATE ON HP 5445 REAL TIME ANALYZER

MEASUREMENT : LINEAR SPECTRUM

AVERAGE :   5   , STABLE

SIGNAL :   TRANSIENT

TRIGGER :   INTERNAL   , CHNL 1

CENT FREQ :   6.12500 KHZ

BANDWIDTH :   100.000 HZ

TIME LENGTH :   2.56000 S

ΔF :   390.625 mHZ   ΔT :   5.00000 mS

			DELAY	CAL (C1/C2)
ADC CHNL	RANGE	AC/DC	50.0000 mS	1.00000
* 1	1 V	AC	0.0 S	1.00000
2	10 V	DC		

L SPEC 1
-10.000

#A: 30

LGMAG
DB

-90.000

0.0   HZ   6.0000 K

FIGURE 4.3.3.   ACOUSTIC SIGNATURE OF A CJ33 WHEEL FROM 0-6.4 kHz
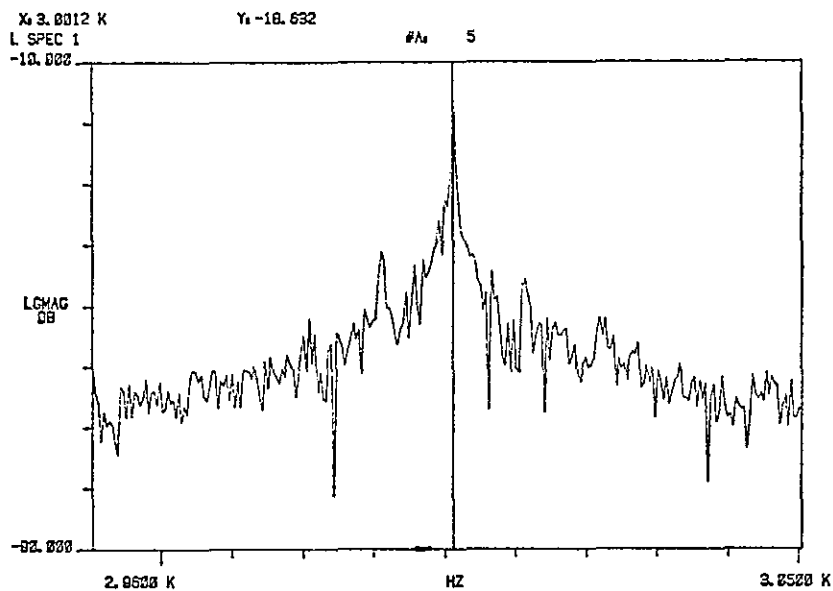
Fig. 4.3.4   Wheel UP 28 A.S. at 3 kHz before the
             Drag Braking Test
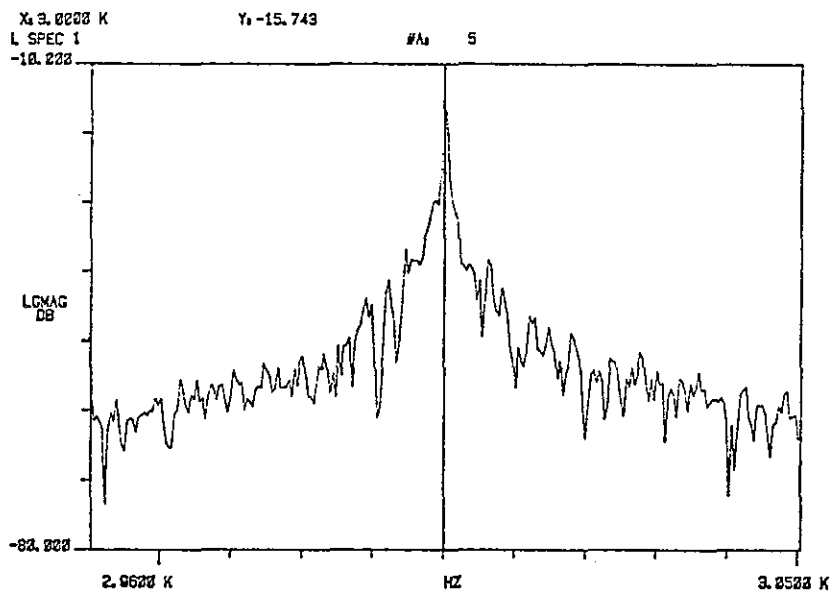
Fig. 4.3.5   Wheel UP 28, A.S. at 3 kHz after the first
             Drag Braking Stop
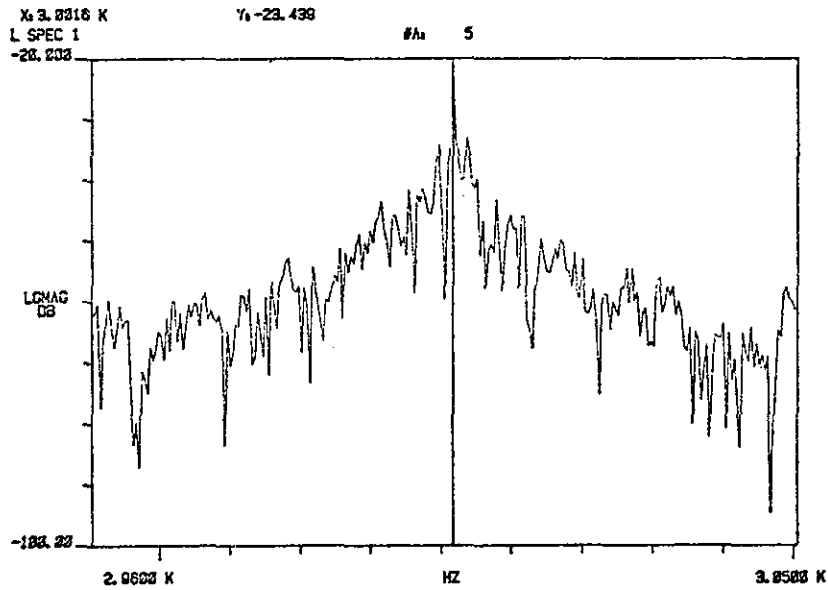
Fig. 4.3.6   Wheel UP 28, A.S. at 3 kHz after the
Second Drag Braking Stop
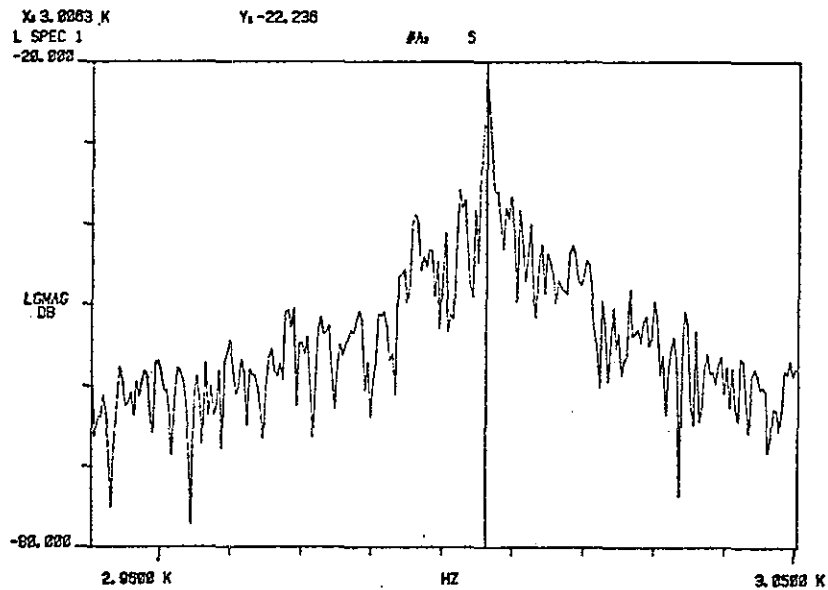
Fig. 4.3.7   Wheel UP 28, A.S. at 3 kHz after the
Third Drag Braking Stop
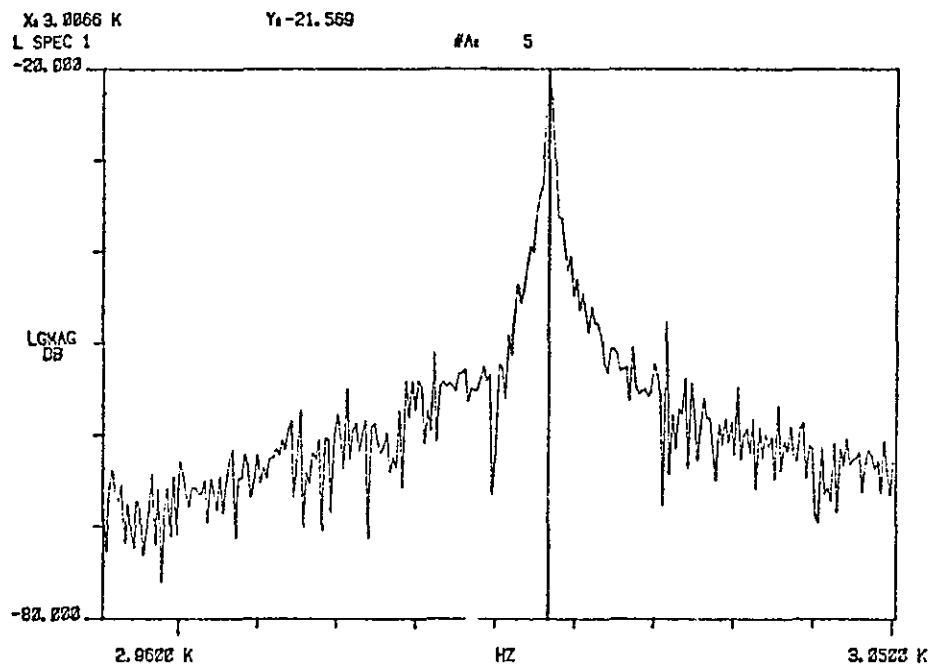
Fig. 4.3.8   Wheel UP 28, A.S. at 3kHz after the
fourth Drag Braking Stop
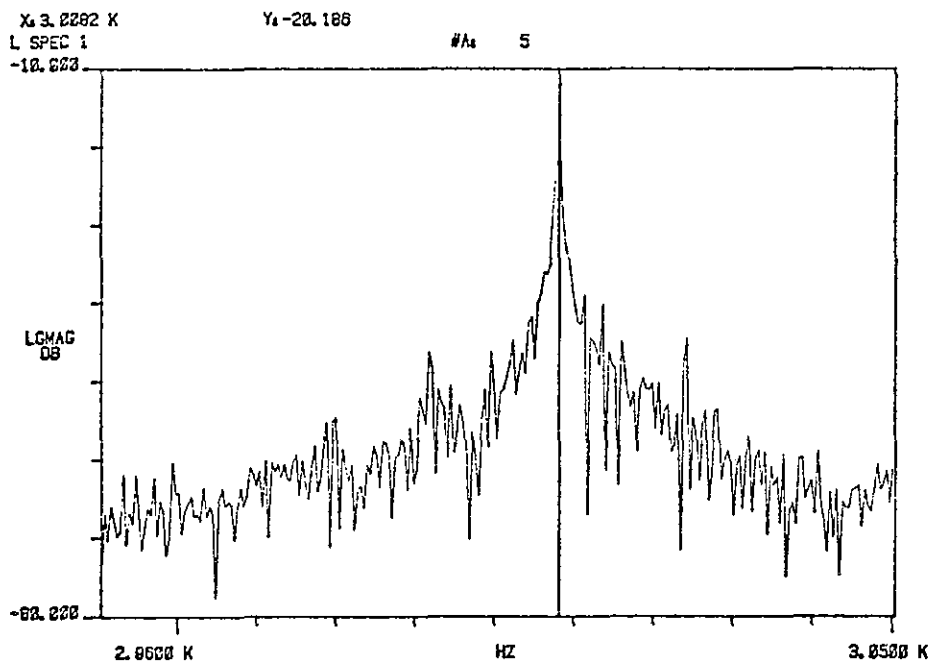
Fig. 4.3.9   Wheel UP 28, A.S. at 3kHz after the
fifth Drag Braking Stop

Hence a shift of 6 Hz corresponds to a stress change of
15 Ksi. It should be noted that this value must cor-
respond to an average stress change in the rim. Strain
gauge readings at the front and back of the rim were often
of different sign and varied from about 50 Ksi tension to
about 25 Ksi compression with a 6 Hz frequency shift. It
is therefore felt that the theory seems to give a
reasonable indication of average stress.

The correspondence between strain indications and
frequency shift is shown in Fig. 4.3.10 and 4.3.11. These
figures show that stress conditions and frequency shift
were best correlated for the readings from strain gauge A
welded on the plate. This seems quite reasonable because
the changes in the stress at gauge A on the plate are due
to the overall condition of the rim. But there may be
considerable local variations in the rim itself. The
least correlated indications were from strain gauge C on
the back rim. Comparison of the readings from gauge C
from wheels UP 27 and 28 under similar drag braking con-
ditions show large differences. Data from gauge B on the
front rim were limited to two values for each wheel
before extreme heat conditions burned them off. As has
been indicated, acoustic signature differences are functions
of the bulk stress, and thus might not be expressed
directly by indications from a single strain gauge. It
is hoped that completing the analyses on wheels UP 27 and
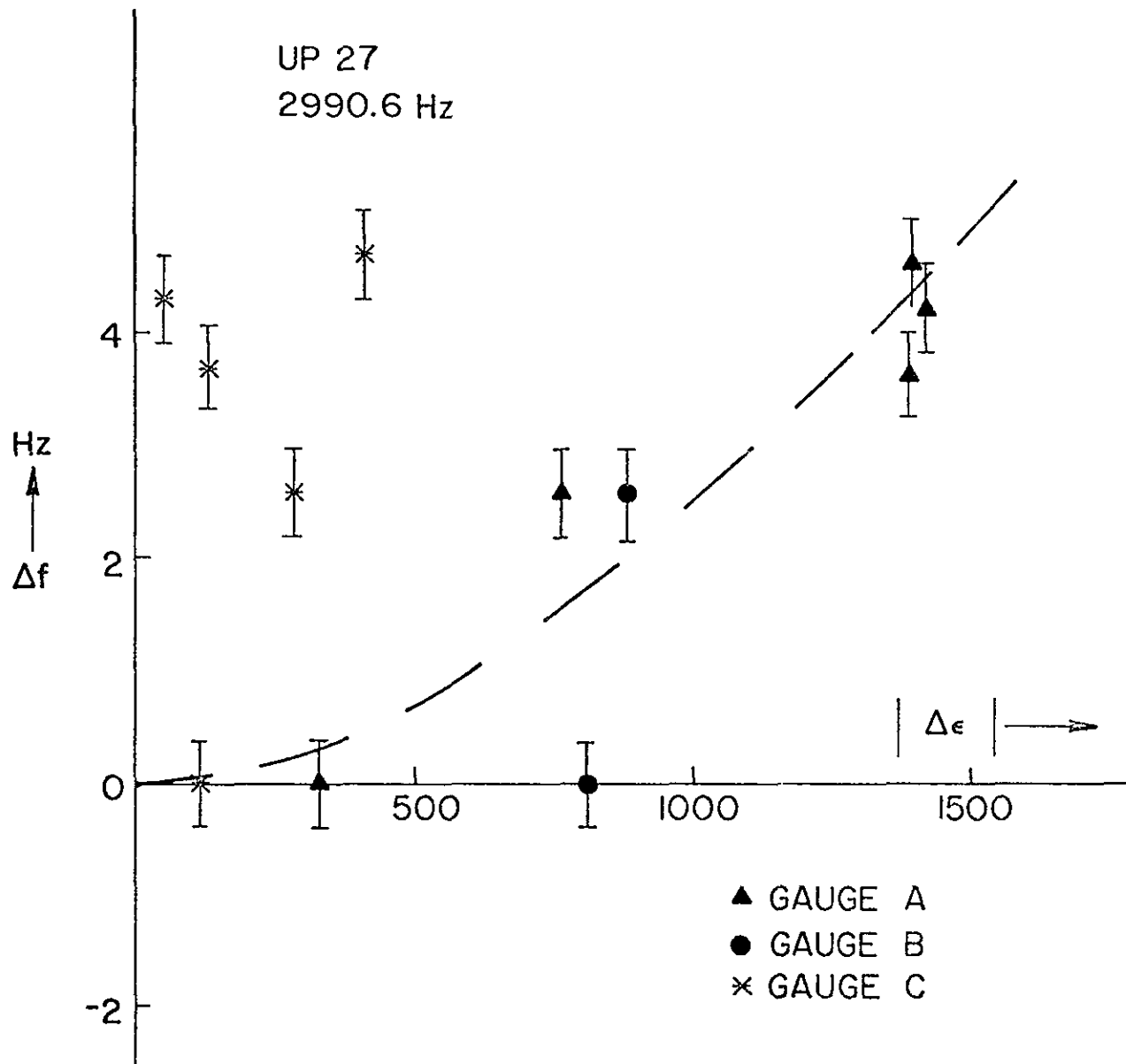
FIG. 4.3.10 FREQUENCY SHIFT Δf VERSUS STRAIN CHANGE
Δε AT 3 kHz FOR WHEELS UP 27 (FIVE DRAG
BRAKING STOPS.)
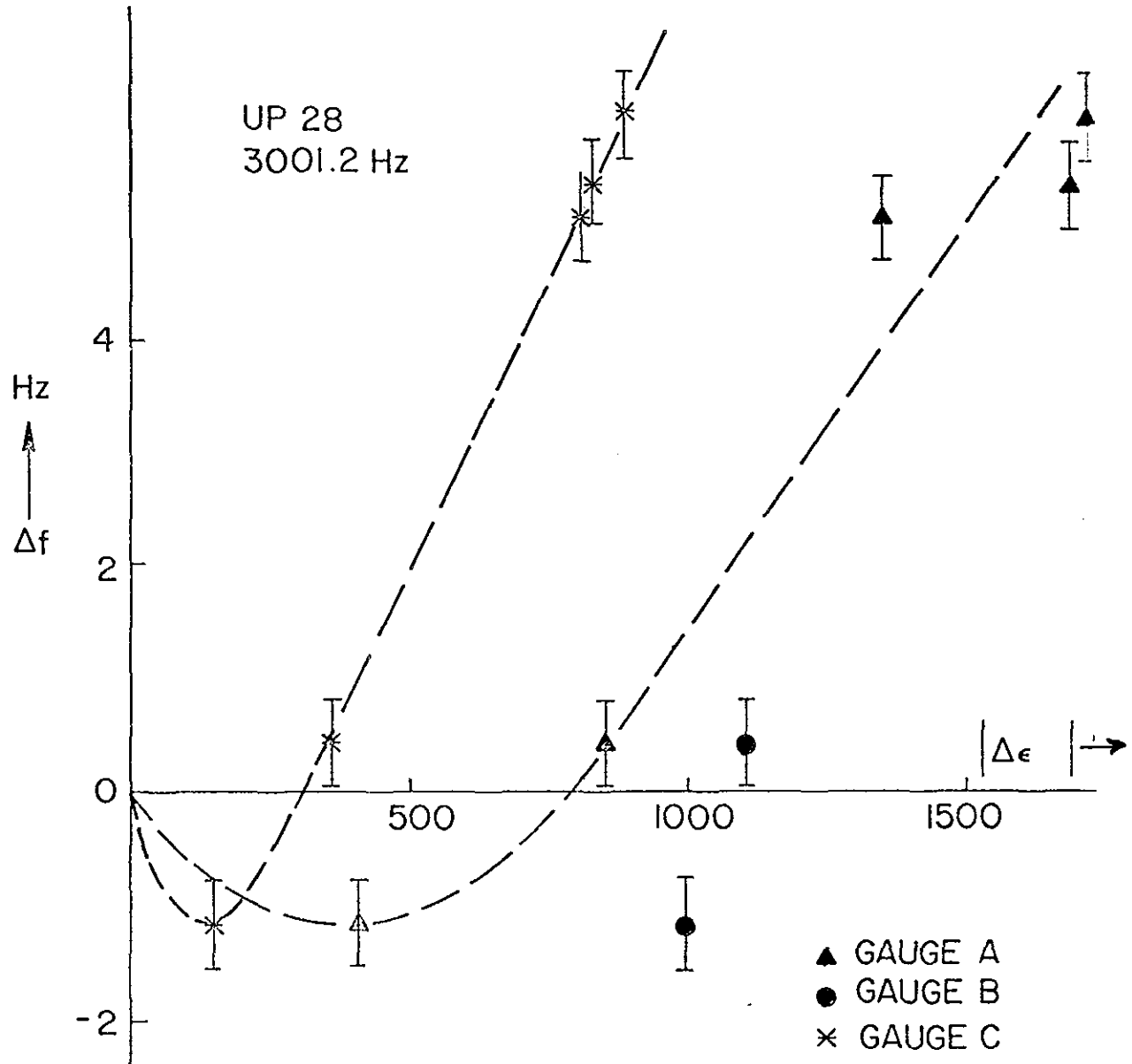
Fig. 4.3.11   Frequency shift Δf versus Strain
change Δε at 3 kHz for wheel
UP 28 (Five Drag Braking Stops)

28 and also on wheels UP 12, 17, 18 and 20 will give a
better understanding of the acoustic signature as a function
of the wheel stress conditions.

The changes in frequency are small, of the order of
a few Hz; hence a rather careful error analysis must be
made. Errors in the data collection and data processing
can be divided into error due to the tape transportation
mechanism of the recorder and errors in the signal processing.
The latter error depends on the sampling rate and time
duration of the signal, which for these analyses was
0.4 Hz. Equally or even more important is the error due
to the tape transport speed and fluctuation. Manufacturer's
data for the NAGRA IV at 15 in/sec indicate a maximum
$\pm$ 0.05% tape speed error which could give an error of
2.5 Hz at 5 KHz. If tape speed changes occurred during
the recording, the resonances ought to show frequency
shifts proportional to frequency. There are indications,
from comparisons of repeated impacts on the same wheel in
the same conditon, that if such an error occurred it was
much smaller than 0.1 Hz at 1000 Hz or less than 0.01%.

A significant experimental error might be included in
some of the Bessemer results. It is believed now that the
results for CJ36 wheels shown in Fig. 4.2.5 are more accurate
than those for CJ33 wheels shown in Fig. 4.2.6. The
maximum frequency difference should be about 10 Hz instead
of 25 Hz. There is no indication at this point of any
important error in the dynamometer test results.

5. SYSTEM COMPONENT DESIGN

5.1 Wheel Exciter

An ideal wheel exciter should:

1. Produce vibrational excitation in the range 0-10 kHz in all types of railroad wheels. The C-weighted intensity at 3 feet must equal or exceed 100 dB. Acoustic signatures resulting from the use of the exciter must be reproducible independent of train speed and not contain resonances other than those of wheels.

2. Induce vibrations in the wheel from a point of contact low on the wheel's rim or flange. This point of contact shall be independent of the train velocity.

3. Have an auxiliary power source (electrical or pneumatic) or be mechanically powered by the train. In the latter case, the exciter must not cause a vertical displacement of the wheel.

4. Excite wheels on both rails with train speeds of up to 45 MPH (for yard operations 10 MPH should be sufficient).

5. Not present a hazard to the train or to itself for train speeds up to 80 MPH (30 MPH for yard operations).

6. Be suitable for use at any railroad track location outdoors within the continental United States.

7. Be designed to comply with requirements for track-
    side apparatus now imposed by the railroads. This
    includes OSHA safety requirements for personnel.

8. Have a Mean Time to Failure such as to allow operation
    for 6 months under normal conditions without probable
    failure.

These specifications represent an ideal to be aimed
at. The designer is confronted with a large variety of
conceivable devices and many choices. In the feasibility
study [1] a mechanism driven by the wheel itself was used.
In the present work it was decided to explore the
feasibility of some alternative approaches and these are
categorized according to the power source. Since some
field experience had been obtained with the original
hammer mechanism it was decided to pursue this design
concept in parallel with the other studies to ensure that
at least one form of operating exciter would be available
for the field tests.

5.1.1 Mechanically Powered Excitation

The original version of the hammer exciter is shown
in Fig. 1.6.1. The device operates as follows: the
flange of the wheel depresses the plunger, 1, whose travel
is guided by the pin, 2. Thus the link, 3, starts to
rotate around the pivot point, 4. Due to this rotation
point A moves towards point B compressing the hammer
spring, 5. At low speeds this spring acts as an energy

storage device. When the torque about B due to the hammer

spring exceeds the torque due to the weight of the hammer the

spring starts to expand and drives the hammer up to impact

the wheel flange. At higher speeds (above 2.5 MPH) the

link, 3, actually impacts the roller 6 thus setting the ham-

mer into essentially free rotation until it impacts the

wheel. The hammer spring then does not contribute much to

the forward motion of the hammer but acts only to reset the

hammer following wheel impact. The forces of acceleration

and deceleration on the hammer mechanism can be very large

(see Appendix E). The associated stresses in this mechanism

probably were excessive in the device tested in Omaha in

1974, and led to its failure when activated by a fast train

passing over it. A tentative solution to this problem was

to make the entire hammer, and hammer mounting, a one-piece

unit cut from steel plate. In addition, the impacting face

of the hammer was heat treated to harden it against wear.

A view of the modified exciter is shown in Fig. 5.1.1.

This is the version of the hammer exciter used in the

field tests to be described in Section 6. It should be

noted that a full dynamic analysis of the hammer mechanism

remains to be completed. However, a simplified model is

discussed in Appendix E. Some snapbuckling mechanisms have

been proposed by Fazekas [41] and these devices were given

some consideration as means of achieving the requirements

of a wheel activated hammer. Although the conceptions are
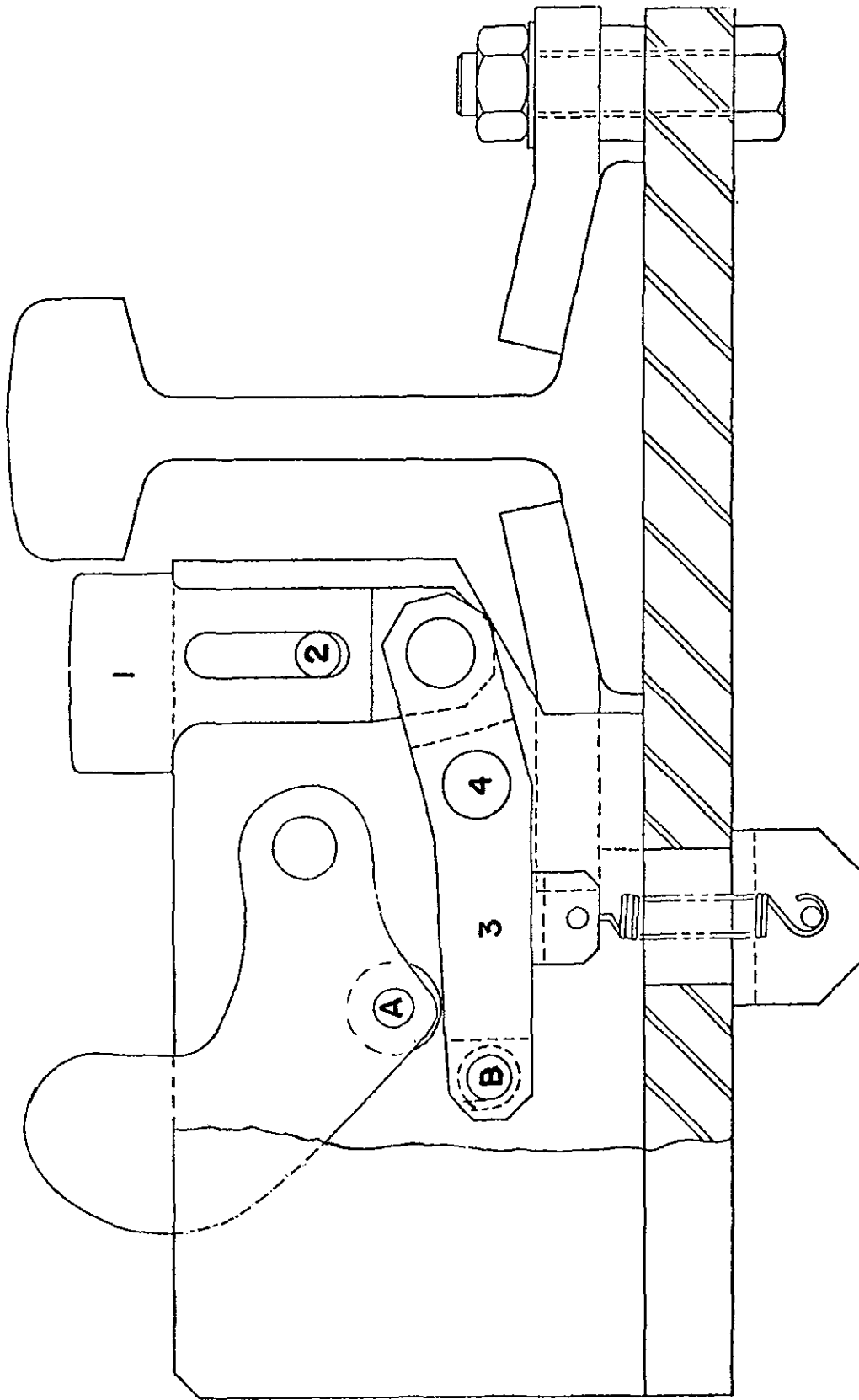
FIG. 5.1.1 DRAWING OF THE MODIFIED MECHANICAL WHEEL EXCITER

elegant, time and resources simply did not permit the design and construction of a working device.

5.1.2 Electrically Powered Excitation

An electric motor to spin two or more impacters, preferably 4, 8, etc., for balance reasons, against the rim of the wheel was also examined (see Fig. 5.1.2). The first tests were performed using a 1/4 HP 1725 rpm motor; in later tests a 1/2 HP universal-type AC-DC motor was used with speed controlled by a VARIAC. The motor exciter represents two significant departures from the hammer type exciter concept. It is electrically powered and therefore the impact is independent of the train speed. However, it may produce multiple impacts on the same wheel. The attraction of this design is its ability to produce impacts at train speeds up to 40-45 MPH and to survive at any train speed. It is a simple design but it must be well guarded for safety reasons. The electric motor and spinning impacter combination was tested on good, bad and greasy wheels. The preliminary conclusions on the feasibility of using this design were: a) the spectra obtained from the good, bad and greasy wheel are noticeably different, and b) spectra from the same wheel were reasonably reproducible.

An impacter to be actuated by a solenoid, such as an automobile starter, was also given some consideraton. However, the concept was not pursued since a triggering pulse would be required and this would involve further
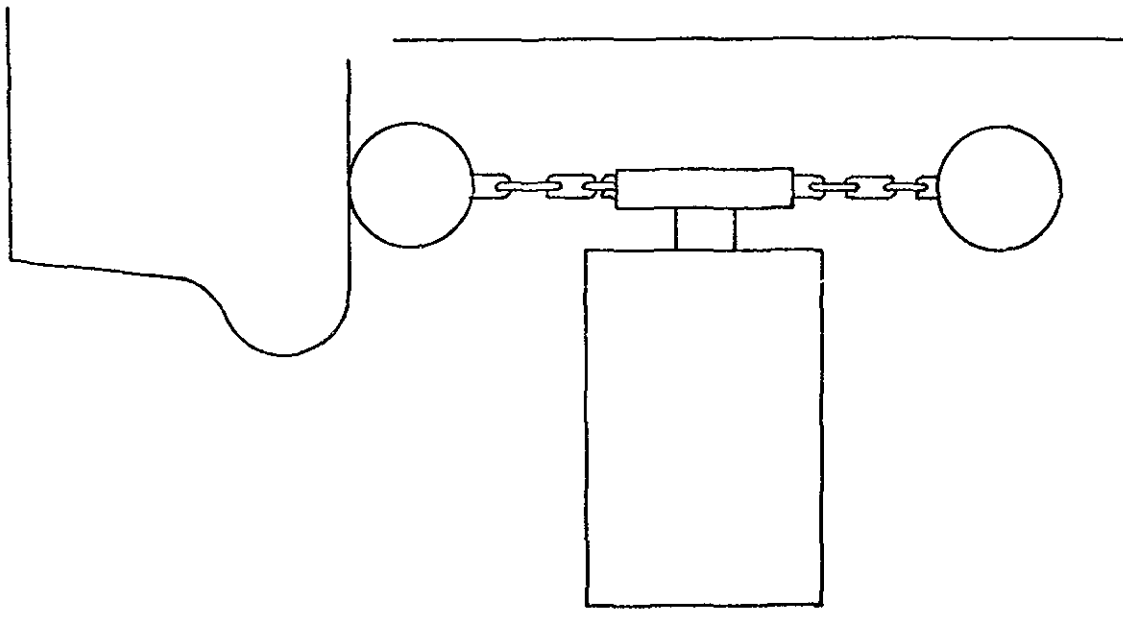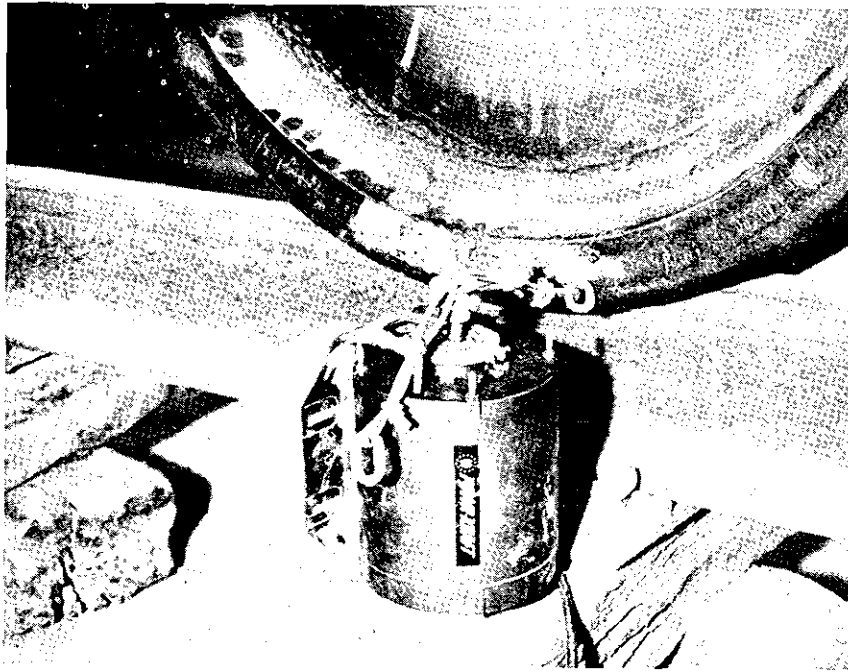
FIG. 5.1.2 MOTOR EXCITER, ROTARY

complication of the system. The motor exciter could be left running during the passage of a train.

5.1.3 Pneumatic Powered Excitation

Another concept examined was that of a pneumatic vibrator impacting a ramp depressed by the wheel flange. The main attraction of such an exciter is the ruggedness and the safety. Pneumatic vibrators are also commercially available in a variety of types, sizes and are low priced. A problem is the background noise of the hammer itself.

Pneumatic vibrators were obtained for preliminary testing of the feasibility of this type of wheel excitation. Included were large and small reciprocating piston types, and five different sizes of rotary vibrators. Testing involved holding each vibrator in contact with the wheel, and obtaining taped wheel signatures associated with differing points of contact and differing air pressures. These tapes were then analyzed using both the 1/3 octave band B & K analyzer and the Spectral Dynamics narrow band analyzer. The results of this investigation were: a) the large piston type vibrator was difficult to keep in contact with the wheel, and therefore no conclusions could be drawn; b) the small piston type vibrator produced usable wheel signatures which were reproducible and comparable in quality to those obtained by rolling ball impact; and c) the rotary vibrators did not excite a broad spectrum of the natural modes of vibration in the wheels. An explanation

for the failure of the rotary vibrators to excite the
wheels is evident in the fact that an off-center spinning
mass produces a frequency of vibration which is the
inverse of its orbital period. This is not comparable
with the rich spectrum of frequencies associated with
the delta function of an impacting mass. Consequently,
the rotary vibrators will only excite the few natural
wheel frequencies which are close to that of the vibrator's
frequency. The piston vibrator, on the other hand,
induces frequencies of vibration almost uniformly
throughout the 0-10 kHz band of interest.

To test the performance of a pneumatic vibrator
and mounting, a NAVCO model BH 1-1/4 impact type was
installed on a custom made leaf spring (K = 150 lbs/in)
which was mounted on the test track. The leaf spring
parallels the inside of one of the rails, with the
vibrator directly attached to the underside center of
the leaf spring. In use, the vibrator operates con-
tinuously. The wheel flange depresses the leaf spring
in passing over it and the impact vibrations are then
transmitted into the wheel. This design is attractive
for its simplicity and suitability for outdoor use.
As it was mentioned earlier the background noise level
produced by the pneumatic vibrator was high but a 6-8 dB reduction
was achieved through the use of an exhaust muffler and
damping compound applied to the vibrator and leaf
spring. Figure 5.1.3 shows the details of this design.

MODIFICATIONS REQUIRED TO MOUNT LEAF SPRING VIBRATOR WHEEL EXCITER TO TEST
TRACK. THIS DEVICE USES 80 PSI·REGULATED AIR SUPPLY. SECTION AA SHOWS A 5
AND 3/8 INCH STEEL BOLT WELDED TO INSIDE OF TRACK PARALLEL TO TOP OF TRACK.
SECTION BB SHOWS THE INSIDE BOTTOM OF THE RAIL CUT AWAY 1/2 INCH BEYOND THE
INSIDE EDGE OF THE TOP OF THE RAIL. THE CUT AWAY IS 5 INCHES LONG. SECTION
CC SHOWS 1/4 INCH STEEL PLATE WELDED TO THE INSIDE BOTTOM OF THE TRACK. THIS
ALLOWS THE FREE END OF THE LEAF SPRING TO FLEX WHEN THE SPRING IS DEPRESSED
BY THE WHEEL. THE LEAF SPRING IS 3 AND 1/16 INCHES WIDE. THE INSIDE EDGE
OF THE LEAF SPRING JUST TOUCHES THE INSIDE EDGE OF THE TOP OF THE RAIL.

A   B   C

3"

$19\frac{1}{2}$"   5"

36"

42"

℄ PIN
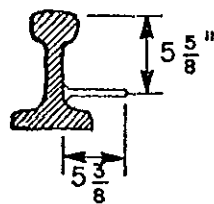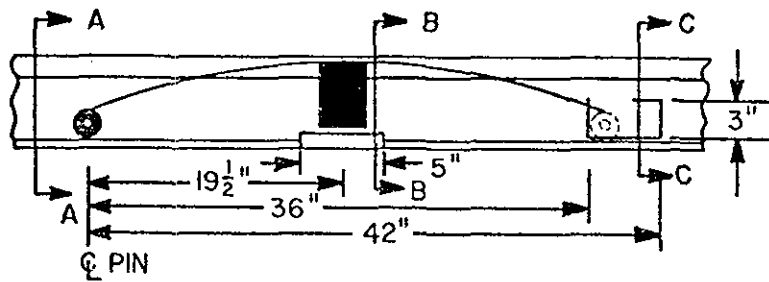
$5\frac{5}{8}$"   INSIDE OF TRACK

(BOLT IS 5/8 INCH DIAMETER)

$5\frac{3}{8}$

SECTION AA

$\frac{1}{2}$"

SECTION BB

-0
$+1/8$
$3\frac{1}{8}$"

$6\frac{1}{2}$"
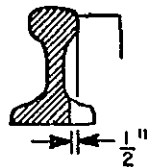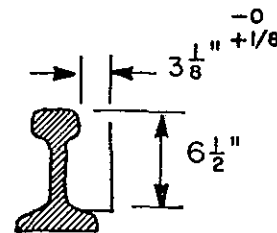
SECTION CC

FIG. 5.1.3.   PNEUMATIC   LEAF   SPRING   EXCITER

The problem with this type of design is that the
amplitude of the sound from a wheel rolling over the
leaf spring is much less than from the directly
impacting devices, such as mechanically and electrically
actuated hammers.

5.1.4 Comparison of Exciter Types

Table 5.1.1 is a summary of ratings of these various
types of exciters assessed according to the specifications
of an ideal exciter. The characteristics of the acoustic signa-
ture are given a higher weighting than the other specifica-
tions since if the device does not give a reproducible signature,
it is useless for the present purpose. Overall the
mechanical hammer appeared to be the best device to use
despite its dependence on wheel speed in its present
form. The pneumatic exciter was downgraded because of
the weakness of the signature intensity. The electric
motor driven impacter was downgraded slightly as regards
signature because of the problem of multiple impacts
and because of possible safety problems. It would also
present a profile above the top of the rail. As a
result of these considerations it was decided to use
the modified hammer exciter in the field test.

5.2 Wheel Sensor

The search for a device to be used to generate a
trigger pulse was restricted to three possible types:

TABLE 5.1.1 RATING OF 3 EXCITER TYPES AGAINST IDEAL SPECIFICATIONS

SPECIFICATION	MECHANICAL HAMMER	PNEUMATIC VIBRATOR	ELECTRIC MOTOR
Signature	5 x 2	1 x 2	4 x 2
Contact Point	4	4	4
Operational to 45 mph	3	4*	4*
No Hazard at 80 mph	3	3*	4*
Weather Resistant	4	4*	3*
Safety	4	4*	2*
Mean Time to Failure	3	4*	4*
TOTAL	32	25	29

Note the quality of the signature is rated twice as important as other considerations.

5 = Excellent
4 = Very Good
3 = Good
2 = Fair
1 = Poor

*Rating based on surmise, rather than experience.

a) microswitches, b) photosensors, and c) commercially
available metal sensors. Microswitches had already
been used in an earlier test. Their performance could
be rated as moderate because they are susceptible to
rough operational conditions. Stable mounting of the
microswitch on the track or exciter was also a problem
due to vibrations induced by the train rolling over it.
Electric contact noise was another problem, although it
could be eliminated with proper electronic filtering.
Photosensors would be an ideal solution if they could
survive the dirt of the yard and severe weather con-
ditions. In the third class the best available wheel
sensor system appeared to be the DUAL DIRECTIONAL WHEEL
SENSOR by ACI, since many engineering problems had been
solved in its development. It has solid state circuitry,
which is shock mounted and temperature independent from
$-40°$ to $+140°F$. It has a waterproof casing and is easily
installed and adjusted. The wheel speed can range from
0 to 80 MPH. The operation of the wheel sensor is based
on the principle of magnetic flux change in a coil to
detect the presence of a wheel. The device has two
sensing units to determine wheel direction. During the
present tests only one unit was used because the
direction of wheel travel was not needed. The basic
elements of each sensor unit are a permanent magnet as
the source of the magnetic flux and a coil whose inductance

changes when a wheel is present due to the

change in the magnetic flux in the core of the coil.

The unit is also equipped with a light-emitting-diode

(LED) which stays on when the sensor indicates a wheel

presence and which can be used to check if the sensor

is functioning. The output voltage circuit is shown in

Fig. 5.2.1. In this figure, S1 is a solid state relay

whose contacts close in the presence of a wheel and are

rated for a maximum current of 25 mA at 24 VDC. The

triggering pulse was the voltage obtained across the

resistor R2 = 1200 Ω. For tape recording, the voltage

E was about 3.0 Volts, for direct real-time sensing it

was about 4.5 Volts.

5.3 Microphone

General Radio had recently introduced a weatherproof

microphone system for outdoor noise monitoring. This

microphone system is shown in Fig. 5.3.1a. The micro-

phone element is an electret condenser random incidence

microphone. It has flat response, wide dynamic range

and high sensitivity. It also has a permanently charged

diaphragm so it does not require a polarization voltage

and it does not become noisy in a humid environment.

The General Radio system includes a preamplifier after

the microphone element to transform the impedance from

high to low, so that long cable can be used. The first

outdoor test of the microphone in Pueblo, Colorado under

very dry and cold weather conditions was satisfactory
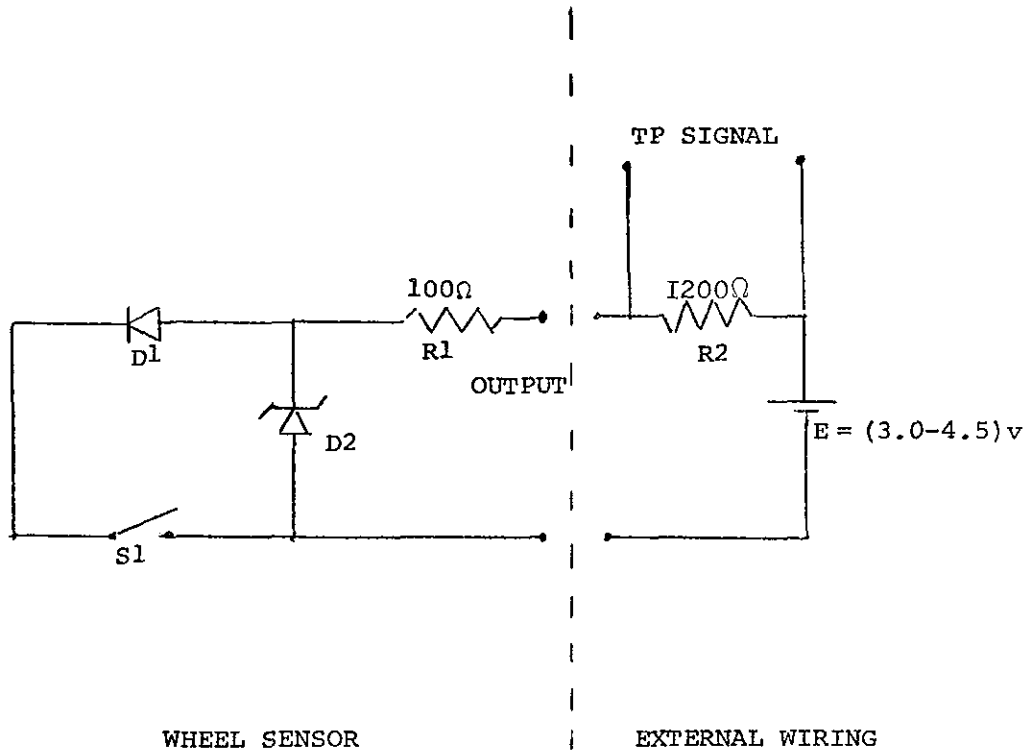
FIG. 5.2.1 OUTPUT VOLTAGE CIRCUIT OF THE WHEEL SENSOR
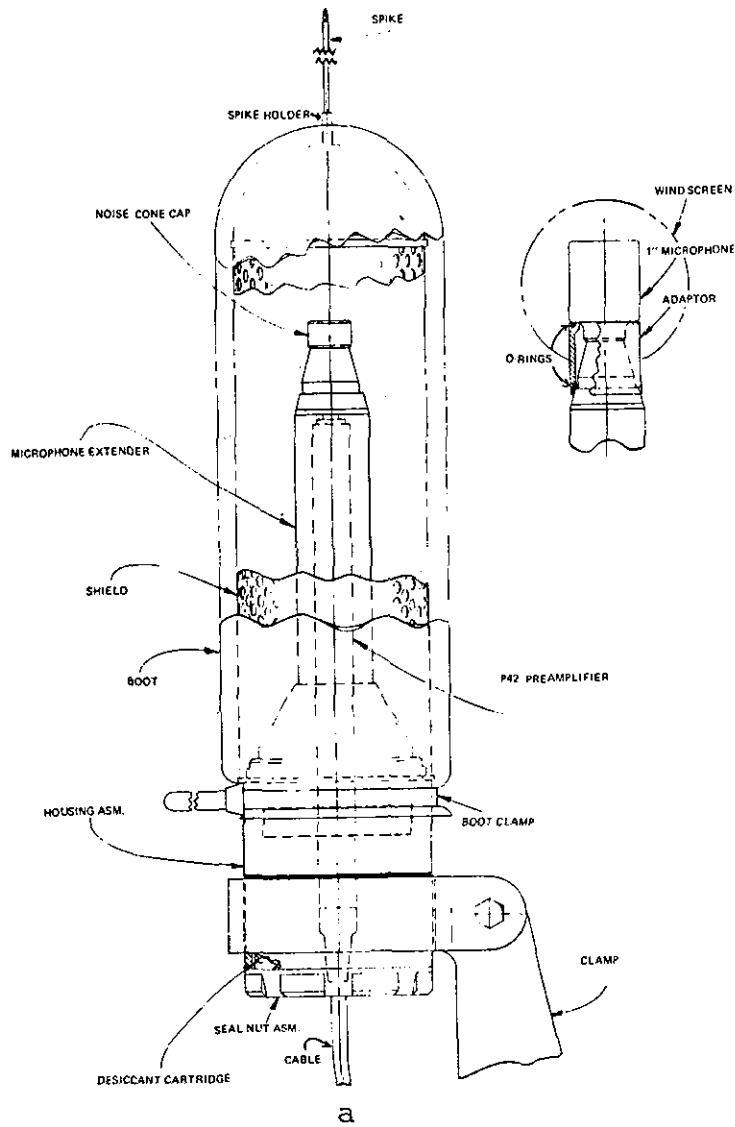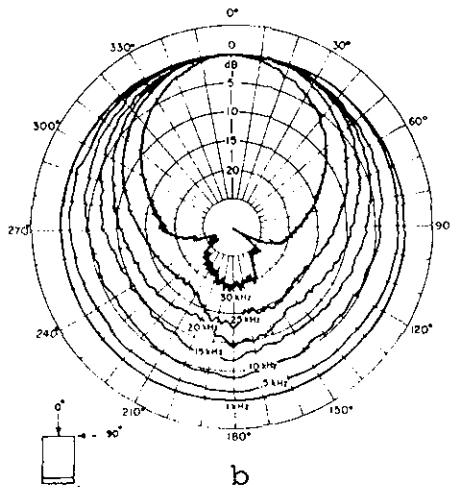
FIG. 5.3.1a ASSEMBLY OF WEATHERPROOF MICROPHONE
b DIRECTIONAL RESPONSE PATTERNS FOR THE GR ½ INCH
ELECTRET-CONDENSER MICROPHONE

and encouraged the acceptance of this type of microphone
for the final field test. The only negative aspect
was the need for a power supply for the microphone's
preamplifier. A directional microphone would have been
a better choice than the random incidence type actually
used. The directional response patterns of the present
microphone are shown in Fig. 5.3.1b. The system used in
the final field test included two microphones installed
on either side of the track. The sound signals go into
a microphone mixer whose output goes to a filter
and then to the real-time analyzer.

5.4 Spectrum Analyzer, Computer and Diskette Interfacing

The most important parts of the system are the
real-time analyzer (RTA) and the mini-computer. At the
present time there are basically two ways to extract
frequency information from a sound signal: a) using an
analog to digital (A/D) converter and subsequently
analyzing the digitized signal through the use of
computer software or b) using a RTA. The selection of
the proper device is based on the duration, frequency
range, amplitude, type (transient or stationary) of the
signal and the frequency resolution of the analyzed
spectrum. Different commercial devices have similar
specifications and it is hard to select the best. Rapid
improvements and development of these products make the
selection even more complicated.

A NOVA 1220 computer interfaced with a 39 channel,
1/3 octave band analyzer had already been used in previous
wheel testing by Nagy [1] and Dousis [4]. Some spectral
analysis had also been done using a Spectral Dynamics
model 330A real-time analyzer on loan from the Company
for a short period of time but without any digital inter-
facing. The cost of the SD330A, its fast signal analysis
for the frequency range needed in the tests and the
familiarity of the researchers with it led to the
selection of this device as the spectrum analyzer for
the system. However the use of an A/D converter should
be given serious consideration as a part of a prototype
system. Some advantages and disadvantages of the SD330A
analyzer in respect of transient signal analysis will
be presented in the appropriate chapter.

The computer for the system was a 16K NOVA 1220.
Because of the medium memory size of the computer the
bulk of the software was written in BASIC language.
The digital output of the SD330A analyzer was interfaced
with the NOVA's I/O board according to Table C.1 in
Appendix C.

The next major task after the interfacing was the
development of NOVA computer software needed to operate
the analyzer and retrieve data from it. To accomplish
this the following software was written:

1. Assembly subroutines for control of the SD330A
    analyzer, including the following commands: start,
    stop, peak, cursor/plotter, sweep or reset [35].

2. Assembly subroutines for use of the NOVA Real-Time
    Clock.

3. Assembly subroutines to read and operate on individual
    spectra (250 channels) from the SD330A using the
    slow speed plotter output mode.

4. Assembly subroutines to read, print, and operate
    on individual spectra in the high speed (53 ms)
    output mode, i.e., levels from the 250 channels
    are sequentially read in 53 ms directly into core
    memory.

5. Assembly subroutines to store complete spectra in
    NOVA core memory in sequential order.

6. BASIC language programs to call the above Assembly
    subroutines for processing spectra.

The core memory requirement for a single spectrum
is 250, 16 bit, words. After the BASIC interpreter
and the program was stored in the memory, 3K of core
was available for data, which means only 10 spectra
could be stored in the computer. Approximately 5 ms
are required to retrieve one data word for
processing. Retrieval of two complete spectra
for an across-the-axle comparison takes about 2.5
seconds which does not include the analysis program
execution time.

Considering this relatively long execution time for BASIC instructions, it was concluded that the analysis for wheel fault detection would not be done immediately following reading the spectra as the train cars pass over the exciters. (For a car speed of 10 MPH, wheels on the same side of a truck will pass over the exciter in approximately 0.4 seconds). Thus it appeared that the analysis ought to be done in near real-time, i.e., immediately after the last wheel spectra is read into the computer. Furthermore, since core memory was limited to approximately 1 car, and since additional core memory boards would not greatly increase this capacity to store wheel spectra, a peripheral memory device of several hundred thousand word capacity was needed if long trains were to be scanned with this apparatus. The speed of data transfer from the SD330A of 4717 words per sec is too fast for the NOVA Cassette which writes at 800 words per second. A Data General Diskette unit, model 6031 was the best technical choice having a transfer rate of approximately 16,000 words per second and a storage capacity of 157,696 words. The track to track head positioning time is 20 ms. Eight spectra may be stored per track. The assembly routines for data transfer from the computer to the Data General Diskettes and retrieval are presented together with the rest of the software in Appendix C.

5.5 System Description and Software Development

The general configuration of the system for railroad wheel inspection is as shown in the layout of Fig. 5.5.1. Airborne sound or vibrations of the test object were detected using a microphone or an accelerometer respectively. The signal was preamplified near the transducer, and then filtered for further signal processing. In the field tests it was recorded in channel No. 1 of a dual channel tape recorder. The triggering pulse was recorded in channel No. 2; this being very important because timing reference and information are essential for short duration transient signals, such as impact recordings. The tape recordings were later analyzed in the laboratory. In the Englewood Yard test the signal could be both recorded and processed in real time. The sound signal was fed into the analyzer for Fourier analysis. During the early stages of the project no digital interfacing and control were available, hence precise data sampling was impossible due to timing errors, and data collection was slow. The analyzer was then operated in the PEAK, STORE mode, because that was the only way to avoide the timing problems. In the peak mode the maximum response of the test object was obtained on the analyzer's screen and it could be traced on the X-Y plotter for permanent record and inspection. Numerical data were taken sweeping the spectrum, through the CURSOR, manually.
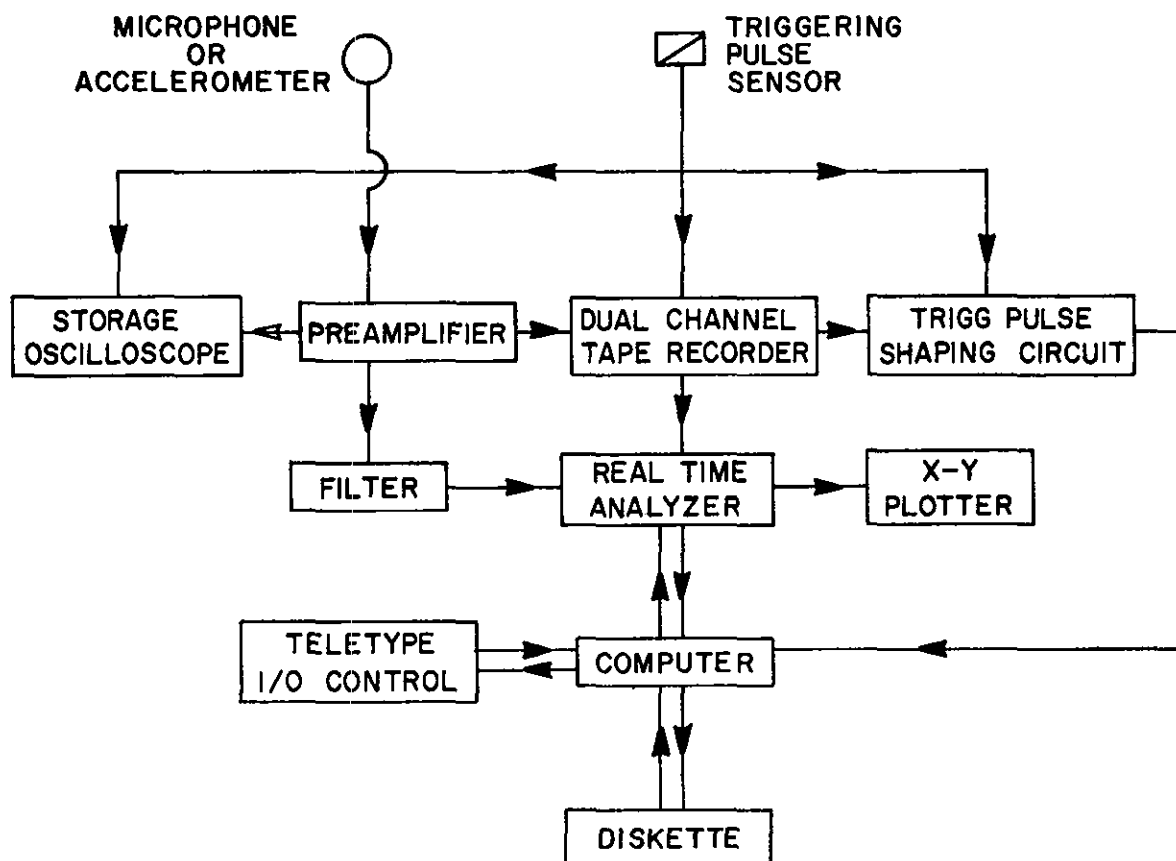
FIG. 5.5.I SCHEMATIC OF DATA COLLECTION AND PROCESSING HARDWARE

One disadvantage in the case of impact analysis using the PEAK mode is the presence of the shock wave produced during the impact together with the response of the test object. This means that the spectrum obtained includes the Fourier components of the shock wave, which theoretically is a continuous spectrum. In practice though (narrow band analysis), it does not appear as continuous, but as a very dense low amplitude line spectrum. When another mode is used such as EXP. AVG. (exponential average) or START where the spectrum in the analyzer's memory is the sum of N successive analyzed spectra divided by N, the number of averages selected, these peaks disappear rapidly due to the short duration of the shock.

One of the recognition and decision schemes used early in the project was line spectra comparison. The line spectrum of a signal is a representation of its spectrum with lines at the resonances whose amplitude is above a certain level. An example of a line spectrum is shown in Fig. 1.4.2. From the finite element analysis studies it was known that a good wheel has fewer resonance lines compared to the same type of defective wheel. Another characteristic is the frequency shift in some of these resonances in defective wheels of the same structure and geometry. Therefore, comparison of good wheels of the same type should give identical or well matched line spectra, whereas a good to bad wheel comparison ought to show significant line mismatching.

During the first experiments line spectra acquisition
was done manually using the X-Y plots of the acoustic
signatures. An example of these results is shown in
Table 5.5.1. The first column of the table has the
wheel code; the second, the wheel description. The
third column has the total average number of lines based
on three or four signatures from impacts on the same
or different points on the rim of the wheel. The fourth
column has the number of common lines between these
spectra and represents the "average" line spectrum of
the wheel.

As an example, the first axle tested had good 33"
cast, single wear wheels. Three different impacts
(signatures) on the same point showed an average of 38
lines on both wheels. On the east side there were 28
common lines, on the west side, 32. Finally, there were
19 lines common to both sides (fifth column). In the
case of a good 33" wheel compared to a 33" wheel with
a partial crack, the number of matched lines was 11, and
comparison between the partially cracked wheel and the
one with the large crack indicated only 4-7 common lines,
although for some lines it was difficult to see if they
had identical frequencies or if there was a one channel
shift. The line spectra comparison procedure was later
automated using BASIC/ASSEMBLY language software.
Analyzing taped acoustic signatures with the above
software, results were obtained as shown in
Table 5.5.2. Important conclusions were obtained from

TABLE 5.5.1

SUMMARY OF THE LINE SPECTRA ANALYSIS
(RESULTS OBTAINED MANUALLY FROM SPECTRA PLOTS)

WHEEL CODE	WHEEL DESCRIPTION	NUMBER OF SPECTRAL LINES (AVERAGE OF 3 OR 4 SPECTRA)	NUMBER OF COMMON SPECTRAL LINES	NUMBER OF COMMON LINES FROM WHEELS ON THE SAME AXLE	REMARKS
SP1E	GOOD 33" CAST 1W	38(3) Same Point	28		
SP1W	GOOD 33" CAST 1W	38(3) Same Point	32	19	Same Axle
15 A	LARGE PLATE CRACK	42(4) Diff. Point	24		
15 C	PARTIAL PLATE CRACK	41(4) Diff. Point	30	6 - 7	Same Axle
15 A	LARGE PLATE CRACK	45(3) Same Point	28		
15 C	PARTIAL PLATE CRACK	44(3) Same Point	31	4 - 7	Same Axle
15 C	PARTIAL PLATE CRACK	40(4) Diff. Point	28		
SP1W	GOOD 33" CAST 1W	41(4) Same Point	32	11	Diff. Axle

TABLE 5.5.2

SUMMARY OF THE LINE SPECTRA ANALYSIS
(TESTS WERE COMPUTER CONTROLLED)

Number of Wheels Tested	% Range of Lines Matched Between Two Signatures	Remarks
18	70-100	Same wheel-same point. All good wheels.
18	40-90	Wheels across the same axle. All good wheels.
14	10-50	Good/Bad wheel, across the same axle.

these tests:

a. There is some overlapping in the percentage of
    matched lines in good/good and good/bad wheels.

b. Large defects (plate cracks) showed a 10-20% line
    matching and therefore should be easily detected
    under this scheme.

c. A comparison was made between the spectra of two
    good wheels on the same axle, one having a very
    worn flange. A low matching percentage of about 30%
    was found.

d. A change in the input attenuation by a few dB caused
    a different percentage of matching. This was to
    be expected, because it changes the discrimination
    window.

e. Small defects, such as thermal cracks, had 50% or
    higher of matching lines.

f. The Line Spectra comparison scheme could not be
    used alone for detection of defective wheels.
    Thermal cracks would be difficult to detect and
    small changes in the wheel geometry, such as worn
    flanges, would appear as defects.

The BASIC software developed for the Englewood Yard
tests is given in Appendix C. A simplified general flow
diagram is shown in Fig. 5.5.2. The most important change
from earlier versions was to base the decision on
consideration of several factors: the number of coincident
resonances, the amplitudes of signals in the same spectral

```
            ┌─────────────┐
            │    START    │
            └─────────────┘
                   │
                   ▼
      ┌──────────────────────────┐
      │ READ, PRINT PROGRAM      │
      │ PARAMETERS               │
      └──────────────────────────┘
                   │
                   ▼
      ┌──────────────────────────┐
      │ READ ALL SIGNATURES FROM │
      │ RTA TO COMPUTER DISKETTE │
      └──────────────────────────┘
                   │
                   ▼
      ┌──────────────────────────┐
      │ READ-OUT ACROSS AXLE     │
      │ SPECTRA                  │
      └──────────────────────────┘
                   │
                   ▼
      ┌──────────────────────────┐
      │ DATA PROCESSING FOR TWO  │
      │ WHEELS ON THE SAME AXLE  │
      └──────────────────────────┘
                   │
                   ▼
             IS THIS
   YES    THE LAST AXLE    NO
            TESTED ?
```
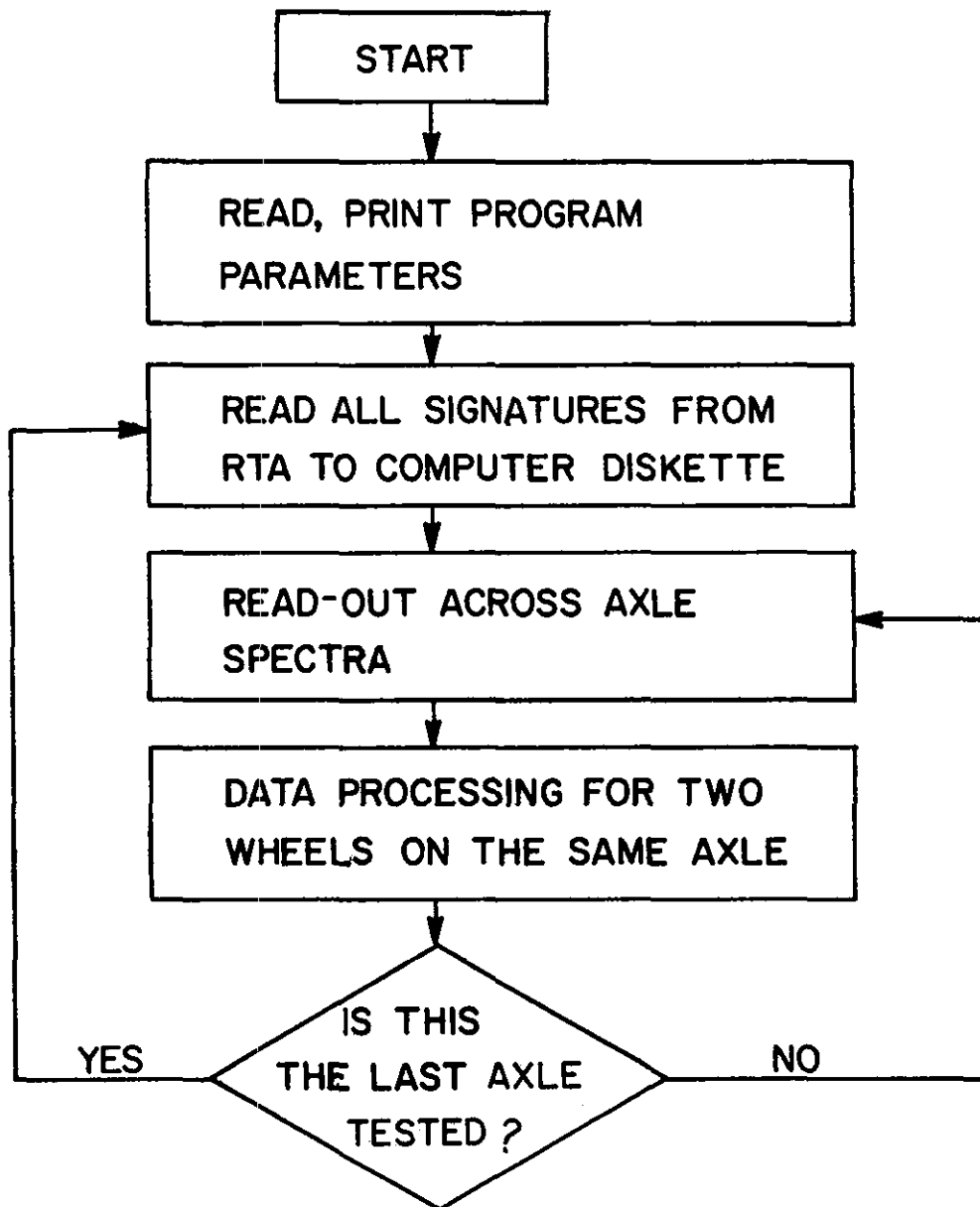
Fig. 5.5.2   Flow diagram for the Series
of Computer Programs used in the
SP Englewood Yard, Houston Tests

range and the decay rates of sound from the two mating

wheels. A number, called the difference index (DI) was

computed as follows:

$$DI = C_1 SD + C_s (1/SP_1 + 1/SP_2) + C_3 (DR_1 - DR_2)$$
$$+ C_4 (DR_1 + DR_2)$$

where C_1, C_2, C_3 and C_4 are weighting coefficients.

SD is the sum of the absolute value of the dif-

ferences between corresponding channels ignoring

3 channels at common resonances. (Resonances are

found using subroutines from the line spectra

comparison program).

SP1 is the sum of all channels for the spectrum

of wheel No. 1.

SP2 is the sum of all channels for the spectrum

of wheel No. 2.

DR1 is the decay rate for wheel No. 1.

DR2 is the decay rate for wheel No. 2 (across the

axle).

Some comments on the terms of this empirical formula

are in order.

1. The first term SD. This is the most important term

and the decision is based mainly on the value of SD.

The amplitude of the resonances depends on the impact,

and spectra from the same wheel under different

impact forces, at the same impact point will give

spectra of varying resonance amplitude. To reduce

the error introduced because of the intensity of the

impact, the differences between the spectra are ignored at common resonances and the differences of the two channels adjacent to the peak are also ignored.

2. The second term, 1/SP1 + 1/SP2. SP1 and SP2 are the sums of all channels for each wheel. Good wheels have low damping compared to defective and greasy wheels, and in that case SP1 and SP2 are large numbers and have small inverse values.

3. The third term, DR1-DR2. Good wheels have low decay rates and hence this term is then a small number. Greasy wheels have significant DR, but they are usually both greasy on the same axle and again this term is small. Only in the case of good/bad wheel pairs does this term contribute to the difference index.

   The decay rate (DR) is defined as the number of channels, K2, which dropped more than L2 dB (L2 = 8 dB in these tests) between the first and second reading, divided by the number of channels, K1, which exceeded P4 dB (P4 = 8 dB in these tests).

4. The fourth term, DR1 + DR2. This term is small when wheels are good, and large in cases of greasy or defective wheels. To separate defective from greasy wheels a subroutine checks the pattern of the signature. If the high frequencies are damped more than the low, this is an indication that the wheel is greasy.

The flow diagram of the READ and acoustic signature sections of the main program is shown in Fig. 5.5.3. Details of the flow diagram of the data processing section of the program are shown in Fig. 5.5.4.

A sample of the computer printout is shown in Fig. 5.5.5. The operator types RUN on the teletype, the date and number of the test, then the computer starts printing information about identification of the program and values of the parameters. The program calls for the time and number of the tape where the test will be recorded. At this point, being ready to start collecting data, the execution goes to a subroutine which checks for a trig-gering pulse. After sensing the TP, the RTA starts sampling and processing the sound signal in the Exponential Average mode for 150 ms, the values on the 250 channels of the analyzer being transferred to the computer through the digital interfacing. A second spectrum is read into the computer 150 ms later (300 ms after the TP). Comparison of the two spectra gives the decay rate of the sound. Following that the two spectra are stored on the diskette, a process which can take from 40 to 200 ms. The computer then gets ready for a new reading, which will start with the next TP. Although the maximum time interval required for one signature is 500 ms, the average is about 385 ms.

When all the signatures initially asked for have been received, the computer calls for the car I.D. For
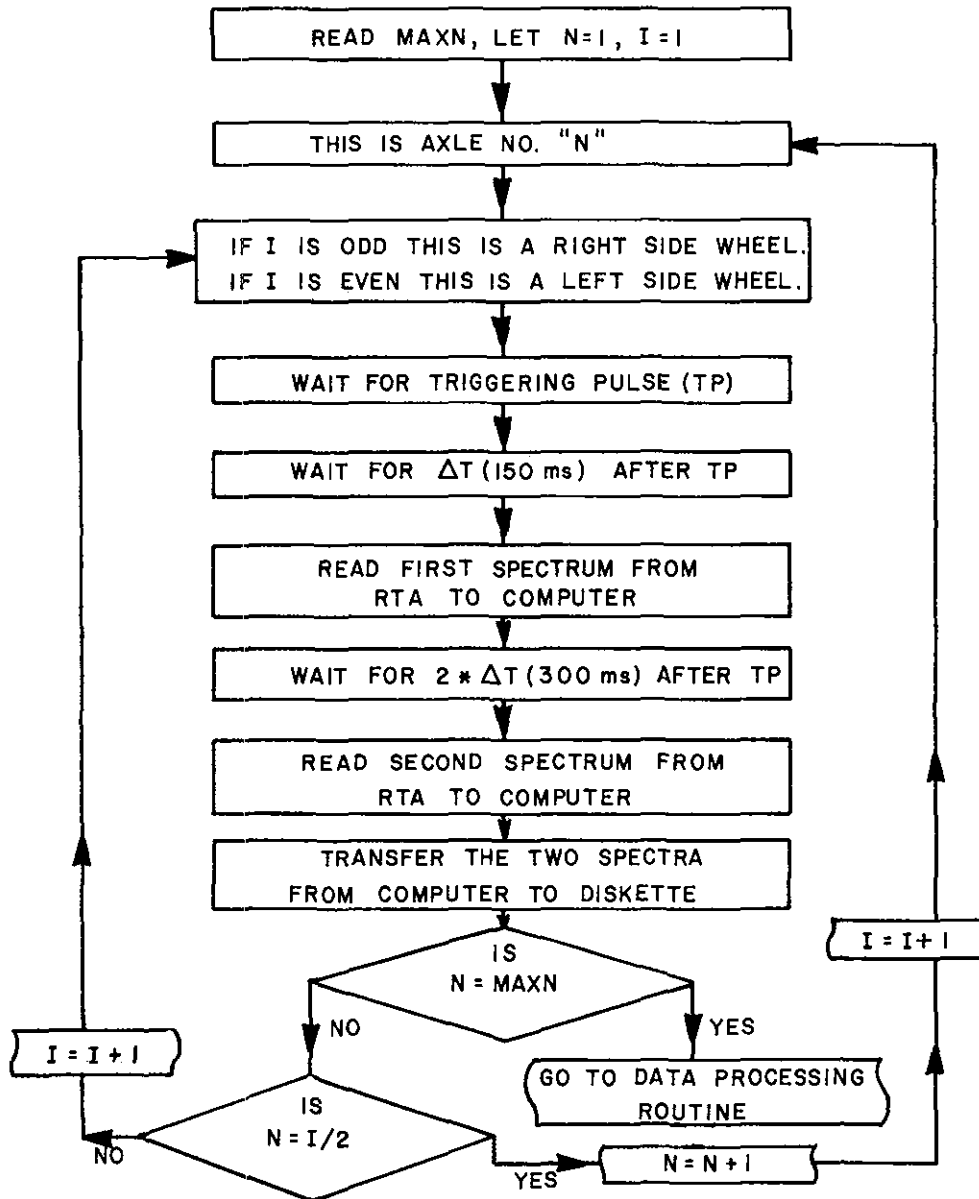
FIG. 5.5.3 FLOW DIAGRAM OF THE READ
ACOUSTIC SIGNATURES PART OF THE
MAIN PROGRAM.

FROM READ ROUTINE

RETURN TO READ ROUTINE

LET N = I , I = I

IF I IS ODD, IT IS A RIGHT SIDE WHEEL
IF I IS EVEN, IT IS A LEFT SIDE WHEEL

READOUT SPECTRA FROM AXLE N₀ N
$SP_{N,I,\Delta T}$ AND $SP_{N,I,2\Delta T}$

NO

IS N=N MAX

YES

EVALUATE THE DECAY RATE $(DR_{N,I})$

PRINT VARIABLES FOR $DR_{N,I}$

OBTAIN LINE SPECTRUM

IS N = $\frac{I}{2}$

NO

I = I + I

3

OBTAIN SUM OF DIFF (SP) FROM ACROSS AXLE SIGNATURES
OBTAIN SUM OF ALL CHANNELS RIGHT WHEEL SPI
OBTAIN SUM OF ALL CHANNELS LEFT WHEEL SP2

PRINT CI*SD , C $SP_{N,I}$,
C * $SP_{N,2}$

EVALUATE DIFFERENCE INDEX (DI)
$DI = C_1 * SD + C_2\left(\frac{I}{SPI} + \frac{I}{SP2}\right) +$
$+ C_3 \left|DR_{N,I} - DR_{N,2}\right| + C_6(DR_{N,I} + DR_{N,2})$

2

FIG. 5.5.4.   FLOW DIAGRAM OF THE DATA PROCESSING SECTION
OF THE MAIN PROGRAM
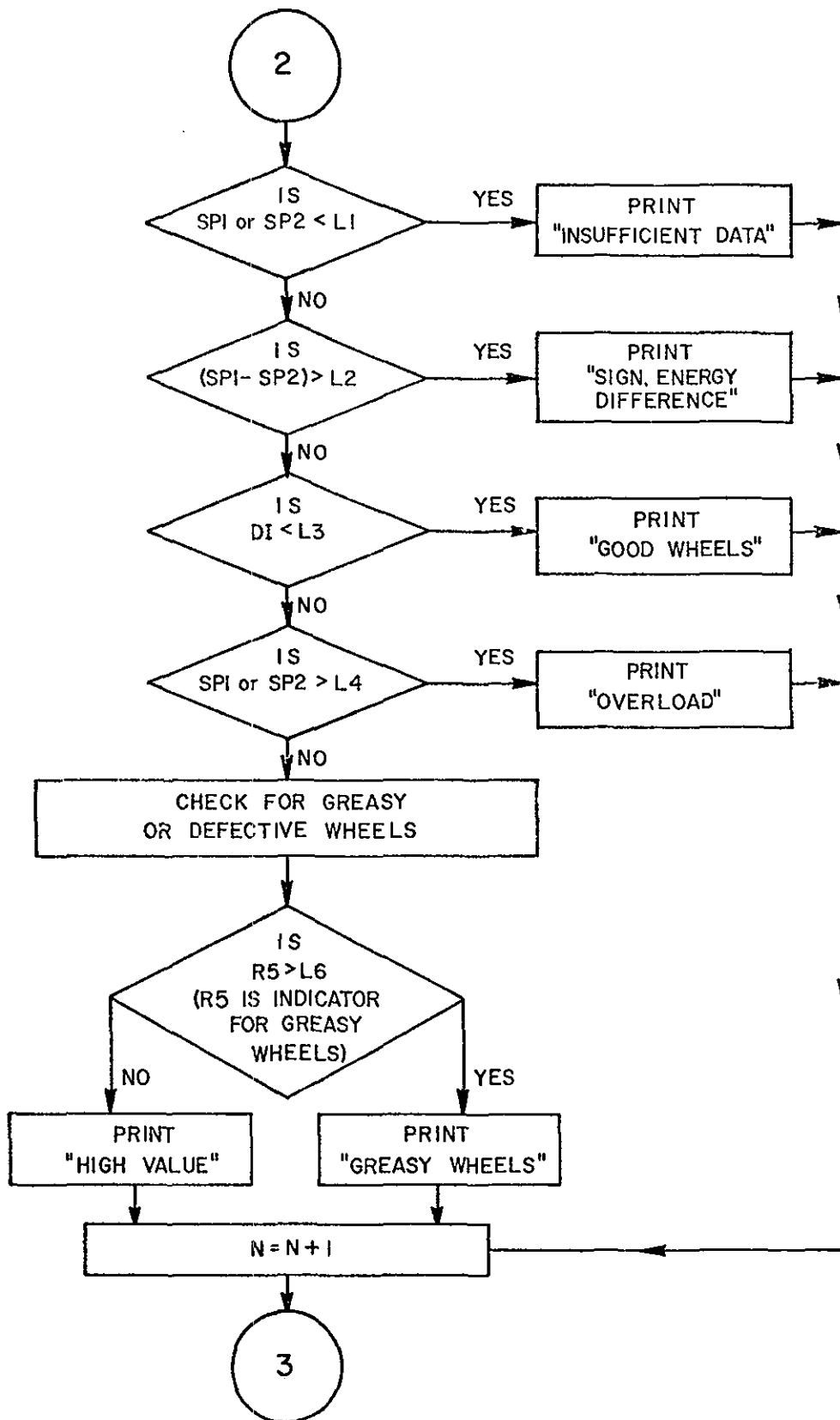
NOTE: LI, L2, ······ L6 ARE INPUT PARAMETERS

FIG. 5.5.4 (continued)

```
RUN 770712-IV
----------------------------------
     T-562-VIII
     EXP. AVG.
  SPECTRA PROCESSING ROUTINES
 ENGLEWOOD YARD TESTS-JUNE 77
  +ASSEMBLY A-140-IX
    12 JULY 1977
----------------------------------

NUMBER OF CHANNELS; 250
NUMBER OF SPECTRA ; 24
FREQUENCY FACTOR  DBAND HZ; 40
DISCRIMINATION LEVEL; 8
D.INDEX DECISION LEVEL; 85
DATE-TIME? 12 JULY 77  15:10:0\? 0
TAPE#? 180
CAR I.D.? TP 78217CL/SSW 79457 CL/ATSF 81338 CL\? 1
J1,K1,K2  0   162   34
J1,K1,K2  1   157   48
 472   39   45   57
```

TEST	SP1	SP2	ID.INDEX	REMARKS
1	188	111	61	GOOD WHEELS

```
J1,K1,K2  0   140   12
J1,K1,K2  1   180   64
 573   47   51   62
```

TEST	SP1	SP2	ID.INDEX	REMARKS
2	239	182	75	GOOD WHEELS

```
J1,K1,K2  0   187   11
J1,K1,K2  1   173   52
 956   79   83   91
```

TEST	SP1	SP2	ID.INDEX	REMARKS
3	274	130	103	SIGNIFF. ENERGY DIFF.

```
J1,K1,K2  0   173   26
J1,K1,K2  1   168   47
 638   53   58   63
```

TEST	SP1	SP2	ID.INDEX	REMARKS
4	176	160	74	GOOD WHEELS

```
J1,K1,K2  0   157   23
J1,K1,K2  1   145   19
 708   59   64   70
```

TEST	SP1	SP2	ID.INDEX	REMARKS
5	234	137	70	GOOD WHEELS

```
J1,K1,K2  0   155   11
J1,K1,K2  1   193   39
 816   68   72   78
```

TEST	SP1	SP2	ID.INDEX	REMARKS
6	238	157	84	GOOD WHEELS

FIG. 5.5.5 SAMPLE OUTPUT OF THE MAIN PROGRAM

long train cuts the first and last car I.D.s were given,
and thus intermediate cars could be identified by consulting
the consist lists. For short tests, of two to four cars,
all I.D.s were typed. Data processing then begins by
retrieving from the diskette the spectra of wheels across
the axle. The decay rate is evaluated from the two
readings with a 150 ms interval.

In order to test the efficiency of the system and
the software, recordings made during the 1975 field test
described in Section 1.8 were analyzed. The distribution
of difference index for 2 runs (Run #21, 23) is shown
in Fig. 5.5.6. The circles indicate a defective wheel.
The distribution of difference index for the same run
(Run #10) for 3 different sampling time intervals is
also shown in Fig. 5.5.7. The analyses indicated better
discrimination and reproducibility compared to analyses
made using the 1/3 octave band RTA.
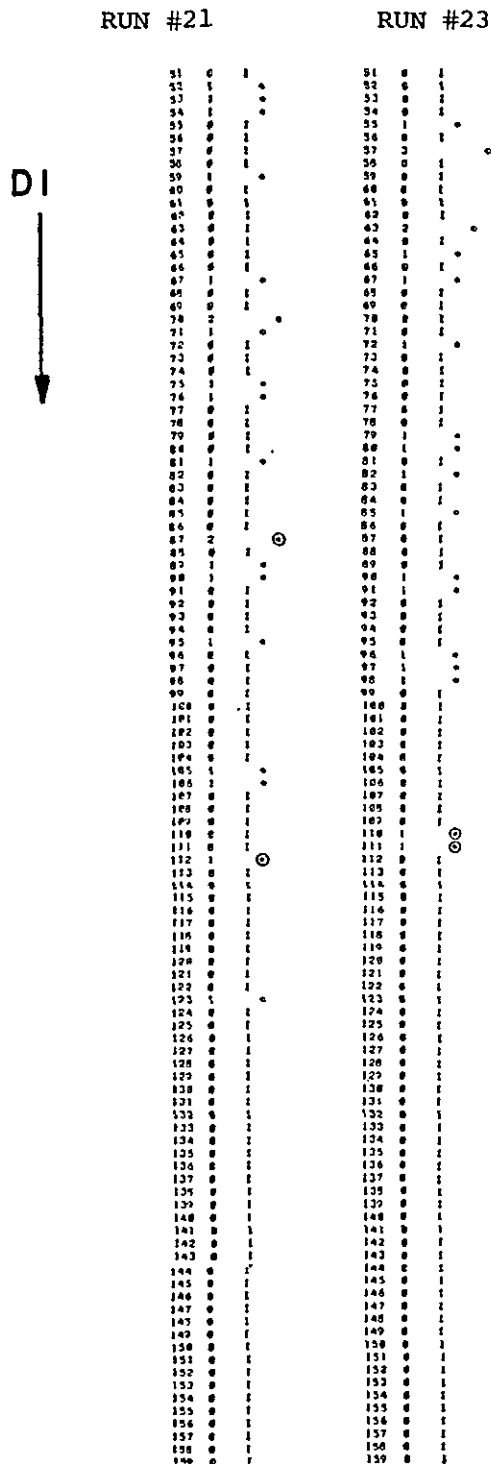
FIG. 5.5.6 DISTRIBUTION OF DIFFERENCE INDEX FOR RUN #21 AND RUN #23
FROM THE FIELD TESTS AT ENGLEWOOD YARD, 18 June 1975

o Indicate D. I. for defective wheel.

FIG. 5.5.7 DISTRIBUTION OF DIFFERENCE INDEX FOR RUN #10, THREE
DIFFERENT SAMPLING TIME INTERVALS, FROM THE FIELD
TESTS AT ENGLEWOOD YARD, 18 June 1975

⊙ Indicate D. I. defective wheel.

6. WAYSIDE TESTS

6.1 Tests at TTC Pueblo, Colorado

Two field tests were performed in the Transportation Test Center (TTC) in Pueblo, Colorado, at a three month interval. The objectives of these tests were:

1. To test certain parts of the system, such as the microphone, the modified exciter, and the wheel sensor, in the field.

2. To simulate the operating conditions for the Acoustic Signature Inspection system under development.

3. To determine the signature change, over a certain time period, due to wear of the wheels.

6.2 First Pueblo Test

In all 10 tests were done on the bypass of the FAST track. These are described as follows.

Test	Date	Description (train speed, direction)
1	11-16-78	5 MPH; counterclockwise
2	11-16-78	5 MPH; counterclockwise
3	11-16-78	8 MPH; counterclockwise
4	11-16-78	8 MPH; counterclockwise
5	11-17-78	5 MPH; clockwise
6	11-17-76	5 MPH; clockwise
7	11-17-76	8 MPH; clockwise
8	11-17-76	8 MPH; clockwise
9	11-17-76	5 MPH; brakes lightly applied
10	11-17-76	12-15 MPH; clockwise

Tape recordings of acoustic signatures were obtained from each of the project FAST train wheels. This was done for all wheels on one side of the train

on Tuesday evening, 16 November 1976 and for the
wheels on the other side on Wednesday evening. A
consist description was obtained for car identification.
The first four cars in the 70-car consist were replaced
in the Wednesday night test, otherwise the consist
remained the same for both tests.

Wheel excitation in these tests was done with the
improved model of the UH mechanical hammer exciter, as
described in section 5.1.1. A photograph of the installed
exciter is shown in Fig. 6.2.1. This hammer exciter
performed without mishap during the tests, and showed
only minor wear following the 3124 test impacts. At the
time the first series of Pueblo tests were made, it
was believed that the hammer could be activated by impact
from the link, 3, (see Fig. 1.6.1), so the springs, 5,
were disconnected from the hammer at point B and instead
connected to the frame. Thus the hammer was allowed to
swing free from the link, 3, on impact and the springs, 5,
served to reset the link, 3, rather than the hammer. This
change, although of interest from the design standpoint,
gave rise to some problems, as indicated below.

The wheel impact response was judged to be best for
the 5-8 MPH train speed. The hammer exciter would not
operate effectively for train speeds above 12 MPH and
did not impact at all below 3 MPH. About 1/3 of the
wheels were not struck by the hammer during the 12-15 MPH
test presumably because the hammer could not reset as
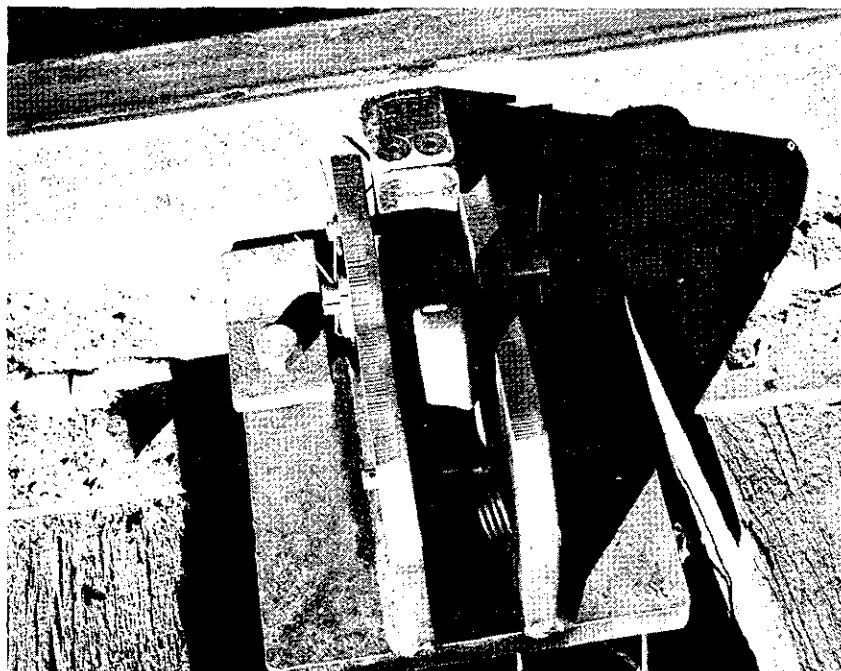
FIG. 6.2.1 MODIFIED MECHANICAL HAMMER EXCITER USED AT TTC,
PUEBLO

needed in the time between the passage of wheels on the same truck. However, the hammer mechanism was not damaged in this test nor did it appear to present a hazard to the train or personnel in attendance. The impact sound levels measured approximately 6 feet from the wheel usually exceeded 95 dB which was at least 10 dB above the background train noise.

The performance of the wheel sensor was good. It was installed and calibrated easily. For calibration a small vehicle provided by TTC was used. Views of the system used at TTC Pueblo are shown in Figs. 6.2.2 and 6.2.3.

The acoustic signature of the wheels was recorded on two different tape recorders simultaneously. One recorder was a General Radio dual channel. It was used for simultaneous recording of the sound in channel No. 1 and the triggering pulse in channel No. 2. This recorder operates with a 115 Volt AC, 60 Hz power supply. Unfortunately there was no such line available at the test location and a portable generator was used. That later proved to be a major obstacle in the analysis, because the speed of the tape transport mechanism is directly dependent on the frequency of the power supply. The other recorder was a NAGRA single channel, battery operated instrument. This is a very good recorder, but only the sound could be recorded on the single channel.
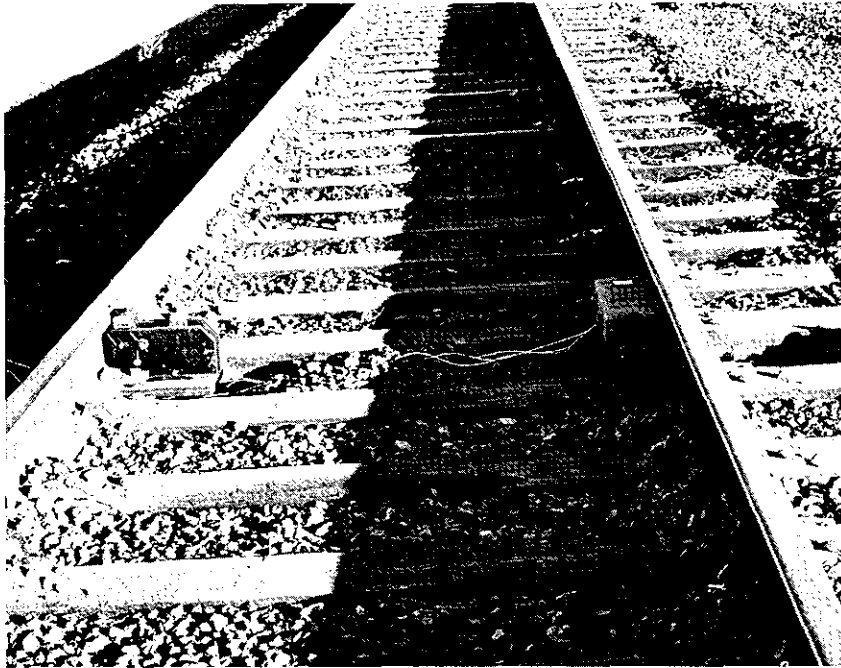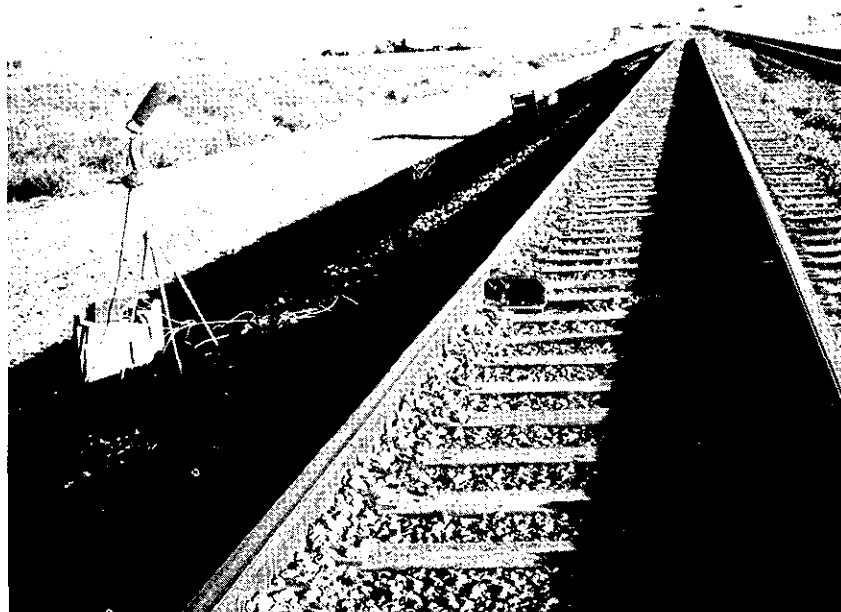
FIG. 6.2.2a VIEW OF THE EXCITER-WHEEL SENSOR
b VIEW OF THE MICROPHONES, EXCITER AND WHEEL SENSOR
ON THE BYPASS SECTION OF THE FAST TRACK AT TTC,
PUEBLO
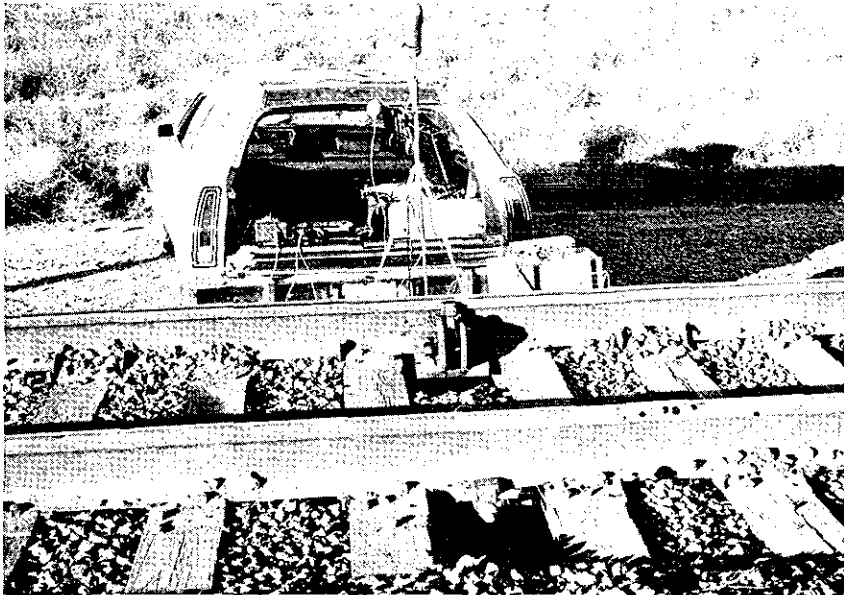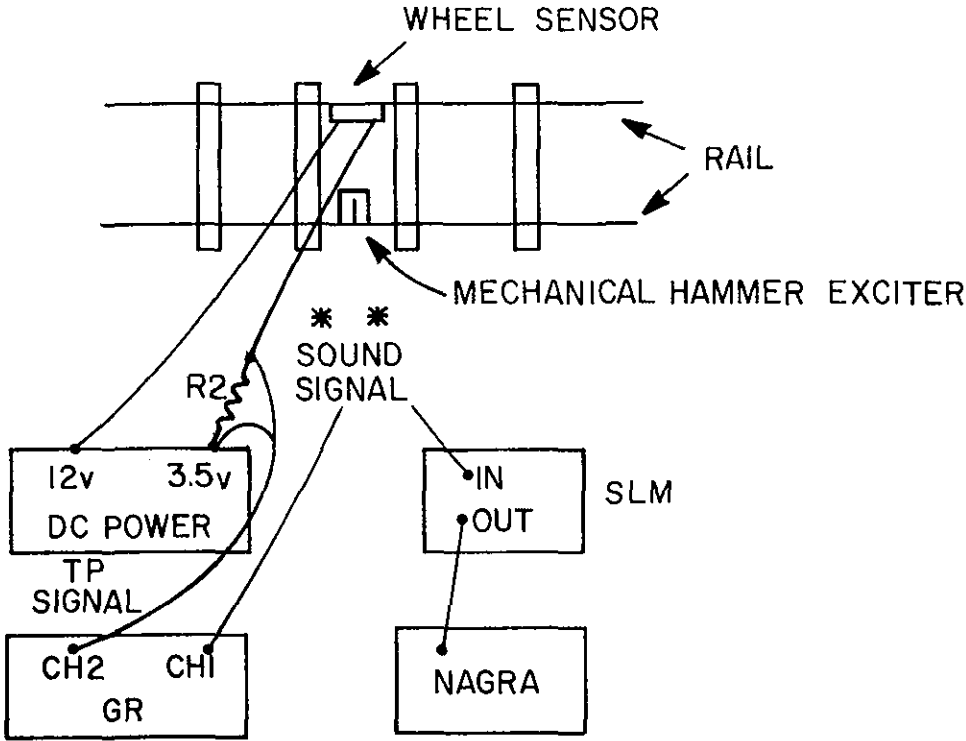
FIG. 6.2.3a. VIEW OF THE SETUP AND EQUIPMENT USED AT TTC, PUEBLO CO

b. SCHEMATIC OF THE SYSTEM AT TTC, PUEBLO CO

Preliminary analyses of these tapes
were made to test and refine the recognition
logic. Comparisons were made between
two impacts on the same wheel, impacts from two wheels
on the same axle, and from two different wheels on the
same side of the train. Some studies of this type are
reported in the next section. Since the train speed of
8 MPH is close to the maximum speed for which the fourier
analysis and data transfer into the computer could be
effected, the tape playback speed was 7-1/2 inch/sec
instead of the recording speed of 15 inch/sec. This
gives double the time for sampling and data transferring,
compared to direct real-time analysis.

6.3 Second Pueblo Test

A second series of tests similar to the first
was conducted in the evening of 10 February 1977 on the
main FAST track. These are described as follows:

Test No.	Description
11	5 MPH; Clockwise
12	5 MPH; Clockwise
13	8 MPH; Clockwise
14	8 MPH; Clockwise
15	5 MPH; Counterclockwise
16	5 MPH; Counterclockwise
17	8 MPH; Counterclockwise
18	8 MPH; Counterclockwise

For these tests the same devices and arrangements as
in the first tests were used (see Fig. 6.2.3). The only
additional precaution taken was continuous monitoring
of the frequency of the AC power line by a frequency

counter. During the second tests a better and bigger
generator was available. The frequency of the generator
was reasonably stable, although it drifted slowly within
the range of 59.0 - 60.2 Hz, during the 5 hour tests.
This introduced a maximum frequency error of 2% in the
acoustic signatures. Errors of this size can be important
in the data analysis, because line spectra comparison
will be impossible. Note that in the line spectra
comparison the tolerable error is 0.4% (a spectrum from
SD330A RTA has 250 channels). During a single test the
frequency of the generator drifted in the range of 0.0 -
0.3 Hz with an average less than 0.2 Hz. Indications
are that during the first test the phase frequency of
the power supplied was between 52.8 and 54.2 Hz. As a
final note on the error introduced by the change of tape
speed, manufacturers data for the GR data recorder type 1525
indicates that 'flutter and wow' is below 0.2% rms.
According to the Houston Lighting & Power Company, the
maximum average frequency change of the power lines is
0.2% - 0.3%. In unusual cases this may go a little
higher. Therefore there is no error introduced in the
analysis due to the tape transport mechanism due to the
frequency of the laboratory power supply.

Most of the recordings made were good. Comparisons
between wheels on the same side, across the axle and at
different speeds were made. The results are presented
in Fig. 6.3.1, Fig. 6.3.2 and in Fig. 6.3.3. These

TESTS #

5/6	6/9	14/18
SAME SIDE	SAME SIDE	ACROSS AXLE
5 MPH	5 MPH	8 MPH

DI
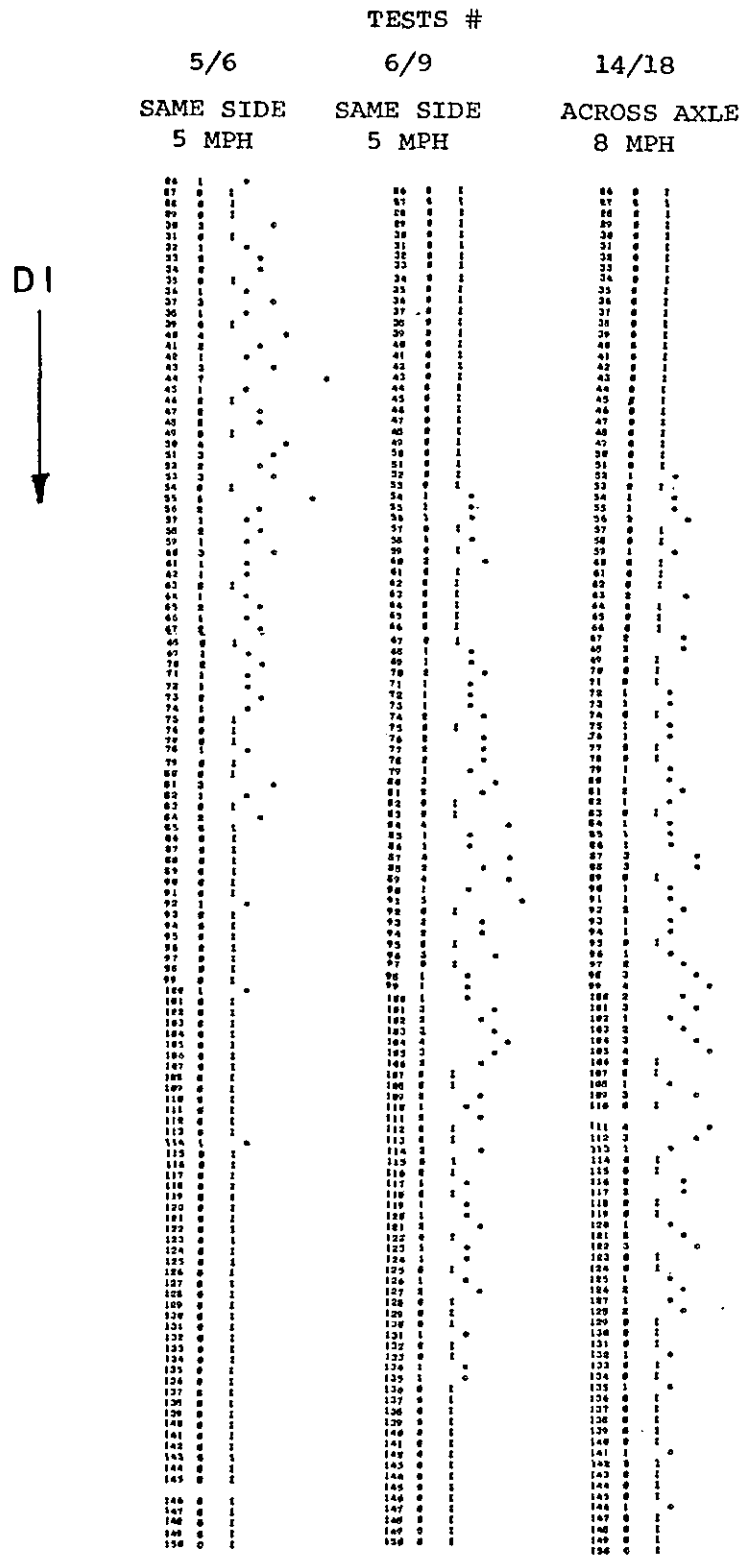
FIG. 6.3.1 DISTRIBUTION OF DIFFERENCE INDEX FOR THE TEST 5/6,
6/9, 14/18 AT TTC PUEBLO COLORADO

TEST #

14/18 6/3 13/13

ACROSS AXLE ACROSS AXLE SAME SIDE RANDOM COMP.

DI
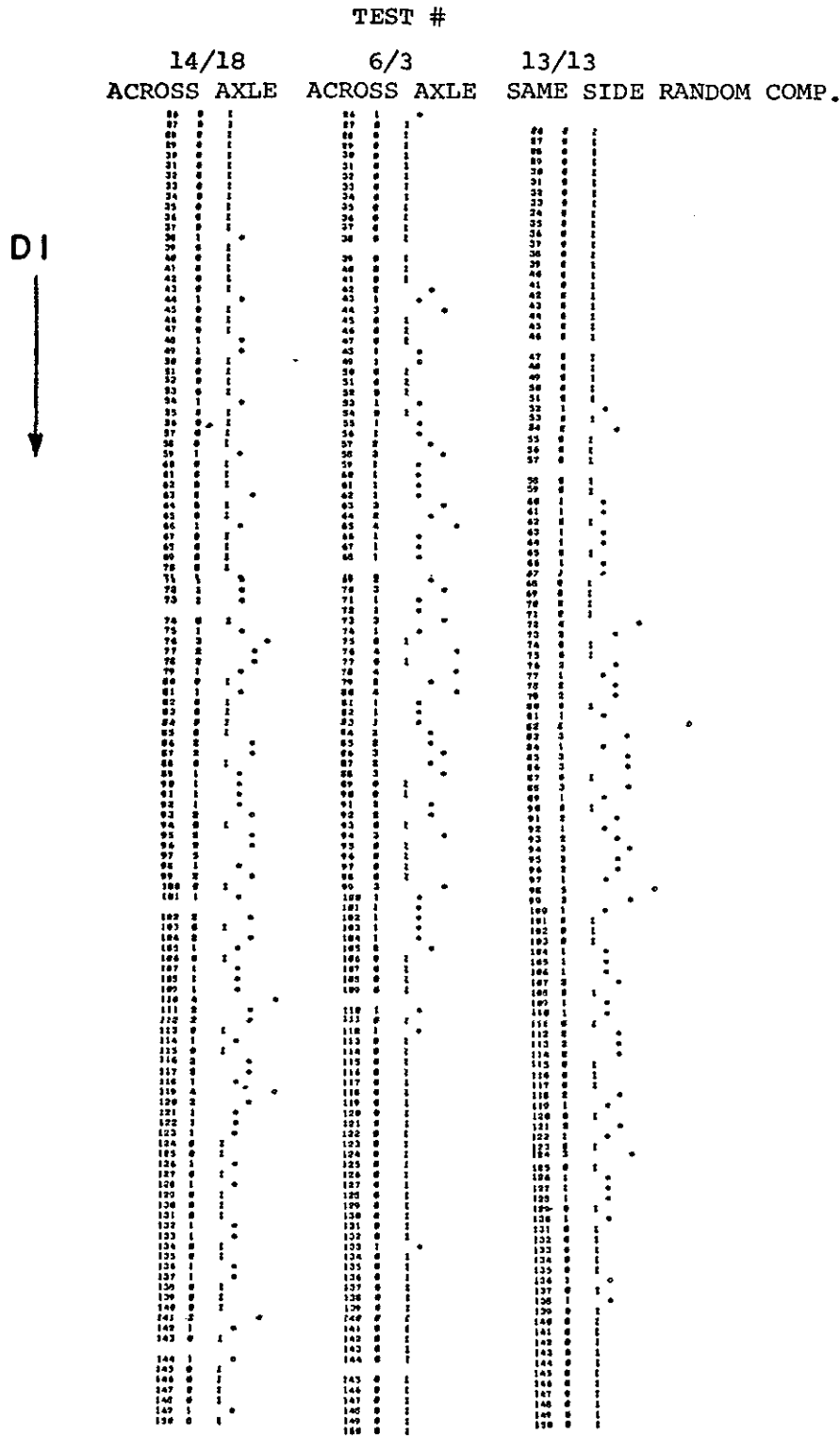
FIG. 6.3.2 DISTRIBUTION OF DIFFERENCE INDEX FOR TESTS 14/18, 6/3,
13/13 AT TTC PUEBLO COLORADO

FIG. 6.3.3 DISTRIBUTION OF DIFFERENCE INDEX FOR THE TESTS
13/17, 17/18, 13/14

figures show the distribution of the difference index
values for most of the tests. The best results were
obtained comparing the same wheels recorded in successive
tests where the train was moving at the same speed.
Problems related to the tests and subsequent laboratory
analyses are:

1. The train speed varied in most of the tests about
    ± 2 MPH from the nominal speed, the reason being the
    steep grade existing in the particular section of
    the FAST track used.

2. The power frequency was different in tests separated
    by long time intervals. This is probably the reason
    why across the axle comparison did not show
    results as good as expected.

3. Because of the large power frequency difference
    between the first and second Pueblo tests (53 and
    60 Hz respectively) it was impossible to come to
    any reliable conclusions on the effect of wheel
    wear.

    The following conclusions were arrived at from
the Pueblo tests:

1. The spring assembly of the mechanical exciter was
    necessary.

2. Distant mounting of the exciters should be avoided.
    A 200 ft separation between exciters was used in
    the 1975 Englewood yard tests where the wheels on
    one side were inspected first and then those on the other.

But the Pueblo tests showed that the greater

the exciter separation the greater is the effect

of varying train speed.

3. The exciter was strong enough to operate and survive

for a large number of impacts.

6.4 Tests at the Southern Pacific Englewood Yard, Houston

The final wayside testing of the Acoustic Signature

wheel inspection system took place in July 1977, in the

Southern Pacific Englewood yard in Houston. Traffic

speed inbound to the yard is sometimes higher than

15 MPH, and hence too fast for the inspection system,

but incoming to the hump the speed is 2-3 MPH. There

are about 3000 cars/day humped in the yard on 3 tracks.

The rail size is 136 lb. (mechanical hammer exciters

were designed for this size of rail). In a previous 2

year period the inspection personnel had discovered 6

broken and 12 overheated wheels.

The objectives for the tests were:

1. To obtain data for a statistically significant

sample of wheels in service. This data sample

could then be used for further studies to find the

optimum DI equation and to ascertain what wheel

conditions, other than cracks, might give rise to

high DI values.

2. To rate the performance of the hardware to identify

weaknesses and problems.

3. Using the best software available at the time to
    permit immediate follow-up on some wheels with high
    DI values. It was hoped that a cracked wheel might
    be found but this was recognized as a somewhat
    unlikely occurrence in the time available.

6.5 Englewood Test Site and Equipment

The location for the tests was selected after a
visit to the site and discussions with representatives
of Southern Pacific. A simple chart of the hump is
shown in Fig. 6.5.1. The figure shows the location of
the trailer, where the electronic equipment of the system
was stored, and the mechanical exciter on the north
track. The location for the trailer had to comply
with and fulfill the objectives and requirements set
for the tests. For that reason it was placed at the
bottom of the slope which is about 400 yards from the
top of the hump. It would then take more than two
minutes for a car moving at the regular humping speed
to cover the distance from the trailer to the inspection
pits. An observer sitting in the trailer had an unob-
structed view of the inbound or outbound traffic as well as
all train cuts moving over the hump. Electric
power was easily accessible from an electric tower a
few feet away.

Modifications in the hammer exciter and the software
were needed under the new operational conditions and

TO YARD

RETARDERS

N

CONTROL ROOM

CREST

INSPECTION PITS

LIBERTY ROAD

EXCITERS

APPROXIMATE
OUTLINE OF
HUMP

TRAILER
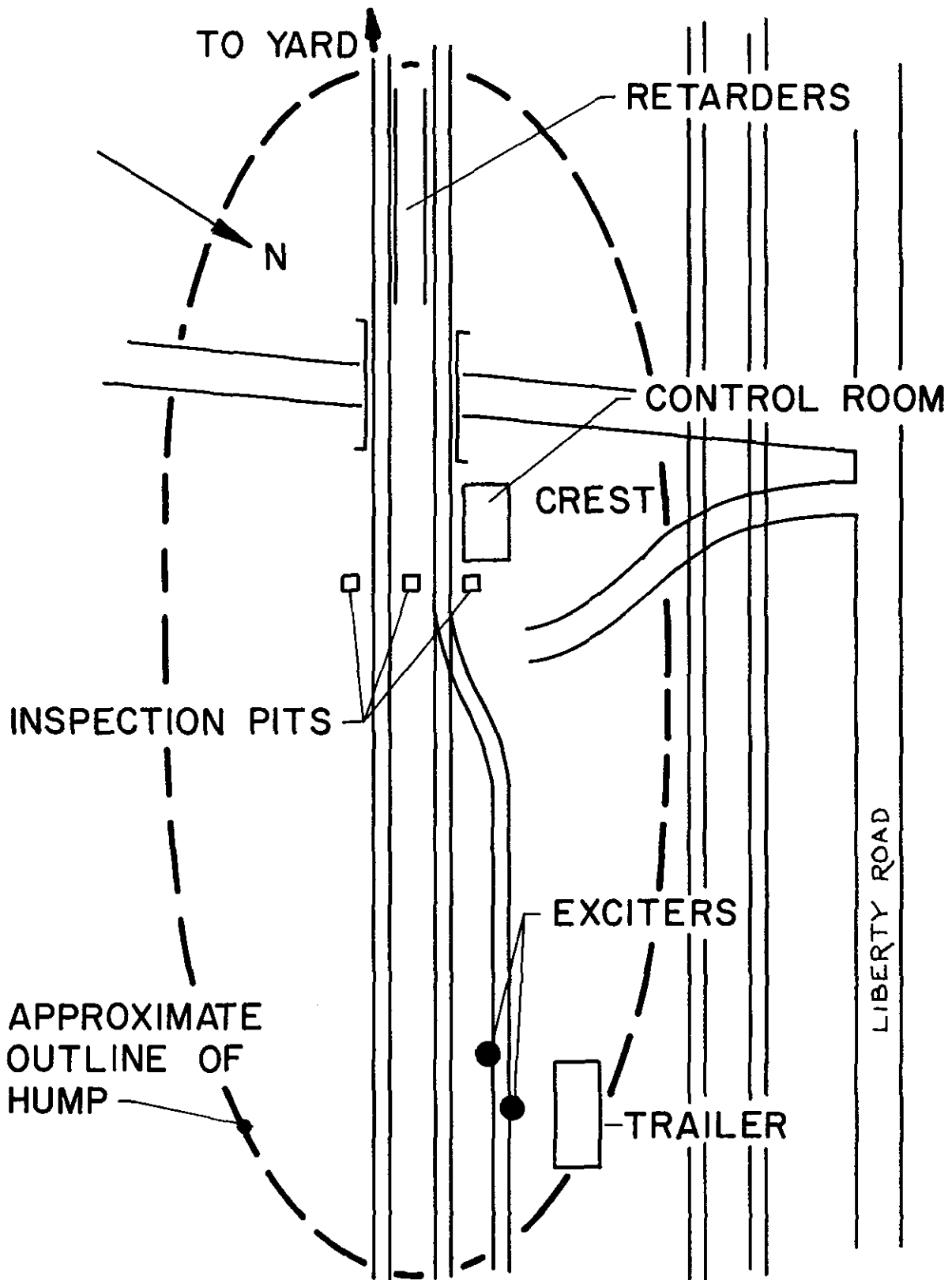
FIG.6.5.1   OUTLINE OF THE SOUTHERN PACIFIC'S
CLASSIFICATION YARD IN HOUSTON.

requirements for these tests. The exciter used at Pueblo did not operate for train speeds below 3 MPH. Consequently, the spring configuration was returned to the original design as shown in Fig. 5.1.1. After these changes the exciter operated best in the range 1.5 to 3.0 MPH. It is obvious that with this design the performance of the exciter is speed and flange depth dependent.

The tests were scheduled daily between 9:00 a.m. and 5:00 p.m. An average of 400 cars/day was estimated to pass through the test location. Only a fraction of those cars were actually tested, hence the chances of finding a defective wheel were remote. To define the discrimination level for good/bad wheels a complete simulation test was performed in the laboratory. The discrimination level of 85 was chosen after testing a selection of wheels, as shown in Table 6.5.1.

An air-conditioned 8' x 21' trailer was installed in the yard on 15 June 1977. It took about a week to install, calibrate and make the first complete test of the system. Two problems arose due to the condition of the rail. i) Although the size of the rail was 136 lbs., parts of the exciters had to be machined and plates of variable thickness were attached to the top of the plunger because the rail was worn down about 3/8 inch. ii) Calibration of the wheel sensor was

TABLE 6.5.1 DIFFERENCE INDEX VALUES FROM WHEELS TESTED IN THE
LABORATORY, FOR DISCRIMINATION LEVEL SELECTION

RUN #,	PROGRAM	TAPE #	AXLE & WHEEL IDENTIFICATION				
			GOOD/BAD				GOOD/GOOD
			15C-15A	8B-8G	4G-4B	1G-1B	13A-13C
770701-II	T-562-V	175	91	101	142	127	69
770615-IV	T-562-I	175	99	93	106	119	71

very difficult for the same reason. No such problem
had been encountered during the test at TTC in Pueblo
or the laboratory simulation. As a result of this
difficulty multiple triggering or missing triggering
pulses were observed. Consequently, the maximum number
of wheel signatures per test had to be reduced to 80,
because faulty triggering invalidates an entire run.

The trailer and the outdoor hardware are shown in
Fig. 6.5.2. Through the window on the left the test
controller could watch the cars moving uphill towards
the crest. The schematic of the inspection system is
shown in Fig. 6.5.2b, distances between different devices
being marked on the drawing. The exciter and the wheel
sensors were mounted between the ties. The clearance
was very small, and therefore inevitably there was some
difference in the time between the triggering pulse and
the impact on the two sides of the track. During the
TTC and simulation tests, the exciter-wheel sensor
alignment was much better. In Fig. 6.5.3, the microphones,
exciters and wheel sensors are shown from the same angle
as seen by the test controller looking through the
window of the trailer. In Fig. 6.5.4a,b the system
and the east part of the hump are shown. The inspection
pits are indicated by arrows (Fig. 6.5.4a).

All testing was performed in real time. During
the last two weeks, when all necessary changes and
corrections had been made the sound and triggering
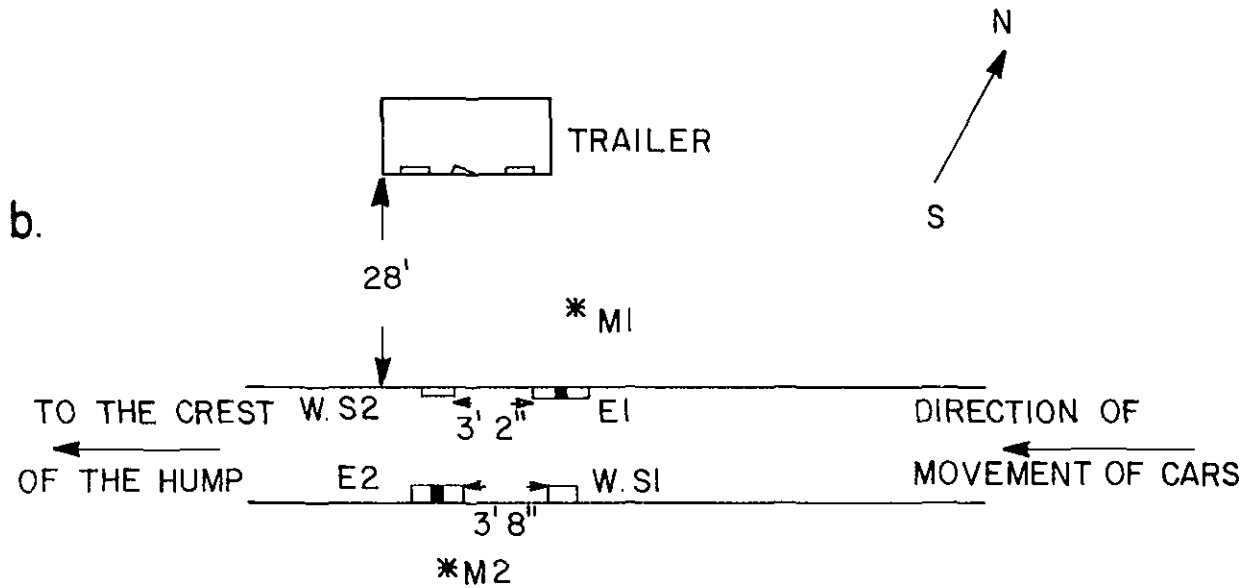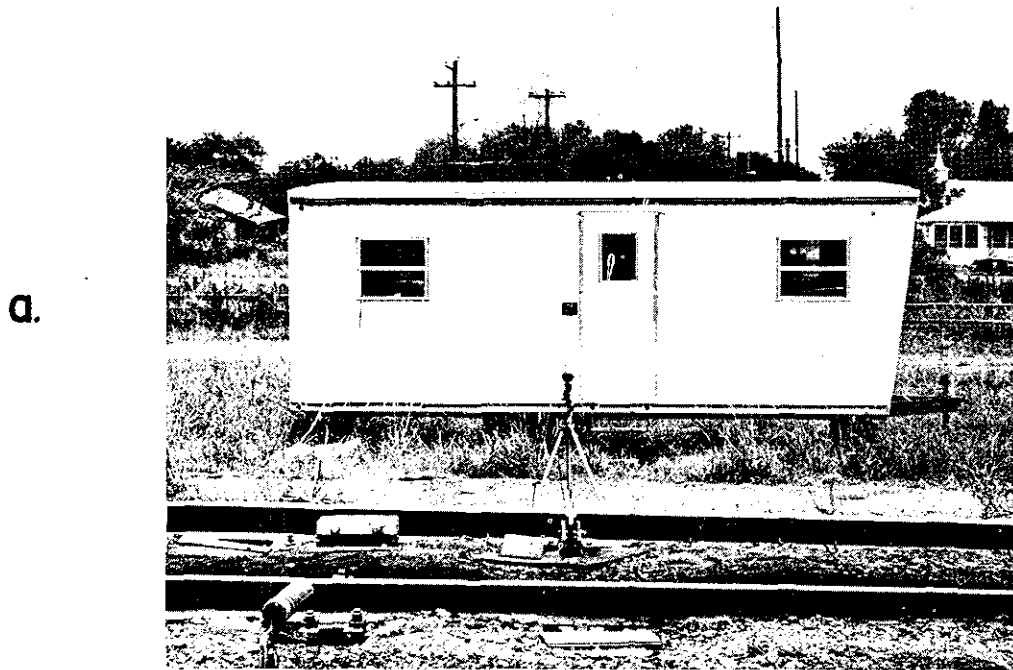
FIG.6.5.2 a VIEW OF THE INSPECTION SYSTEM

b SCHEMATIC OF THE SYSTEM LAYOUT

FIG. 6.5.3 VIEW OF THE MICROPHONES, EXCITERS AND WHEEL SENSORS
THROUGH THE WINDOW OF THE TRAILER
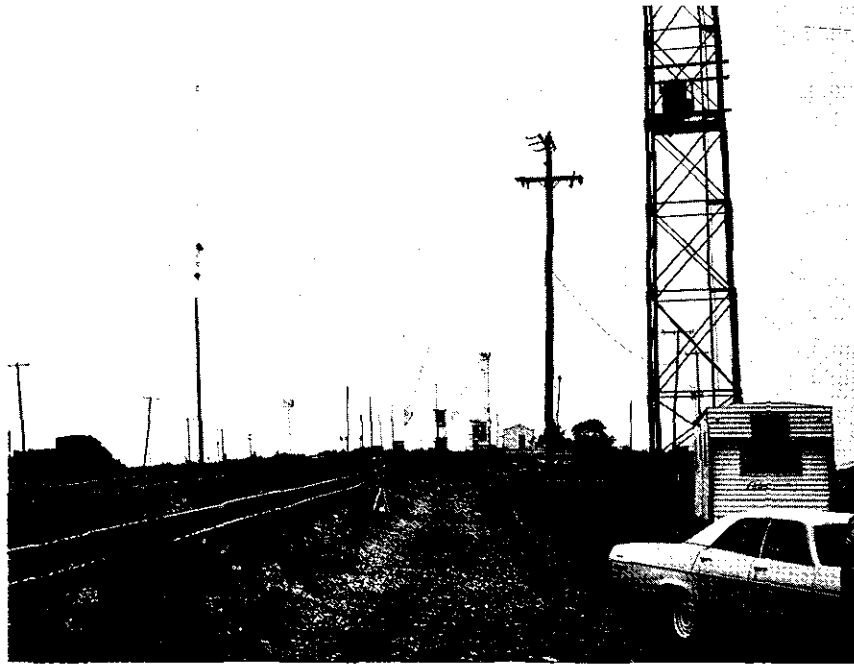
FIG. 6.5.4a VIEW OF THE EAST SIDE OF THE HUMP, INSPECTION PITS
            ARE INDICATED BY ARROW
         b VIEW OF THE MICROPHONES, EXCITERS AND WHEEL SENSORS

pulse signals were tape-recorded simultaneously with the real time testing.

6.6 Performance of Hardware during the Englewood Test

The duration of the tests was approximately five weeks instead of the scheduled four due to the initial one week delay in the installation of the system.

The components of the system performed as follows during the tests:

a) Microphones: No problem or failure. Some indications of excessive attenuation or low gain in the pre-amplifier of one of the microphones during the second week of the tests were finally attributed to a bad cable. Rain did not have any adverse effect on the microphones which survived three heavy rainstorms during the test period.

b) Wheel Sensors: One of the dual wheel sensing units failed a couple of days before the end of the tests. It was easily replaced by the other unit. Some triggering problems could be attributed to wheel sensors. In the late afternoon hours, under extreme heat, the temperature on the cover of the wheel sensors was estimated to be above 130°F.

c) Mechanical Hammer Exciters: Most of the parts operated satisfactorily. Each exciter performed about 27,000 impacts. One hammer had to be replaced due to excessive wear, possibly because of improper

heat treatment. One pair of springs was also replaced with new and stiffer springs.

d) SD330A Real Time Analyzer: Some problems developed when the temperature inside the trailer was above 85°F.

e) NOVA 1220 Minicomputer: Some serious problems (computer failure) occurred when the temperature inside the trailer was above 85°F. The temperature related problems in the RTA and computer were corrected by improving the air circulation in the trailer.

f) Diskette System: No problems. Further verification of proper data transferral from the computer to diskette and vice-versa was checked with a specially written test program.

The performance of the exciter is shown in the figures 6.6.1 through 6.6.4. In each figure the top trace is the triggering pulse signal, and the bottom trace is the sound signal. These pictures were taken during the tests using a TEKTRONIX 564 storage oscilloscope and a polaroid camera.

The events shown in the pictures from left to right are: The triggering pulse (TP) and the corresponding impact on the north wheel of the first axle is shown first, then the TP and the impact on the south wheel of the same axle, then the TP and impact on the north wheel of the second axle, etc.

Figures 6.6.1.a and b show the typical form of the sig-
nals. The top picture which shows normal impact during the
last few days of the test after all possible improvements were
made may be compared to the bottom picture which was taken in the
early experiments. Figures 6.6.2a and b show some of
the impact problems. In the top figure double impact
of the hammer on the wheel is shown. This impact is
more prominent on one side. In the bottom figure very
weak impact or no impact occurred at low speed when new
wheels with low flanges were passing over the exciter.
These impacts usually appeared as "insufficient data"
in the printout. Figure 6.6.3a shows, two
impacts on old used wheels with high flanges,
followed by two impacts on rather new
wheels with low flanges. In Figures 6.6.3b are shown
impacts of the type which sometimes gave rise to
the indication Significant Energy Difference. In
Figs. 6.6.1 through 6.6.3 the sweep speed of the
oscilloscope was 500 ms/div., except in Fig. 6.2.3b where
it was 200 ms/div. Figure 6.6.4a shows the signals from
the south exciter, at a sweep speed of 50 ms/div.
Figure 6.6.4b shows the corresponding signals from the
north exciter. On the south side the impact occurred
45-50 ms after the TP, on the north side the impact
occurred 100-105 ms after the TP, hence there was a
difference of 50-60 ms in the data processing between
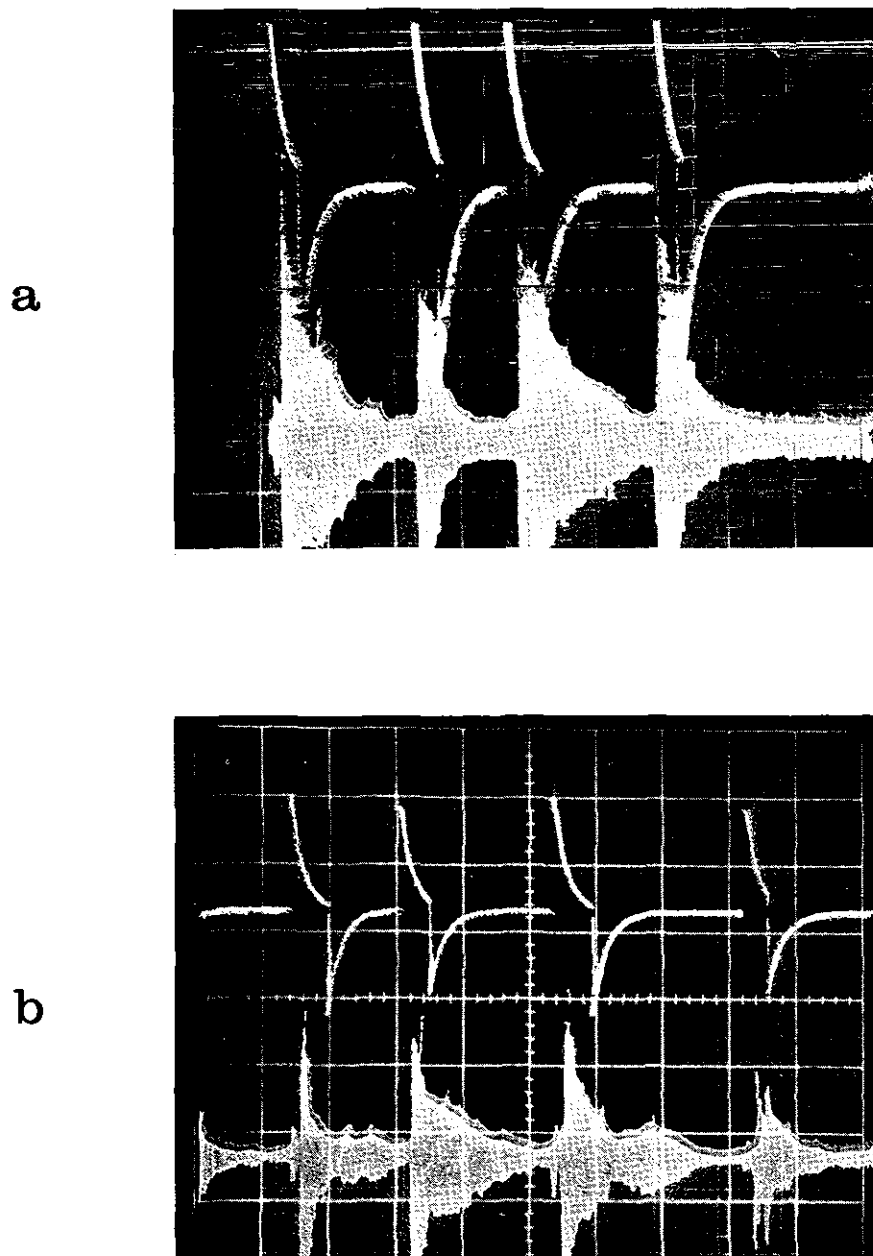
FIG. 6.6.1a   TYPICAL PERFORMANCE OF THE EXCITERS DURING THE LATE
              TESTS
        b   TYPICAL PERFORMANCE OF THE EXCITERS DURING THE EARLY
              TESTS, SWEEP SPEED 500 ms/DIV
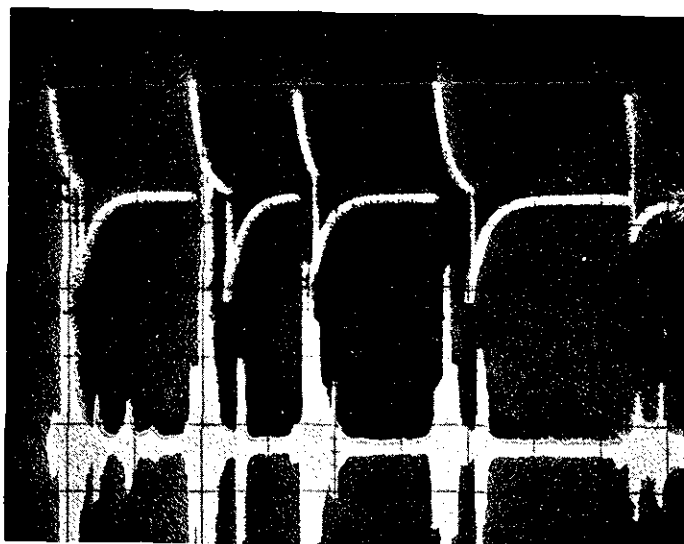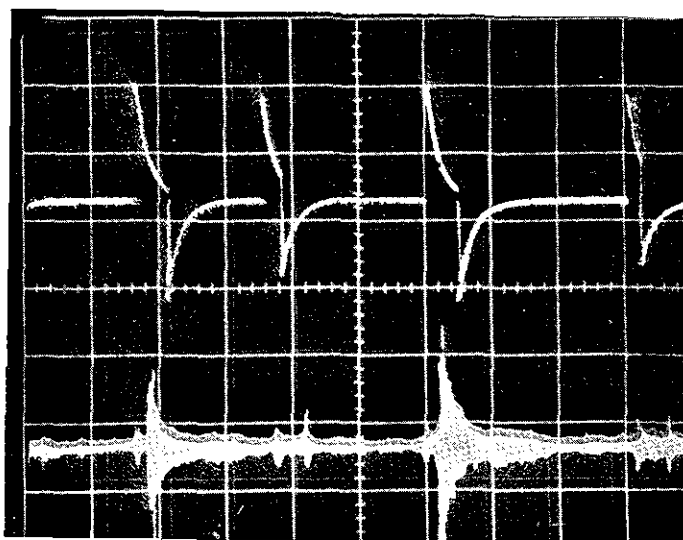
FIG. 6.6.2a EXCITER PERFORMANCE, DOUBLE IMPACT
         b EXCITER PERFORMANCE, NEW WHEELS, LOW OR NO IMPACT;
            SWEEP SPEED 500 ms/DIV
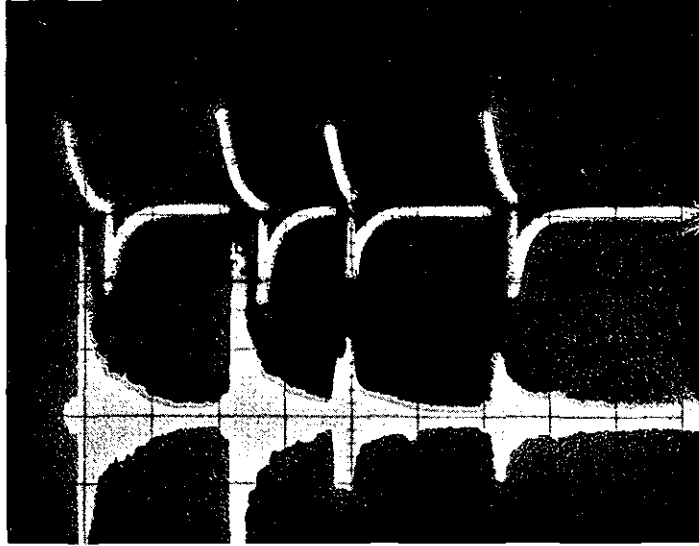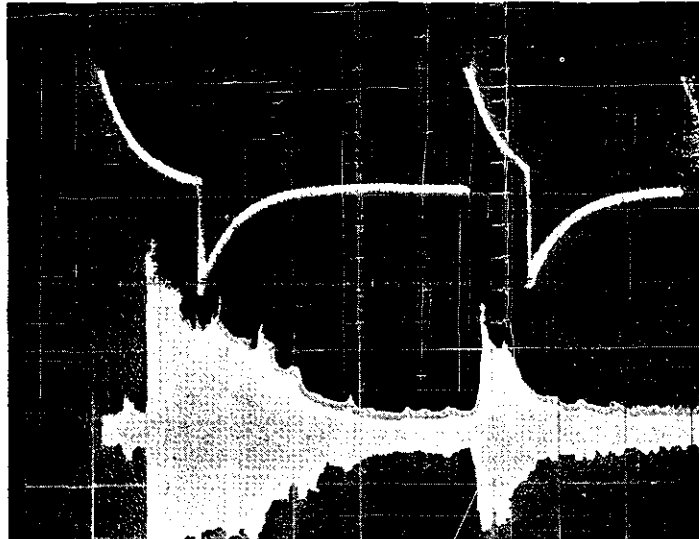
FIG. 6.6.3a IMPACTS ON WHEELS WITH HIGH FLANGES FOLLOWED BY
IMPACTS ON NEW WHEELS WITH LOW FLANGES
b UNEVEN IMPACT ON WHEELS ACROSS THE AXLE
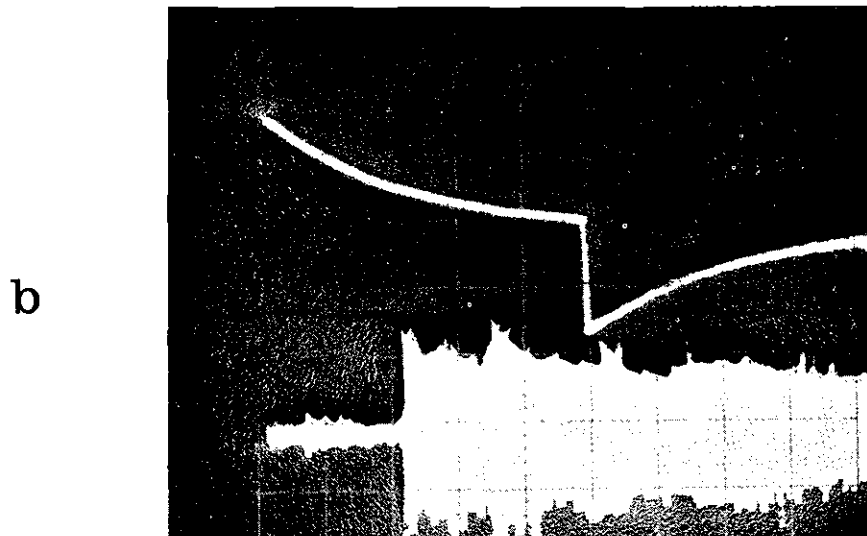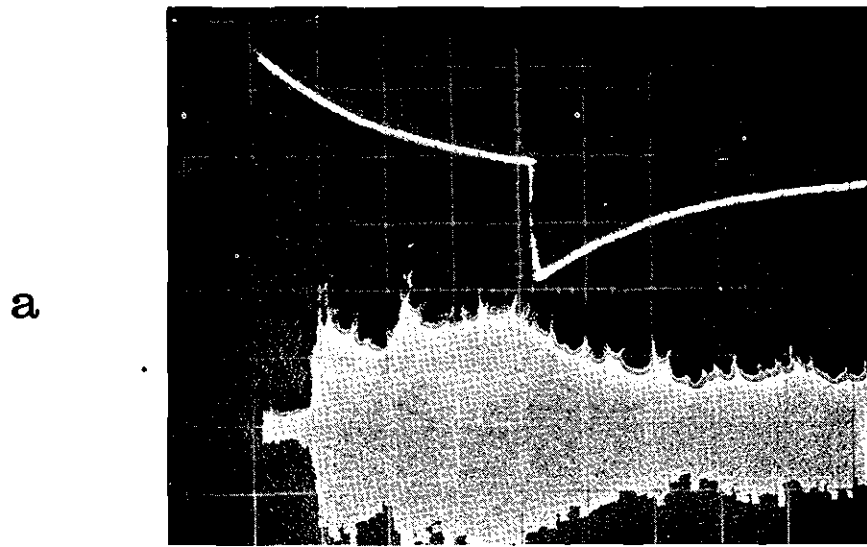
FIG. 6.6.4a TIMING RELATION, SOUTH EXCITER, IMPACT ABOUT 40 ms
            AFTER THE TIMING PULSE
         b TIMING RELATION, NORTH EXCITER, IMPACT ABOUT 110 ms
            AFTER THE TIMING PULSE; SWEEP SPEED 50 ms/DIV

the two sides. This time interval corresponded to one sampling cycle of the analyzer and obviously introduced some error. This difference could have been corrected with alignment of the exciter-wheel sensor, but due to the tie spacing that was impossible. The alternative way to correct this error is through the software which was also difficult because of the lack of time for major software changes during the test.

6.7 Performance of Software during the Englewood Test

Table 6.7.1 has a summary of the printout obtained during the last ten days of the tests. The first column has the RUN identification number. The second column has the number of cars tested during the run. The third column has the number of the tape on which the run was recorded. The fourth column has the total number and condition of the wheels tested (clean, greasy, etc.). The next five columns have the results, which include "good," "insufficient data," "significant energy difference," "overload" and "high value." The next column contains the levels of the high values. Visual inspection on some of those wheels with difference index over 110 did not show any apparent defect. The axle with the highest difference index (164) had 9 year old iron wheels but without any cracks. Only one axle was in rather bad condition. It had extensive built-up tread, but was not condemnable according to the railroad inspectors. During the period

TABLE 6.7.1

SUMMARY OF THE LAST TEN DAYS OF TESTS AT THE
SOUTHERN PACIFIC ENGLEWOOD YARD, HOUSTON

RUN NUMBER	NUMBER OF CARS	TAPE NUMBER	NUMBER OF WHEELS GR-GREASY CL-CLEAN	RESULTS NUMBER OF AXLES					LEVELS OF H.V.	REMARKS
				GOOD	INSUFF. DATA	SIGNIFICANT ENERGY DIF.	OVER-LOAD	HIGH VALUE		
770721-I	3	184	16CL-8GR	6	6	–	–	–	–	
770721-II	3	184	24CL	5	–	5	–	2	85,90	
770721-III	3	185	24CL	11	1	–	–	–	–	
770721-IV	3	185	24CL	7	–	2	–	3	90,90,105	
770719-Ib	10	183	80CL	19	21	–	–	–	–	New Wheels
770719-II	10	183	64CL-16GR	21	12	3	–	4	97,91,112, 164	
770719-IIb	10	183	72CL-8GR	26	12	1	–	1	93	
770718-I	9	183	72CL	21	10	3	–	2	89,95	
770718-II	6	183	48CL	12	3	4	–	5	100,103,93, 107,91	
770718-IIb	6	183	48CL	15	8	–	–	1	94	
770716-I	3	–	24CL	10	1	–	–	1	90	
770715-I	3	–	16CL-8GR	6	6	–	–	–	–	
770714-I	1	182	4CL	20	16	–	–	–	–	
770714-II	9	182	72CL	3	1	–	–	–	–	
770713-III	5	181	32CL-8GR	15	5	–	–	–	–	Possible microphone mixing problem
770713-IV	6	181	48CL	14	–	1	–	9	91,97,104 105,104,103 91,90,96	
770712-IV	6	180	48CL	12	–	1	4	7	93,118,86,115 92,94,126	
770712-III	6	180	40CL-8GR	18	5	–	–	1	85	
770712-II	15	180	104CL-16GR	39	6	3	–	12	110,86,95,90, 93,95,88,109, 102,88,95,118	
TOTAL	117		864CL-72GR	280	113	23	4	48		

of the tests the READ assembly subroutine did not have
an error flag for the case of improper reading of the
digital output of the RTA by the computer. When this
error flag was added later it showed on average that 2%
of the indications contained a reading error. It is
not known how much this error might have affected the
results.

In some of the runs with a large number of high
values, certain indications showed improper setting or
calibration in parts of the system. For example in run
770713-IV improper microphone mixing was indicated from
the fact that north side readings had a substantially
higher overall sum compared to the south side. In the
case of run 770712-IV the 4 overload indications showed
low input attentuation in the RTA. Indications of
Insufficient Data, Significant Energy Difference, and
Overload are related to the performance of the exciter,
as shown in Fig. 6.6.1 through 6.6.3.

Another point that should be mentioned is the large
number of insufficient data indications. This is mostly
due to greasy wheels. The majority of these wheels are
on cars with plain journal bearings where oil has leaked
from the journal box. For spectral comparisons, the
second reading, 300 ms after the TP, was used. The
signal from greasy wheels in that instance is very low
or completely decayed. This problem could be corrected

by checking the first spectrum in cases of fast decay. Another point of some interest is that wheels with dragging brake shoes or even squealing under the application of brake shoe pressure did not appear to generate especially high Difference Index values.

The distribution of DI values for the last ten days of field test in SP Englewood yard (July 1977) is shown in Fig. 6.7.1. In the same figure indications from defective axles tested in the UH laboratory are marked with circles.
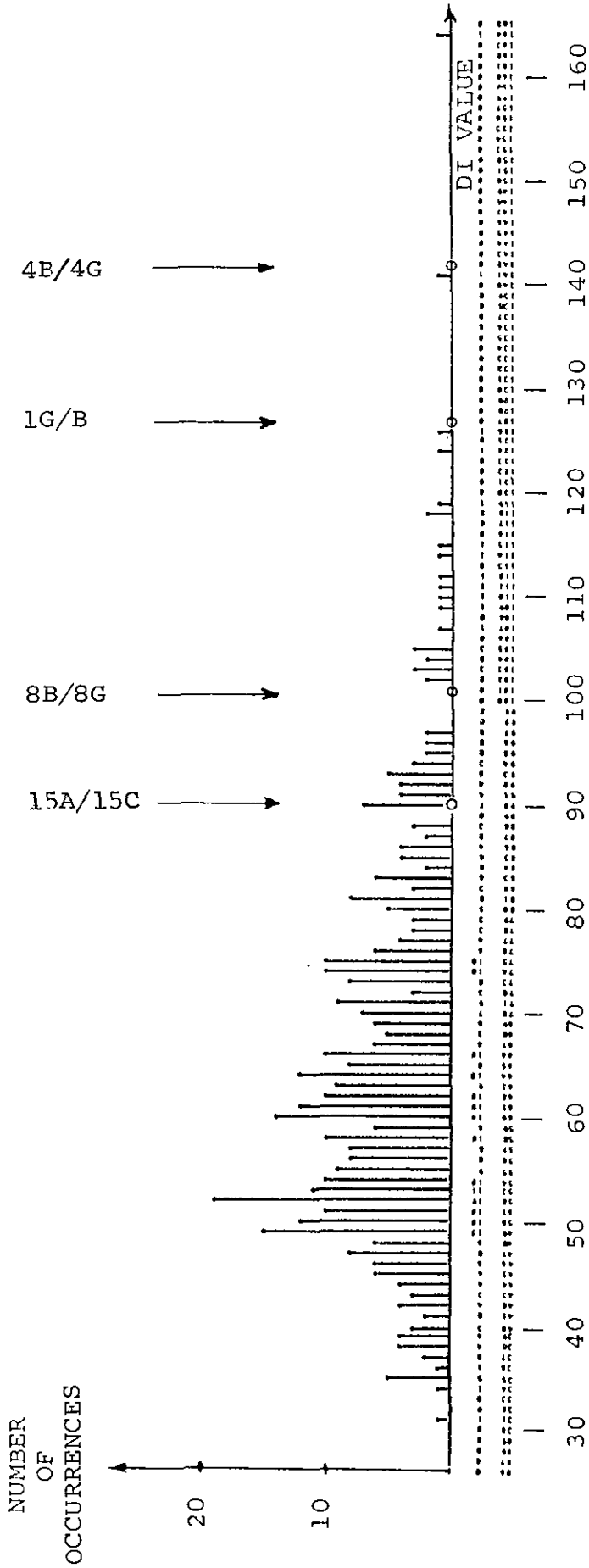
FIG. 6.7.1 DISTRIBUTION OF DIFFERENCE INDEX FOR THE LAST TEN
DAYS OF FIELD TEST AT SOUTHERN PACIFIC YARD (July 1977)

⊙ Indicate DI for defective wheels

Sample size: 443   Frequency Range: 0-10,000 Hz
Real Time Data. No correction for timing difference
DI includes terms in SD, DR, LD

7. SENSITIVITY ANALYSIS

7.1 Introduction

Figure 6.7.1 is the histogram of DI values obtained in real time during the tests. It was pointed out in section 6.7 that a number of system problems occurred during the tests and that the DI equation used was based on prior experience with small samples. The idea at the time of the test was to follow up on a few wheels with high values. Further study of the analog tape recordings taken during the test was divided into three parts with the following objectives:

1) to identify recordings with system problems and to correct for deficiencies, where possible, in the data processing software,

2) to use the corrected data to find the optimum DI equation, and

3) to study the remaining high DI values from the Englewood data to ascertain what wheel conditions besides cracks could cause high values.

The maximum sample size (number of axles) used in this study was 370, a little smaller than the sample shown in Fig. 6.7.1. The reason for this difference is that analog tape recordings were not made for a few cars included in the real-time data. Each time a correction was introduced into the data processing or a change was

made in the DI equation, the procedure was to plot a
histogram of the results. If, as a result of the change,
the modal value of the histogram showed an increased
separation from a reference sample of defective wheels,
the change was regarded as an improvement. In some cases
improvements were obvious with relatively small sample
sizes (130 to 170 axle pairs) and the histogram plot was
discontinued to save processing and analysis time.

The good/bad wheels used for reference are 15A/15C,
1G/1B and 4G/4B. They were tested on the UH laboratory
track, where the wheel sensors and exciters were spaced
as in the SP Englewood Yard. The setup prevented data
collection from axle 8B/8G which appears in the reference
sample of Fig. 6.7.1. The indications for the bad axles
shown in this report are the average values of seven runs.
Two good wheel pairs were also included in the laboratory
measurements and these are also shown in comparison to
each histogram.

7.2   Identification and Correction of System Problems

The hardware performance during the Englewood tests
was described in Section 6.6. Some of the problems that
are important for data processing are summarized and
explained below.

1. Difference in timing of the triggering pulse: As
mentioned in section 6.6 the tie spacing prevented the
proper alignment between impacters and wheel sensors, thus
introducing an average difference of $\Delta t = t_N - t_S = 60$ ms,

where t_N is the time interval between triggering pulse
(TP) and impact on the north side of the track and t_s is
the time interval between TP and impact on the south side,
as shown in Figs. 6.6.4a and b. This problem was partially
overcome by introducing an additional 60 ms delay after
the TP and before the first data reading for the north
side exciter. The word "partially" is used because not
every axle shows this 60 ms timing difference which is dependent
on the train speed and the condition of the axle. There
was a considerable improvement in data analysis shown by
the corresponding DI histograms before and after the time
delay correction (see Figs. 7.2.1 and 7.2.2). Obviously
with an electronically activated exciter these timing
problems could be eliminated completely.

2. Difference in impact force: This problem was also
described in section 6.6. Examples are shown in
Figs. 6.6.3a and b. To overcome this problem a redesign
of the exciter in order to make the impact independent
of the flange depth and train speed will be necessary.
An important requirement of the new design must be electric
or electronic disengagement of the hammer mechanism when
trains are moving at speeds beyond the operational limit
of the exciter. At this time no corrective action in
the data processing is possible.

3. Failure to read the RTA or to read twice: This problem
could introduce significant errors in the data processing.
During the Englewood tests there was no error flag in the

NUMBER
OF
OCCURRENCES

5

0

DI

4B/G

1B/G

15A/C
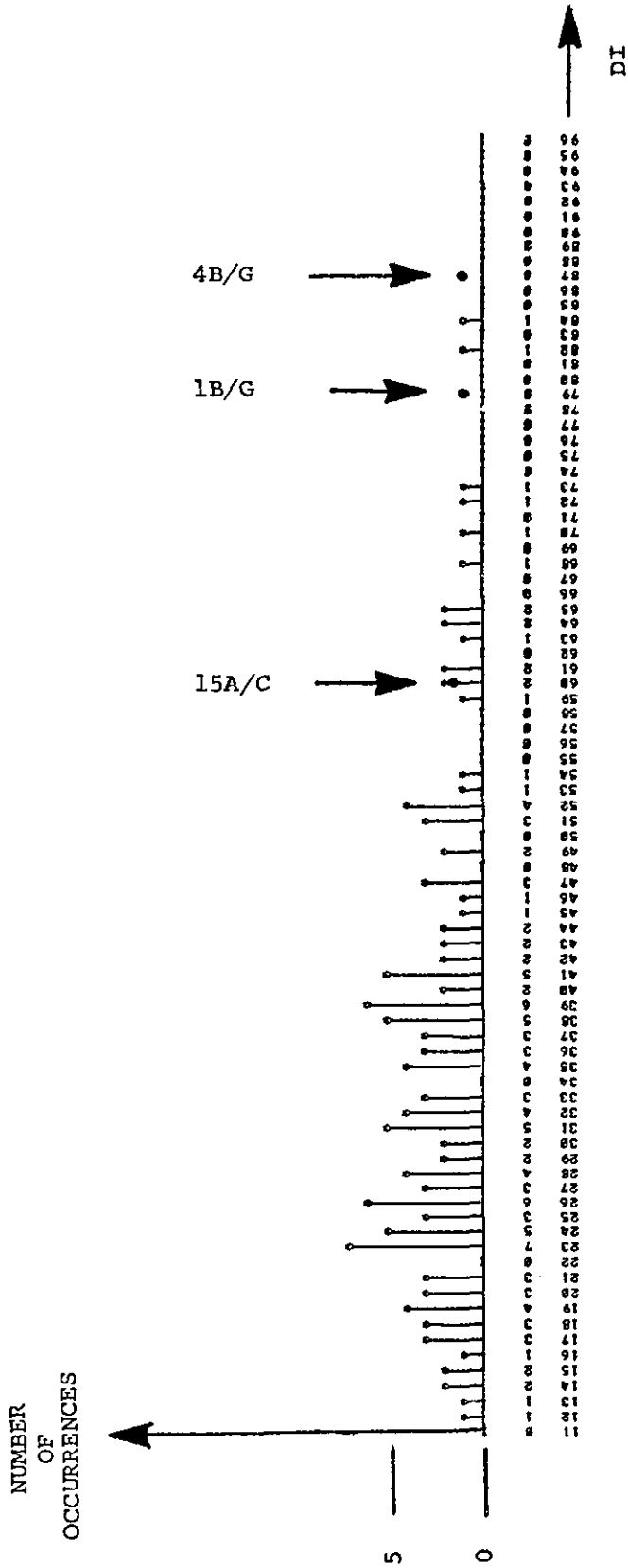
FIGURE 7.2.1. DISTRIBUTION OF DIFFERENCE INDEX VALUES

$$DI = C_1 SD$$

—— INDICATES DI FOR DEFECTIVE WHEELS

---- INDICATES DI FOR GOOD WHEELS IN LAB. TEST

SAMPLE SIZE: 137 FREQUENCY RANGE 0-10 kHz

COMPARE WITH FIG. 7.2.2

NO CORRECTION FOR TIMING PULSE DIFFERENCE.
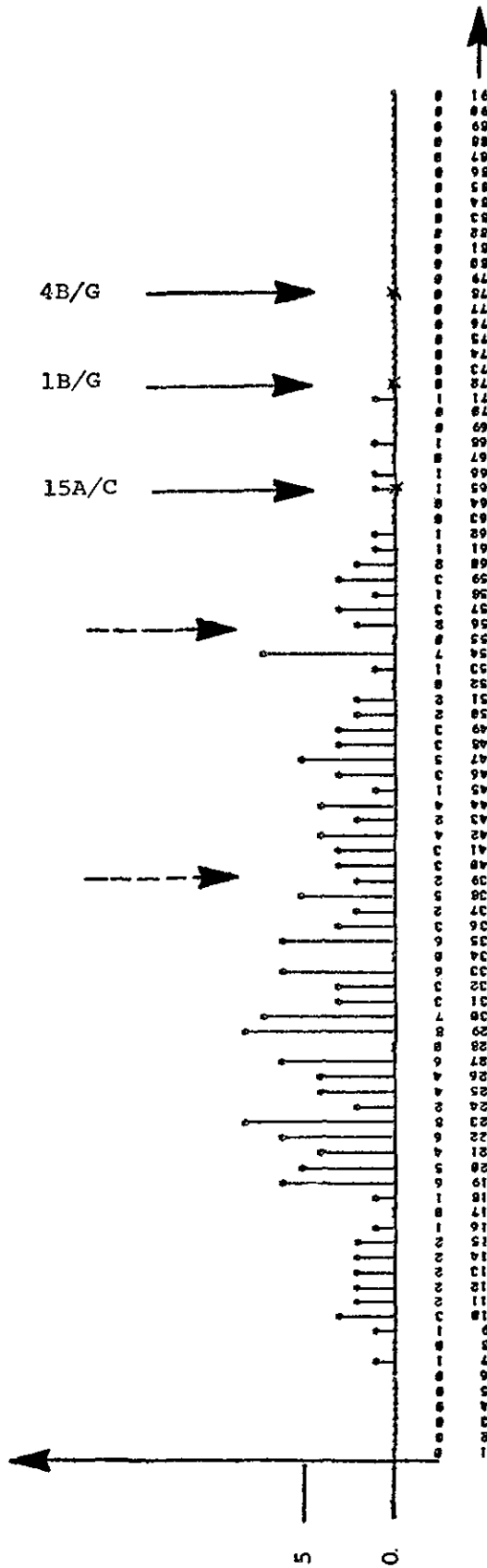
FIGURE 7.2.2. DISTRIBUTION OF DIFFERENCE INDEX VALUES
DI = C1SD
——→ INDICATES DI FOR DEFECTIVE WHEELS
----→ INDICATES DI FOR GOOD WHEELS IN LAB. TEST
SAMPLE SIZE: 168 FREQUENCY RANGE 0-10 kHz

WITH CORRECTION FOR TIMING PULSE DIFFERENCE. COMPARE WITH FIG. 7.2.1

software to pinpoint this anomaly. The problem has been overcome now by making appropriate changes in the assembly software. The misreadings appear to be related to overload of the RTA.

4. Missing timing pulse: This is another serious problem, because the computer starts comparing signatures from wheels on different axles. The problem is probably due to the position of the wheel flange in respect to the sensing element of the proximity detector. The difficulty was recognized early during the field tests but despite continuous efforts to make an ideal adjustment of the sensors, it was not possible to store data from a long train without missing one or more TP's. This was the main reason that it was decided to test only a few cars at a time. Similar problems at other installations using this type of proximity detector have been reported. The highest DI indication (164) in Fig. 6.7.1 was due to a missing TP. For the present the few axles in the Englewood data with missing TP are not included in the analysis. The recommended solution is to avoid using this type of sensor, with prefer-ence for strain gauges, or photocells. An alternative solution is to incorporate circuitry and an error flag in the software when two successive TP's come from the same sensor.

5. Missing timing pulse at high train speed: This is due to the length of sampling time for data collection and storage. No action has been taken at present. The

recommended solution is a hardware-software change to give an error flag. No recordings at high speed are included in the present sample.

7.3 Optimizing the DI equation

There are several features of the acoustic signals from two wheels which could be used for comparison purposes:

SD: the sum of the absolute values of the differences between the sound pressure levels of the two signals in the same frequency channels.

NC: the number of common resonances, i.e., the number of resonances occurring in the same frequency channels in the two signals.

DR: the difference in decay rates of the two signals.

LD: the difference in the overall levels of the two signals.

NR: the difference in the total numbers of resonances in each signal.

A variety of experiments were performed to obtain the optimum DI equation. In each case a histogram of the results was obtained in the same manner as for Figs. 7.2.1 and 7.2.2 which showed the effects of making a correction for the time delay.

It was decided to take one variable at a time and only add additional terms to the equation as proven to be efficacious. The first tests were made using the sum of the differences, SD. The principal issue here is the

most effective frequency range. In order to resolve this issue, 25 different histograms were plotted dividing the frequency range between 0 and 10 kHz into 400 Hz bands. It was clear from these histograms that the separation between the Englewood sample and the bad wheels was lost at frequencies above about 7200 Hz. Consequently, in all subsequent tests the frequency range was restricted to 0-7200 Hz. The improvement resulting from this restriction of the frequency range can be seen by comparing Figs. 7.3.1 and 7.3.2. Note that in Fig. 7.3.2 only one wheel from the Englewood sample appears in the range of the bad wheel reference set. This was the first histogram obtained in which one of the bad wheel sets showed a DI value higher than any in the Englewood sample.

This test was followed by several attempts to incorporate terms involving the differences in decay rates. Although earlier laboratory tests had shown that the sound from cracked wheels damps more rapidly than from good wheels the present set of tests did not lead to an improvement in separation. It is believed that this disappointing outcome was because of the uncertainties in the time reference, and the availability of only two data samples of the sound from each impact. It is possible that when the TP problems have been completely eliminated, then terms involving the difference in decay rate may still lead to improvement in the DI separation.

NUMBER OF OCCURRENCES

4B/G

1B/A

15A/C

10

0

DI
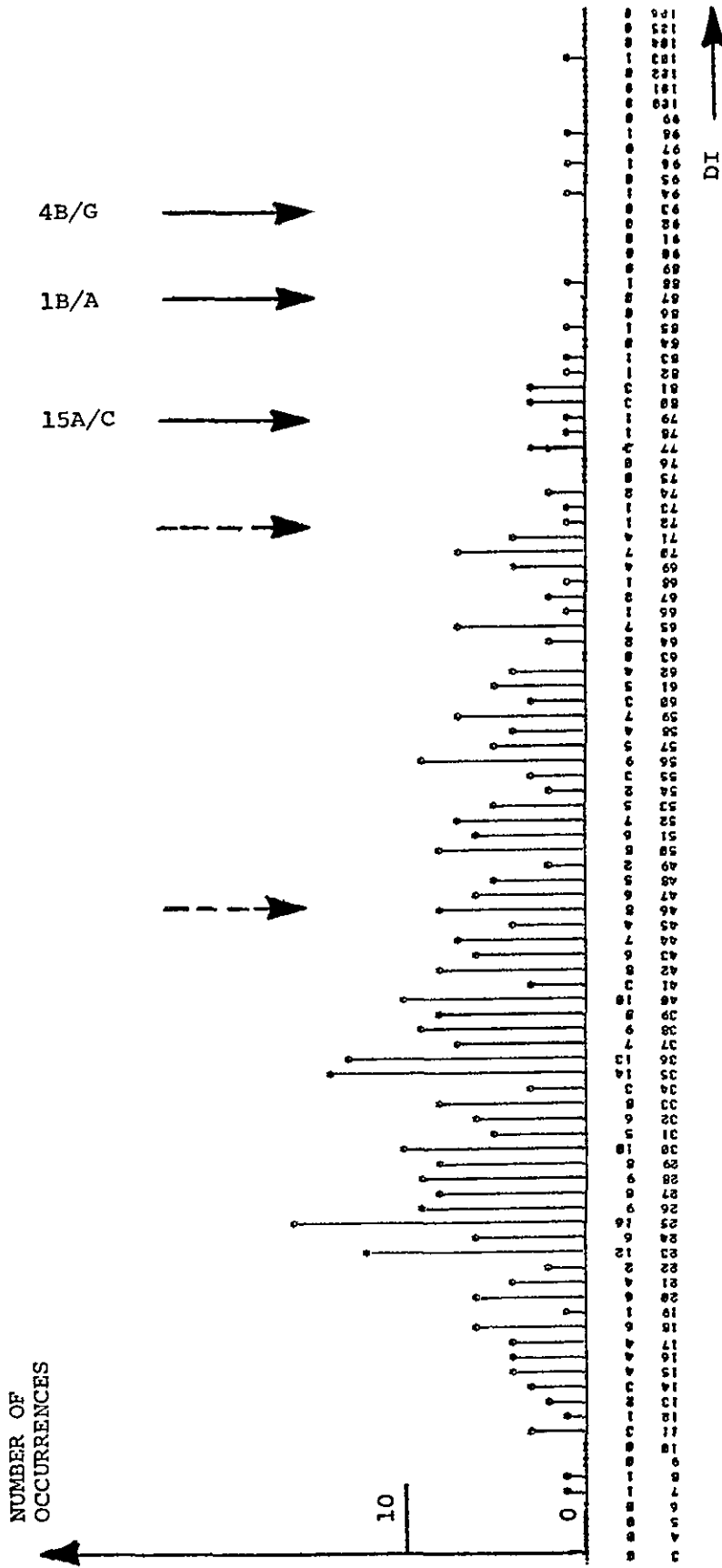
FIGURE 7.3.1. DISTRIBUTION OF DIFFERENCE INDEX VALUES

DI = C₁SD

⟶ INDICATES DI FOR DEFECTIVE WHEELS

⇢ INDICATES DI FOR GOOD WHEELS IN LAB. TEST

SAMPLE SIZE: 372 WITH CORRECTION FOR TIMING PULSE DIFFERENCE

Frequency Range is 0-10 kHz. Compare with Fig. 7.3.2

NUMBER OF
OCCURRENCES

10

5

4B/G

1B/G
15A/C

DI
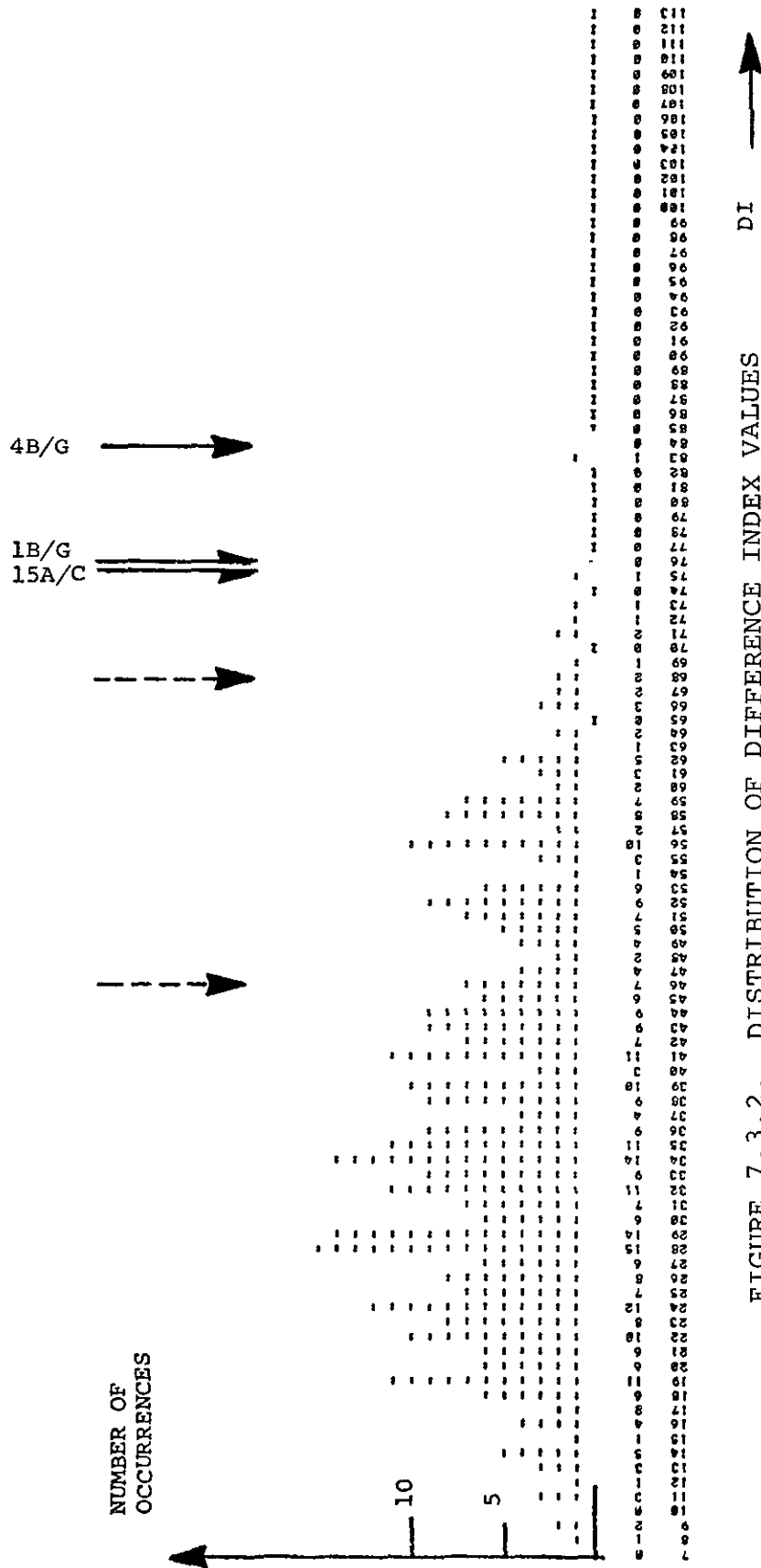
FIGURE 7.3.2. DISTRIBUTION OF DIFFERENCE INDEX VALUES
DI = C_1SD

——— INDICATES DI FOR DEFECTIVE WHEELS
----- INDICATES DI FOR GOOD WHEELS IN LAB. TEST

SAMPLE SIZE: 369. WITH CORRECTION FOR TIMING PULSE DIFFERENCE
Frequency Range is 0-7.2 kHz. Compare with Fig. 7.3.1

The last set of experiments involved the inclusion
of a term in NC, the number of common resonances. Figure
7.3.3 is a histogram of NC values from the Englewood
sample with those from the reference bad wheel set. Note
that the bad wheels show up to 5 common resonances, but
the modal value is around 6 or 7. It was felt that this
feature could be used by putting a heavy emphasis on the
similarity of wheels with a high number of common resonances.
Consequently, experiments were run using the following
DI equations:

$$DI = c_1 SD - c_2 NC \qquad (7.3.1)$$

and

$$DI = c_1 SD - c_2 (NC)^2 \qquad (7.3.2)$$

The best results were obtained from equation (7.3.2) with
the ratio

$$\frac{c_2}{c_1} = 5.$$

These results are shown in Fig. 7.3.4. In comparison
with Fig. 7.3.2 it may be argued that there is an improve-
ment in that there are now two bad wheels with DI values
higher than any from the Englewood sample.
On the other hand, there are still three values from
the Englewood sample falling in the range of the bad
wheel reference group.
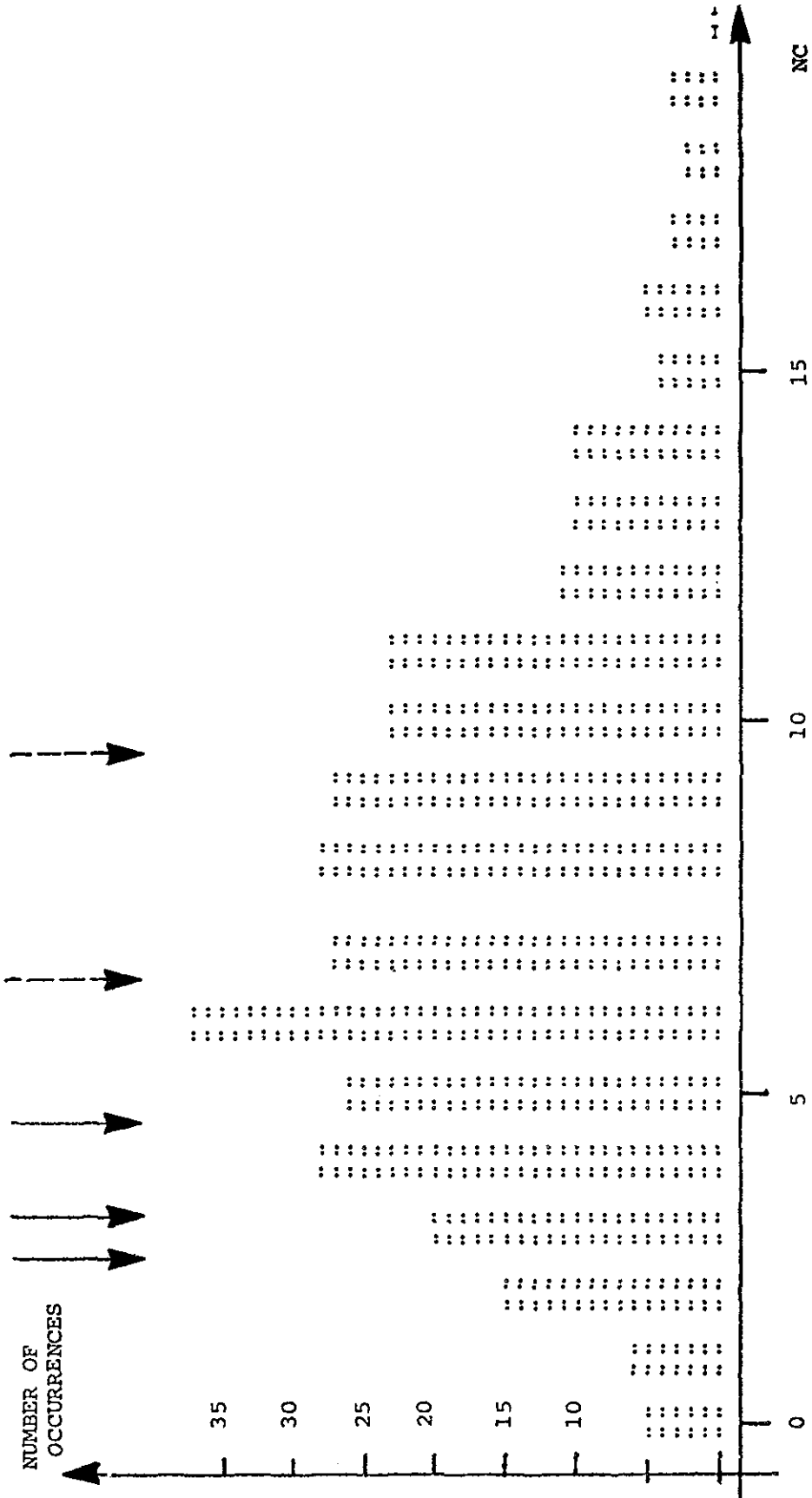
FIGURE 7.3.3. DISTRIBUTION OF NUMBER OF COMMON RESONANCES, NC
——→ INDICATES AVERAGE VALUE OF NC FOR DEFECTIVE WHEELS
‒‒→ INDICATES AVERAGE VALUE OF NC FOR GOOD WHEELS IN LAB. TEST

Sample Size: 313. Frequency Range is 0-10 kHz

NUMBER OF
OCCURRENCES

5

0

DI
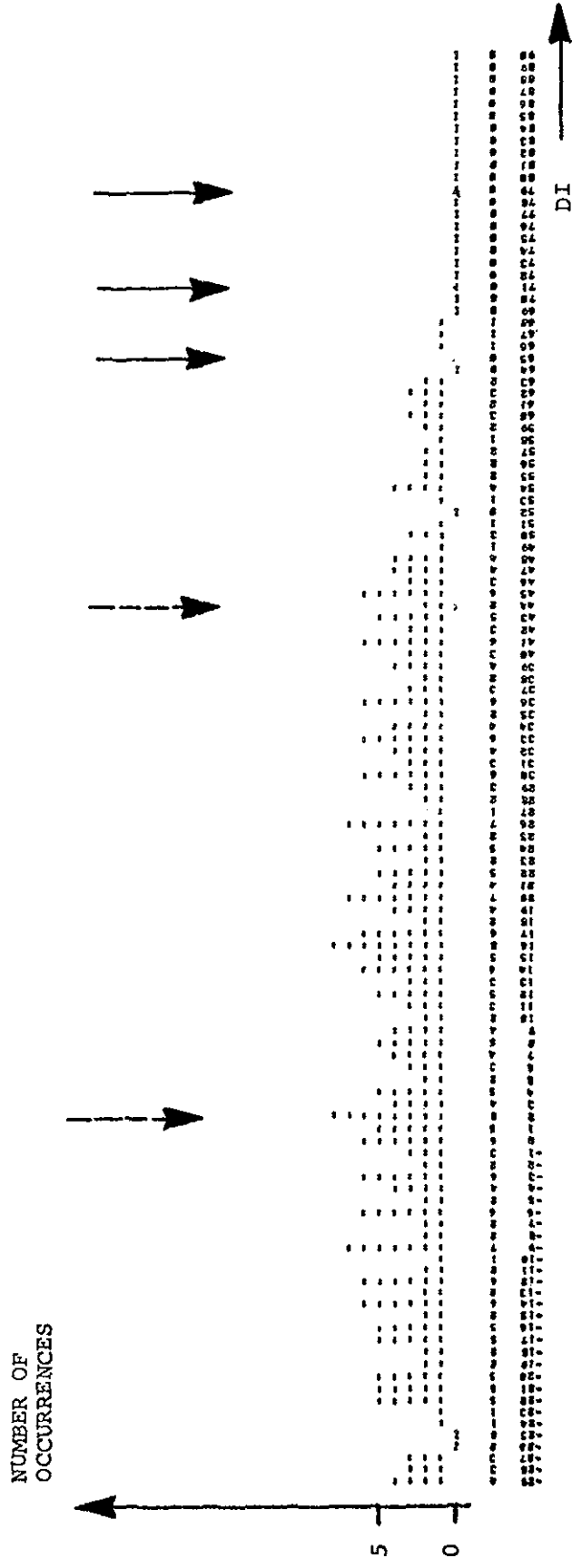
FIGURE 7.3.4.   DISTRIBUTION OF DIFFERENCE INDEX VALUES

$DI = C_1 SD - C_2 (NC)2$

———INDICATES DI FOR DEFECTIVE WHEELS
- - -INDICATES DI FOR GOOD WHEELS IN LAB. TEST

Sample Size: 371.   With correction for Timing Pulse Difference
Frequency Range is 0-7.2 kHz.   Compare with Fig. 7.3.2

Several other histograms were made for DI equations including terms in the difference of total levels LD and terms in the difference of total numbers of resonances in each spectrum NR. None of the variations tried led to any further improvement in the separation.

At this stage therefore there are two variations of the DI equation which appear to be promising as illustrated in Figs. 7.3.2 and 7.3.4. The question to be addressed in the next section is whether or not the high DI values shown in Figs. 7.3.2 and 7.3.4 are indicative of wheel/axle conditions, and, if so, what conditions.

7.4   The Effect of Wheel Conditions

7.4.1   Introduction

In the previous sections the identification and correction of system problems and the optimization of the DI equation was presented. As a result of these studies there was a considerable improvement in the histogram of DI values in the sense that the DI values for defective wheels showed the greatest separation yet from the modal value of the rest of the population. But there is clearly a wide spread in DI values among the sample. The purpose of the study reported now was to ascertain, if possible, what wheel conditions, besides cracks, could give rise to high DI values. Before starting this phase of the investigation it was anticipated that a variety of possible conditions might have caused such high values:

1. skewed axles

2. uneven load

3. uneven wear

4. greasy wheels

5. differences in internal stress

6. cracks.

There is evidence that some skewed axles were
present in the Englewood sample, but these occurrences
did not result in extremely high DI values. Greasy wheels
are highly damped at high frequencies and usually resulted
in an "insufficient data indication." None of the very
high DI values in Fig. 7.3.5 showed very high damping,
and consequently grease is not believed to be the cause
of the high values. Although changes in internal stress
do cause changes in resonant frequencies, such changes are
very small. Even if there were substantial differences
in internal stress between two wheels of a given axle set
(which is hard to believe), the effect in the DI value
should still be very small. The effects of uneven load
should presumably be similarly small since the effect
on the acoustic properties of the wheel does not depend on
whether the stress field is residual or is applied
externally.

Thus, by this process of elimination uneven wear and
cracks were left as potential causes of the high DI values.
However, in a sample of 400 wheel sets, it is very unlikely
that there is a cracked wheel as mentioned previously.

One therefore suspects that uneven wear is the most likely
cause of the large number of high DI values.

7.4.2 Data Reduction

In order to investigate this hypothesis it was
decided to make a further study of the data on the ten
wheel sets from the Englewood sample showing the highest
DI values. For these wheel sets the following data was
available:

1)   plots of the acoustic spectra from the two wheels

2)   oscillograms of the impact and timing pulse

and 3)   the car identification number.

In each case the first point of concern was to ascertain
if uneven impact level was a problem. In only two of the
ten cases investigated was there a substantial difference
in impact levels. Figures 7.4.1 and 7.4.2 show the effect
for one of these cases. The impact level was about the
same in the other eight instances. However, all of these
other eight instances showed a common feature in the
spectral comparisons as seen in Figs. 7.4.3 and 7.4.4 for
a typical case.

The feature of importance which distinguishes these
cases is a frequency shift between resonance peaks. Such
shifts are marked in Fig. 7.4.3, The interesting aspect
of this phenomenon is that the amount of the shift appears
to increase proportionally with frequency to a first
approximation. This effect is illustrated in Fig. 7.4.5
where the frequency shifts are plotted as a function of
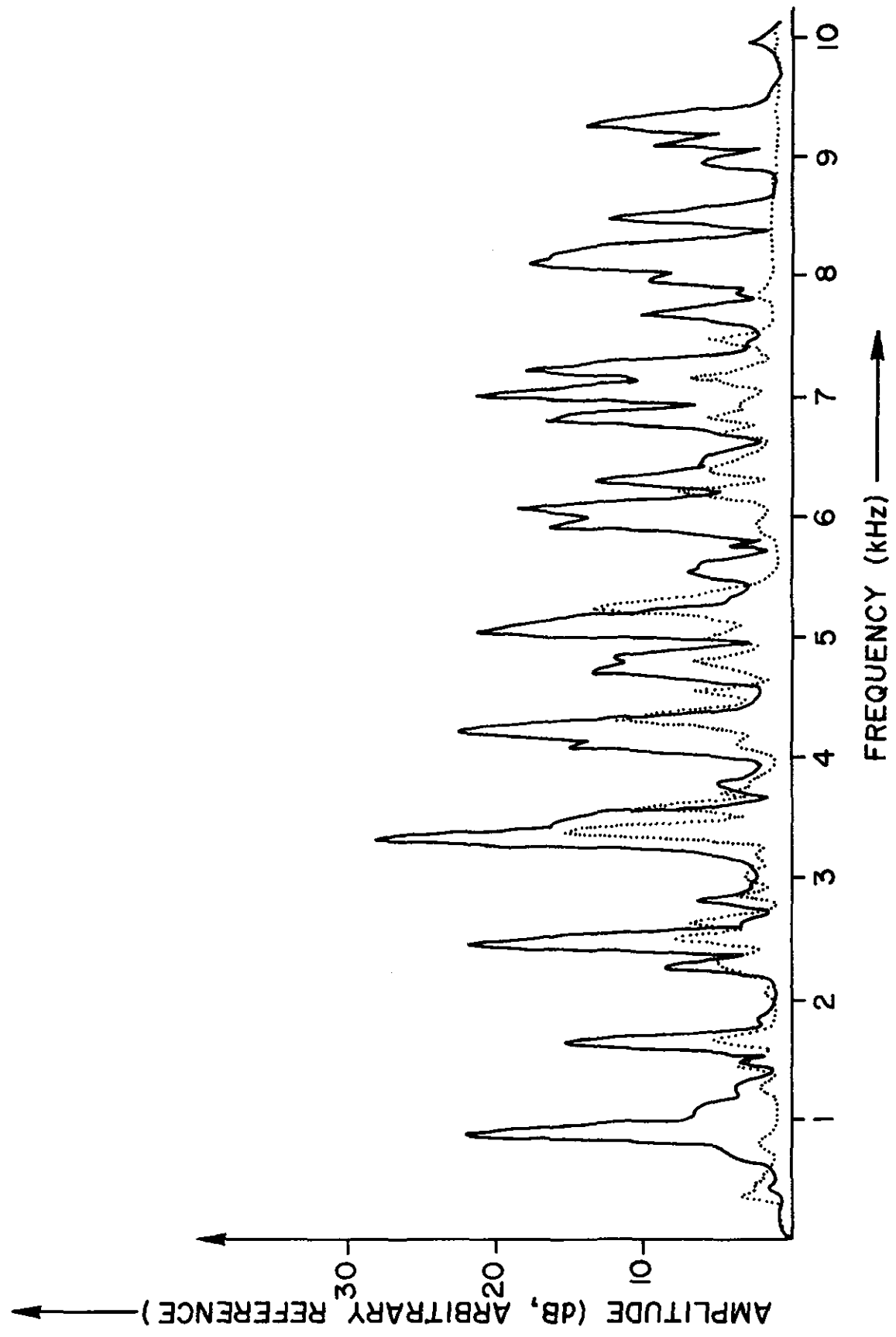
FIGURE 7.4.1 SIGNATURES OF WHEELS DUE TO UNEVEN IMPACT
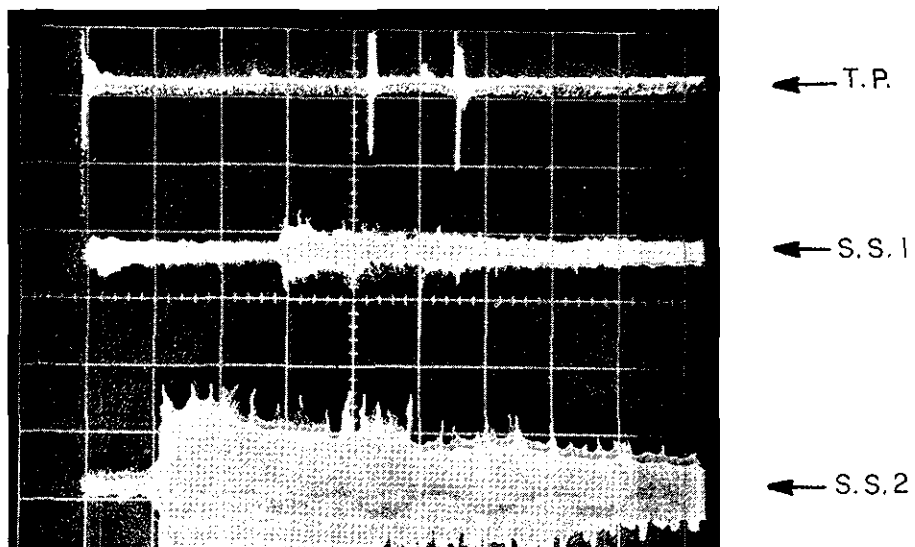
Fig. 7.4.2   Timing pulses (T.P.) and sound signals
(S.S.) from two unevenly impacted wheels.
Sweeping speed 50 ms/div. (The signatures
in Fig. 7.4.1 correspond to the above
signals.)
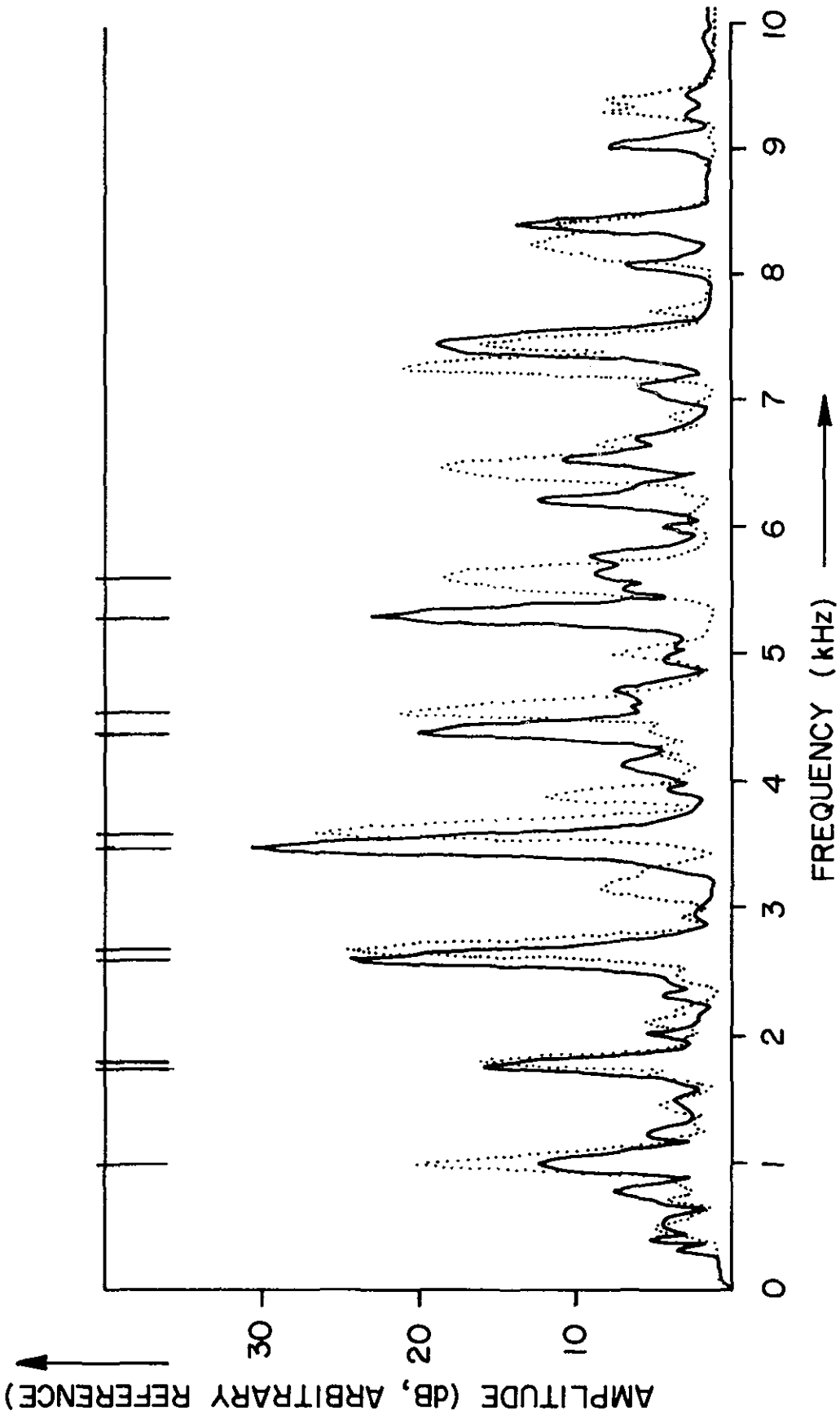
FIGURE 7.4.3   SIGNATURES OF WHEELS ON AXLE 3 , CAR GTAX 13286
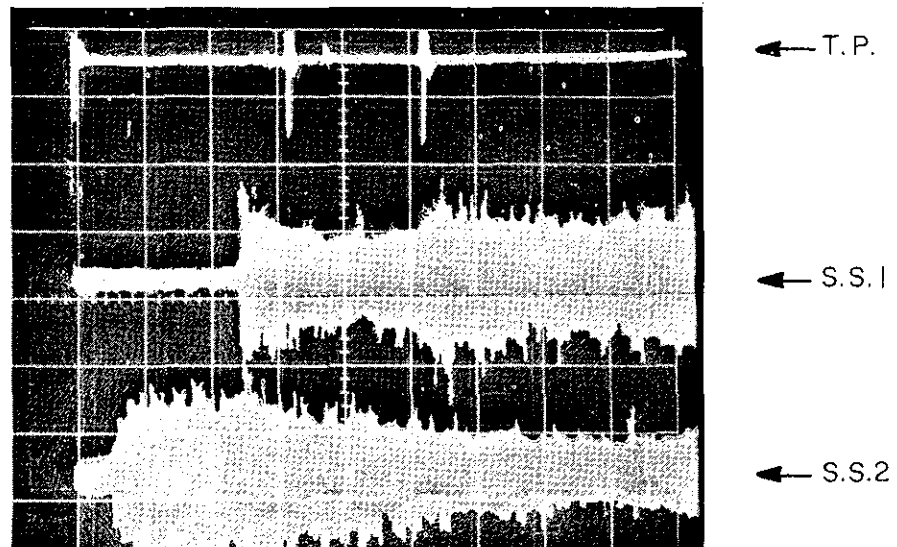
Fig. 7.4.4   Typical timing pulses and sound signals
from a pair of wheels tested at the
Englewood yard.   Sweeping speed 50 ms/div.
(The signatures in Fig. 7.4.3 correspond
to the above signals.)

Fig. 7.4.5 Frequency shift Δf_n of a pair of unevenly worn wheels, as a function of frequency f. Corresponding spectra are illustrated in Fig. 7.4.3.
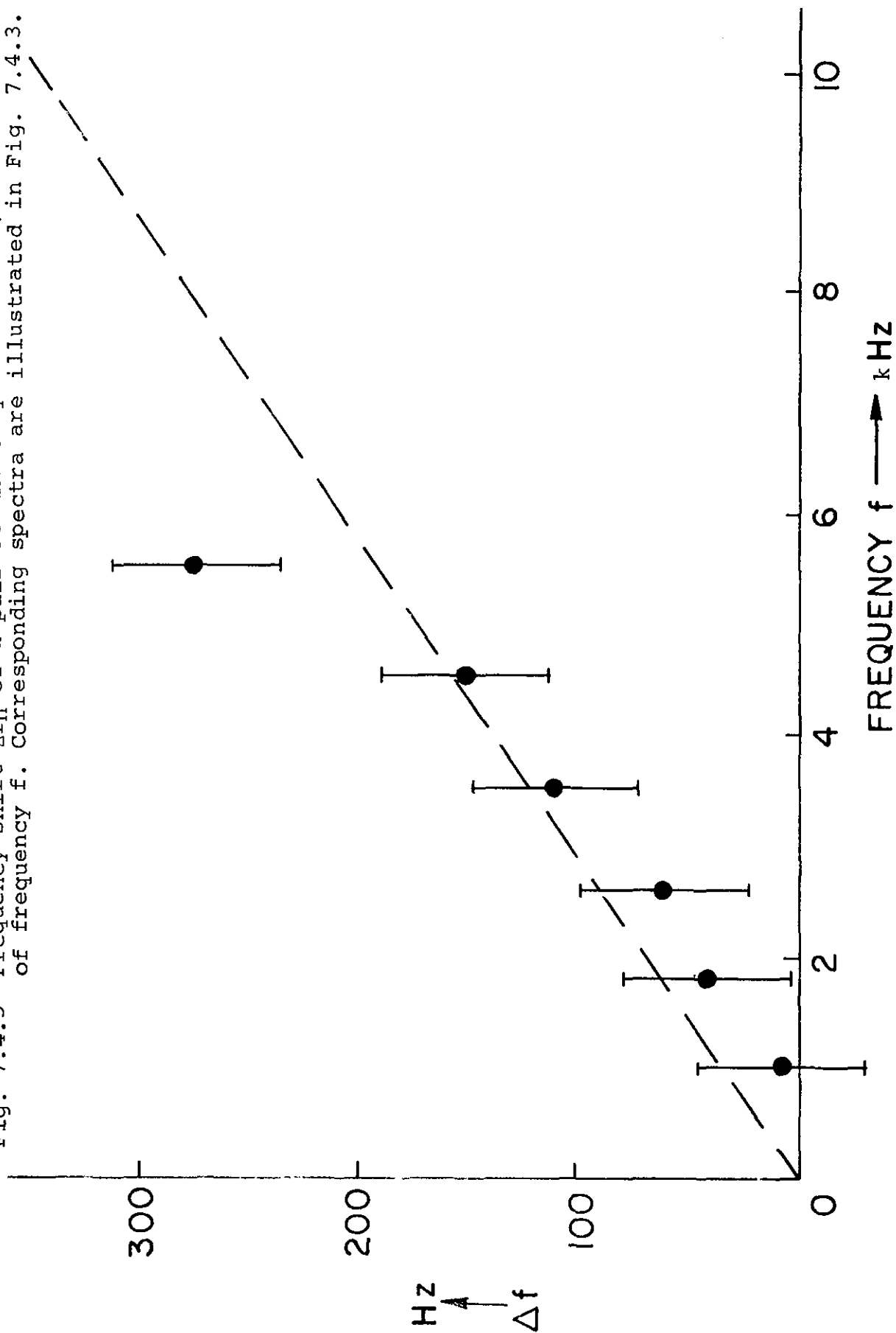
resonant frequency, as measured from the spectrum of one of the wheel pairs illustrated in Fig. 7.4.3. In most cases it was found that the frequency shifts at the higher resonances (above about 5 kHz) departed from the linear relation to even higher values, as seen in Fig. 7.4.5 for the resonance at 5.5 kHz. This made it increasingly difficult to recognize the corresponding modes at the higher frequencies.

A theoretical study on the effect of uneven wear on wheel vibrations was presented in Chapter II and the conclusion was that for small changes in rim thickness, Δh the frequency shift in the nth mode, Δf_n is given by

$$\left| \Delta f_n \right| = \left| \frac{\Delta h}{r} \right| f_n \qquad (7.4.1)$$

This simple theory offers a qualitative explanation of the results shown in Fig. 7.4.5. It is of interest to see if the theory and experiment have a reasonable quantitative relationship. From Fig. 7.4.5 the slope of the fitted line is about 250 Hz in 10 KHz, thus from eqn. (7.4.1)

$$\frac{\Delta h}{r} = \frac{250}{10 \times 10^3}$$

Assuming r to be about 16 in. we estimate $\Delta h = 0.40$ in. (10 mm). Table 7.4.1 shows the slopes and differential wear estimated for the eight wheel sets investigated. These values range from 9 to 18 mm. Obviously the theory given above has a number of simplifying approximations and the question arose as to whether such amounts of differ-

TABLE 7.4.1   THEORETICAL ESTIMATE OF DIFFERENTIAL WEAR

ON WHEELS WITH HIGH DI VALUES

Car Identification and Axle Number	DI Value	$\frac{\Delta f}{f}$	Estimated Δh in (mm)
GN 171932 axle 1	63	0.045	0.72 (18)
IC 75536 axle 4	39	0.040	0.64 (16)
ATSF 521735 axle 2	55	0.021	0.34 (9)
SSW 76704 axle 2	61	0.025	0.40 (10)
C & S 565500 axle 4	61	0.030	0.48 (12)
C & S 565500 axle 2	66	0.035	0.56 (14)
ATSF 81338 axle 4	68	0.045	0.72 (18)
GTAX 13286 axle 3	67	0.035	0.56 (14)

ential wear are encountered in practice. The expense of recalling the wheels in question was not felt to be justifiable, and in any case the wheels would have received almost a year of additional usage since the Englewood test. Instead it was decided to make some careful measurements on wheels in the laboratory collection at the University.

7.4.3 Laboratory Measurement of Wear

Measurements of the tread and flange thicknesses were made between the points indicated in Fig. 7.4.6 using a pair of calipers. Because of difficulty in positioning the calipers at precisely the same orientation it is estimated that the accuracy was $\pm$ 0.5 mm for tread measurements and $\pm$ 1.5 mm for flange measurements. The results are given in Table 7.4.2. Measurements made at different circumferential positions showed no more than $\pm$ 1 mm variation.

The first observation to be made is that the range of values of differential tread wear, from 0.0 to 6.9 mm, while not showing values as high as those hypothesized is, nevertheless, of the same order of magnitude. It was decided to study the spectra of the laboratory wheel sets to ascertain the magnitude of frequency shifts, if any. Wheels 6B/C, showing the highest differential tread wear, are 36 in. wheels with thermal cracks and the spectra are very complex. The next highest values of differential wear are for wheels 10A/C and 11A/C. Both of these sets also show considerable differential flange wear.

Figures 3.3.1 and 7.4.7 show the spectra for these wheel
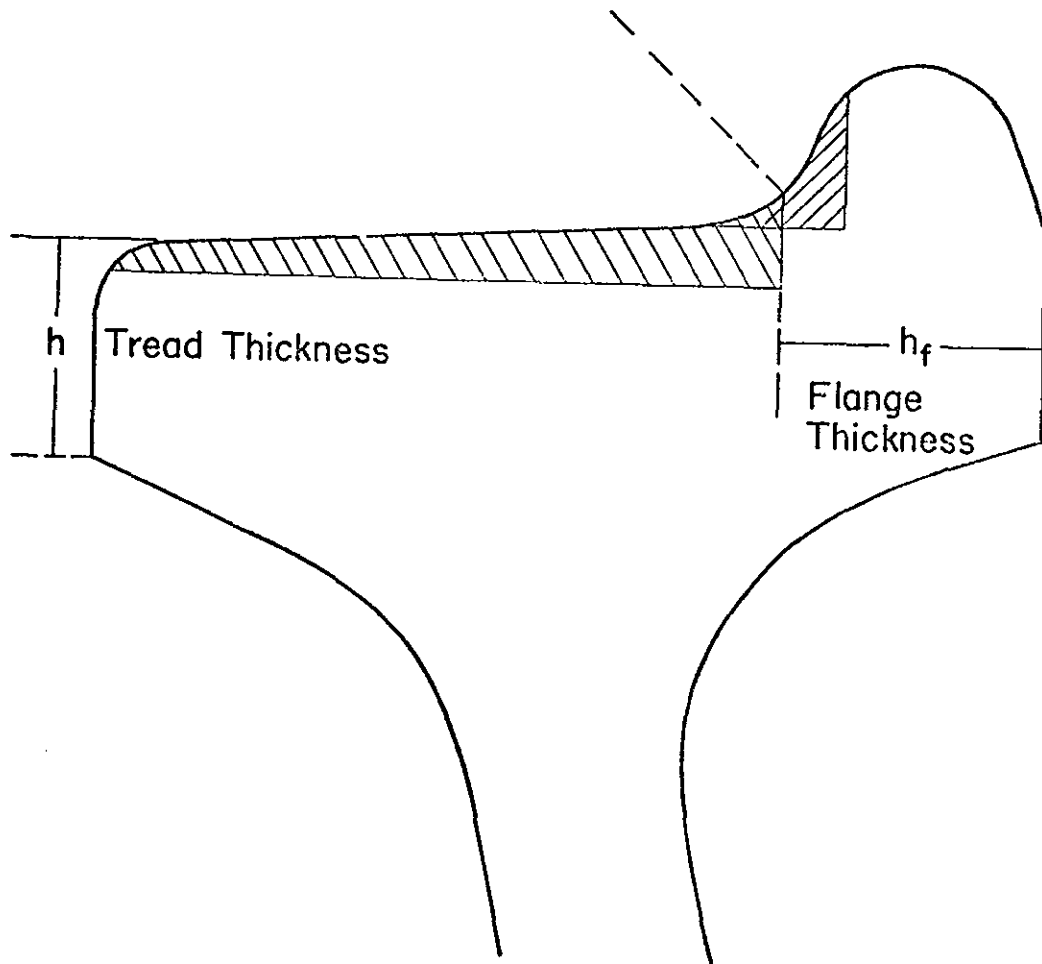
FIG. 7.4.6 Actual Cross Section of a Wheel Showing
How the Tread and Flange Thickness Were
Measured. Crosshatched Area Reveals
the Relative Importance of the Tread and
Flange Wear.

TABLE 7.4.2.   TREAD AND FLANGE THICKNESS OF WHEELS
               AT THE UNIVERSITY OF HOUSTON LABORATORY

UH Wheel Identification Number	Flange mm	Tread mm	Δh for Tread mm
9A	32.6	35.5	1.5
9C	26.2	34.0	
10A	29.5	29.5	3.7
10C	38.4	25.8	
11A	29.3	33.6	3.6
11C	39.0	30.0	
12A	31.4	28.2	0.9
12C	32.4	27.3	
13A	40.0	25.0	0.0
13C	41.0	25.0	
14A	41.0	31.2	0.0
14C	42.0	31.2	
15A	36.0	35.2	0.2
15C	34.4	35.0	
1B	33.0	34.0	1.8
1G	37.3	32.2	
2B	29.0	32.2	0.2
2G	36.2	32.0	
4B	41.0	32.5	0.5
4G	40.5	32.0	
5B	42.5	47.0	1.5
5G	30.2	48.5	
6B	38.3	42.1	6.9
6G	33.7	49.0	
8B	38.8	24.0	0.5
8G	33.5	24.5	
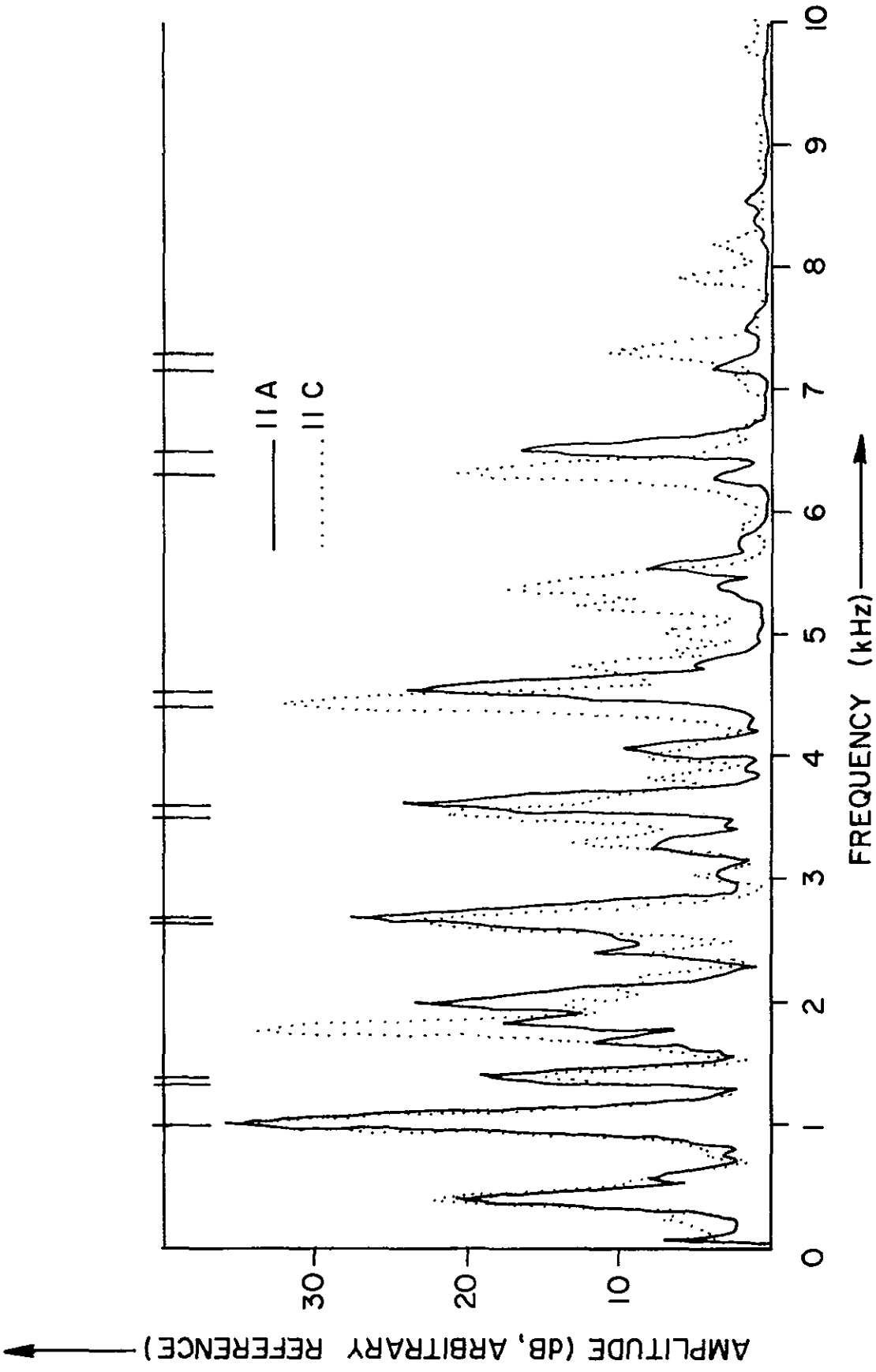
FIGURE 7.4.7 SIGNATURE OF WHEELS IIA and IIC

sets. Proportional frequency shifts are more easily seen in the spectra of 11A/C. Plotting Δf_n versus f_n for 11A/C results in the plot shown in Fig. 7.4.8. From the slope of the best straight line fit, using eqn (7.4.1) Δh is estimated to be 8 mm, about twice the measured value. A possible explanation for this apparent discrepancy could be that wear on the inside of the tread is greater than on the edge, where the measurement was made.
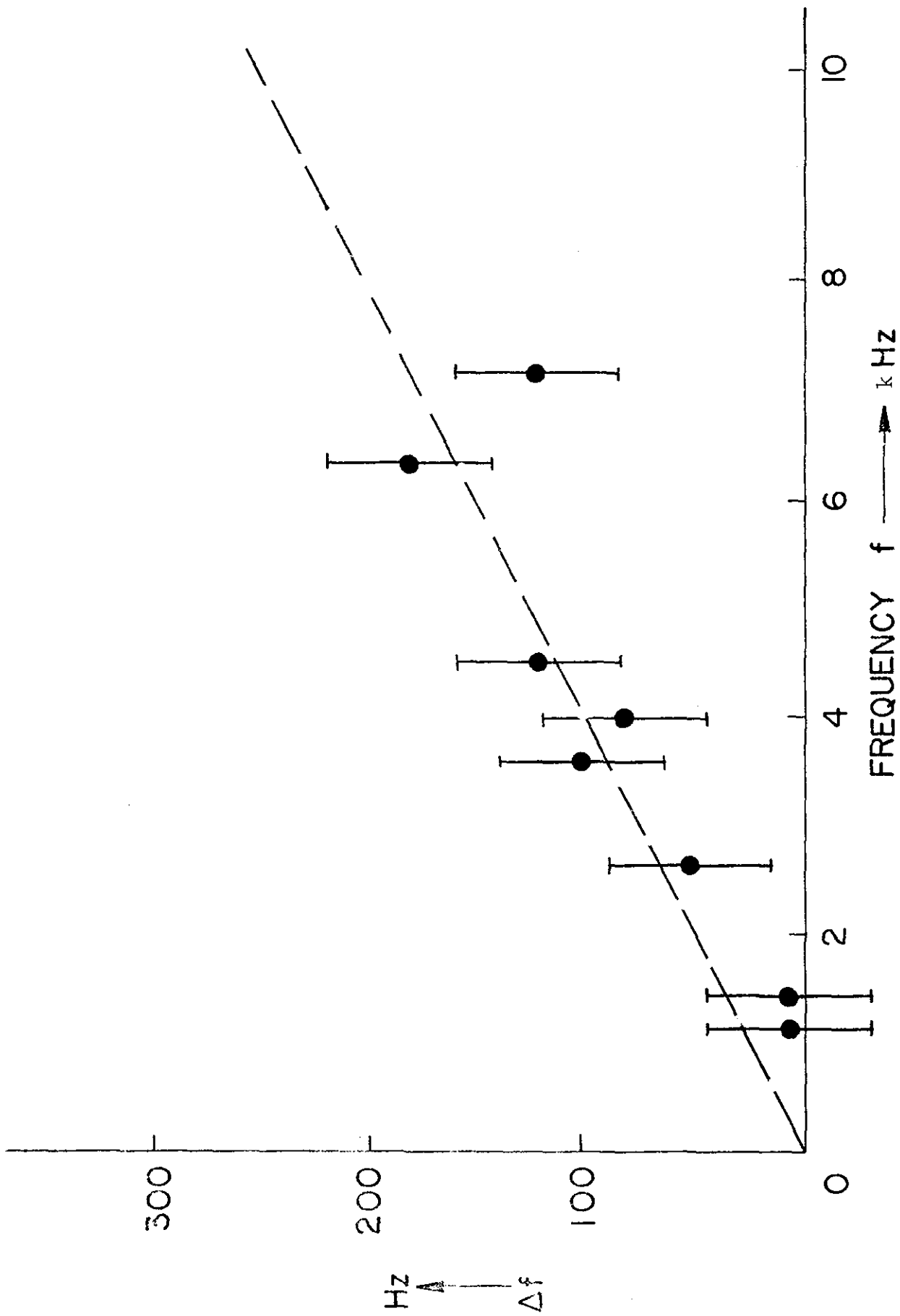
FIGURE 7.4.8.   SIGNATURE DIFFERENCES AT THE RESONANT MODES FOR WHEELS
11A/C, DUE TO UNEVEN WEAR.   CORRESPONDING SPECTRA ARE
ILLUSTRATED IN FIG. 7.4.7

8. CONCLUSIONS AND SUGGESTIONS FOR

FURTHER WORK

8.1 Conclusions

In these studies the development of a wayside
system for inspection of railroad wheels in service using
acoustic signature analysis was presented. The basic
claim is that the improvements and modifications of Nagy's
laboratory system have reached the point that the installa-
tion of a prototype system can now be contemplated. This
transitional phase included hardware interfacing for
wayside installation, and software development for real
time operation, data acquisition and data analysis.
Experimental studies and theoretical models were used to
obtain more information on the effects on vibrations of
wheels of geometrical variations, wear, internal stress etc.
Finally a field test was performed to elucidate system
problems. Tape recordings were made to permit further
study of these problems, to optimize the software and to
discover other wheel conditions influencing the acoustic
signature. It is appropriate to review these efforts in
more detail.

8.1.1 Advances in Scientific Understanding

A better understanding of wheel vibrations under
various conditions and under varying forcing functions
was needed for the development of the recognition logic.

A number of analyses were made using a finite element program. This is the best theoretical approach because there is no closed form solution for vibrations of elastic solids with complex geometries, such as the railroad wheels. A summary of the work is presented in Appendix F.

Parallel studies were made in the development of Stappenbeck's simple ring model for comparison and evaluation of the experimental results. It was successfully used in the evaluation of the lowest flexural modes of a 33" wheel, and later in the studies of differential wear on the tread of two wheels. Finally the effect of residual stress on wheel vibrations was demonstrated to be plausible from the theory of the effect of externally applied forces on beam vibration. In order to verify some of these theoretical predictions, several laboratory experiments were conducted. The results reconfirmed earlier indications that the important modes are those with nodal diameters.

Further experimental studies on the acoustic signatures from wheels in manufacture and under drag braking, with different residual stress, yielded a very important discovery, namely that there are measurable frequency shifts which are in agreement with theoretical evaluations. These shifts are of the order of 0-10 Hz.

8.1.2 System Improvements

The major change and improvement over the earlier laboratory system was the use of a narrow band instead of a 1/3 octave band real time analyzer. Most of the fre-

quency information of 28" to 40" railroad wheels is between 400 to 10,000 Hz. For this range a 250 channel narrow band real time analyzer has a 40 Hz per channel resolution, compared to several hundred Hz for the corresponding 1/3 octave band analyzer operating in the same frequency range. Although this is a significant improvement some experiments, such as residual stress evaluation, required even higher resolution.

A second area of improvement was in the wheel excitation. Several alternatives were evaluated and tested. The study led to the selection of a mechanical hammer, which rated superior to two other possible exciters. A redesign of the mechanical exciter with the emphasis on ruggedness produced an exciter which withstood some 27,000 impacts with minimal wear and without breaking. Despite the improvements impacts were speed dependent. Commercial all weather microphones were used and performed without problems despite high temperatures, humidity and rainstorms. A timing pulse was used in the data processing. The sound from impact excitation of a moving railroad wheel is a transient signal of short duration, and the maximum train speed restricts the sampling time to about 300 ms. Thus precise sampling becomes an important factor. A reasonable choice of a timing pulse generator seemed to be a wheel proximity detector already in use on several railroads. Field experience indicated that the actual device chosen sometimes failed to generate the required pulse, and

consideration of this must be made in the installation of a prototype. The addition of two floppy diskettes as mass memory storage devices was another improvement. Laboratory tests required a relatively small amount of memory for data storage. But in actual operation the fast collection of a large amount of data prevented true real time analysis. However, near real time operation was possible in that data processing started after the transfer of the last wheel signature. The processing time could and should be reduced in a prototype system.

8.1.3 Software and Signature Recognition Improvements

The field tests at TTC, Pueblo were made as a rehearsal for the complete test of the system at the Englewood Yard in Houston. The treatment of the data obtained during those tests led to the following principal conclusions:

1. Timing differences between the triggering pulse and impact for the two pairs of wheel sensors and exciters was found to be an important problem but could be partially corrected in the data processing.

2. Improper data transfer from the RTA to the computer can be flagged now, with appropriate changes in the assembly software.

3. Missing triggering pulses were a problem but could be accounted for in the data processing.

4. The optimum frequency range to be used in the analysis has been shown to be 0-7200 Hz.

5. The optimum DI equation has been found to be:

$$DI = C_1 SD - C_2 (NC)^2$$

where SD is the sum of the absolute values of the differences between the sound pressure levels of the two signals in the same frequency channel. NC is the number of common resonances, i.e., the number of the resonances occurring in the same frequency channels in the two signals. This simplified DI equation was obtained after the analysis of the field data, which had shown that terms such as Decay Rate (DR) or $SP_{1,2}$ (indicating the overall sound pressure level) did not improve the separation between DI values for good and defective wheels.

The criterion for the optimum DI equation was the achievement of a maximum separation between the modal DI value in a histogram of results using the sample of recordings made in the Englewood Yard and some recordings of bad wheels made in the laboratory. The improvement in this separation can be related to system reliability and false alarm rate (see Appendix G). Using such criteria, two thirds of the defective wheels could be found with one hundred percent reliability and zero false alarm rate, based on the small statistical sample presently available.

Uneven or differential wear on wheelsets was established as the major cause of high DI values. This was concluded on the following bases:

1) An argument on the basis of prior knowledge

2) A study of the data for the 10 highest DI values found in the Englewood sample using the optimum DI equation.

These instances showed a characteristic shifting of resonance peaks by amounts approximately proportional to frequency.

3) A simple theoretical treatment showing that such an effect is to be expected if there is different wear on the treads of two wheels.

4) Some measurements of wear differences among wheels in the collection at the University.

5) A comparison of the frequency shifts in the spectra of worn wheels in the laboratory, and hence a demonstration that the wear differential predicted using the theory mentioned in 3) agrees with the measurement mentioned in 4) within a factor of two.

Some method of recognition of unevenly worn wheel sets would probably yield the most significant improvement over the existing system.

8.2 Suggestions for Further Work

It is advocated that the work on Acoustic Signature Inspection should be advanced on three fronts:

a) Installation of a prototype system by a railroad. The Union Pacific Railroad is planning to install a prototype system. Certain obvious system design improvements should be made, as detailed below.

b) Improvement of scientific knowledge. The measurement of internal stress in wheels and its effects on crack growth is probably the most important gap in knowledge at present. The effect of cyclic loading on crack growth

rates is another unknown area. It will be difficult to improve on wheel removal criteria without such knowledge.

c) <u>System Interaction Studies, Calibrations, etc.</u> There is a need for a centrally located establishment where comparisons and interactions of various inspection systems could be carried out. Suggestions for development of an ASI system at such a location are also detailed below.

8.2.1 <u>Installation of a Prototype ASI System</u>

Planning for the installation of a prototype ASI system by the Union Pacific Railroad has already reached an advanced stage. The system will be installed in the Las Vegas, Nevada yard and the target date for commencement of operations is January 1979. The hardware will consist of a Hewlett-Packard computer system interfaced with the Spectral Dynamics RTA presently on loan to the University of Houston. A single General Radio all-weather microphone will be used. Two commercial microswitch wheel sensors have been selected. The wheel exciters will be of the same type used in the 1977 test at the Englewood Yard.

The Union Pacific plans to assemble the system at Omaha prior to installing it at Las Vegas. Implementation of the software is considered to be part of the assembly task. It will be necessary to rewrite the existing programs in FORTRAN in order to reduce the data processing time.

After installation of the system at a low speed location it is anticipated that a period of "debugging"

will be necessary. The Union Pacific intends to assign
a qualified person to work full time with the system.

It is recommended that additional work to support
the Union Pacific's effort could be directed toward
the detection of uneven wheel wear. Successful identifica-
tion of such wheels should further reduce the false alarm
rate. One way to do this would be to incorporate a
subroutine in the computer software to recognize resonant
frequency shifts. Two possible algorithms can be envisaged:
a) multiplication of the frequency values of one spectrum
by a variable and use of the minimum DI value obtained,
for decision making; b) elimination from consideration of
wheel sets in which the DI value increases rapidly at high
frequency. Obviously such a subroutine would require
development time and need careful study before incorpora-
tion in the program. One problem might be that a wheel
set with a cracked member could also show high differential
wear. Another method to offset the high DI value of sets
with high differential wear would be to include a term
in the DI equation based on input from a system capable
of directly measuring differential wear, such as a flange
height sensor or a rim circumference indicator.

It is also suggested that some effort could be devoted
to exciter design as follows:

a) Improve the present exciter by modifying the impact
    delivered so that it shall be independent of train
    speed. A solenoid could be used to activate the
    impacter. Other changes, not in the exciter alone, are

needed to improve the effectiveness of the system at
higher speeds.

b) Instrument the plunger of the present hammer to permit
a reading of flange depth. This reading should be
used to detect uneven wear on wheels of an axle set
and to indicate wear beyond condemnable limits.

c) Instrument the hammer of the present exciter to give
a reading of the impact force. This reading could be
used to indicate a failure of the system or to indicate
the presence of foreign material on the wheel tread.
This could be used to detect wheels liable to slip
through retarders.

d) Reconfigure the mounting of the exciter to permit
speedier attachment to the rail and ready adaptability
to rail of different weights, between 110 lb/yd and
136 lb/yd.

e) Design an electrical control unit to activate the
hammer and provide the means to program the sequence
of wheels to be struck and to deactivate the exciter
entirely if so required.

Finally it is important that a data bank of tapes
be compiled to permit further sensitivity studies and
improvement of the DI equation. This would also permit
the system reliability and false alarm rate to be monitored.
Causes of high DI values should be ascertained. In order
to allow such studies to be made the system should include
a 2 or 4 channel analog tape recorder. Tapes should be
catalogued and stored.

8.2.2 System Interaction Studies

Beyond the installation of the prototype at Las Vegas, and benefitting from experience therewith, a second system should be installed at the Transportation Test Center at Pueblo, Colorado. In order to permit systems interaction studies, operation of calibration consists, etc. the following additional developments should be undertaken:

a) Use of A/D Conversion

If the microphone signal were converted directly into digital form and stored in memory it could then be processed by a Fast Fourier Transform (FFT) program and the use of the RTA could be avoided. Hardwired FFT programs are available. If this task were successfully accomplished it appears that there would also be an improvement in system reliability. However elimination of the RTA is not recommended until it is demonstrated that the task can be accomplished without sacrifice in frequency resolution, and even then the RTA has other desirable features. The use of a line printer instead of the teletype will speed up the computer output 10 to 25 times which is another important factor in the development and use of the system.

b) Provision of Automatic Turn-on

It would be desirable to provide automatic turn-on for the system when a train approaches. This will entail the selection of a train proximity detector and turn-on

of the electronics with adequate warm-up time. Equipment costs are uncertain estimates.

c) Interfacing to a Central Processor

The minicomputer of the ASI system would need to be interfaced with the Central Processor of the Automated Wayside Facility. In addition an analog signal from the microphones should be available to the Central Processor.

8.2.3 Further Research on Residual Stress, Crack Growth and Wheel Removal Criteria

Further research is necessary in order to develop a better understanding of crack initiation and growth, the influence of internal stress, the influence of cyclic loading, etc., with a view to improving wheel removal criteria.

The Wilmerding data, together with the previous information on loading and the results of the Bessemer tests, indicate that changes in resonant frequencies occur with changes in internal stress. There is a need for additional data, and there is a need to establish a firm theoretical explanation of the effect for any complex residual stress field combined with the rotating stress field due to the external load. There also arises the question of the engineering application of the effect.

The major problem in applying the effect is that the occurrence of a resonance at a certain frequency can only be used as an indicator of internal stress if the frequency of resonance in a normally stressed wheel is known.

In principle a wayside stress measuring system could be developed by cataloguing the acoustic signatures of all the extant wheel types (about 40) under conditions of normal stress and then comparing the given wheel signature with this catalog. It would not be possible to use across the axle comparison since the likelihood is that mating wheels would have very similar conditions of internal stress. One difficulty with the wheel recognition scheme is the problem of recognizing the wheel type. This might be done by reading the wheel ID lettering or by identifying the acoustic signature. Another difficulty is that the acoustic signature is affected by wear, grease, load, etc. Thus the comparison signature of the wheel type after identification would need to be corrected according to these wheel conditions. While these difficulties appear to be almost insurmountable at present for a wayside system a program of research might be started with the aim of developing a machine shop system.

Another method that could be envisaged for shop use involves a determination of the slope of the $\Delta f - \Delta \sigma$ curve by applying a stress. If an additional load is applied to a wheel, by means of a hydraulic jack for instance, then a given resonance line will shift by different amounts in frequency, depending on its initial internal stress, and the slope of the curve at the point represented by this condition. If the curve indeed exhibits a change in slope from negative to positive for certain resonances as in

Fig. 4.3.10 then the resonance line will shift to higher values for highly stressed wheels or lower values for normally stressed wheels. The effect of frequency shift for flexural vibration with circular modal lines may be different from frequency shifts for vibration with modal diameters. If this were found to be the case the absolute stress field might be inferred again by an incremental loading.

In order to elucidate these questions the following research tasks are suggested:

a) Development of Research Instrumentation to Measure Internal Stress

In order to establish the effect of internal stress on acoustic signatures in various wheel types and under various conditions it will be necessary to select and procure or develop instrumentation to make absolute stress measurements. The ultrasonic method is favored for this purpose because it yields bulk values. It will also be necessary to secure equipment for accurate tread profile measurements.

b) Collection of Data

Data on residual stress, as measured by the ultrasonic method, together with acoustic signatures needs to be collected for a variety of wheels and for various vibrational modes. New wheels as well as wheels in service need to be evaluated. Accurate wear profiles need to be measured.

c) Establishment of $\Delta f/\sigma$ Curves

Further work needs to be done to establish the nature of the $\Delta f/\sigma$ curves. It will be necessary to secure a

frequency translator in order to accomplish this. The
first order of business should be to process the remaining
tape recordings from the Wilmerding tests. The apparent
lack of correlation with some strain gauge readings on
the rim needs to be explained. It is desirable to establish
the repeatability of these curves and to correlate
frequencies with absolute stress. Further dynamometer
tests will be necessary although some information may be
forthcoming from the data collection of task b.

d) Theoretical Prediction of Frequency Shifts

If the changes in resonant frequency are indeed due
to changes in internal stress it should be possible to
simulate the changes using one of the standard finite
element programs. NASTRAN, for example, permits such
stress distributions to be imposed. Not only would a
correct prediction of natural frequency shifts enhance
confidence but the study could also be of enormous value
in predicting $\Delta f/\sigma$ curves because of the difficulties
envisaged in collecting data.

e) Demonstration System for Residual Stress Measurement

After the tasks outlined above have been performed it
should be possible to assemble a laboratory demonstration
system. This should be evaluated by comparing residual
stress measured by ASI with values obtained from ultrasonic
tests.

f) Theoretical Prediction of Crack Growth

While the work of Carter and Caton emphasizes many
important aspects of fracture in wheels, it evidently

does not treat fatigue crack growth except in an elementary
manner. Even though the results reported there provide
some idea of crack sizes which ought to result in a wheel
being taken out of service, they do not establish any
basis for estimating the number of cycles to failure for a
crack of subcritical size. It is proposed that this problem
could be tackled on a theoretical basis, using recent
developments in fracture mechanics. There are two possible
avenues of approach. One way would be to use a finite
element technique, modelling the crack tip with a plastic
element and having a moving network of grid points. The
other way would be to use an analytical approach using
path invariant integral. It is not clear at present
which method would be the most satisfactory. The output
of such a study would be predictions of crack growth paths
and crack growth rates under various conditions of cyclic
load and stress.

g) Experimental Study of Crack Growth

Some further experimental studies of crack initiation,
due to braking, cyclic loading, etc. would serve to comple-
ment and confirm task f. It is possible that such a study
would best be carried out on model wheels, with accelerated
cycling techniques. The detailed mechanism of crack
initiation needs further study.

REFERENCES

1. Nagy, K., "Feasibility Study of Flaw Detection in Railway wheels Using Acoustic Signatures," Ph.D. Thesis, University of Houston, August 1974. See also: Report No. FRA/OR & D 76-290, National Technical Information Service, Springfield, Virginia 22161.

2. Nagy, K., Dousis, D. A., Finch, R. D., "Detection of Flaws in Railway Wheels Using Acoustic Signatures," ASME paper No. 77-WA/RT-1, 1977.

3. Bray, D. E. and Finch, R. D., "Flaw Detection in Model Railway Wheels," Report No. FRA-RT-71-75, National Technical Information Service, Springfield, Virginia 22161, PB-199-956, February 1971. See also: Bray, D. E., Dalvi, N. G. and Finch, R. D., Ultrasonics II, 1973, 66-72.

4. Dousis, D., "Acoustic Signature Processing for Railroad Wheel Flat Spot Detection," M.S. Thesis, University of Houston, December 1975.

5. Bray, P. E., "Pulse Excitation of Railway Wheels," M.S. Thesis, M-2165, University Microfilms, Ann Arbor, Michigan, 48106 111 pp. 1969.

6. Leissa, A. W., "Vibration of Plates," NASA SP-160, 1969.

7. Leissa, A. W., "Vibration of Wheels," NASA SP-288, 1973.

8. Soni, S. R., Amba-Rao, C. L., "Axisymmetric Vibrations of Annular Plates of Variable Thickness," J. Sound Vibr., 38 (4), 465-473, 1975.

9. Banerjee, M. M., "On the Non-linear Vibrations of Elastic Circular Plates of Variable Thickness," J. Sound Vibr. 47 (3), 341-346, 1976.

10. Appl, F. C., Byers, J. R., "Fundamental Frequency of Simply Supported Rectangular Plates with Linearly Varying Thickness," J. Appl. Mech., 32, 163-168 (65).

11. Eastep, F. E., "Estimation of the Fundamental Frequency of Beams and Plates with Varying Thickness," AIAA, 14 (11) 1647-1649, 1976.

12. Sakata, T., "Approximate Formulas for Natural Frequencies of Rectangular Plates with Linearly Varying Thickness," J. Acoust. Soc. Am., 61 (4), 982-985, 1977.

13. Soni, S. R., Sankara-Rao, K., "Vibrations of Non-uniform Rectangular Plates: A Spline Technique Method of Solution," J. Sound Vibr., 35 (1), 35-45, 1974.

14. Mote, C. D., Szymani, R., "Circular Saw Vibration Research," The Shock Vibr. Dig., 10 (6), 15-26, 1978.

15. Harris, C. M., Crede, C. E., Shock and Vibration Handbook, McGraw-Hill Book Co., New York, 1976.

16. Beranek, L. L., Noise and Vibration Control, McGraw-Hill Book Co., New York, 1971.

17. Stappenbeck, Von H., "Das Kurvengerausch Der Strassenbahn," Z VDI, Bd. 96, Nr. 6, 21 February 1954. (Re: Noise made by streetcar as it takes a curve)

18. Bray, D. E., "Report on the 5th International Wheelset Congress," Report No. FRA/ORD-77/65, January 1978.

19. Wetenkamp, H. R., and Kipp, R. M., "Thermal Damage in a 33-inch Railroad Car Wheel," J. Eng. Ind., 100, 363-369, August 1978.

20. Biot, M. A., "The Influence of Initial Stress on Elastic Waves," J. Appl. Phys., 11 (8) 522-530, 1940.

21. Biot, M. A., "Mechanics of Incremental Deformations," John Wiley & Sons, New York, 1965.

22. Libai, A., Rosen, A., "Transverse Vibrations of Compressed Annular Plates," J. Sound Vibr. 40 (1), 149-153, 1975.

23. Brunell, E. J., Robertson, S. R., "Vibration of an Initially Stressed Thick Plate," J. Sound Vibr. 45 (3), 405-416, 1976.

24. Nogfeh, A. H., Kamat, P. M., "Numerical-Perturbation Technique for the Transverse Vibrations of Highly Prestressed Plates," J. Acoust. Soc. Am., 61 (1), 95-100, 1977.

25. Chehil, D. S., Dua, S. S., "Buckling of Rectangular Plates with General Variation in Thickness," J. Appl. Mech., 40 (3) 745-751, 1973.

26. Dickinson, S. M., "Modified Bolotin's Method Applied to Buckling and Vibration of Stressed Plates," AIAA, 13 (12), 1672-1673, 1975.

27. Dickinson, S. M., "The Flexural Vibration of Rectangular Orthotropic Plates Subject to In-Plane Forces," J. Appl. Mech., 38, 699-700 (1971).

28. Nieh, L. T., Mote, C. D., "Vibration Stability in Thermally Stressed Rotating Disks," Exper. Mech., 15 (7) 258-264, 1975.

29. Aggarwal, R. R., Biswas, R. N., "Flexural Vibration of a Circular Plate," Acustica, 33, 238-242, (1975).

30. Carter, C. S., Caton, R. G., Fracture Resistance of Railroad Wheels, DOT, Interim Report, No. FRA-OR & D-75-12, September 1974.

31. Wandrisco, J. M., Dewey, F. J., "Service Defects in Treads of Railroad Wheels During Service," ASME Paper 60-RR-1, 1960.

32. Cullity, B. D., Elements of X-Ray Diffraction, Addison-Wesley, third edition, New York, 1967.

33. Hirooka, T., et al., "Residual Stresses in the Rim of a Railroad Solid Wheel Due to on Tread Drag Braking and Their Effect on Wheel Failure," Proc. Fourth International Wheelset Congress, Paris, 1972, p. 91.

34. King, et al., "Stress Measurement in Railroad Wheels Via the Barkhausen Effect," Final Report, Office of R & D FRA/DOT, December 1974. Contract No. DOT-TSC-713, SWRI, Prof. No. 15-3486.

35. Spectral Dynamics Corporation, Instruction Manual for SD330A Spectrascope Real Time Analyzer, San Diego, California, May 1974.

36. Association of American Railroads, Manual of Standards and Recommended Practices, AAR Issue of 1976, pp. G-174-1973/G-178-1973.

37. Car and Locomotive Cyclopedia, Centennial Edition, (1974 by Simmons-Boardmen Publishing, New York).

38. Clotfelter, W. N. and Risch, E. R., "Ultrasonic Measurement of Stress in Railroad Wheels and in Long Lengths of Welded Rails," NASA TM X-64863, July 1974.

39. Osgood, W. R., Residual Stresses in Metals and Metal Construction Reinhold Publishing Corp., New York, 1954.

40. Treuting, R. G., Residual Stress Measurements, American Society for Metals, Cleveland, Ohio, 1952.

41. Fazekas, G. A., "On Bidirectional Snapping Linkages," J. Eng. Ind., November 1976, 1363-1366,

42. Hetenyi, M., Handbook of Experimental Stress Analysis, J. Wiley, New York, 1950.

43. Smith, R. T., "Stress-Induced Anisotropy in Solids - The Acoustoelastic Effect," Ultrasonics, July-September 1963.

44. Toupin, R. A., Bernstein, B., "Sound Waves in Deformed Perfectly Elastic Materials, Acoustoelastic Effect," J. Acoust. Soc. Am., 33, 216-225, 1961.

45. Beauchamp, K. G., Signal Processing Using Analog and Digital Techniques, Halsted Press, J. Wiley, New York, 1973.

46. Box, G., and Jenkings, G., Time Series Analysis Forecasting and Control, Holden Day, San Francisco, 1976.

47. Blackman, R. B., Tukey, J. W., The Measurement of Power Spectra, Dover Publications, Inc., New York, 1958.

48. Kapur, K. C., Lamberson, L. R., Reliability in Engineering Design, J. Wiley, New York, 1977.

49. Burton, R., Vibration and Impact, Addison Wesley, Reading, Massachusetts, 1958, pp. 248-250.

50. Timoshenko, S., Young, D. H., Weaver, W., Vibration Problems in Engineering, Fourth Edition, John Wiley & Sons, 1974, pp. 453-455.

51. Carter, C. S., Caton, R. G., Guthrie, J. L., "Fracture Resistance and Fatigue Crack Growth Characteristics of Railroad Wheels and Axles," DOT, Final Report, No. FRA/ORD-77/50, November 1977.

52. Michell, J. H., Messenger of Math., Vol. 19 (1890).

53. Yanelak, J. J., Scott, C. N., "Requirements of Residual Stress Measurements Peculiar to the Railway-Freight Industry," Extended Summaries of the Technical Papers Presented at the 1978 SESA (Society of Experimental Stress Analysis) Fall Meeting, pp. 17-18.

APPENDIX A

LIST OF WHEELS ON INVENTORY
AT UNIVERSITY OF HOUSTON

Axle Number	Wheel Size	Good Wheel Description	Bad Wheel Description	Manufacturer
1	33"	No defect, light rusting	Thermal crack to axle	Southern
2	33"	No defect, light rusting	Overheated rim	Griffin
3	33"	No defect, heavy coat of dirt and grease on outside of plate	Large crack running circumferentially in rim fillet, heavy coat of dirt and grease on outside of plate	Southern
4	33"	No defect, light rusting	Large plate crack	ARMCO
5	36"	No defect, light rusting	Thermal crack partially extending into plate	Standard
6	36"	No defect, light rusting	Thermal cracks on outside of tread, extending into rim only	Griffin
7	33"	New wheel	New wheel	Southern
8	33"	No defect	Rim fillet crack	Griffin
9	33"	No defect	Crack on rim face	Bethlehem
10	33"	No defect	No defect	Griffin
11	33"	No defect	No defect	Southern
12	36"	12A-large flat spot (6.5 inch)	12C-large flat spot	Bethlehem
13	33"	13A-small flat spot	13C-small flat spot	Griffin
14	33"	14A-small flat spot	14C-small flat spot	Griffin
15	33"	Partial plate crack	Large plate crack	

APPENDIX B

EQUIPMENT LIST USED IN THE ENGLEWOOD YARD TESTS

1. SD330A REAL TIME ANALYZER

2. NOVA 1220 MINI-COMPUTER

3. DATA GENERAL DISKETTE SYSTEM

4. DATA GENERAL FAST PAPER TAPE READER

5. (2) BAND-PASS FILTERS

6. TRIGGERING-PULSE CIRCUIT

7. DC POWER SUPPLY FOR ITEM NO. 6

8. HP AMPLIFIER

9. GR TAPE RECORDER

10. (2) GR MICROPHONES

11. (1) OSCILLOSCOPE

12. (10) DISKETTES FOR ITEM NO. 3

13. CABLES

14. (2) MECHANICAL EXCITERS

15. SPARE PARTS FOR ITEM NO. 14

16. HAND TOOLS

17. (2) ACI WHEEL DETECTORS

18. (2) WALKY-TALKY'S

APPENDIX C

SOFTWARE FOR COMPUTER INTERFACING
AND DATA PROCESSING

APPENDIX C.1

PIN ASSIGNMENT

In general loading narrowband spectra into a digital computer
can be done in two ways. First, using the FRAME-SYNC and WORD-SYNC.
pulses to trigger separate computer interrupt lines. These inter-
rupts cause the computer to abandon its current processing task
and jump to an interrupt routine, and service the device which is
requesting the interrupt (in this case the SD330A). The computer
then returns to normal processing. Second, if it is required to
load spectra only at certain defined times, the FRAME-SYNC. and
WORD-SYNC. lines can be connected as data lines to the computer
data register. In this case spectra would be loaded under program
control by testing the individual bits in the data word which
correspond to the FRAME-SYNC. and WORD-SYNC. lines. Under the
present interfacing scheme the WORD-SYNC. line is connected to
the External Interrupt pin and the FRAME-SYNC. to a DATA in pin
(see Table C.1.1).

TABLE C.1.1   COMPUTER-ANALYZER INTERFACING

PIN ASSIGNMENT

REAL TIME ANALYZER SD330A			COMPUTER NOVA 1220	
SIGNAL NAME	PIN	PIN	SIGNAL NAME	
DATA LINES (LSB) (OUTPUT)	J-17	28	22	DATA IN 15
	J-17	27	20	DATA IN 14
	J-17	26	4	DATA IN 13
	J-17	25	19	DATA IN 12
	J-17	24	5	DATA IN 11
	J-17	23	6	DATA IN 10
	J-17	22	8	DATA IN 9
	J-17	21	7	DATA IN 8
	J-17	19	9	DATA IN 7
(MSB)	J-17	18	10	DATA IN 6
WORD SYNC. (OUTPUT)	J-17	29	46	DIO. EXT. INT.
SWEEP FRAME SYNC. (OUTPUT)	J-17	31	11	DATA IN 4
SWEEP (OUTPUT)	J-17	16	13	DATA IN 3
GROUND	J-17	34	1	GROUND
EXT. START (INPUT)	J-18	1	21	DATA OUT 1
EXT. PEAK HOLD (INPUT)	J-18	3	24	DATA OUT 3
EXT. STOP (INPUT)	J-18	4	27	DATA OUT 4
EXT. TR. PULSE (TAPE RECORDER)	⟶		16	DATA IN 1
EXT. RESET (INPUT)	J-18	5	25	DATA OUT 5
EXT. SWEEP (INPUT)	J-18	6	3	DATA OUT 6
EXT. EXP. AVG.	J-18	2	23	DATA OUT 0

213
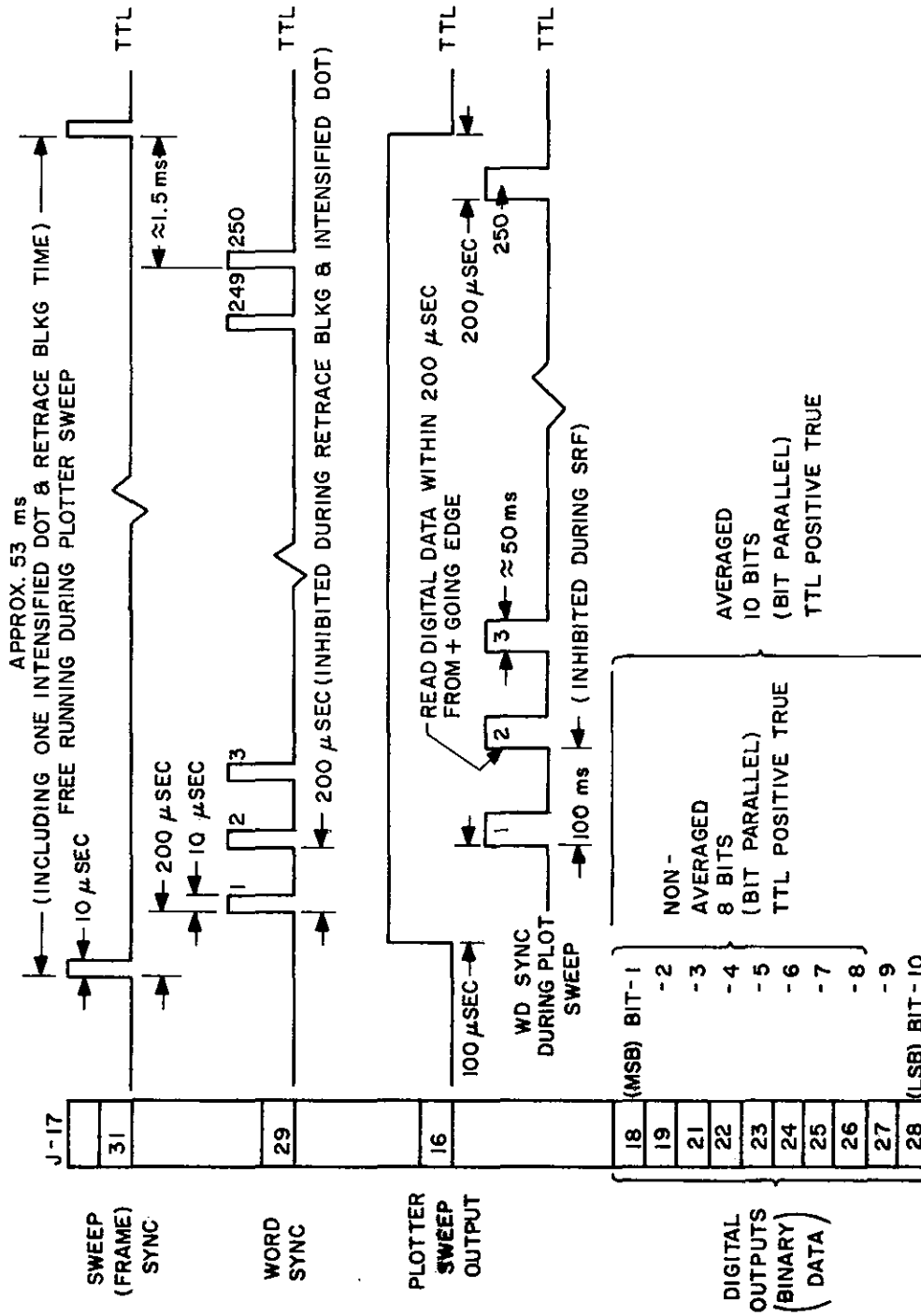
FIGURE C.1.2 SD 330A DIGITAL OUTPUT TIMING

APPENDIX C.2

LIST OF THE ASSEMBLER SOFTWARE USED FOR DIGITAL CONTROL OF THE
REAL TIME ANALYZER AND DATA TRANSFER TO THE COMPUTER/DISKETTE

```
0001   .MAIN
01              ; ----------------------------------------------
02              ;    TAPE  A-140-XII-N
03              ;    14 SEPT. 1977
04              ;
05              ;  DECK STBN.01
06              ;
07              ; ----------------------------------------------
08              ; THIS TAPE CONTAINS THE FOLLOWING ASSEMBLY S/R
09              ; #1   START     :START SAMPLING
10              ; #2   STOP      :STOP AND STORE
11              ; #3   PEAK      :GET PEAK SPECTRUM
12              ; #4   RESET     :RESET  CURSOR OR PLOTTER
13              ; #5   SWEEP     :START SWEEPING
14              ; #6   CLKST     :START THE CLOCK--CL.FR. 60HZ
15              ; #7   CLOCK     :READ THE CLOCK
16              ; #8(10) SFRAME :SENSE THE SWEEP FRAME PULSE (53MSEC)
17              ; #9(11) SPEC   :READ THE VALUE OF A CHANNEL
18              ; #10(12) RSTCL :RESET CLOCK
19              ; #11(13) EXTRG :EXTERNAL TRIGGERING
20              ; #12(14) SP250 :READ-IN SP. IN 53MSEC
21              ;                   USING INTERRUPT
22              ; #13(15) PNTER :RESET INPUT-OUTPUT POINTER
23              ; #14(16) OUT   :READ-OUT SPECTRUM
24              ; #16(20) SPNMR :SPECTRUM NUMBER (INPUT-OUTPUT)
25              ; #17(21) EXPAV :EXPONENTIAL AVERAGING
26              ; #18(22) PLSP  :PLOTTER SWEEP OUTPUT
27              ; #19(23) OPEN  :OPEN DISK FOR R/W
28              ; #20(24) WRITE :WRITE ON DISK
29              ; #21(25) READ  :READ FROM DISK
30              ; #22(26) CLOSE :CLOSE A R/W CALL
31              ; #23(27) CDISK :CLEAR I/O TABLES
32              ; #24(30) FLTA  :CHANGE TO FLOAT AN INT. ARRAY
33              ;
34              ; ----------------------------------------------
35
36       033000          .LOC 33000
37
38 33000 034470 SBRTB:  CKINT
39 33001 000001          1
40 33002 033107          START
41       000004          .RDX 4
42 33003 100000          20000000
43
44 33004 000002          2
45 33005 033117          STOP
46 33006 140000          30000000
47
48 33007 000003          3
49 33010 033137          PEAK
50 33011 100000          20000000
51
52 33012 000004          4.
53 33013 033147          RESET
54 33014 140000          30000000
55
56 33015 000005          5.
57 33016 033157          SWEEP
 3 33017 100000          20000000
 )
```

```
    0002  .MAIN
01 33020 000006            6.
02 33021 033175            CLKST
03 33022 100000            20000000
04
05 33023 000007            7.
06 33024 033206            CLOCK
07 33025 140000            30000000
08
09 33026 000010            8.
10 33027 033276            SFRAME
11 33030 100000            20000000
12
13 33031 000011            9.
14 33032 033304            SPEC
15 33033 140000            30000000
16
17 33034 000012            10.
18 33035 033222            RSTCL
19 33036 100000            20000000
20
21 33037 000013            11.
22 33040 033261            EXTRG
23 33041 100000            20000000
24
25 33042 000014            12.
26 33043 033352            SP250
27 33044 170000            33000000
28
29 33045 000015            13.
30 33046 033417            PNTER
31 33047 140000            30000000
32
33 33050 000016            14.
34 33051 033424            OUT
35 33052 140000            30000000
36
37 33053 000020            16.
38 33054 033437            SPNMR
39 33055 100000            20000000
40
41 33056 000021            17.
42 33057 033127            EXPAV
43 33060 100000            20000000
44
45 33061 000022            18.
46 33062 033267            PLSP
47 33063 140000            30000000
48
49 33064 000023            19.
50 33065 033501            OPEN
51 33066 125260            22222300
52
53 33067 000024            20.
54 33070 033610            WRITE
55 33071 136000            23300000
56
57 33072 000025            21.
   3073 034015            READ
   3074 136000            23300000
```

```
     0003   .MAIN
01
02  33075  000026              22.
03  33076  034137              CLOSE
04  33077  136000              23300000
05
06  33100  000027              23.
07  33101  034212              CDISK
08  33102  100000              20000000
09
10  33103  000030              24.
11  33104  034251              FLTA
12  33105  174000              33200000
13
14         000010              .RDX  8   ;RESTORE RADIX TO OCTAL
15
16  33106  177777              -1
17
19  33107  054544  START:  STA     3,S1     ;CALL  1,<DUMMY CHARACTER>
20  33110  030535          LDA     2,MASK1
21  33111  071042          DOA     2,42
22  33112  004455          JSR     DELAY
23  33113  030506          LDA     2,ZERO
24  33114  071042          DOA     2,42
25  33115  034536          LDA     3,S1
26  33116  001401          JMP     1,3      ;RETURN
27
28  33117  054534  STOP:   STA     3,S1     ;CALL  2,<DUMMY CHAR.>
29  33120  030530          LDA     2,MASK4
30  33121  071042          DOA     2,42
31  33122  004445          JSR     DELAY
32  33123  030476          LDA     2,ZERO
33  33124  071042          DOA     2,42
34  33125  034526          LDA     3,S1
35  33126  001401          JMP     1,3      ;RETURN
36
37  33127  054524  EXPAV:  STA     3,S1     ;CALL  17,<DUMMY CHAR.>
38  33130  030516          LDA     2,MASK2
39  33131  071042          DOA     2,42
40  33132  004435          JSR     DELAY
41  33133  030466          LDA     2,ZERO
42  33134  071042          DOA     2,42
43  33135  034516          LDA     3,S1
44  33136  001401          JMP     1,3      ;RETURN
45
46  33137  054514  PEAK:   STA     3,S1     ;CALL  3,<DUMMY CHAR.>
47  33140  030507          LDA     2,MASK3
48  33141  071042          DOA     2,42
49  33142  004425          JSR     DELAY
50  33143  030456          LDA     2,ZERO
51  33144  071042          DOA     2,42
52  33145  034506          LDA     3,S1
53  33146  001401          JMP     1,3      ;RETURN
54
55  33147  054504  RESET:  STA     3,S1     ;CALL  4,<DUMMY CHAR.>
56  33150  030501          LDA     2,MASK5
57  33151  071042          DOA     2,42
58  33152  004415          JSR     DELAY
59  33153  030446          LDA     2,ZERO
 0  33154  071042          DOA     2,42
```

```
      0004  .MAIN
01  33155  034476              LDA      3,S1
02  33156  001401              JMP      1,3       ;RETURN
03
04  33157  054474  SWEEP:      STA      3,S1      ;CALL  5,<DUMMY CHAR.>
05  33160  030472              LDA      2,MASK6
06  33161  071042              DOA      2,42
07  33162  004405              JSR      DELAY
08  33163  030436              LDA      2,ZERO
09  33164  071042              DOA      2,42
10  33165  034466              LDA      3,S1
11  33166  001401              JMP      1,3       ;RETURN
12
13  33167  054471  DELAY:      STA      3,SAVE
14  33170  020465              LDA      0,NUM
15  33171  040463              STA      0,CNT0
16  33172  014462              DSZ      CNT0
17  33173  000777              JMP      .-1
18  33174  002464              JMP      @ SAVE
19
20  33175  054456  CLKST:      STA      3,S1      ;CALL  6,<INPUT/CLOCK FREQU.>
21  33176  031400              LDA      2,0,3     ; A. IF INPUT 0 THEN  60HZ
22  33177  021000              LDA      0,0,2     ; B. IF INPUT 1 THEN  10HZ
23  33200  025001              LDA      1,1,2     ; C. IF INPUT 2 THEN  100HZ
24  33201  006130              JSR      @.FIX     ; D. IF INPUT 3 THEN  1000HZ
25  33202  044442              STA      1,INTVL   ;WARNING:AVOID C OR D
26  33203  065114              DOAS     1,RTC
27  33204  034447              LDA      3,S1
28  33205  001401              JMP      1,3       ;RETURN
29
30  33206  054445  CLOCK:      STA      3,S1      ;CALL 7,<OUTPUT/CLOCK READING>
31  33207  060277              INTDS
32  33210  020433              LDA      0,CLK02
33  33211  024431              LDA      1,CLK01
34  33212  006132              JSR      @.FLOT
35  33213  034440              LDA      3,S1
36  33214  031400              LDA      2,0,3
37  33215  041000              STA      0,0,2
38  33216  045001              STA      1,1,2
39  33217  060177              INTEN
40  33220  001401              JMP      1,3       ;RETURN
41
42  33221  000000  ZERO:0
43
44  33222  054431  RSTCL:      STA      3,S1      ;CALL 10,<DUMMY CHAR.>
45  33223  020776              LDA      0,ZERO    ;RESET CLOCK TO ZERO
46  33224  040417              STA      0,CLK02
47  33225  040415              STA      0,CLK01
48  33226  034425              LDA      3,S1
49  33227  001401              JMP      1,3       ;RETURN
50
51  33230  000000              0
52  33231  020413  SRTC:       LDA      0,INTVL
53  33232  061114              DOAS     0,RTC
54  33233  010407              ISZ      CLK01
55  33234  002404              JMP      @E.RET
56  33235  010406              ISZ      CLK02
57  33236  101000              MOV      0,0
58  33237  002401              JMP      @E.RET
      3240  034447  E.RET:      RET
```

```
      0005  .MAIN
01  33241  000400  CMASK:000400
02  33242  000000  CLK01:  0
03  33243  000000  CLK02:  0
04  33244  000000  INTVL:  0
05  33245  040000  MASK1:040000
06  33246  100000  MASK2:100000
07  33247  010000  MASK3:010000
08  33250  004000  MASK4:004000
09  33251  002000  MASK5:002000
10  33252  001000  MASK6:001000
11  33253  000000  S1:0
12  33254  000000  CNT0:0
13  33255  000002  NUM:2
14  33256  000042  FTWO:42
15  33257  000000  TELOS:0
16  33260  000000  SAVE:0
17          000130  .FIX=130
18
19
20  33261  054772  EXTRG:   STA     3,S1     ;CALL 11,<DUMMY CHAR.>
21  33262  020453           LDA     0,NUM1
22  33263  064442           DIA     1,42
23  33264  107404           AND     0,1,SZR
24  33265  000776           JMP     .-2      ;WAIT FOR TRIG. PULSE
25  33266  001401           JMP     1,3      ;RETURN
26
27  33267  054764  PLSP:    STA     3,S1     ;CALL 18,<D. CHAR.>
28  33270  020447           LDA     0,NUM3
29  33271  064442           DIA     1,42
30  33272  107404           AND     0,1,SZR
31  33273  000776           JMP     .-2      ;WAIT WHEN PL. OUTPUT IS HIGH
32  33274  034757           LDA     3,S1
33  33275  001401           JMP     1,3      ;RETURN
34
35  33276  054755  SFRAME:  STA     3,S1     ;CALL 8,<DUMMY CHAR.>
36  33277  020441           LDA     0,NUM4
37  33300  064442           DIA     1,42
38  33301  107405           AND     0,1,SNR
39  33302  000776           JMP     .-2      ;WAIT FOR SWEEP FRAME P.
40  33303  001401           JMP     1,3      ;RETURN
41
42  33304  054747  SPEC:    STA     3,S1     ;CALL 9,<OUTPUT/ READ VALUE
43  33305  020431           LDA     0,NUM2   ;   OF EACH CHANNEL,SLOW MODE>
44  33306  064442           DIA     1,42
45  33307  107405           AND     0,1,SNR
46  33310  000776           JMP     .-2
47  33311  004403           JSR     WAIT
48  33312  004410           JSR     READ0
49  33313  001401           JMP     1,3      ;RETURN
50
51  33314  054432  WAIT:    STA     3,SAV6
52  33315  020421           LDA     0,NUM2
53  33316  064442           DIA     1,42
54  33317  107404           AND     0,1,SZR
55  33320  000776           JMP     .-2
56  33321  002425           JMP     @ SAV6
57
    33322  054417  READ0:   STA     3,SAV1
    33323  020426           LDA     0,MASK
```

```
    0006  .MAIN
01 33324 064442          DI A      1,42
02 33325 107400          AND       0,1
03 33326 102400          SUB       0,0
04 33327 006132          JSR       •.FLOT
05 33330 034413          LDA       3,SAV3
06 33331 031400          LDA       2,0,3
07 33332 041000          STA       0,0,2
08 33333 045001          STA       1,1,2
09 33334 002405          JMP       • SAV1
10
11 33335 040000 NUM1:040000
12 33336 020000 NUM2:020000
13 33337 010000 NUM3:010000
14 33340 004000 NUM4:004000
15 33341 000000 SAV1:0
16 33342 000000 SAV2:0
17 33343 000000 SAV3:0
18 33344 000000 SAV4:0
19 33345 000000 SAV5:0
20 33346 000000 SAV6:0
21 33347 000007 CN7:7
22 33350 033603 S.PAR:    .PAR
23 33351 001777 MASK:001777
24
25 33352 054514 SP250:    STA       3,SAV25
26 33353 060277           INTDS
27 33354 021401           LDA       0,1,3
28 33355 040516           STA       0,LINPT
29 33356 020762 SWFR:     LDA       0,NUM4
30 33357 064442           DI A      1,42
31 33360 107405           AND       0,1,SNR
32 33361 000776           JMP       .-2
33 33362 020515           LDA       0,NUM25
34 33363 040512           STA       0,CNT1
35 33364 000401 WSYNC:    JMP       .+1
36 33365 060142           NIOS      42
37 33366 020752           LDA       0,NUM4
38 33367 064442           DI A      1,42
39 33370 107404           AND       0,1,SZR
40 33371 000414           JMP       EXODO
41 33372 063642           SKPDN     42
42 33373 000774           JMP       .-4
43 33374 060242           NIOC      42
44 33375 030476           LDA       2,LINPT
45 33376 020753           LDA       0,MASK
46 33377 064442           DI A      1,42
47 33400 107400           AND       0,1
48 33401 045000           STA       1,0,2
49 33402 010471           ISZ       LINPT
50 33403 014472           DSZ       CNT1
51 33404 000760           JMP       WSYNC
52 33405 000401 EXODO:    JMP       .+1
53 33406 024467           LDA       1,CNT1
54 33407 102400           SUB       0,0
55 33410 006132           JSR       @.FLOT
56 33411 034455           LDA       3,SAV25
57 33412 031400           LDA       2,0,3
-- 33413 041000           STA       0,0,2
   33414 045001           STA       1,1,2
```

```
     0007    .MAIN
01  33415  060177  EX1:      INTEN
02  33416  001402            JMP       2,3
03
04  33417  054445  PNTER:    STA       3,SAV12
05  33420  021400            LDA       0,0,3
06  33421  040452            STA       0,LINPT
07  33422  040440            STA       0,LOUT
08  33423  001401            JMP       1,3       ; RETURN
09
10  33424  054441  OUT:      STA       3,SAV13
11  33425  030435            LDA       2, LOUT
12  33426  010434            ISZ       LOUT
13  33427  025000            LDA       1,0,2
14  33430  102400            SUB       0,0
15  33431  006132            JSR       @.FLOT
16  33432  034433            LDA       3,SAV13
17  33433  031400            LDA       2,0,3
18  33434  041000            STA       0,0,2
19  33435  045001            STA       1,1,2
20  33436  001401            JMP       1,3       ; RETURN
21
22  33437  054430  SPNMR:    STA       3,SAV31
23  33440  035400            LDA       3,0,3
24  33441  021400            LDA       0,0,3
25  33442  025401            LDA       1,1,3
26  33443  006130            JSR       @.FIX
27  33444  044430            STA       1,NSP
28  33445  014427            DSZ       NSP
29  33446  000402            JMP       .+2
30  33447  000411            JMP       EXO
31  33450  020427  LSNP:     LDA       0,NUM25
32  33451  040424            STA       0,CNT1
33  33452  010421            ISZ       LINPT
34  33453  010407            ISZ       LOUT
35  33454  014421            DSZ       CNT1
36  33455  000775            JMP       .-3
37  33456  014416            DSZ       NSP
38  33457  000771            JMP       LSNP
39  33460  034407  EXO:      LDA       3,SAV31
40  33461  001401            JMP       1,3       ; RETURN
41
42  33462  000000  LOUT:     0
43  33463  000000  ZER1:     0
44  33464  000000  SAV12:    0
45  33465  000000  SAV13:    0
46  33466  000000  SAV25:    0
47  33467  000000  SAV31:    0
48  33470  000400  B7:       000400
49  33471  000001  ONE:      1
50  33472  034000  L34:      34000
51  33473  000000  LINPT:    0
52  33474  000000  NSP:      0
53  33475  000000  CNT1:     0
54  33476  000000  SAVN:     0
55  33477  000373  NUM25:    251.
57                          ;****************************
58                          ;
59                          ; DECK SKIPS.SR
                            ;
```

```
  0008   .MAIN
01      102033 .DALC SLT =     ADCZ#   0,0,SNC
02      102433 .DALC SLE =     SUBZ#   0,0,SNC
03      102032 .DALC SGE =     ADCZ#   0,0,SZC
04      102432 .DALC SGT =     SUBZ#   0,0,SZC
05              ;
06              ;      ----------
```

```
 ↑ 0009   .MAIN
02                  ;*********************************
03                  ;
04                  ;** DECK OPEN.01      16 APRIL 1977
05                  ;
06                  ;** CALL (OPEN),<CHANNEL>,<UNIT>,<FIRST SECTOR>
07                  ;   ,<NUMBER SECTORS>,<RECORD SIZE>,<ERROR FLAG> **
08                  ;
09 33500 000006            6
10 33501 171000 OPEN:   MOV     3,2
11 33502 006406          JSR     @0.PRE
12 33503 000406          JMP     OP1
13 33504 024402          LDA     1,ECAOP ; ALREADY OPEN
14 33505 002402          JMP     @0.ERT
15                  ;   --------
16 33506 000151 ECAOP:  105.    ;CODE FOR ALREADY OPEN
17 33507 033770 0.ERT:  CERTN
18 33510 033720 0.PRE:  CPREP
19                  ;   CONVERT 4 PARAMETERS UNIT THRU
20                  ;   RECORD SIZE TO INTEGER
21 33511 020416 OP1:    LDA     0,C4
22 33512 040416          STA     0,CNT
23 33513 020416          LDA     0,.OPP
24 33514 040416          STA     0,.OPX
25 33515 010466 OP2:    ISZ     .PAR
26 33516 036465          LDA     3,@.PAR
27 33517 021400          LDA     0,0,3
28 33520 025401          LDA     1,1,3
29 33521 006130          JSR     @.IFIX
30 33522 046410          STA     1,@.OPX
31 33523 010407          ISZ     .OPX
32 33524 014404          DSZ     CNT
33 33525 000770          JMP     OP2
34 33526 000412          JMP     OP3
35                  ;   --------
36 33527 000004 C4:     4
37 33530 000000 CNT:    0
38 33531 033533 .OPP:   OUNIT
39 33532 000000 .OPX:   0
40 33533 000000 OUNIT:  0
41 33534 000000 OFSEC:  0
42 33535 000000 ONSEC:  0
43 33536 000000 ORSZ:   0
44 33537 033761 0.CT:   .CT
45                  ;   --------
46                  ;   LOOK FOR UNIT
47 33540 032777 OP3:    LDA     2,@0.CT
48 33541 020772          LDA     0,OUNIT
49 33542 034411          LDA     3,0.UT0
50 33543 025402          LDA     1,UTUN,3;TABLE NUMBER
51 33544 106475          SUBC#   0,1,SNR ;OURS?
52 33545 000410          JMP     OP4      ;YES FOUND IT
53 33546 035400          LDA     3,0,3
54 33547 174014          COM#    3,3,SZR ;CHECK FOR MORE
55 33550 000773          JMP     .-5
56 33551 024403          LDA     1,ECNSU ; * NO SUCH UNIT *
57 33552 002735          JMP     @0.ERT
58                  ;   --------
59 33553 035226 0.UT0:  UT330
   33554 000152 ECNSU:  106.    ;CODE FOR NO SUCH UNIT
```

```
     0010   .MAIN
01                      ;         --------
02 33555 055002 OP4:    STA      3,CT.UT,2;REMEMBER UNIT
03                      ;       TREAT OTHER PARS
04 33556 020756         LDA      0,OFSEC
05 33557 024756         LDA      1,ONSEC
06 33560 107000         ADD      0,1
07 33561 034421         LDA      3,D616
08 33562 101113         MOVL#    0,0,SNC
09 33563 136433         SLE      1,3
10 33564 002415         JMP      @O.EOF  ;EOF ERROR
11 33565 041003         STA      0,CTSST,2
12 33566 041005         STA      0,CTSEC,2
13 33567 045004         STA      1,CTSLM,2;POSITION FILE
14 33570 102460         SUBC     0,0
15 33571 041006         STA      0,CTCWD,2
16 33572 020744         LDA      0,ORSZ
17 33573 101120         MOVZL    0,0
18 33574 024553         LDA      1,C400
19 33575 106433         SLE      0,1
20 33576 000407         JMP      OP5
21 33577 041007         STA      0,CTRSZ,2
22 33600 000567         JMP      COKR     ;OK RETURN
23                      ;         --------
24 33601 034002 O.EOF:  CEEOF
25 33602 001150 D616:   616.
26 33603 000000 .PAR:   0
27 33604 000153 ECBRS:  107.
28 33605 024777 OP5:    LDA      1,ECBRS
29 33606 000562         JMP      CERTN
```

```
↑ 0011   .MAIN
02                  ;********************************
03                  ;
04                  ;** DECK WRITE.01 **
05                  ;
06                  ;** CALL (WRITE),<CHANNEL>,<DATA>,<ERROR FLAG> **
07                  ;
08                  ;
09 33607 000003             3                    ;PAR'S   CHANN.,DATA,ERF
10 33610 171000 WRITE:  MOV     3,2        ;LOC. RETURN
11 33611 004507         JSR     CPREP
12 33612 000566         JMP     CENOP    ;  NOT OPEN
13 33613 035010         LDA     3,CT.BH,2;IS A BUFFER ASSIGNED?
14 33614 174014         COM#    3,3,SZR
15 33615 000426         JMP     WC       ;YES
16 33616 021005         LDA     0,CTSEC,2;NO
17 33617 025004         LDA     1,CTSLM,2;CHECK FOR EOF
18 33620 106033         SLT     0,1
19 33621 000561         JMP     CEEOF
20              ;   FIND A FREE BUFFER
21 33622 034472         LDA     3,W.BH0
22 33623 021406 W1:     LDA     0,BHNU,3;THIS BUFFER IN USE?
23 33624 101014         MOV#    0,0,SZR
24 33625 000404         JMP     W3
25 33626 021405         LDA     0,BHQL,3
26 33627 101015         MOV#    0,0,SNR ;ON AN IO QUEUE?
27 33630 000405         JMP     W2       ;NO
28 33631 035400 W3:     LDA     3,BHCL,3
29 33632 174014         COM#    3,3,SZR
30 33633 000770         JMP     W1
31 33634 000550         JMP     CENBA    ;NO BUFFER
32              ;   --------
33 33635 011406 W2:     ISZ     BHNU,3
34 33636 055010         STA     3,CT.BH,2
35 33637 021002         LDA     0,CT.UT,2
36 33640 041403         STA     0,BH.UT,3
37 33641 021005         LDA     0,CTSEC,2
38 33642 041404         STA     0,BHSEC,3
39              ;   COPY DATA INTO BUFFER
40 33643 035401 WC:     LDA     3,BH.BF,3
41 33644 021006         LDA     0,CTCWD,2
42 33645 117000         ADD     0,3      ;NEXT BUFFER WORD LOC.
43 33646 025007         LDA     1,CTRSZ,2;NUMBER OF WORDS IN RECORD
44 33647 123000         ADD     1,0
45 33650 041006         STA     0,CTCWD,2
46 33651 030732         LDA     2,.PAR
47 33652 031001         LDA     2,1,2    ;LOC. OF DATA
48 33653 124400         NEG     1,1
49 33654 021000 WCL:    LDA     0,0,2
50 33655 041400         STA     0,0,3
51 33656 151400         INC     2,2      ;THE COPY LOOP
52 33657 175400         INC     3,3
53 33660 125404         INC     1,1,SZR
54 33661 000773         JMP     .-5
55 33662 030477         LDA     2,.CT
56 33663 035010         LDA     3,CT.BH,2
57 33664 011402         ISZ     BHMOD,3
58              ;   CHECK FOR BUFFER FULL
59 33665 021006         LDA     0,CTCWD,2
   33666 025007         LDA     1,CTRSZ,2
```

```
       0012  .MAIN
 01 33667 123000          ADD     1,0
 02 33670 024457          LDA     1,C400   ;IS THERE ROOM FOR ANOTHER RECOB
 03 33671 106432          SGT     0,1
 04 33672 000475          JMP     COKR     ;YES. SO JUST RETURN
 05                  ;                      ;NO.  SO ENQUE FOR WRITING
 06 33673 031010          LDA     2,CT.BH,2
 07 33674 035003          LDA     3,BH.UT,2
 08 33675 020420          LDA     0,W.UQH
 09 33676 024420          LDA     1,W.BQL ;ENQUEUE BUFFER ON UNIT QUEUE
 10 33677 163000          ADD     3,0
 11 33700 147000          ADD     2,1
 12 33701 006416          JSR     @W.CAL
 13 33702 034321          ENQUE
 14 33703 015006          DSZ     BHNU,2   ;DECREMENT USE COUNT
 15 33704 000401          JMP     .+1
 16 33705 030454          LDA     2,.CT
 17 33706 102000          ADC     0,0      ;CLEAR THE BUFFER
 18 33707 041010          STA     0,CT.BH,2;   ASSIGNMENT
 19 33710 102460          SUBC    0,0      ;
 20 33711 041006          STA     0,CTCWD,2
 21 33712 011005          ISZ     CTSEC,2
 22 33713 000454          JMP     COKR     ;RETURN
 23                  ;        --------
 24 33714 035270 W.BH0:   BH0
 25 33715 000005 W.UQH:   UTQH
 26 33716 000005 W.BQL:   BHQL
 27 33717 034403 W.CAL:   CAL
 28                  ;        --------
 30                  ;************************************
 31                  ;
 32                  ;** DECK CPREP.01 **
 33                  ;
 34                  ;**CPREP -- SUPPORT FOR CHANNEL IO CALLS **
 35                  ;
 36                  ;   USAGE:
 37                  ;        NP       ;NUMBER OF PARAMETERS
 38                  ;<ENTRY>:MOV  3,2      SAVE RETURN FROM NEXT JSR
 39                  ;        JSR  CPREP
 40                  ;
 41 33720 050663 CPREP:   STA     2,.PAR
 42 33721 021775          LDA     0,-3,3
 43 33722 143000          ADD     2,0
 44 33723 040427          STA     0,.RTEN
 45 33724 054427          STA     3,CTMP
 46                  ;        SET UP STACK
 47 33725 020432          LDA     0,C.STK
 48 33726 042426          STA     0,@C.TP
 49 33727 042427          STA     0,@C.FP
 50 33730 020430          LDA     0,C.STL
 51 33731 042424          STA     0,@C.LP
 52 33732 035000          LDA     3,0,2
 53 33733 021400          LDA     0,0,3
 54 33734 025401          LDA     1,1,3
 55 33735 006130          JSR     @.IFIX
 56                  ;     LOCATE CHANNEL TABLE
  7 33736 030412          LDA     2,C.CT0
  8 33737 021001          LDA     0,CTNB,2
      '40 106415          SUB#    0,1,SNR ;OURS?
      '41 000421          JMP     CP4      ;YES
```

```
    0013    .MAIN
01  33742  031000            LDA     2,CTCL,2;NO
02  33743  150014            COM#    2,2,SZR ;OS THERE ANOTHER
03  33744  000773            JMP     .-5      ;YES
04  33745  024404            LDA     1,ECNSC ; NO SUCH CHANNEL
05  33746  000422            JMP     CERTN    ;TO ERROR RETURN
06                   ;       --------
07  33747  000400 C400:      400
08  33750  035331 C.CT0:     CT0
09  33751  000144 ECNSC:     100.      ;CODE FOR NO SUCH CHANNEL
10  33752  000000 .RTEN:     0
11  33753  000000 CTMP:      0
12  33754  034443 C.TP:      TP
13  33755  034444 C.LP:      LP
14  33756  034442 C.FP:      FP
15  33757  036755 C.STK:     BUF+1400
16  33760  037206 C.STL:     BUF+1640-LH
17  33761  000000 .CT:       0
18                   ;       --------
19                   ;    CHECK FOR OPEN
20  33762  050777 CP4:       STA     2,.CT
21  33763  021002            LDA     0,CT.UT,2;THE OPEN FLAG
22  33764  100014            COM#    0,0,SZR
23  33765  010766            ISZ     CTMP
24  33766  002765            JMP     @CTMP
25                   ;       --------
26  33767  126460 COKR:      SUBC    1,1       ;OK RETURN
27  33770  102460 CERTN:     SUBC    0,0
28  33771  006132            JSR     @.FLOT
29  33772  034760            LDA     3,.RTEN
30  33773  035777            LDA     3,-1,3   ;LOC OF <ERROR FLAG>
31  33774  041400            STA     0,0,3
32  33775  000401            JMP     .+1       ;  **DEG. **
33  33776  045401            STA     1,1,3
34  33777  002753            JMP     @.RTEN
35                   ;       --------
36                   ;    SPECIAL ERROR RETURNS
37  34000  024410 CENOP:     LDA     1,ECNOP ;NOT OPEN
38  34001  000767            JMP     CERTN
39  34002  024407 CEEOF:     LDA     1,ECEOF ;END OF FILE
40  34003  000765            JMP     CERTN
41  34004  024406 CENBA:     LDA     1,ECNBA ;NO BUF AVAIL.
42  34005  000763            JMP     CERTN
43  34006  024405 CETMO:     LDA     1,ECTMO ;TIME OUT
44  34007  000761            JMP     CERTN
45                   ;       --------
46  34010  000145 ECNOP:     101.
47  34011  000146 ECEOF:     102.
48  34012  000147 ECNBA:     103.
49  34013  000150 ECTMO:     104.
50         000130 .IFIX=130
51         000132 .FLOT=132
52                   ;       --------
54                   ;*****************************
55                   ;
56                   ;DECK   READ.01          28 APR 77.
57                   ;
58                   ;** CALL (READ),<CHANNEL>,<DATA>,<ERROR FLAG> **
                     ;
    34014  000003            3                ;PAR'S -- CHANN,DATA,ERF
```

```
     0014  .MAIN
01 34015 171000 READ:     MOV      3,2
02 34016 004702           JSR      CPREP
03 34017 000761           JMP      CENOP    ;*NOT OPEN*
04 34020 035010           LDA      3,CT.BH,2
05 34021 174014           COM#     3,3,SZR ;(JUST LIKE WRITE)
06 34022 000455           JMP      R5
07 34023 021005           LDA      0,CTSEC,2
03 34024 025004           LDA      1,CTSLM,2
09 34025 106033           SLT      0,1
10 34026 000754           JMP      CEEOF    ; EOF ERROR
11                 ;      FIND A FREE BUFFER
12 34027 034665           LDA      3,W.BH0
13 34030 021406 R1:       LDA      0,BHNU,3
14 34031 101014           MOV#     0,0,SZR
15 34032 000404           JMP      R3
16 34033 021405           LDA      0,BHQL,3
17 34034 101015           MOV#     0,0,SNR
18 34035 000405           JMP      R2
19 34036 035400 R3:       LDA      3,BHCL,3
20 34037 174014           COM#     3,3,SZR
21 34040 000770           JMP      R1
22 34041 000743           JMP      CENBA    ;*NO BUFFER AVAILABLE*
23                 ;      ---------
24 34042 011406 R2:       ISZ      BHNU,3
25 34043 055010           STA      3,CT.BH,2
26 34044 021002           LDA      0,CT.UT,2
27 34045 041403           STA      0,BH.UT,3
23 34046 021005           LDA      0,CTSEC,2
29 34047 041404           STA      0,BHSEC,3
30                 ;      ENQUE FOR READING
31 34050 102460           SUBC     0,0
32 34051 041402           STA      0,BHMOD,3;CLEAR WRITE FLAG
33 34052 031403           LDA      2,BH.UT,3
34 34053 020642           LDA      0,W.UQH
35 34054 024642           LDA      1,W.BQL
36 34055 143000           ADD      2,0        ;  ENQUE FOR READING
37 34056 167000           ADD      3,1
38 34057 006640           JSR      @W.CAL
39 34060 034321           ENQUE
40                 ;      WAIT TILL READ
41 34061 030700           LDA      2,.CT
42 34062 035010           LDA      3,CT.BH,2
43 34063 030412           LDA      2,RWAIT
44 34064 126460 R4:       SUBC     1,1
45 34065 021405           LDA      0,BHQL,3
46 34066 101015           MOV#     0,0,SNR
47 34067 000407           JMP      R5A
48 34070 125404           INC      1,1,SZR
49 34071 000774           JMP      .-4
50 34072 151404           INC      2,2,SZR
51 34073 000771           JMP      R4
52 34074 000712           JMP      CETMO    ;* TIME OUT *
53                 ;      ---------
54 34075 177773 RWAIT:    -5
55                 ;      ---------
56                 ;      COPY DATA OUT OF BUFFER
57 34076 030663 R5A:      LDA      2,.CT
   34077 035401 R5:       LDA      3,BH.BF,3
   34100 021006           LDA      0,CTCWD,2
```

```
     0015  .MAIN
01 34101 117000          ADD       0,3     ;NEXT BUFFER WORD LOC.
02 34102 025007          LDA       1,CTRSZ,2;NUMBER OF WORDS
03 34103 123000          ADD       1,0
04 34104 041006          STA       0,CTCWD,2
05 34105 032501          LDA       2,@C.PAR
06 34106 031001          LDA       2,1,2   ;LOC. DATA
07 34107 124400          NEG       1,1
08 34110 021400 RCL:     LDA       0,0,3
09 34111 041000          STA       0,0,2
10 34112 175400          INC       3,3
11 34113 151400          INC       2,2
12 34114 125404          INC       1,1,SZR
13 34115 000773          JMP       .-5
14               ;       CHECK FOR BUFFER EMPTY
15 34116 030643          LDA       2,.CT
16 34117 021006          LDA       0,CTCWD,2
17 34120 025007          LDA       1,CTRSZ,2;INCREMENT NEXT POINTER
18 34121 123000          ADD       1,0
19 34122 024625          LDA       1,C400   ;IS BUFFER OUT?
20 34123 106432          SGT       0,1
21 34124 000643          JMP       COKR      ;OK RETURN
22               ;       REMOVE BUFFER
23 34125 011005          ISZ       CTSEC,2
24 34126 102460          SUBC      0,0
25 34127 041006          STA       0,CTCWD,2
26 34130 035010          LDA       3,CT.BH,2
27 34131 015406          DSZ       BHNU,3
28 34132 000401          JMP       .+1
29 34133 102000          ADC       0,0
30 34134 041010          STA       0,CT.BH,2
31 34135 000632          JMP       COKR
32               ;       --------
34               ;****************************
35               ;
36               ; DECK CLOSE.01
37               ;
38               ;** CALL (CLOSE),<CHANNEL>,<NEXT SECTOR>,<ERROR FLAG> **
39               ;
40 34136 000003          3
41 34137 171000 CLOSE:   MOV       3,2
42 34140 006451          JSR       @C.PRP
43 34141 000637          JMP       CENOP   ;*NOT OPEN*
44               ;       RETURN THAT SECTOR NUMBER
45 34142 025005          LDA       1,CTSEC,2
46 34143 021006          LDA       0,CTCWD,2
47 34144 101004          MOV       0,0,SZR
48 34145 125400          INC       1,1
49 34146 102460          SUBC      0,0
50 34147 006132          JSR       @.FLOT
51 34150 032436          LDA       2,@C.PAR
52 34151 031001          LDA       2,1,2
53 34152 041000          STA       0,0,2
54 34153 045001          STA       1,1,2
55 34154 032433          LDA       2,@C.CT
56               ;       IF A BUFFER IS IN USE,CK FOR WRITE REQUIRED
57 34155 035010          LDA       3,CT.BH,2
58 34156 174015          COM#      3,3,SNR
   4157 000421          JMP       CL4     ;NO BUFFER
   4160 021402          LDA       0,BHMOD,3;YES BUF.
```

```
     0016   .MAIN
01  34161  101015              MOV#      0,0,SNR ;WRITE REQ.?
02  34162  000410              JMP       CL3        ;NO
03  34163  031403              LDA       2,BH.UT,3;YES
04  34164  020421              LDA       0,C.UQH
05  34165  024417              LDA       1,C.BQL
06  34166  143000              ADD       2,0
07  34167  167000              ADD       3,1
08  34170  006413              JSR       @C.CAL
09  34171  034321              ENQUE
10  34172  032415  CL3:        LDA       2,@C.CT
11  34173  035010              LDA       3,CT.BH,2
12  34174  015406              DSZ       BHNU,3
13  34175  000401              JMP       .+1
14  34176  102000              ADC       0,0
15  34177  041010              STA       0,CT.BH,2
16                  CL4:
17                  ;          CLOSE CHANNEL
18  34200  102000              ADC       0,0
19  34201  041002              STA       0,CT.UT,2
20  34202  002406              JMP       @C.OKR
21                  ;          ----------
22  34203  034403  C.CAL:      CAL
23  34204  000005  C.BQL:      BHQL
24  34205  000005  C.UQH:      UTQH
25  34206  033603  C.PAR:      .PAR
26  34207  033761  C.CT:       .CT
27  34210  033767  C.OKR:      COKR
28  34211  033720  C.PRP:      CPREP
29                  ;          ----------
31                  ;****************************
32                  ;
33                  ; CALL <(23) CLR DISK>
34                  ;
35                  ; FOR RESETTING ALL I/O TABLES
36                  ;
37  34212  060277  CDISK:      INTDS
38  34213  060233              NIOC      DP0
39  34214  102400              SUB       0,0
40  34215  126000              ADC       1,1
41  34216  030427              LDA       2,L.DT
42  34217  045005              STA       1,DTQH,2
43  34220  030426              LDA       2,L.UT
44  34221  041010              STA       0,UTQL,2
45  34222  045005              STA       1,UTQH,2
46  34223  031000              LDA       2,UTCL,2
47  34224  150014              COM#      2,2,SZR
48  34225  000774              JMP       .-4
49
50  34226  030421              LDA       2,L.BH
51  34227  041005              STA       0,BHQL,2
52  34230  041006              STA       0,BHNU,2
53  34231  045003              STA       1,BH.UT,2
54  34232  031000              LDA       2,BHCL,2
55  34233  150014              COM#      2,2,SZR
56  34234  000773              JMP       .-5
57
58  34235  030413              LDA       2,L.CT
59  34236  045002              STA       1,CT.UT,2
    34237  045010              STA       1,CT.BH,2
```

```
   0017   .MAIN
01 34240 031000          LDA     2,CTCL,2
02 34241 150014          COM#    2,2,SZR
03 34242 000774          JMP     .-4
04
05 34243 060177          INTEN
06 34244 001401          JMP     1,3
07                ;      -------
08 34245 035172 L.DT:    DT33
09 34246 035226 L.UT:    UT330
10 34247 035270 L.BH:    BH0
11 34250 035331 L.CT:    CT0
12                ;      --------
↑ 0018   .MAIN
02                ;***********************************
03                ;   DECK   FLT.01
04                ;
05                ;   CALL (NUMBER-24), <ARRAY1>,<ARRAY2>,<NO. OF DATA>
06                ;
07 34251 175400 FLTA:    INC     3,3
08 34252 175400          INC     3,3
09 34253 175400          INC     3,3
10 34254 054441          STA     3,RTN1
11 34255 031777          LDA     2,-1,3
12 34256 021000          LDA     0,0,2
13 34257 025001          LDA     1,1,2
14 34260 006130          JSR     @.FIX
15 34261 131000          MOV     1,2
16 34262 034433          LDA     3,RTN1
17 34263 021775          LDA     0,-3,3
18 34264 025776          LDA     1,-2,3
19 34265 004402          JSR     FLX
20 34266 002427          JMP     @RTN1
21
22 34267 143000 FLX:     ADD     2,0
23 34270 147000          ADD     2,1
24 34271 147000          ADD     2,1
25 34272 040421          STA     0,.A1
26 34273 044421          STA     1,.A2
27 34274 050423          STA     2,N3
28 34275 054421          STA     3,RTFX
29 34276 014415 LOOP:    DSZ     .A1
30 34277 026414          LDA     1,@.A1
31 34300 125113          MOVL#   1,1,SNC
32 34301 102461          SUBC    0,0,SKP
33 34302 102000          ADC     0,0
34 34303 006132          JSR     @.FLOT
35 34304 014410          DSZ     .A2
36 34305 044407          STA     1,.A2
37 34306 014406          DSZ     .A2
38 34307 040405          STA     0,.A2
39 34310 014407          DSZ     N3
40 34311 000765          JMP     LOOP
41 34312 002404          JMP     @RTFX
42
43 34313 000000 .A1:     0
44 34314 000000 .A2:     0
45 34315 000000 RTN1:    0
 ; 34316 000000 RTFX:    0
 ' 34317 000000 N3:      0
```

```
↑ 0019   .MAIN
02                    ;*************************
03                    ;
04                    ;DECK   QUEUE.01   31 MARCH 77
05                    ;
06                    ;**ENQUEUE AND DEQUEUE SUBROUTINES **
07                    ;
08                    ;USAGE:
09                    ;        TO  QUEUE UP AN ITEM.
10                    ;        JSR      CAL      ;WITH AC0=HEAD LOC.,AND
11                    ;        ENQUE             ;     AC1=LINK LOC.
12                    ;     TO DEQUEUE THE TOP ITEM
13                    ;        JSR      CAL      ;WITH AC0=HEAD LOC.
14                    ;        DEQUE
15                    ;
16        000002 QFL =    2         ;LENGTH OF FRAME REQUIRED
17        000000 QIF =    0         ;DISPL. FOR INTERRUPT ENABLE FLAG.
18        000001 QSV =    1         ;FOR SERVER ADDRESS
19                    ;
20 34320 000002           QFL               ;REQUIRED FRAME SIZE (2 WORDS)
21 34321 063577 ENQUE:   SKPBZ    CPU       ;INTERRUPT ENABLED?
22 34322 152461           SUBC     2,2,SKP   ; 0 IF ON
23 34323 152001           ADC      2,2,SKP   ;-1 IF OFF
24 34324 060277           INTDS
25 34325 051400           STA      2,QIF,3   ;REMEMBER ENTRY STATE
26 34326 111000           MOV      0,2       ;HEAD LOC.
27 34327 021000           LDA      0,0,2     ;TOP LINK
28 34330 100014           COM#     0,0,SZR   ;IS IT THE END
29 34331 000775           JMP      .-3       ;NO, SO CHAIN TO NEXT
30 34332 043773           STA      0,@AC1,3  ;YES. SET NEW ITEM'S LINK -1
31 34333 045000           STA      1,0,2     ;LINK NEW ITEM INTO CHAIN
32 34334 021772           LDA      0,AC0,3   ;HEAD LOC.
33 34335 112414           SUB#     0,2,SZR   ;WAS IT THE FIRST ENTRY?
34 34336 000437           JMP      QRT       ;NO, SO RETURN
35                    ;  NOTE: AC2=HEAD AND AC1=LINK
36 34337 021001 QE2:     LDA      0,1,2     ;YES. CALL SERVER BUT FIRST
37 34340 041401           STA      0,QSV,3   ;    MOVE SERVER ADDRESS
38 34341 141000           MOV      2,0       ;AC0=HEAD AND AC1=LINK
39 34342 006436           JSR      @Q.CAL    ;CALL SERVER
40 34343 000001           QSV
41 34344 101013           MOV#     0,0,SNC   ;WAS THERE AN ERROR?
42 34345 000430           JMP      QRT       ;NO, SO RETURN
43 34346 000407           JMP      QD2       ;YES, SO DEQUE
44                    ;     -------------
45                    ;  DEQUEUE.  AC0=HEAD
46 34347 000002           QFL
47 34350 063577 DEQUE:   SKPBZ    CPU
48 34351 152461           SUBC     2,2,SKP
49 34352 152001           ADC      2,2,SKP
50 34353 060277           INTDS
51 34354 051400           STA      2,QIF,3
52 34355 031772 QD2:     LDA      2,AC0,3   ;AC2=HEAD LOC
53 34356 035000           LDA      3,0,2     ;AC3=TOP LINK
54 34357 025400           LDA      1,0,3     ;SECOND LINK
55 34360 045000           STA      1,0,2     ;MOVE IT TO TOP
56 34361 102460           SUBC     0,0       ;SET REMOVED LINK WORD TO 0.
57 34362 041400           STA      0,0,3
58 34363 034457           LDA      3,FP      ;RECOVER FRAME POINTER
   1364 124014           COM#     1,1,SZR   ;IS THE NEW TOP EMPTY?
   1365 000752           JMP      QE2       ;NO AC2=HEAD AC1=LINK
```

```
      0020   .MAIN
01 34366 021002              LDA     0,2,2     ;IDLER S/R LOC.
02 34367 100015              COM#    0,0,SNR   ;IS THERE ONE?
03 34370 000405              JMP     QRT
04 34371 041401              STA     0,QSV,3
05 34372 141000              MOV     2,0       ;LOC. HEAD
06 34373 006405              JSR     @Q.CAL
07 34374 000001              QSV
08 34375 011400 QRT:         ISZ     QIF,3     ;TEST INTERRUPT ENABLE
09 34376 060177              INTEN
10 34377 006402              JSR     @Q.RET    ;RETURN
11              ;           -----------
12 34400 034403 Q.CAL:       CAL
13 34401 034447 Q.RET:       RET
14 34402 034442 Q.FP:        FP
15              ;           -----------
17              ;*******************************
18              ;
19              ;DECK   STACK.01        08 APR 77.
20              ;
21              ;** CALL,RETURN,AND STACK MECHANISM **
22              ;
23              ;  A CALL SAVES THE CALLER'S REGISTERS AND ALLOCATES
24              ;  A FRAME ON THE STACK FOR USE BY THE SUBROUTINE.
25              ;  A RETURN RELEASES THE FRAME AND RETURNS
26              ;  TO THE CALLER. A FRAME POINTER,FP,POINTS TO THE
27              ;  BASE OF THE CURRENT FRAME. A TOP POINTER,TP,POINTS
28              ;  TO THE NEXT AVAILABLE WORD IN THE FRAME, AND A
29              ;  LIMIT POINTER,LP,IS THE HIGHEST VALUE ALLOWED FOR
30              ;  FP AND SP. LP SHOULD BE 7 LESS THAN THE END OF THE
31              ;  STACK. THE SBED (S/R ENTRY DESIGNATOR)
32              ;  BELOW MAY BE EITHER THR ADDRESS OF THE
33              ;  FIRST INSTRUCTION OF A S/R OR (IF BITS
34              ;  0 THRU 7 ARE 0) A DISPLACEMENT IN THE
35              ;  CALLER'S FRAME WHICH CONTAINS THE  ADDRESS OF
36              ;  THE S/R. THE ENTRY INSTRUCTION OF EACH S/R MUST
37              ;  BE PRECEDED BY THE NUMBER OF WORDS REQUIRED
38              ;  IN THE STACK FRAME.
39
40              ;
41              ;
42              ;
43              ;  USAGE:
44              ;       JSR      CAL       ;TO CALL A S/R
45              ;       <SBED>
46              ;       <RETURN>
47              ;
48              ;       JSR      RET       :TO RETURN TO CALLER
49              ;  DESIGNED BY J F HERBSTER, 23-27 MAR 77
50              ;
51      000007 LH  =     7          ;LENGTH OF FRAME HEADER
52      177771 RTN =     -LH        ;DISPLACEMENT FOR RETURN ADDRESS
53      177772 AC0 =     RTN+1
54      177773 AC1 =     RTN+2
55      177774 AC2 =     RTN+3
56      177775 OFP =     RTN+4      ;FOR OLD FRAME POINTER
57      177776 SBE =     RTN+5      ;FOR S/R ENTRY
58      177777 FSZ =     RTN+6      ;FOR FRAME SIZE (FSZ=-1)
              ;  BEGINNING OF CALL
   34403 175400 CAL:         INC     3,3       ;PREPARE RETURN ADDRESS
```

```
     0021    .MAIN
01  34404  056437              STA     3,@TP    ;AND SAVE
02  34405  034436              LDA     3,TP     ;TOP OF STACK
03  34406  051403              STA     2,AC2+LH,3
04  34407  045402              STA     1,AC1+LH,3
05  34410  041401              STA     0,AC0+LH,3
06  34411  030434              LDA     2,.LH    ;LENGTH OF HEADER
07  34412  157000              ADD     2,3      ;NEW FRAME POINTER
08  34413  024427              LDA     1,FP     ;OLD FRAME POINTER
09  34414  045775              STA     1,OFP,3  ;SAVE IT
10  34415  054425              STA     3,FP
11  34416  031771              LDA     2,RTN,3  ;ADDRESS OF SBED PLUS 1.
12  34417  031377              LDA     2,-1,2   ;THE SBE DESIGNATOR
13  34420  020426              LDA     0,SBEDM  ;MASK WITH BITS 0-7
14  34421  113414              AND#    0,2,SZR  ;IS SBED THE ENTRY ADDRESS?
15  34422  000403              JMP     .+3      ;YES
16  34423  133000              ADD     1,2      ;NO. ITS A DISPL. ON OFP
17  34424  031000              LDA     2,0,2    ;SO GET ADDRESS FROM OLD FRAME
18  34425  051776              STA     2,SBE,3  ;SAVE IN HEADER
19  34426  031377              LDA     2,-1,2   ;REQUIRED FRAME SIZE
20  34427  051777              STA     2,FSZ,3  ;SAVE
21  34430  173000              ADD     3,2      ;NEW TOP OF STACK
22  34431  020413              LDA     0,LP     ;LIMIT FOR TP AND FP
23  34432  112432              SUBZ#   0,2,SZC  ;IS LP.GT.TP?
24  34433  004431              JSR     PANIC    ;NO
25  34434  050407              STA     2,TP     ;SET NEW POINTER
26  34435  021772              LDA     0,AC0,3
27  34436  025773              LDA     1,AC1,3  ;LOAD UP AND ENTER S/R
28  34437  031774              LDA     2,AC2,3
29  34440  003776              JMP     @SBE,3
30                     ;      ---------------
31  34441  000000  RTMP:  0
32  34442  000000  FP:  0
33  34443  000000  TP:  0
34  34444  000000  LP:  0
35  34445  000007  .LH:      LH
36  34446  177400  SBEDM:    177400
37                     ;      ---------------
38                     ;
39                     ;   THE BEGINNING OF THE RETURN
40  34447  030773  RET:    LDA     2,FP
41  34450  021371              LDA     0,RTN,2
42  34451  040770              STA     0,RTMP
43  34452  020773              LDA     0,.LH    ;PREPARE OLD TOP POINTER
44  34453  112460              SUBC    0,2
45  34454  050767              STA     2,TP     ;SET TP
46  34455  035004              LDA     3,OFP+LH,2;RESTORE OLD FRAME POINT.
47  34456  054764              STA     3,FP
48  34457  021001              LDA     0,AC0+LH,2
49  34460  025002              LDA     1,AC1+LH,2;RESTORE REGISTERS AND
50  34461  031003              LDA     2,AC2+LH,2;   RETURN TO CALLER
51  34462  000401              JMP     .+1      ;****DEBBUG POINT*****
52  34463  002756              JMP     @RTMP
53                     ;      -----------------
54  34464  063077  PANIC:  HALT
 5  34465  000777              JMP     .-1
 6                     ;      -----------------
```

```
↑ 0022   .MAIN
02                 ;********************************
03                 ;
04                 ; DECK ISTEAL.01           APRIL 1977
05                 ;
06                 ;** INTERRUPT STEALER, SAVE, AND RESTORE **
07                 ;
08                 ;  THE FOLLOWING IS AN INTERRUPT PREPROCESSER
09                 ;  WHICH WILL PICK OUT OUR OWN INTERRUPTS
10                 ;  AND PASS THE OTHERS TO THE REGULAR
11                 ;  PROCESSER.
12                 ;
13                 ;
14                 ;  TO ADD DEVICE CODES SEE THE EXAMPLE BELOW
15                 ;
16                 ;        --------
17 34466 000530 I.REG:  530
18 34467 035172 I.DT:   DT33
19                 ;        --------
20 34470 040466 CKINT:  STA     0,SV+0
21 34471 044466         STA     1,SV+1
22 34472 050466         STA     2,SV+2
23 34473 000401 CK2:    JMP     .+1
24 34474 061477         INTA    0
25 34475 030772         LDA     2,I.DT
26 34476 025001         LDA     1,DTDC,2
27 34477 106475         SUBC#   0,1,SNR
28 34500 000412         JMP     ISAVE
29 34501 031000         LDA     2,DTCL,2
30 34502 150014         COM#    2,2,SZR
31 34503 000773         JMP     .-5
32 34504 020452         LDA     0,SV+0
33 34505 024452         LDA     1,SV+1
34 34506 030452         LDA     2,SV+2
35 34507 002757         JMP     @I.REG
36                 ;        --------
37 34510 035172 I.D33:  DT33
38 34511 000400 CMSK:400
39                 ;        --------
40                 ;  COMMON SAVE STATE PROCESSER
41 34512 054447 ISAVE:  STA     3,SV+3
42 34513 102560         SUBCL   0,0
43 34514 040446         STA     0,SV+4
44 34515 020725         LDA     0,FP
45 34516 040445         STA     0,SV+5
46 34517 020724         LDA     0,TP
47 34520 040444         STA     0,SV+6
48 34521 020723         LDA     0,LP
49 34522 040443         STA     0,SV+7
50 34523 020716         LDA     0,RTMP
51 34524 040442         STA     0,SV+10
52 34525 034445         LDA     3,IFP  ; SET UP STACK FOR INTERRUPT
53 34526 054714         STA     3,FP   ; PROCESSING
54 34527 054714         STA     3,TP
55 34530 020443         LDA     0,ILP
56 34531 040713         STA     0,LP
57 34532 021003         LDA     0,DT.IS,2
58 34533 010710         ISZ     TP     ; PUT OUR SERVER'S ADDRESS
   34534 041400         STA     0,0,3  ; ON THE STACK AND CALL IT
   34535 004646         JSR     CAL
```

```
     0023  .MAIN
01 34536 000000                  0
02 34537 020427 DISM:    LDA     0,SV+10
03 34540 040701          STA     0,RTMP
04 34541 020424          LDA     0,SV+7   ; RESTORE STACK
05 34542 040702          STA     0,LP
06 34543 020421          LDA     0,SV+6
07 34544 040677          STA     0,TP
08 34545 020416          LDA     0,SV+5
09 34546 040674          STA     0,FP
10 34547 020413          LDA     0,SV+4
11 34550 101200          MOVR    0,0      ; RESTORE REGISTERS
12 34551 034410          LDA     3,SV+3
13 34552 030406          LDA     2,SV+2
14 34553 024404          LDA     1,SV+1
15 34554 020402          LDA     0,SV+0
16 34555 002711          JMP     @I.REG   ; AND RETURN
17               ;       --------
18 34556 000000 SV:      0
19 34557 000000          0
20 34560 000000          0
21 34561 000000          0
22 34562 000000          0
23 34563 000000          0
24 34564 000000          0
25 34565 000000          0
26 34566 000000          0
27 34567 000000          0
28 34570 000000          0
29 34571 000000          0
30 34572 037215 IFP:     BUF+1640
31 34573 037346 ILP:     BUF+2000-LH
32               ;       --------
```

```
t 0024   .MAIN
02              ;*****************************
03              ;
04              ;** DECK SEEK.01 **
05              ;
06              ;** SEEK AND RECALL INITIATION **
07              ;
08  34574 000001          1
09  34575 030444 ISEEK:  LDA   2,S.UQH ;NEG. OF Q HEAD DISPL. IN UT
10  34576 113000          ADD   0,2      ;LOC. UT
11  34577 034443          LDA   3,S.BQL ;NEG OF Q LINK DISPL. IN BH.
12  34600 137000          ADD   1,3
13  34601 055011          STA   3,UT.BH,2
14  34602 020447          LDA   0,NTRY  ;NUMBER OF TRIES ALLOWED
15  34603 041016          STA   0,UTTTG,2        ;TRIES TO GO
16  34604 025404          LDA   1,BHSEC,3
17  34605 020443          LDA   0,D7
18  34606 123400          AND   1,0
19  34607 125220          MOVZR 1,1
20  34610 125220          MOVZR 1,1
21  34611 125220          MOVZR 1,1
22  34612 045013          STA   1,UTRCY,2;REQUESTED CYLINDER
23  34613 035015          LDA   3,UTNCY,2;NUMBER OF CYL. ON DISK
24  34614 136033          ADCZ# 1,3,SNC ;SKIP IF RCY LESS THAN NCY
25  34615 000437          JMP   SERC     ;**NO. OF CYL. TOO LARGE**
26  34616 103120          ADDZL 0,0
27  34617 103120          ADDZL 0,0
28  34620 035003          LDA   3,UTUN1,2
29  34621 163000          ADD   3,0
30  34622 041012          STA   0,UTSSC,2
31  34623 006415          JSR   @S.USL ;SELECT UNIT
32  34624 000426          JMP   SERT     ;TIME OUT ERROR RETURN
33  34625 000402          JMP   RSEEK
34              ;      --------
35  34626 000001          1
36  34627 021013 RSEEK:  LDA   0,UTRCY,2
37  34630 024414          LDA   1,SKCMD
38  34631 123000          ADD   1,0
39  34632 025014          LDA   1,UTCCY,2
40  34633 124015          COM#  1,1,SNR
41  34634 020411          LDA   0,RCCMD
42  34635 061333          DOAP  0,DP0   ;START THE SEEK AND RECAL.
43  34636 101020          MOVZ  0,0
44  34637 006404          JSR   @S.RET
45              ;      -------------
46  34640 035142 S.USL:  USEL
47  34641 177773 S.UQH:  -UTQH
48  34642 177773 S.BQL:  -BHQL
49  34643 034447 S.RET:  RET
50  34644 001000 SKCMD:  1000
51  34645 001400 RCCMD:  1400
52  34646 000001 ERCY:   1
53  34647 000002 ERT0:   2
54  34650 000007 D7:     7
55  34651 000012 NTRY:   10.
56              ;      --------
57  34652 024775 SERT:   LDA   1,ERT0 ;TIME OUT ERROR
58  34653 000402          JMP   .+2
    34654 024772 SERC:   LDA   1,ERCY ;CYL. NO. ERROR
    34655 035011          LDA   3,UT.BH,2
```

```
      0025  .MAIN
01  34656  041410           STA     0,BHEC0,3;RETURN ERROR DATA
02  34657  045411           STA     1,BHEC1,3
03  34660  101040           MOVO    0,0       ;SET ERROR FLAG
04  34661  002762           JMP     @S.RET  ;RETURN
05                  ;       ----------
07                  ;****************************
08                  ;
09                  ;  DECK DMA.01
10                  ;
11                  ;   ** READ AND WRITE QUEUE SERVER **
12                  ;
13                  ;
14  34662  000000           0               ;FRAME SIZE
15  34663  030433  IDMA:    LDA     2,I.DQH ;NEG. OF Q HEAD DISPL. IN DT.
16  34664  113000           ADD     0,2       ;LOC. DT.
17  34665  034432           LDA     3,I.UQL ;NEG. OF Q LINK DISPL. IN UT.
18  34666  137000           ADD     1,3       ;LOC. UT.
19  34667  055011           STA     3,DT.UT,2;REMEMBER WHICH UNIT IN DT
20  34670  021412           LDA     0,UTSSC,3
21  34671  041014           STA     0,DTSSC,2
22  34672  021413           LDA     0,UTRCY,3;REQUESTED CYLINDER
23  34673  035411           LDA     3,UT.BH,3;BUFFER HEAD
24  34674  055012           STA     3,DT.BH,2
25  34675  025401           LDA     1,BH.BF,3;BUFFER ADDRESS
26  34676  045013           STA     1,DT.BF,2
27  34677  035402           LDA     3,BHMOD,3
28  34700  055016           STA     3,DTMOD,2
29  34701  126460           SUBC    1,1
30  34702  175014           MOV#    3,3,SZR
31  34703  125700           INCS    1,1
32  34704  123000           ADD     1,0
33  34705  041015           STA     0,DTCCW,2
34  34706  061033  ID2:     DOA     0,DP0     ;SET COMMAND AND CYLINDER
35  34707  021013           LDA     0,DT.BF,2
36  34710  062133           DOBS    0,DP0
37  34711  101020  ID3:     MOVZ    0,0
38  34712  002406           JMP     @I.RET
39                  ;       ----------
40                  ;
41                  ;   ENTRY FOR DMA RW RETRIES   AC2=LOC DT
42  34713  000000           0
43  34714  021015  RDMA:    LDA     0,DTCCW,2
44  34715  000771           JMP     ID2
45                  ;       ----------
46  34716  177773  I.DQH:   -DTQH
47  34717  177770  I.UQL:   -UTQL
48  34720  034447  I.RET:   RET      ;LOC RETURN ROUTINE
49                  ;       ----------
50                  ;
51                  ; THIS S/R IS CALLED WHEN A RW QUEUE BECOMES EMPTY
52                  ; AC0 = LOC. OF DT
53  34721  000000           0
54  34722  111000  SDMA:    MOV     0,2
55  34723  021377           LDA     0,DTDNF-DTQH,2
56  34724  061233           DOAC    0,DP0
57  34725  000764           JMP     ID3       ;RETURN
58                  ;       ----------
                    ;****************************
                    ;
```

```
     0026  .MAIN
01                  ;  DECK  DPIS.01        APRIL 1977
02                  ;
03                  ;** DISK INTERRUPT SERVER **
04                  ;
05                  ;  THIS ROUTINES RECEIVES CONTROL ON DISK
06                  ;  INTERRUPTS WITH AC2=LOC. OF THE DEVICE
07                  ;  TABLE. SEE THE FLOW CHART FOR AN OVERALL
08                  ;  PICTURE OF ITS ACTIONS. THE EXIT MUST BE
09                  ;  TO LOC. DISM
10                  ;
11                  ;
12                  ;  DESIGNED DY JFH 1 APRIL 77
13                  ;
14        000000 SHOLD = 0
15 34726 000001              1
16 34727 060433 D33SV:  DIA       0,DP0    ;GET STATUS DONE FLAG
17 34730 025004          LDA       1,DTDNF,2
1
 8 34731 123415          AND#      1,0,SNR ;IS A READ OR WRITE DONE?
19 34732 000465          JMP       D3CKS    ;NO
20 34733 021014          LDA       0,DTSSC,2;YES. SO RESELECT AND GET STATS
21 34734 006535          JSR       @D.US
22 34735 000411          JMP       D3REC    ;SELECT FAILURE
23 34736 101213          MOVR#     0,0,SNC ;SEL. OK. CHECK RW STATUS
24 34737 000440          JMP       DOK      ;OK
25 34740 024532          LDA       1,DFEM   ;NOT OK. CHECK RW STATUS
26 34741 123414          AND#      1,0,SZR
27 34742 000404          JMP       D3REC    ;ITS FATAL
28 34743 035011          LDA       3,DT.UT,2
29 34744 015416          DSZ       UTTTG,3
30 34745 000406          JMP       D3CSE
31 34746 035411 D3REC:  LDA       3,UT.BH,3
32 34747 024524          LDA       1,DEC5   ;RETURN ERROR CODES
33 34750 041410          STA       0,BHEC0,3
34 34751 045411          STA       1,BHEC1,3
35 34752 000434          JMP       D3DQ     ;DEQUE RW.
36                  ;      --------
37 34753 024521 D3CSE:  LDA       1,DSEF
38 34754 123414          AND#      1,0,SZR ;IS IT A SEEK ERROR
39 34755 000406          JMP       D3RSK
40 34756 006526          JSR       @D.CAL
41 34757 034714          RDMA
42 34760 101012          MOV#      0,0,SZC
43 34761 000425          JMP       D3DQ     ;YES,SO GIVE UP
44 34762 000435          JMP       D3CKS    ;NO ERROR
45                  ;      --------
46 34763 020512 D3RSK:  LDA       0,D.DQH
47 34764 143000          ADD       2,0
48 34765 006517          JSR       @D.CAL
49 34766 034350          DEQUE
50 34767 031011          LDA       2,DT.UT,2
51 34770 102000          ADC       0,0      ;THEN INDICATE UNKNOWN CYLINDER
52 34771 041014          STA       0,UTCCY,2;AND START A RECALL
53 34772 006512          JSR       @D.CAL
54 34773 034627          RSEEK
55 34774 101012          MOV#      0,0,SZC
56 34775 000416          JMP       D3DQS
57 34776 000421          JMP       D3CKS
                   ;      --------
   34777 021016 DOK:    LDA       0,DTMOD,2
```

```
     0027  .MAIN
01 35000 101015              MOV#    0,0,SNR
02 35001 000405              JMP     .+5
03 35002 035012              LDA     3,DT.BH,2
04 35003 025402              LDA     1,BHMOD,3 ;THE BHMOD COUNTER GETS DECRE-
05 35004 106400              SUB     0,1       ; MENTED BY ITS VALUE BEFORE THE
06 35005 045402              STA     1,BHMOD,3 ;WRITE STARTED. NO CHG ON REAS
07 35006 020467  D3DQ:       LDA     0,D.DQH
08 35007 143000              ADD     2,0
09 35010 006474              JSR     @D.CAL    ;DEQUE THE READ-WRITE OP.
10 35011 034350              DEQUE
11 35012 031011              LDA     2,DT.UT,2
12 35013 020465  D3DQS:      LDA     0,D.UQH
13 35014 143000              ADD     2,0
14 35015 006467              JSR     @D.CAL    ;DEQUE THE UNIT
15 35016 034350              DEQUE
16                   ;   PROCESS SEEK AND RECAL DONES BELOW
17                           D3CKS:
18 35017 060433              DIA     0,DP0      ;FETCH STATUS DONE FLAGS.
19 35020 024456              LDA     1,D3DM
20 35021 123405              AND     1,0,SNR ;SAVE ONLY UNIT FLAGS.
21 35022 006463              JSR     @D.RET
22 35023 031010              LDA     2,DTUCH,2
23 35024 000411              JMP     D3CKF
24                   ;      --------
25 35025 021400  D3LFM:      LDA     0,SHOLD,3;CHECK FOR MORE WORK
26 35026 101015              MOV#    0,0,SNR
27 35027 002456              JMP     @D.RET
28 35030 031000  D3TNX:      LDA     2,UTCL,2;NEXT UNIT TABLE
29 35031 150014              COM#    2,2,SZR ;IS THERE MORE?
30 35032 000403              JMP     .+3
31 35033 061033              DOA     0,DP0      ;CLEAR THE GHOSTS
32 35034 002451              JMP     @D.RET
33 35035 025004  D3CKF:      LDA     1,UTDNF,2
34 35036 123415              AND#    1,0,SNR
35 35037 000771              JMP     D3TNX
36 35040 122400              SUB     1,0
37 35041 041400              STA     0,SHOLD,3
38 35042 065033              DOA     1,DP0
39 35043 021005              LDA     0,UTQH,2
40 35044 100015              COM#    0,0,SNR
41 35045 000760              JMP     D3LFM
42 35046 021012              LDA     0,UTSSC,2
43 35047 006422              JSR     @D.US      ;SELECT AND GET STATUS
44 35050 000457              JMP     D3TOX
45 35051 024452              LDA     1,D3SER ;SEEK ERROR MASK
46 35052 123414              AND#    1,0,SZR
47 35053 000442              JMP     D3CFE
48 35054 021014              LDA     0,UTCCY,2;WAS IT A RECAL.
49 35055 100015              COM#    0,0,SNR ;
50 35056 000430              JMP     D3FRC      ;YES
51 35057 021013              LDA     0,UTRCY,2;MOVE REQUESTED CYLINDER
52 35060 041014              STA     0,UTCCY,2;TO CURRENT CYLINDER
53 35061 020414              LDA     0,D.DQH
54 35062 024415              LDA     1,D3.UL ;ENQUQE A READ OR WR.
55 35063 035001              LDA     3,UT.DT,2
56 35064 147000              ADD     2,1
57 35065 163000              ADD     3,0
-- --066 006416              JSR     @D.CAL
    067 034321              ENQUE
```

```
     0028  .MAIN
01 35070 000735           JMP     D3LFM
02                    ;       --------
03 35071 035142 D.US:  USEL
04 35072 000200 DFEM:  200       ;FATAL RW ERRORS
05 35073 000015 DEC5:  15        ;ERROR CODE
06 35074 000040 DSEF:  40        ;SEEK ERROR
07 35075 000005 D.DQH: DTQH
08 35076 074000 D3DM:  074000
09 35077 000010 D3.UL: UTQL
10 35100 000005 D.UQH: UTQH
11 35101 000022 D3TOE: 22
12 35102 000023 D3STE: 23
13 35103 000005 D3.UH: UTQH
14 35104 034403 D.CAL: CAL
15 35105 034447 D.RET: RET
16                    ;       --------
17 35106 102460 D3FRC: SUBC    0,0       ;A RECAL IS COMPLETE.
18 35107 041014         STA     0,UTCCY,2;SET CURRENT CYLINDER TO 0
19 35110 006774         JSR     @D.CAL
20 35111 034627         RSEEK             ;SEEK REQUESTED CYLINDER
21 35112 101012         MOV#    0,0,SZC ;ERROR?
22 35113 000422         JMP     D3SDQ   ;YES
23 35114 000711         JMP     D3LFM
24                    ;       --------
25 35115 024407 D3CFE: LDA     1,D3SFT ;ERROR, BUT WAS IT FATAL
26 35116 123414         AND#    1,0,SZR
27 35117 000412         JMP     D3STX   ;YES
28 35120 015016         DSZ     UTTTG,2 ;NO. HAVE WE TRIED ENOUGH?
29 35121 000404         JMP     D3IRC   ;NO
30 35122 000407         JMP     D3STX   ;YES
31                    ;       --------
32 35123 000240 D3SER: 240       ;SEEK ERROR FLAGS
33 35124 000200 D3SFT: 200       ;SEEK FATAL ERROR FLAGS
34                    ;       --------
35 35125 102000 D3IRC: ADC     0,0       ;CHANGE TO RECALL REQUEST
36 35126 000761         JMP     D3FRC+1 ;    AND RESTART SEEK
37                    ;       --------
38 35127 024752 D3TOX: LDA     1,D3TOE ;TIME OUT ERROR CODE
39 35130 000402         JMP     .+2
40 35131 024751 D3STX: LDA     1,D3STE ;STATUS ERROR CODE
41 35132 035011         LDA     3,UT.BH,2
42 35133 041410         STA     0,BHEC0,3;RETURN ERRORS
43 35134 045411         STA     1,BHEC1,3
44 35135 020746 D3SDQ: LDA     0,D3.UH ;DEQUE DISK UNIT
45 35136 143000         ADD     2,0
46 35137 006745         JSR     @D.CAL
47 35140 034350         DEQUE
48 35141 000664         JMP     D3LFM    ;LOOK FOR MORE WORK
49                    ;       --------
51                    ;***************************
52                    ;
53                    ;  DECK UNSEL.01
54                    ;
55                    ;** UNIT SELECT **
56                    ;
57 35142 054426 USEL:  STA     3,RLOC  ; NOR REENTRANT
58 35143 115000         MOV     0,3       ;SELECT AND SECTOR COMMAND
'  35144 024423         LDA     1,USTT
3  35145 125405 US1:  INC     1,1,SNR
```

```
     0029   .MAIN
01 35146 000416              JMP     USER
02 35147 060433              DIA     0,DP0      ;READ STATUS
03 35150 101300              MOVS    0,0
04 35151 103133              ADDZL#  0,0,SNC
05 35152 000773              JMP     US1
06                    ;
07 35153 077033              DOC     3,DP0      ;OUTPUT SELECT COMMAND
08                    ;
09 35154 024413              LDA     1,USTT
10 35155 125405 US2:         INC     1,1,SNR
11 35156 000406              JMP     USER
12 35157 060433              DIA     0,DP0
13 35160 101300              MOVS    0,0
14 35161 103133              ADDZL#  0,0,SNC
15 35162 000773              JMP     US2
16 35163 010405              ISZ     RLOC
17 35164 101300 USER:        MOVS    0,0
18 35165 036404              LDA     3,@U.FP
19 35166 002402              JMP     @RLOC
20                    ;      --------
21 35167 177266 USTT:        -330.
22 35170 000000 RLOC:        0
23 35171 034442 U.FP:        FP
24                    ;      --------
26                    ;*******************************
27                    ;    DECK   DDTBL.0
28                    ;
29                    ;** DISKETTE DEVICE TABLE **
30                    ;    DISPLACEMENT DEFINITIONS:
31        000000 DTCL  = 0              ;DEVICE TBL LINK
32        000001 DTDC  = DTCL+1  ;DEVICE CODE
33        000002 DTMSK = DTDC+1  ;RESERVED
34        000003 DT.IS = DTMSK+1 ; ADDRESS OF INTERRUPT SERVER
35        000004 DTDNF = DT.IS+1 ; DMA DONE FLAG POSITION(100000)
36        000005 DTQH = DTDNF+1  ; DMA QUEUE HEAD(INIT. TO -1)
37                    ;DTQH+1          ADDRESS OF QUEUE SERVER
38                    ;DTQH+2 ;ADDRESS OF QUEUE IDLER (OR -1,IF NONE)
39        000010 DTUCH = DTQH+3
40        000011 DT.UT = DTUCH+1 ; LOC. OF UT BEING SERVED
41        000012 DT.BH = DT.UT+1 ; LOC. OF BH BEING SERVED
42        000013 DT.BF = DT.BH+1 ; LOC. OF BUFFER BEING READ OR WRITTEN
43        000014 DTSSC = DT.BF+1 ;SELECT AND SECTOR COMMAND
44        000015 DTCCW = DTSSC+1 ; CYLINDER AND COMMAND WORD
45        000016 DTMOD = DTCCW+1 ;COPY OF BHMOD,JUST BEFORE READ OR WRITE
46                    ;      --------
47 35172 035212 DT33:        DT14
48 35173 000033              33
49 35174 000000              0
50 35175 034727              D33SV   ;DT.IS
51 35176 100000              100000  ;DTDNF
52 35177 177777              -1      ;DTQH
53 35200 034663              IDMA    ;SERVER
54 35201 034722              SDMA    ;IDLER
55 35202 035226              UT330   ;DTUCH
56 35203 000000              0       ;DT.UT
57 35204 000000              0       ;DT.BH
58 35205 000000              0       ;DT.BF
      206 000000              0       ;DTSSC
      207 000000              0       ;DTCCW
```

```
     0030  .MAIN
01 35210 000000              Ø         ;DTMOD
02 35211 000000              Ø         ;SPARE
03                    ;      --------
04 35212 035216 DT14:        DT42
05 35213 000014              14
06 35214 000000              Ø
07 35215 033231              SRTC
08
09 35216 177777 DT42:        -1
10 35217 000042              42
11 35220 000000              Ø
12 35221 035223              SV42
13
14 35222 000000              Ø
15 35223 060242 SV42:        NIOC      42
16 35224 002401              JMP       @D.RT
17
18 35225 034447 D.RT:        RET
19        000033 DPØ = 33
21               ;*************************************
22               ;
23               ;    DECK DUTBL.Ø1
24               ;
25               ;** DISK UNIT TABLES **
26               ;
27               ;    DISPLACEMENT DEFINITIONS:
23        000000 UTCL = Ø               ;LINK TO OTHER DT'S(DON'T CHANGE)
29        000001 UT.DT = UTCL+1         ;MOTHER DEVICE TABLE
30        000002 UTUN = UT.DT+1         ;UNIT NUMBER
31        000003 UTUN1 = UTUN+1         ;UNIT NUMBER FOR SELECT & SECTOR
32        000004 UTDNF =UTUN1+1         ;POSITION OF DONE FLAG
33        000005 UTQH = UTDNF+1         ;UNIT'S QUEUE HEAD(FOR BHQL'S)
34               ;UTQH+1                ;QUEUE SERVER
35               ;UTQH+2                ;QUEUE IDLER (PROBABLY -1.)
36        000010 UTQL = UTQH+3          ;LINK FOR DMA. QUEUE
37        000011 UT.BH = UTQL+1         ;BUFFER HEADER  BEING SERVED
38        000012 UTSSC = UT.BH+1        ;SELECT AND SECTOR COMMAND
39        000013 UTRCY = UTSSC+1        ;REQUIRED CYLINDER
40        000014 UTCCY = UTRCY+1        ;CURRENT CYLINDER (OR -1 IF UNKNOWN)
41        000015 UTNCY = UTCCY+1        ;NUMBER OF CYLINDERS ON DISK
42        000016 UTTTG = UTNCY+1        ;TRIES TO GO BERORE GIVING UP
43        000017 UTTMP = UTTTG+1        ;TEMPORARY
44               ; UNIT Ø TABLE
45 35226 035247 UT330:        UT331     ;UTCL
46 35227 035172               DT33      ;UT.DT
47 35230 000000               Ø         ;UTUN
48 35231 000017               000017    ;UTUN1
49 35232 040000               040000    ;UTDNF
50 35233 177777               -1        ;UTQH
51 35234 034575               ISEEK     ;SERVER
52 35235 177777               -1        ;IDLER
53 35236 000000               Ø         ;UTQL
54 35237 000000               Ø         ;UT.BH
55 35240 000000               Ø         ;UTSSC
56 35241 000000               Ø         ;UTRCY
57 35242 177777               -1        ;UTCCY
58 35243 000115               77.       ;UTNCY
   35244 000000               Ø         ;UTTTG
   35245 000000               Ø         ;UTTMP
```

```
   0031  .MAIN
01 35246 000000              0           ; SPARE
02                   ;          --------
03                   ;
04                   ; UNIT 1 TABLE
05 35247 177777 UT331:       -1          ; UTCL
06 35250 035172              DT33        ; UT.DT
07 35251 000001              1           ; UTUN
08 35252 040017              040017      ; UTUN1
09 35253 020000              020000      ; UTDNF
10 35254 177777              -1          ; UTQH
11 35255 034575              ISEEK       ; SERVER
12 35256 177777              -1          ; IDLER
13 35257 000000              0           ; UTQL
14 35260 000000              0           ; UT.BH
15 35261 000000              0           ; UTSSC
16 35262 000000              0           ; UTRCY
17 35263 177777              -1          ; UTCCY
18 35264 000115              77.         ; UTNCY
19 35265 000000              0           ; UTTTG
20 35266 000000              0           ; UTTMP
21 35267 000000              0           ; SPARE
22                   ;          --------
24                   ;***********************************
25                   ;
26                   ;    DECK   BHTBL.01
27                   ;
28                   ;** BUFFER HEADER TABLES **
29                   ;
30                   ;    DISPLACEMENT DEFINITIONS
31       000000 BHCL = 0               ;LINK TO OTHER BH'S(SHOULD BE ZERO)
32       000001 BH.BF = BHCL+1         ;LOC. BUFFER
33       000002 BHMOD = BH.BF+1        ;INCREMENTED EACH TIME BUFFER IS MODIFIE
34       000003 BH.UT = BHMOD+1        ;UNIT TABLE (OR -1)
35       000004 BHSEC = BH.UT+1        ;SECTOR CORRESPONDING TO BUFFER (OR -1)
36       000005 BHQL = BHSEC+1         ;UNIT QUEUE LINK
37       000006 BHNU = BHQL+1          ;NUMBER OF USERS
38       000007 BHLRU = BHNU+1         ;LEAST RECENTLY USED COUNTER
39       000010 BHEC0 = BHLRU+1        ;FOR RETURNED ERROR CODES
40       000011 BHEC1 = BHEC0+1  ;
41                   ;          --------
42                   ;
43 35270 035303 BH0:       BH1         ; BHCL
44 35271 035355            BUF         ; BH.BF
45 35272 000000            0           ; BHMOD
46 35273 177777            -1          ; BH.UT
47 35274 000000            0           ; BHSEC
48 35275 000000            0           ; BHQL
49 35276 000000            0           ; BHNU
50 35277 000000            0           ; BHLRU
51 35300 000000            0           ; BHEC0
52 35301 000000            0           ; BHEC1
53 35302 000000            0           ; SPARE
54                   ;          --------
55 35303 035316 BH1:       BH2
56 35304 035755            BUF+400
57 35305 000000            0
58 35306 177777            -1
-- 35307 000000            0
   5310 000000            0
```

```
     0032  .MAIN
01 35311 000000            0
02 35312 000000            0
03 35313 000000            0
04 35314 000000            0
05 35315 000000            0
06                 ;       --------
07 35316 177777 BH2:       -1
08 35317 036355            BUF+1000
09 35320 000000            0
10 35321 177777            -1
11 35322 000000            0
12 35323 000000            0
13 35324 000000            0
14 35325 000000            0
15 35326 000000            0
16 35327 000000            0
17 35330 000000            0
18                 ;       --------
20                 ;******************************
21                 ;
22                 ;DECK CHTBL.01
23                 ;
24                 ;** CHANNEL TABLES **
25                 ;
26                 ;   DISPLACEMENT DEFINITIONS
27     000000 CTCL    = 0         ;CHANNEL TABLES LINK
28     000001 CTNB    = 1         ;CHANNEL NO.
29     000002 CT.UT   = CTNB+1    ;LOC. UNIT TABLE (OR -1)
30     000003 CTSST   = CT.UT+1   ;START SECTOR
31     000004 CTSLM   = CTSST+1   ;LIMIT SECTOR
32     000005 CTSEC   = CTSLM+1   ;CURRENT SECTOR
33     000006 CTCWD   = CTSEC+1   ;CURRENT WORD
34     000007 CTRSZ   = CTCWD+1   ;RECORD SIZE(IN 16-BIT WORDS)
35     000010 CT.BH   = CTRSZ+1   ;CURRENT BUFFER LOC.
36     000010 CTSPT   = CT.BH     ;SPARE
37                 ;       --------
38                 ;
39 35331 035343 CT0:       CT1         ;CTCL
40 35332 000001            1           ;CTNB
41 35333 177777            -1          ;CT.UT
42 35334 000000            0           ;CTSST
43 35335 000000            0           ;CTSLM
44 35336 000000            0           ;CTSEC
45 35337 000000            0           ;CTCWD
46 35340 000000            0           ;CTRSZ
47 35341 177777            -1          ;CT.BH
48 35342 000000            0           ;CTSPR
49                 ;       -------
50                 ;
51 35343 177777 CT1:       -1          ;CTCL
52 35344 000002            2           ;CTNB
53 35345 177777            -1          ;CT.UT
54 35346 000000            0           ;CTSST
55 35347 000000            0           ;CTSLM
56 35350 000000            0           ;CTSEC
57 35351 000000            0           ;CTCWD
58 35352 000000            0           ;CTRSZ
   35353 177777            -1          ;CT.BH
   35354 000000            0           ;CTSPR
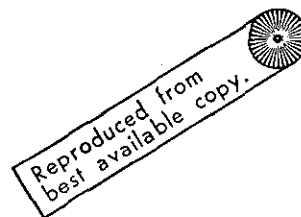```

```
   0033   .MAIN
01                  ;        --------
↑ 0034   .MAIN
02        002000 BUF:     .BLK 2000
03        000010         .LOC 10
04 00010 033000 LOC10:   SBRTB
05                        .END
```

APPENDIX C.3

LIST OF THE BASIC SOFTWARE USED IN THE ENGLEWOOD YARD FIELD TESTS

```
50   PRINT "-----------------------------"
52   PRINT "        T-562-VIII"
53   PRINT "        EXP. AVG."
54   PRINT "   SPECTRA PROCESSING ROUTINES"
55   PRINT " ENGLEWOOD YARD TESTS-JUNE 77"
56   PRINT "   +ASSEMBLY A-140-IX"
58   PRINT "      12 JULY 1977"
60   PRINT "-----------------------------"
65   REM    **REF:T-560-A140-IX**
66   REM    **REF:T-560-II**
67   REM    **REF:T-562-I,VII**
75   LET K5= 0
90   DEF   FNE(X)=8.68589* LOG (X)-8.6
95   CALL  23,D3
100  LET N=250
102  LET N8=N/2
104  DIM Q[2]
105  DIM A[N],C[N]
110  DIM B[N],M[N],S[N],Y[N],W[15]
114  READ L2,L5,L6,L7,L8
116  DATA  8,  4400,  25,  50,  12
120  READ T2,T3,T4,T7
122  DATA  30,  30,  800,  10
124  READ N1,N2,N3,N4,N5,N6
126  DATA  250,  24,  2,  40,  8,  0
128  READ P1,P2,P3,P4,P5,P6
130  DATA  61,  85,  110,  8,  .2,  8
132  READ U,U1,U2,U3,U8,U9
134  DATA  1,  0,-1,  150,  500,  280
136  LET N9=N2/2
```

```
140    PRINT
145    PRINT "NUMBER OF CHANNELS;";N1
150    PRINT "NUMBER OF SPECTRA ;";N2
160    PRINT "FREQUENCY FACTOR  DBAND HZ;";N4
165    PRINT "DISCRIMINATION LEVEL;";N5
170    PRINT "D.INDEX DECISION LEVEL;";P2
180    PRINT "DATE-TIME";
185    INPUT T1
190    PRINT
195    PRINT "TAPE#";
200    INPUT T0
205    PRINT
215    REM      ------------------------
220    GOSUB  800
222    PRINT "CAR I.D.";
223    INPUT P8
224    PRINT
225    GOSUB  1100
228    PRINT
230    GOTO  220
249    REM      ---------------------------------
250    REM                        ** START CLOCK **
255    CALL 6,B6
780    REM      -----------------------------------
790    REM               ** READ IN EXP. AVG. **
800    CALL 2,B2
802    LET U2=-1
806    FOR I=1 TO N9
808      LET U2=U2+2
810      FOR I1= 0 TO 1
811        CALL 22,U,J6,E
820        CALL 19,U,I1,U2,U3,126,E
822        IF E= 0 GOTO  840
824        STOP
840        CALL 17,D7
865        IF I>T4 GOTO  880
870        CALL 11,D1
890        REM              ** DELAY LOOP **
892        FOR J9=1 TO 2
895          FOR J3=1 TO 222
900          NEXT J3
910          IF J9=2 GOTO  925
920          CALL 12,AC 0]
921          GOTO  926
925          CALL 12,BC 0]
926        NEXT J9
928        CALL 20,U,AC 0],E
929        CALL 20,U,BC 0],E
930        IF E> 0 GOTO  990
935      NEXT I1
950    NEXT I
975    RETURN
```

```
 990   STOP
1099   REM           ------------SUB 1100------------
1100   REM             ----*** READ-OUT FROM MEMORY ***----
1110   LET I5=-1
1115   LET I5=I5+2
1120   FOR J1= 0 TO 1
1122     FOR I9= 0 TO 1
1125       CALL 22,U,J6,E
1130       CALL 19,U,J1,(I5+I9),1,126,E
1135       IF E= 0 GOTO  1145
1140       STOP
1145       LET A[ 0]= 0
1150       CALL 21,U,A[ 0],E
1155       CALL 13,A[ 0]
1160       FOR J= 0 TO N1
1165         CALL 14,P7
1170         IF P7>4 GOTO  1180
1175         LET P7=4
1180         LET B[J]= FNE(P7)
1185       NEXT J
1190       IF I9=1 GOTO  1200
1192       FOR I=1 TO N
1194         LET M[I]=B[I]
1196       NEXT I
1200     NEXT I9
1205     LET K1=1
1210     LET K2= 0
1215     FOR L1=1 TO N
1220       IF M[L1]<P4 GOTO  1260
1225       LET K1=K1+1
1230       LET K4=M[L1]-B[L1]
1240       IF K4<L2 GOTO  1260
1250       LET K2=K2+1
1260     NEXT L1
1270     PRINT "J1,K1,K2 ";J1;K1;K2
1280     LET Q[J1]=K2/K1
1290     IF J1=1 GOTO  1400
1300     GOSUB  7500
1400     GOSUB  8000
1410     IF J1=1 GOTO  1430
1420     GOSUB  8500
1430   NEXT J1
1450   GOSUB  1500
1460   IF I5=(N2-1) GOTO  1480
1470   GOTO  1115
1480   RETURN
```

```
1499   REM              ------------SUB 1500-----------------
1500   REM                        S/R TO COMPUTE SP. DIFFERENCE
1520   LET R0= 0
1530   LET R1= 0
1540   LET R2= 0
1545   LET Z3= 0
1550   LET Z4= 0
1555   LET Z5= 0
1560   LET Z6= 0
1760   FOR J=1 TO (N-1)
1770     LET Z1=S[J]
1780     LET Z2=B[J]
1790     IF Z1>P4 GOTO  1810
1800     LET Z1= 0
1810     IF Z2>P4 GOTO  1830
1820     LET Z2= 0
1830     IF Y[J+1]=1 GOTO  1850
1840     GOTO  1880
1850     LET R3= 0
1860     IF Y[J+1]=C[J+1] GOTO  1880
1870     GOTO  1920
1880     LET R3=R3+1
1890     IF R3<3 GOTO  1920
1900     LET D= ABS (Z1-Z2)
1910     LET R0=R0+D
1920     LET R1=R1+Z1
1930     LET R2=R2+Z2
1931     LET C[J]= 0
1932     IF J>N8 GOTO  1940
1934     LET Z3=R1
1936     LET Z4=R2
1940   NEXT J
1942   LET Z5=R1-Z3
1944   LET Z6=R2-Z4
1946   LET R0= INT (R0- ABS ((R1-R2)/P6))
1949   PRINT R0;
1950   LET R0= INT (R0/L3)
1951   PRINT R0;
1952   LET R0= INT (R0+L5*(1/R1+1/R2))
1953   PRINT R0;
1954   LET R0= INT (R0+L6*(Q[ 0]+Q[1]))
1955   PRINT R0
1956   LET R0= INT (R0+L7* ABS (Q[ 0]-Q[1]))
1960   LET R1= INT (R1/10)
1970   LET R2= INT (R2/10)
1980   GOTO  2100
1990   PRINT
```

```
2000    FOR I= 0 TO N1
2002      IF I>5 GOTO  2020
2010      PRINT I,B[I],S[I]
2020    NEXT I
2022    GOTO  2100
2060    FOR J=1 TO N
2070      LET M[J]=J*N4
2075      LET C[J]= INT (S[J]-B[J])
2080      PRINT M[J],B[J],S[J],C[J];
2085      PRINT
2090    NEXT J
2095    STOP
2100    LET K5=K5+1
2110    IF P9>1 GOTO  2200
2120    LET P9=2
2130    PRINT
2140    PRINT "I--------------------------------";
2150    PRINT "------------------------------------I"
2160    PRINT "I TEST I  SP1   I   SP2  I";
2170    PRINT "D.INDEX I            REMARKS                I"
2180    PRINT "I-------I--------I-------I";
2190    PRINT "---------I------------------------------I"
2200    PRINT "I"; TAB (2);K5; TAB (7);"I";R1;
2210    PRINT  TAB (15);"I";R2; TAB (23);"I";R0;
2220    PRINT  TAB (32);"I";
2400    IF R1<P1 GOTO  2430
2410    IF R2<P1 GOTO  2450
2420    GOTO  2470
2430    PRINT " INSUFFICIENT DATA WHEEL #1   I"
2440    RETURN
2450    PRINT " INSUFFICIENT DATA WHEEL #2   I"
2460    RETURN
2470    IF  ABS (R1-R2)<P3 GOTO  2500
2480    PRINT "SIGNIFF. ENERGY DIFF."; TAB (63);"I"
2490    RETURN
2500    IF R0<P2 GOTO  2630
2505    IF (R1+R2)>U8 GOTO  2660
2510    IF R1>U9 GOTO  2660
2515    IF R2>U9 GOTO  2660
2520    REM   **CHECK FOR GREASY OR DEFECTIVE WHEELS**
2555    GOTO  2565
2560    PRINT Z3,Z4,Z5,Z6
2565    LET R5=Z5/Z3
2570    LET R6=Z6/Z4
2575    IF R5<P5 GOTO  2590
2580    IF R6<P5 GOTO  2590
2585    GOTO  2600
```

```
2590  PRINT "   GREASY WHEELS"; TAB (63);"I"
2595  RETURN
2600  PRINT "   HIGH VALUE";
2610  PRINT  TAB (63);"I"
2620  RETURN
2630  PRINT "   GOOD WHEELS";
2640  PRINT  TAB (63);"I"
2650  RETURN
2660  PRINT "   OVERLOAD"; TAB (63);"I"
2670  RETURN
6999  REM            -----------SUB 7000---------------
7000  FOR J1=1 TO N6
7010    CALL 11,D1
7020    FOR J2=1 TO 333
7025    NEXT J2
7030  NEXT J1
7040  RETURN
7499  REM            -----------SUB 7500--------------
7500  FOR I=1 TO N
7520    LET S[I]=B[I]
7540  NEXT I
7550  RETURN
7600  FOR I=1 TO N
7620    LET M[I]=B[I]
7640  NEXT I
7660  RETURN
7989  REM          -----------SUB 8000-------------
7990  REM                ** LINE SPECTRA S/R **
8000  FOR I=2 TO (N-2)
8010    IF B[I]<N5 GOTO  8100
8020    IF B[I]>B[I-1] GOTO  8040
8030    GOTO  8090
8040    IF B[I+1]<B[I] GOTO  8130
8050    IF B[I+1]>B[I] GOTO  8090
8080    IF B[I+2]<B[I+1] GOTO  8120
8090    IF C[I]=1 GOTO  8140
8100    LET C[I]= 0
8110    GOTO  8140
8120    LET C[I+1]=1
8130    LET C[I]=1
8140  NEXT I
8150  RETURN
8499  REM            --------------SUB 8500--------------
8500  FOR I=1 TO N
8520    LET Y[I]=C[I]
8540  NEXT I
8550  RETURN
```

APPENDIX D

RESONANCES OF THE WHEELS TESTED AT THE GRIFFIN
WHEEL PLANT IN BESSEMER, ALABAMA
(A spectrum translator was used to obtain the recorded resonant
frequencies)

TABLE   D.1   Resonances of CJ33 Type Wheels   with
Different Internal Stresses

WHEEL TYPE/I.D.	CJ33 11092	CJ33 97803	CJ33 30695	CJ33 31029
INTERNAL STRESS	Normal Stress	Normal Stress	High Stress	High Stress
TAPE NO. (EVENT)	152(110)	149(82)	152(101)	149(92)
RESONANCES	440.4	434.4	444.4	432.8
	1142.4	1135.2	1136.0	1129.6
	2030.8	2021.2	2019.6	2014.0
	3020.8	3011.6	3008.8	3003.2
	4061.8	4052.8	4044.8	4036.0

TABLE D.2 Resonances of CJ36 Type Wheels with Different Internal Stresses

WHEEL TYPE/I.D.	CJ36-32769	CJ36-32784	CJ36-23089	CJ36-27910	CJ36-26425	CJ36-26171
INTERNAL STRESS	Normal Stress	Normal Stress	Normal Stress	High Stress	High Stress	High Stress
TAPE NO. (EVENT)	154(128)	145(42)	148(65)	148(56)	141(1)	144(24)
RESONANCES	390.4	390.8	392.4	386.8	395.2	395.6
	1040.0	1041.2	1043.2	1038.0	1038.0	--
	1865.2	1867.2	1868.4	1866.0	1862.0	1863.6
	2350.0	--	--	2350.0	2341.6	2343.2
	Weak Resonance	Weak Resonance	Weak Resonance	Weak Resonance		
	2468.8	2465.6	2470.0	2478.8	2483.2	2493.6
	2794.8	2798.8	2795.6	2795.2	2788.0 2789.6	2785.6 2787.2
	2935.6	2941.2	2943.6 W.R. 2966.4	2973.2 W.R 2975.6	2994.0	2995.6 2998.4
	3780.0	3787.2	3787.6	3790.0	3780.4	3784.0 3785.6
	4821.2	4820.0	4818.0	4826.4	4808.6	4809.6
	5856.8	5864.8	5864.8 5875.6	5873.6	5860.0	5861.2

APPENDIX E

DYNAMICS OF A HAMMER EXCITER

Fig. A.E.1 shows a rigid hammer to be used as an exciter, in a generalized form. The hammer is pivoted at point M and impacts at point N. The dynamics of the hammer are governed by the rotational form of Newton's 2nd Law:

$$\tau = I\ddot{\theta} \tag{E.1}$$

where τ is the applied torque, I the moment of inertia of the hammer about M and $\ddot{\theta}$ is the angular acceleration. Let F_i be the component of a driving force in a transverse (i.e. nonradial) direction. Then

$$\Sigma F_i \ell_i - mgk\cos\theta = I\ddot{\theta} \tag{E.2}$$

where ℓ_i is the moment arm of the driving force F_i, k is the distance from M to the center of mass of the hammer and m is its mass.

In the exciter used in the tests there were two driving forces: due to the coiled spring and due to impact at the roller (see Fig. 4.1.1). Both of these forces are time varying, and in the case of the spring force the moment arm is also time varying. Consequently, a full solution of eqn. (E.2) is complicated and has yet to be achieved. However, some insight into the problem can be achieved by solving some simple versions of eqn. (E.2).
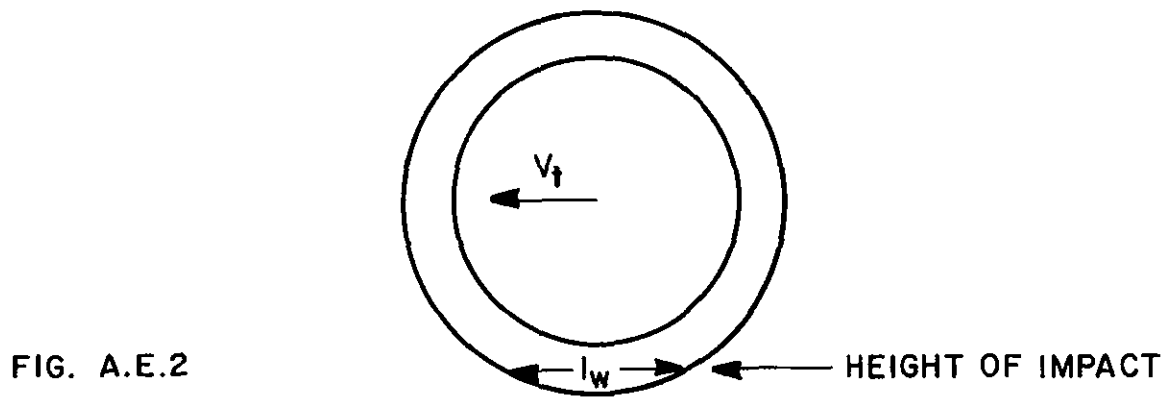
IMPACT POINT

PIVOT POINT

(a)

REST POSITION   IMPACT POSITION

(b)

FIG. A.E.I

FIG. A.E.2   HEIGHT OF IMPACT
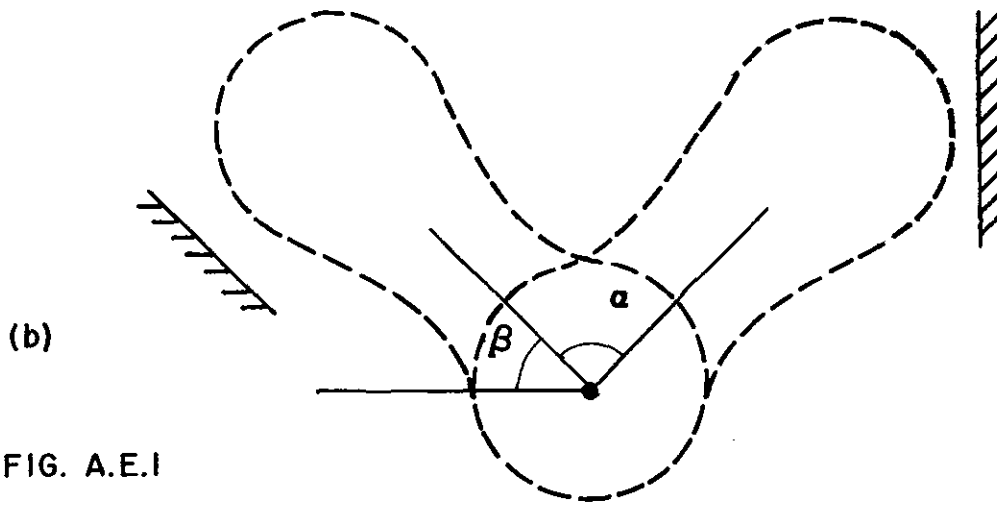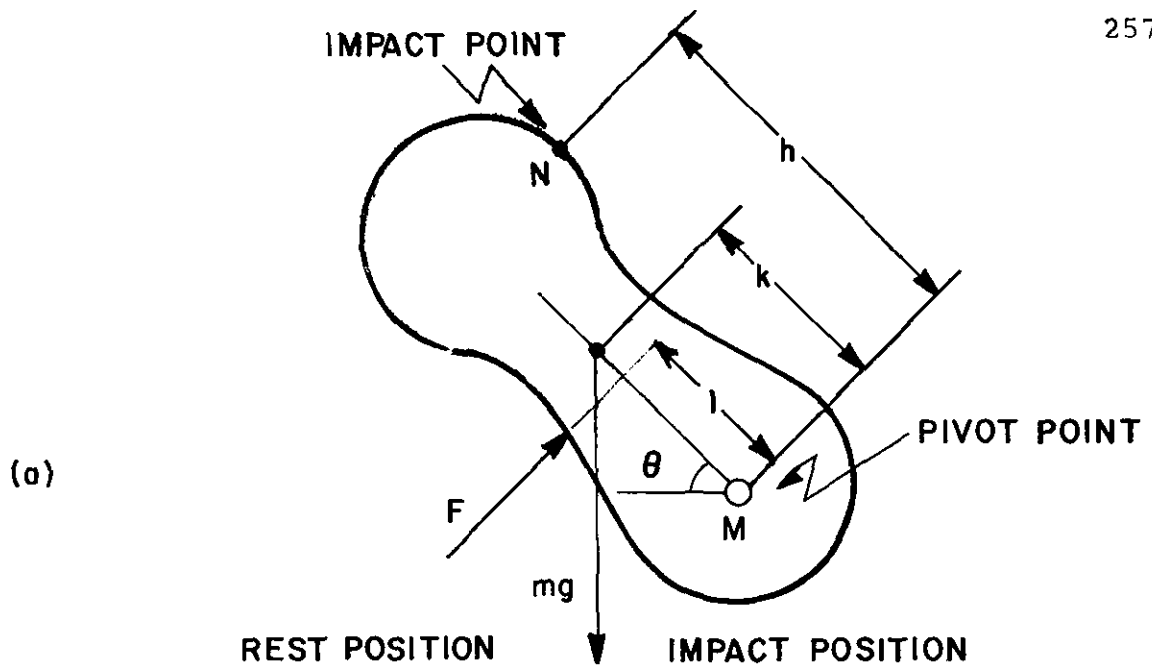
Consider a single constant driving force F and suppose that this force were much greater than the weight mg, then

$$\dot{\theta} = \frac{F\ell}{I} t \tag{E.3}$$

assuming the hammer started from rest and where t is time. Similarly,

$$\theta = \frac{F\ell}{I} \frac{t^2}{2} + \beta \tag{E.4}$$

Thus the time taken to contact the wheel will be given by:

$$t_c = \left(\frac{2\alpha I}{\ell F}\right)^{\frac{1}{2}} \tag{E.5}$$

and the velocity on impact will be:

$$v_c = h\dot{\theta}_c = h \frac{F\ell}{I} t_c$$

$$= h \left(\frac{2\alpha \ell F}{I}\right)^{\frac{1}{2}}. \tag{E.6}$$

If the hammer hits the wheel, it must do so within a time ℓ_w/v_t where ℓ_w is a chord on the wheel at the height of impact and v_t is the train speed (see Fig. A.E.2).

Thus

$$t_c < \frac{\ell_w}{v_t}$$

or

$$\frac{2\alpha I}{\ell F} < \frac{\ell_w^2}{v_t^2} \tag{E.7}$$

Hence

$$F > \frac{2\alpha I v_t^2}{\ell . \ell_w^2} \tag{E.8}$$

Now in the case of a hammer consisting of a heavy ball on a light shaft,

$$I = mh^2 \qquad (E.9)$$

and from (6) and (8)

$$F > \frac{2\alpha mh^2 v^2}{\iota \iota_w^2} t$$

and

$$v_c = \left(\frac{2\alpha \iota F}{m}\right)^{\frac{1}{2}} \qquad (E.10)$$

Thus at 20 mph $\triangleq$ 10 m/sec, with $\iota_w \triangleq 10^{-1}$m; $\iota = 10^{-2}$m; m = 0.5 kg; h = 10^{-1}m and $\alpha = \pi/2$ radians,

$$F > 15 \times 10^3 n = 3,000 \text{ lb}$$

and

$$v_c = 30\text{m/sec}$$

This crude calculation shows that at relatively high train speeds, since the hammer does indeed impact the wheel, that the driving force must be very large. It is inconceivable that these forces are generated by compression of the coil spring and can only be brought about by an impulsive force at impact. On the other hand, at a low speed, e.g. 2 mph $\triangleq$ 1 m/sec

$$F \triangleq 30 \text{ lb}$$

and

$$v_c = 3 \text{ m/sec}$$

At this end of the speed range the spring force is probably effective.

APPENDIX F

FINITE ELEMENT ANALYSIS

F.1 Finite Element Analysis of a Railway Wheel

The finite element method of structural analysis
was used for the mode-frequency analysis of railway wheel
vibrations. The method embodies the concept of representing
the distributed continuum of a physical structure by a
model consisting of a finite number of idealized elements
that are inter-connected at a finite number of points.
The analysis is performed utilizing the ANSYS computer
program developed by Swanson Analysis Systems, Inc.

The ANSYS program employs the matrix displacement
method of finite element analysis. The stiffness matrix
[K] must be generated from a description of the geometrical
and physical properties of the structure. To solve the
resulting system of simultaneous linear equations, ANSYS
uses the wavefront solution method. The "wavefront" is
equal to the number of equations active at any point in
the solution procedure. Each equation is associated with
a particular degree of freedom in the structure. An
active equation is one which has been identified and
previously used in the solution and is required again at
a further point. Equations are activated by the element
to which they are connected as the solution progresses
from element to element.

F.2 Mode Frequency Analysis

The equation of motion for a structural system is

$$[M]\{\ddot{u}\} + [c]\{\dot{u}\} + [K]\{u\} = \{F(t)\}$$

where

[M] = Structure Mass Matrix

[c] = Structure Damping Matrix

[K] = Structure Stiffness Matrix

{u} = Vector of Nodal Displacements

{F(t)} = Force at Each Node as a Function of Time.

For an undamped structure with no force applied,

$$[M]\{\ddot{u}\} + [K]\{u\} = 0$$

If $\qquad \{u\} = \{u_n\}\ \cos\ \omega_n t,$

there are n values of ω^2 and n eigenvectors which satisfy the equation above.

The ANSYS program forms the matrices [M] and [K] by forming the matrices $[M_e]$ and $[K_e]$ for each element. The eigenvalue problem is solved by a technique called "Matrix Condensation" (Guyan Reduction). In this process a set of n "master" degrees of freedom which characterize the natural frequencies of interest in the system are specified, and the eigenvalue problem is solved for the n degrees of freedom.

In the force spectrum option of the ANSYS program, the input consists of a force distribution on the structure nodes and a table of force amplitude multipliers vs. frequency. The structural response to force loading is obtained by superimposing the response of individual

vibrational modes and weighting by their "modal participation factors". The output contains the eigenvalue solution, the corresponding participation factors, mode coefficients and equivalent masses, the eigenvector solution, the expanded mode shapes and the element stress solution.

Natural frequencies and mode shapes are obtained from

$$([k] - \omega_i^2 [m])\{\Psi\}_i = 0$$

where

[k] = the stiffness matrix of the structure

[m] = the mass matrix of the structure

ω_i = the circular natural frequency of mode i

$\{\Psi\}_i$ = the mode shape vector of mode

$\{\Psi\}_i$ is normalized such that

$$\{\Psi\}_i^T [m]\{\Psi\} = 1.$$

The equivalent mass for the ith mode

$$m_{ei} = 1/\{\Psi\}_i^T\{\Psi\}_i$$

The participation factor is defined as

$$\gamma_i = \{\Psi\}_i^T [m]\{F\}$$

where {F} is the force vector.

The mode coefficient is defined as

$$(m.c.)_i = \frac{\gamma_i}{\omega_i} F_i$$

Assumptions

(i) The wheel is rigidly fixed at the hub (UX = UY = UZ = 0) and constrained in radial and circumferential directions at a point on the tread just above the

wheel flange where it is in contact with the railway track, (UX = UY = 0).

(ii) The wheel is made of homogeneous material with Young's Modulus E = 30 x 10^6 psi, and Poisson's ratio ν = 0.3 and density ρ = 7.3 x 10^{-4} $\frac{lb \cdot sec^2}{in4}$.

In the previous contract the ANSYS finite element analysis program has been used to determine the natural frequencies and mode shapes for a 33 in. wheel with i) no cracks and ii) a large plate crack. This study was extended further as follows:

1. The finite element model showing the 33 in. wheel geometry was improved by increasing the number of elements from 192 to 240.

2. The boundary conditions were changed slightly. In addition to fixing all the node points on the hub, an additional node on the tread of the wheel just above the flange was fixed in radial and circumferential directions. This is the point where the wheel is in contact with the railway track.

3. The wavefront size is dependent upon the order in which elements are input. In the case of a railway wheel model there are two possible ways in which the elements can be input to determine the size of the wavefront - radial and circumferential. Both ways were scanned to find out which one gives the smaller wavefront. It was found that the wavefront is smaller if the elements are input in a radial arrangement.

4. A modification of the ANSYS model for the plate portion of the 33 in. wheel was made to determine if a significant cost reduction could be achieved in the execution of this program when the plate geometry was simplified. The simplification involved modeling the plate portion of the wheel by 3-D plate elements having 6 degrees-of-freedom per node instead of the 3-D solid elements having 3 degrees-of-freedom per node. It was hoped that this type of element simplification would allow more computer runs for the same cost. However, this attempt was unsuccessful in achieving a reduction in computer costs. The increase in the degrees-of-freedom for the four nodes for each plate element from 3 to 6 (to allow for plate element rotation) caused the number of simultaneous equations associated with the computer generated wavefront to exceed that of the previous element description.

Various cracks were simulated in the ANSYS model of the wheel by providing double and disconnected nodes in the crack area. The following cracks were simulated:

1. One small radial crack, provided by detaching one boundary on one of the rim elements (Fig. F.2.1).

2. One small radial crack through the rim, but not extending into the plate (Fig. F.2.2).

3. One large radial crack extending from the rim through to the axle (Fig. F.2.3).

4. One large plate crack (open on both sides and extending slightly in the radial direction at both ends (Fig. F.2.4).
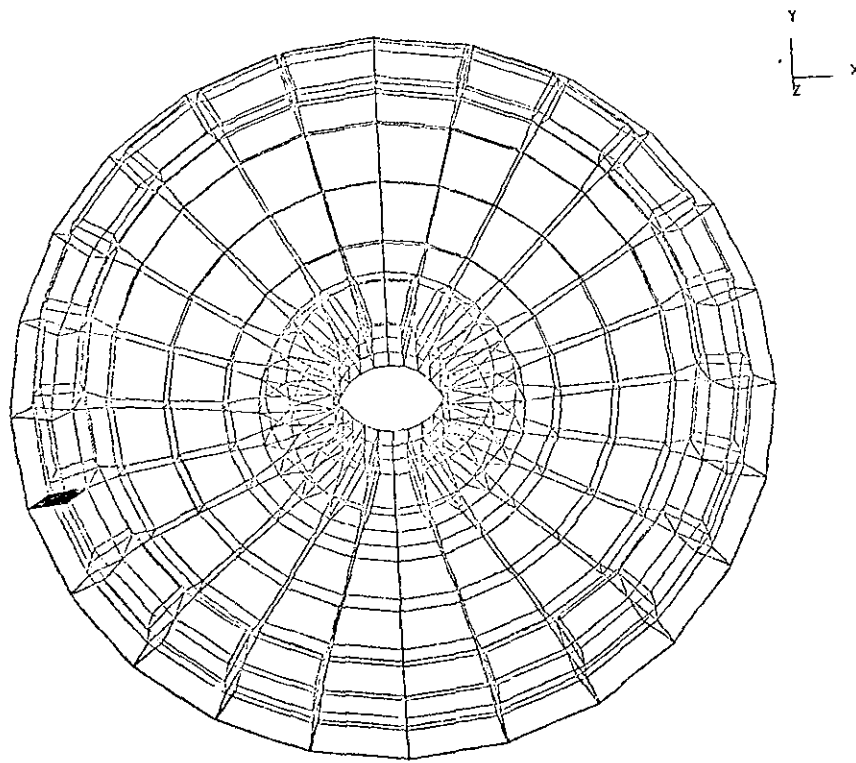
FIG. F.2.1   VIEW OF A 33 INCH WHEEL WITH ONE SMALL RADIAL FLANGE
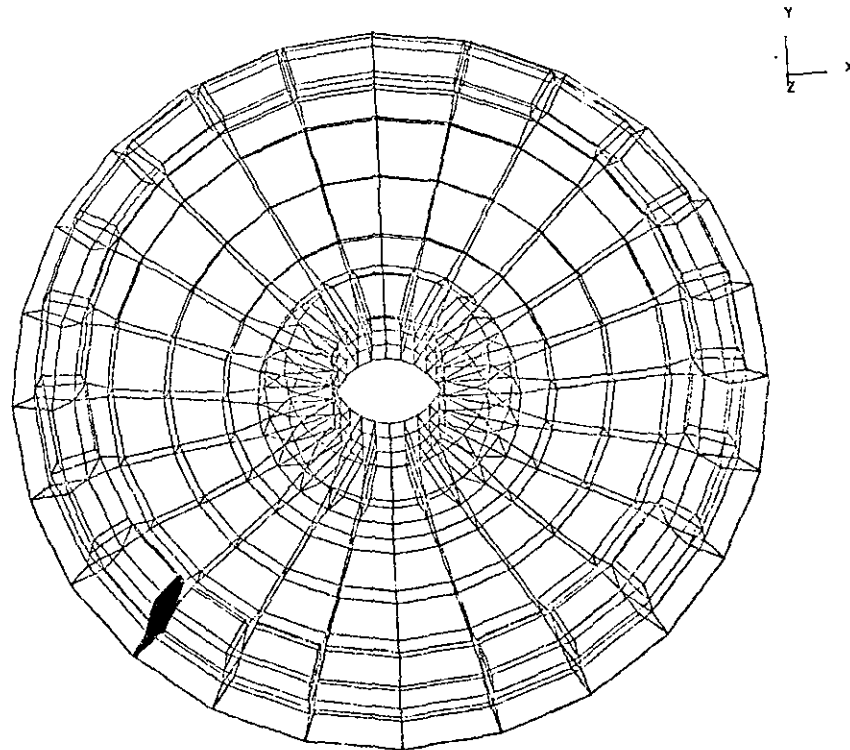CRACK - ANSYS GEOMETRY

FIG. F.2.2   VIEW OF A 33 INCH WHEEL WITH ONE COMPLETE RADIAL
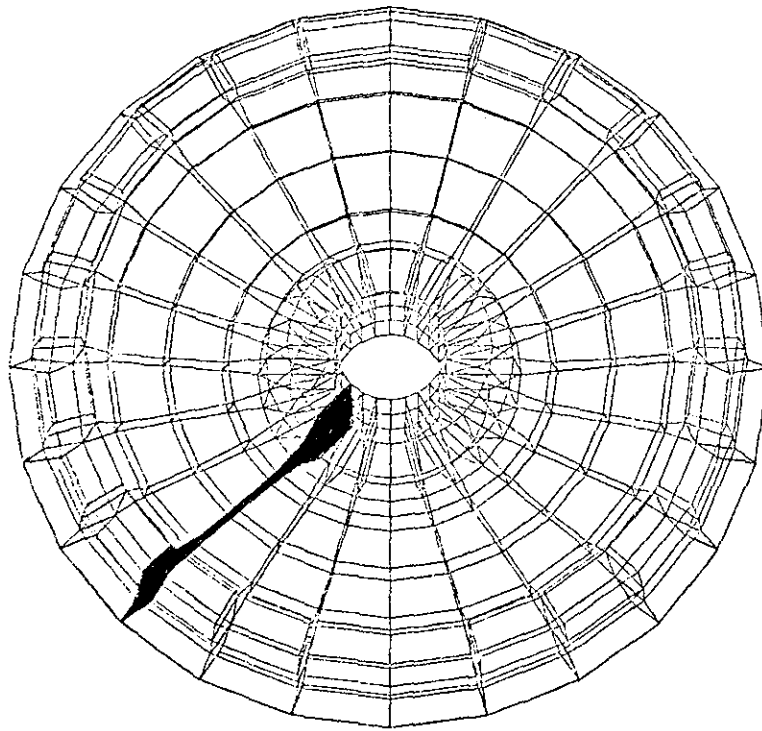FLANGE AND TREAD CRACK - ANSYS GEOMETRY

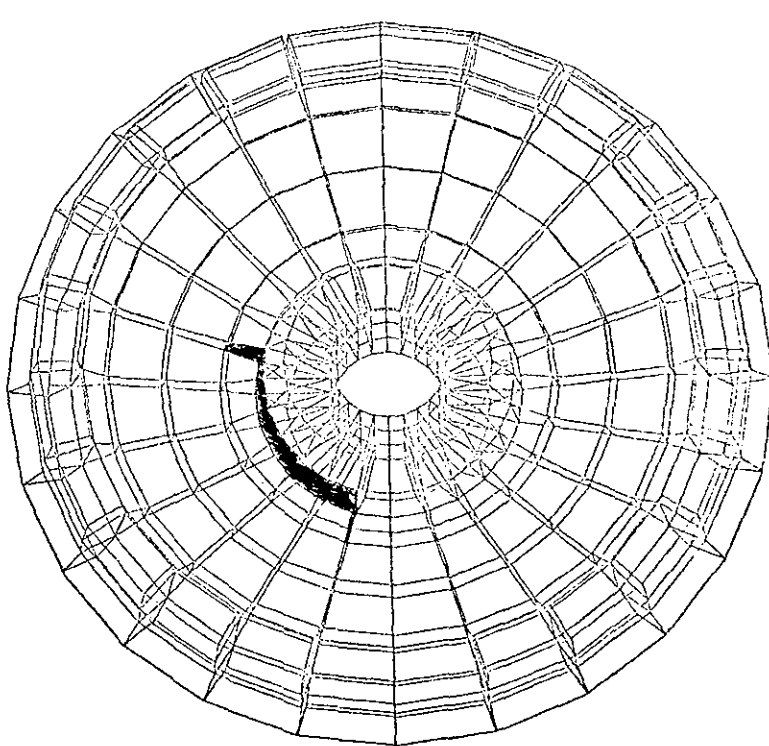FIG. F.2.3 VIEW OF A 33 INCH WHEEL WITH ONE COMPLETE RADIAL CRACK -
ANSYS GEOMETRY

FIG. F.2.4 VIEW OF A 33 INCH WHEEL WITH ONE LARGE PLATE CRACK -
ANSYS GEOMETRY

The following forcing functions were investigated
to determine the vibration response of a wheel with or
without simulated cracks.

(i)   a square pulse: to simulate a single impact

(ii)   repetitive square pulses: to simulate repetitive
        impact

(iii)   a sawtooth: to simulate slip-stick action such
        as with a retarder or brake shoe.

Excitation of Cracked Wheels

Several studies were made to determine the effect
on the spectrum of cracks of various sizes and in various
locations. In addition there was some interest in deter-
mining the effect of varying the direction and point of
contact on the wheel of the forcing function and the position
of this point relative to the crack. These studies are
summarized in Table F.2.1.

Figure F.2.5 shows the calculated line spectra for
the good wheel and for wheels with different cracks.

In general, the introduction of a crack results in
removal of degeneracy of modes and the introduction of
new resonances. Both of these effects cause the appearnce
of additional lines in the spectrum. Even one small
crack in the flange causes significant differences in the
spectrum, especially in the range 2000 to 4000 Hz.

Figures F.2.6 and F.2.8 show Mode Coefficient (related
to the amplitude) vs. Frequency plots for good wheel and

TABLE F.2.1 SUMMARY OF ANALYSIS

| Study No.	Wheel Description	Type of Excitation	Direction and Location of Excitation
1	33 in. wheel – no cracks	Square pulse	Axial on load line and 30 degree from load line
2	"	Square pulse with extended duration	"
3	"	Two successive square pulses	"
4	33 in. wheel – one small radial flange crack	Square pulse	Axial on load line and 30, 60, 90, 120, 150 and 180 degree from load line
5	"	Square pulse	Radial on load line and 30, 60, 90, 120, 150 and 180 degree from load line
6	33 in. wheel – one large plate crack	Square pulse	Radial on load line
7	33 in. wheel – one complete radial crack	–	–
8	33 in. wheel – one radial rim crack	–	–
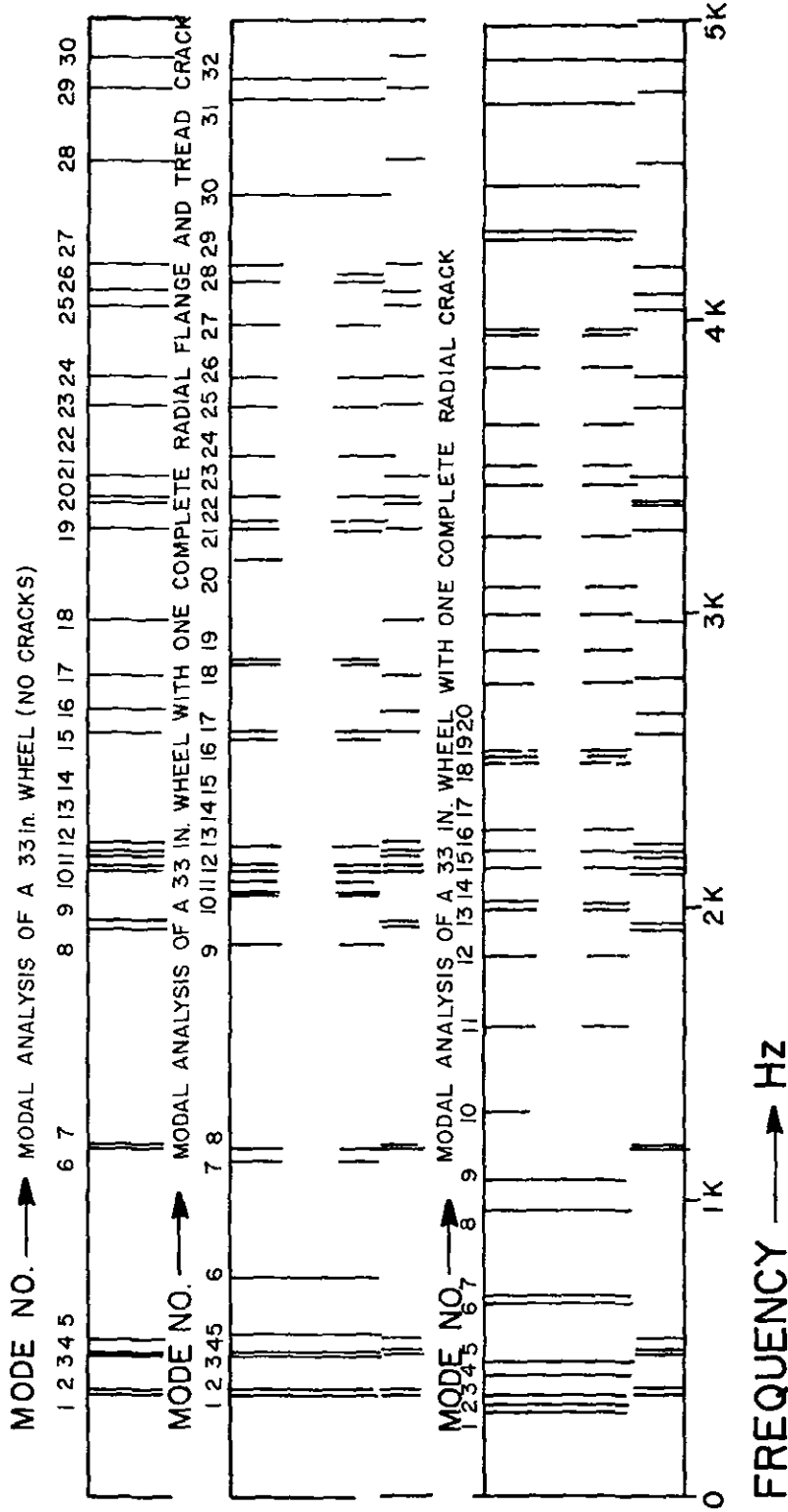
FIG. F.2.5 COMPARISON OF NATURAL MODES FOR 33 in. WHEELS

FIG. F.2.6a 33" GOOD WHEEL MODAL ANALYSIS SINGLE PULSE ON THE LOAD LINE. LOAD STEP NO 1.
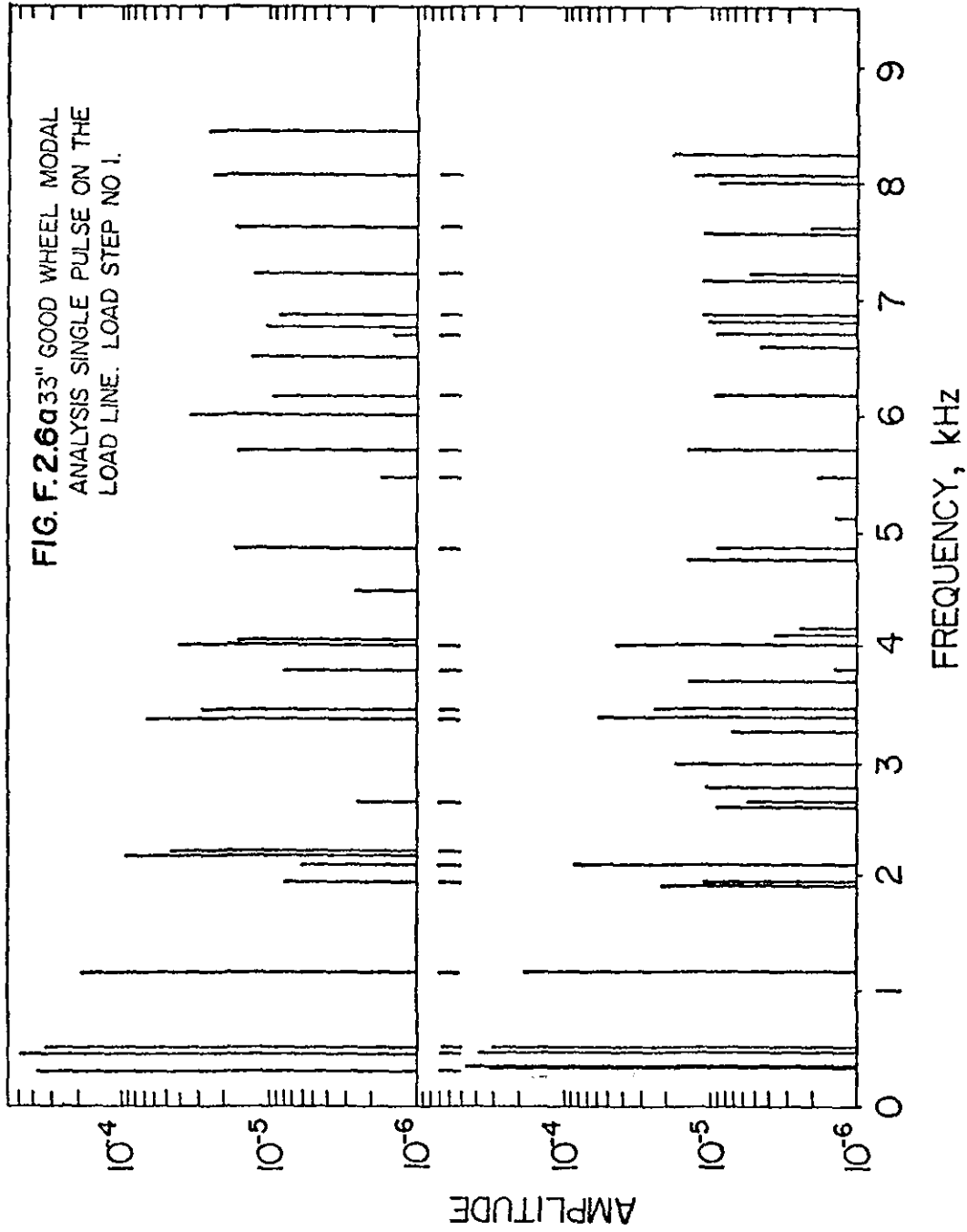
FIGURE F.2.6b 33" GOOD WHEEL MODAL ANALYSIS SINGLE PULSE 30° FROM LOAD LINE LOAD STEP NO. 2
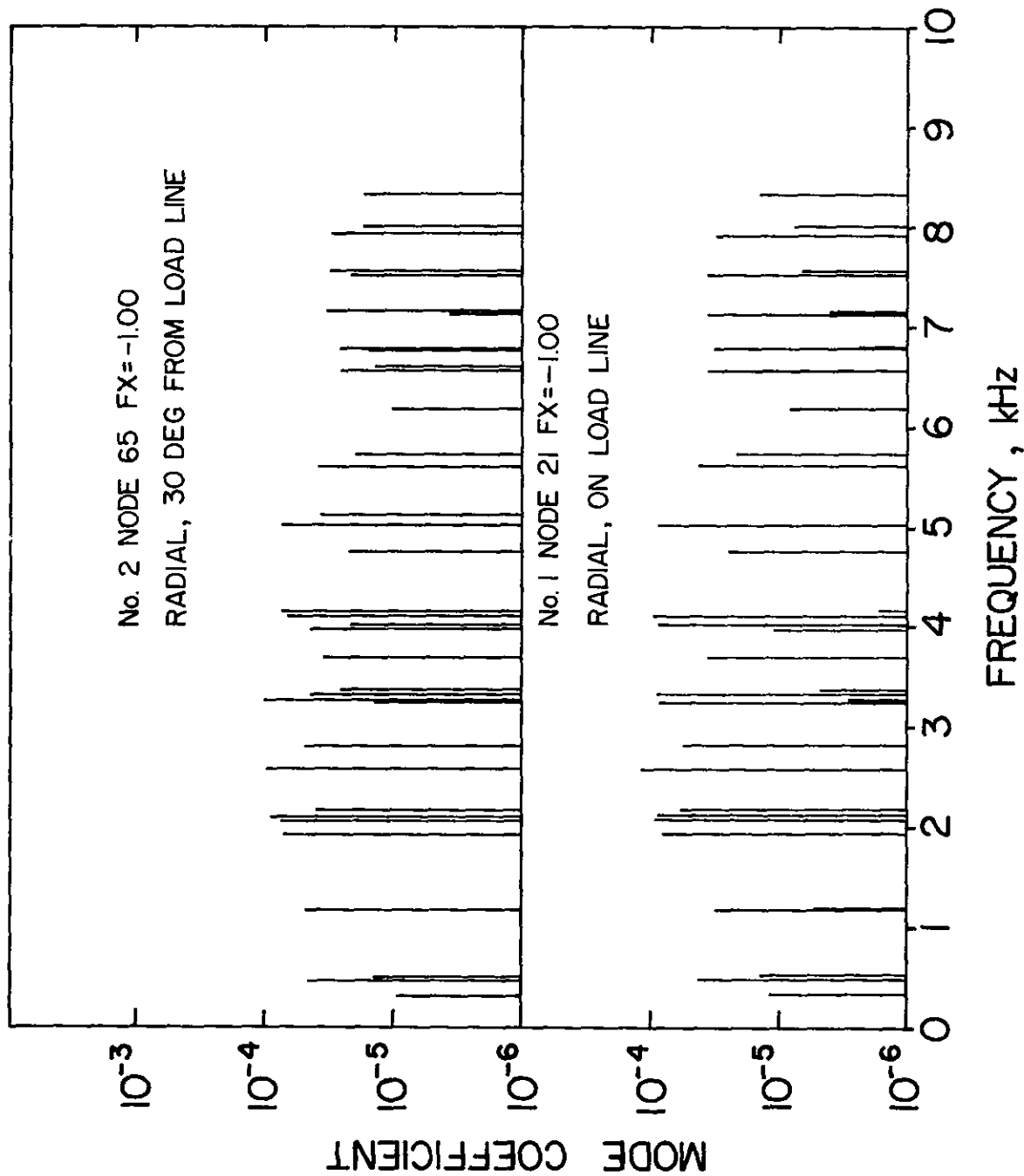
FIGURE F.2.7   MODAL ANALYSIS OF A 33in WHEEL WITH ONE SMALL
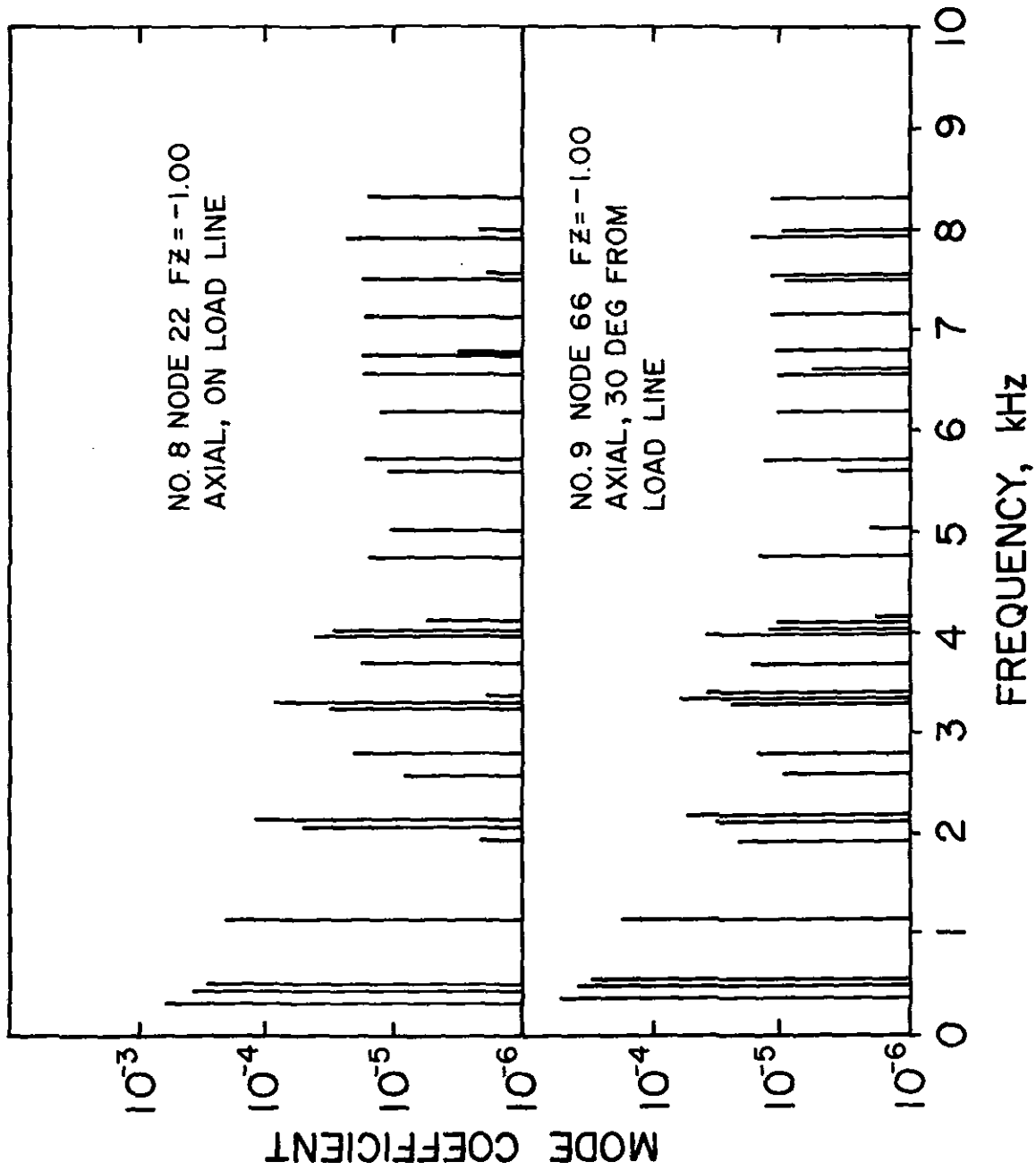RADIAL FLANGE CRACK–A SINGLE PULSE APPLIED

FIGURE F.2.8 MODAL ANALYSIS OF A 33in. WHEEL WITH ONE SMALL
RADIAL FLANGE CRACK - A SINGLE PULSE APPLIED.

wheels with different cracks excited by a square pulse.
For good wheel excitation, it is seen that different modes
are excited depending upon location of the point of excitation
relative to the load line. Also the modal amplitude
varies somewhat. A study of the effect of different impact
points was made for the wheel with the smallest possible
rim crack.

Axial and radial excitation on the flange by a square
pulse was carried out separately at various angular dis-
tances (15 degrees apart) from the load line. The purpose
was to determine if the small crack so simulated is evident
in spectral changes, and secondly, to determine if the small
crack may be discovered regardless of the point of wheel
excitation. The results show that the number of resonances
excited between 300 and 10000 Hz in the faulty wheel varied
between 27 and 40 depending upon the nodal location on
which the impulse was applied, and on whether this impulse
was applied axially or radially. However, the amplitude
of the major resonances was not greatly affected and it
was concluded that there was no great advantage to be gained
by impacting the wheel off the load line.

APPENDIX G

RELATIONSHIP AMONG OPERATING PARAMETERS

In assessing progress towards the goal of helping
the Railroads find defective wheels it is necessary to have
some "yardsticks" or "figures of merit" by which to measure
the performance of the acoustic signature system in
comparison with current practice and other systems and to
measure the cost/benefit ratio of developing and operating
such systems. Such measures are not easy to come by
partly because some of the information that it is necessary
to have (e.g., the percentage of defective wheels in
service) is not available in a precise form.

It is possible to define two figures of merit which
could be used to assess progress. First, reliability is
defined as:

$$R = \frac{\text{Number of correct decisions}}{\text{Total number of decisions}}$$

where a decision is a good/bad wheel choice as made by
the system. The false alarm rate is defined as:

$$F = \frac{\text{Number of unconfirmed indications}}{\text{Total number of bad wheel indications}}$$

Let the number of axles passing the inspection point in
a given period be N_A. Suppose that N_D of these axles
carry a defective wheel and that the fraction of these
identifiable by acoustic signature inspection is g. Then
the number of bad wheels correctly found will be

$$N_B = gN_D.$$

Let:

$$N_D = fN_A,$$

so that f is the fraction of axles with defective wheels.

Now if the total number of indications made during this period is N_i the false alarm rate will be:

$$F = \frac{N_i - N_B}{N_i},$$

so that,

$$N_i = \frac{N_B}{1-F} = \frac{gfN_A}{1-F}.$$

The number of incorrect indications will be $(N_i - N_B)$ and so the number of correct decisions will be $(N_A + N_B - N_i)$. Thus the system reliability for this period will be given by:

$$R = \frac{N_A + N_B - N_i}{N_A} = 1 - \frac{Fgf}{1-F}.$$

Rearranging

$$F = \frac{1-R}{1+gf-R} = 1 - \frac{gf}{1+gf-R}$$

This formula states the problem in a nutshell. F, the false alarm rate, is an operating parameter. The question is how many wrong indications would be accepted by the railroads for every bad wheel detected. Suppose an acceptable value is $F = 1/2$. To accomplish such a low value we would need a reliability of the order $(1 - gf)$. Now g is a measure of our scientific knowledge i.e., our ability to recognize defective wheels. Using the optimum ID equation, it can be seen from Fig. 7.3.4 that if a decision level of 64 is selected then g is unity, but if a

decision level of 69 is selected then g is two thirds.
Let us assume g = 1. The real problem is with f, the
fraction of axles with defective wheels, which is a very
small number. Despite the lack of precise information on
the exact figure, estimating from the number of wheel
failures reported to the AAR and the total size of the U.S.
fleet of cars indicates that there is one defective wheel
in every 10,000

$$\text{i.e., } f = 10^{-4}$$

and the reliability has to be about $(1-10^{-4})$ i.e.,
(1-0.001) = 0.9999 or 99.99%. Putting it another way,
the system has to work so well that only 1 incorrect
decision is made in 10^4.

On the other hand, consider the following case

$$F = 0.9 \text{ (one bad wheel indication in}$$
$$10 \text{ is substantiated)}$$

$$f = 10^{-4}$$

then $R \approx 1 - 9gr \approx 1 - 10^{-3}$ = 99.9%, representing one
incorrect decision in 10^{+3}. As can be seen from the
statistics in Fig. 7.3.4 there were 3 incorrect decisions
in 371 or about 1 in 123. Thus to find all the defective
wheels would require a reduction of the incorrect decisions
by a factor of 8. This would not appear to be beyond the
bounds of possibility for a prototype system. On the other
hand, with a decision level of 69, based on the same sample,
two thirds of the defective wheels would be found with
100% reliability and zero false alarm rate.

APPENDIX H

REPORT OF NEW TECHNOLOGY

In the earlier report (FRA/OR&D 76-290 or DOT-TSC-FRA-76-6),
three items were listed as possibly patentable. In the present work,
a number of improvements are described and these are now listed under
the same three headings:

1) The system for Acoustic Signature Inspection of Railroad
Wheels is described again on page 6-9 and 109-110 with some new
ideas to bypass some problem areas.

2) The mechanical impacter, as actuated by the wheel itself, is
described with improvements on pages 93, 13-14, and 90-94. Additional
ideas for excitation methods are given on pages 94-99.

3) The improved computer programs for analysis of acoustic signa-
tures are described on pages 107-122 and printed in full in Appendix C
on pages 211-252.